Morphodynamics of Texel Inlet

Morfodynamica van het Zeegat van Texel

Cover: ebb-tidal delta bathymetry of Texel Inlet
(image made available by Rijkswaterstaat RIKZ, Den Haag).

Morphodynamics of Texel Inlet

Proefschrift

ter verkrijging van de graad van doctor

aan de Technische Universiteit Delft

op gezag van de Rector Magnificus prof. dr. ir. J.T. Fokkema

voorzitter van het College voor Promoties

in het openbaar te verdedigen op dinsdag 3 oktober 2006 om 12.30 uur

door

Edwin ELIAS

civiel ingenieur

geboren te Hontenisse

Dit proefschrift is goedgekeurd door de promotoren:

Prof. dr. ir. M.J.F. Stive
Prof. dr. ir. J.A. Roelvink

Samenstelling promotiecommissie:

Rector Magnificus	voorzitter
Prof. dr. ir. M.J.F. Stive	Technische Universiteit Delft, promotor
Prof. dr. ir. J.A. Roelvink	Technische Universiteit Delft, promotor
Prof. dr. ir. H.J. de Vriend	WL | Delft Hydraulics
Prof. dr. ir. J. van de Kreeke	University of Miami, Florida, United States
Prof. dr. S.B. Kroonenberg	Technische Universiteit Delft
Dr. A.J.F. van der Spek	TNO-NITG Bouw en Ondergrond
Dr. J. Cleveringa	Alkyon

This research was carried out as cooperation between Delft University of Technology, the Directorate-General of Public Works and Water Management (Rijkswaterstaat-RIKZ) and WL | Delft Hydraulics. Funding was provided by the Dr. Ir. Cornelis Lely Foundation and the Delft Cluster Project: Coasts 03.01.03.

ISBN 1-58603-676-9

Keywords: morphodynamics, process-based models, tidal inlet systems

Published and distributed by IOS Press under the imprint of Delft University Press

Publisher
IOS Press; Nieuwe Hemweg 6b; 1013 BG Amsterdam; The Netherlands
tel: +31-20-688 3355; fax: +31-20-687 0019
email: info@iospress.nl; www.iospress.nl; www.dupress.nl

"Peacefully drifting just waiting for sets.

A little breeze, a few friends its as good as it gets"

Ed Angulo (2005)

Abstract

Texel inlet, the largest inlet in the Dutch Wadden Sea, has undergone drastic changes in the morphology of its back-barrier basin, ebb-tidal delta and adjacent coastlines after the closure of the Zuiderzee (1926-1932). As a result large sand losses were observed along the adjacent coastlines and still until today the maintenance of this part of the coast is the most intensive of the entire Dutch coast. The processes controlling the sediment exchange between the North-Holland and Texel coasts, the ebb-tidal delta, tidal inlet and back-barrier basin are insufficiently understood despite intensive monitoring and analysis. The research reported in this thesis aims to acquire more understanding of this sediment exchange and of the morphodynamics of Texel Inlet in general.

The morphodynamics of Texel Inlet are studied over a wide range of temporal and spatial scales ranging from long-term descriptions of historic inlet evolution, from 1550 A.D. to present, to detailed analyses of hydrodynamics and morphodynamics on a tidal and seasonal process-scale. Although, the focus is on Texel Inlet, where possible, findings are generalized to contribute to the understanding of generic tidal inlet dynamics.

To a varying degree of accuracy Texel Inlet's ebb-tidal delta bathymetry has been monitored over the last 400 years. This series of regular bathymetric observations is unique in the world and allows the description of the inlets long-term morphodynamic evolution. An evolution governed by an increasing impact of major engineering works such as seawall construction (Helderse Zeewering) and damming of a main part of the basin (closure of the Zuiderzee). The well-monitored changes in the ebb-tidal delta morphology show the cumulative impact of inlet modification and of anthropogenic interventions in the back-barrier basin. Different stages of ebb-delta evolution, each characterized by specific orientations of the main channels and shoals, can be discerned. Prior to construction of extensive coastal defence works on the southern shore of the inlet in 1750 A.D. (predecessors of what is now known as Helderse Zeewering) the ebb-tidal delta showed a downdrift asymmetry. Periodic shoal breaching and downdrift channel relocation were the dominant mechanisms for sediment bypassing (major shoal bypassing). After construction of the coastal defence works a stable ebb-tidal delta with a westward stretching main ebb-channel developed over a period of approximately 60 years. Damming of the Zuiderzee, separating the major part of the back-barrier basin and completed in 1932 A.D., distorted this stable state and over a period of about 40 years the main channel switched to a southward, updrift course, remaining in position ever since. During the pre- and post-damming stable states the sediment bypassing took place as minor shoal bypassing;

the main channel remained in position and smaller parts of the swash platform (periodically) migrated landward over the ebb-tidal delta.

The well-monitored large-scale changes on the ebb-tidal delta, which were initiated by the construction of the coastal defence works and closure of the Zuiderzee, show that incorporation of inlet modifications and back-barrier processes is vital for a correct description of the ebb-tidal delta dynamics and processes. The expression 'back-barrier steering' is introduced to describe this 'forcing' induced by the basin.

Analysis of observations significantly contributes to an improved understanding of the inlet behaviour and evolution on higher levels of aggregation. However, a major shortcoming is the lack of comprehensive descriptions of the underlying physics; observed morphological changes and expert judgement form the principal source of information. Knowledge of the underlying physical processes, and their interaction with sediments and sediment bodies is important for understanding ebb-tidal delta behaviour. Due to the non-linear interaction between water motion (wind-, wave-, density- and tide-driven) and variable channel and shoal structures compound (residual) flow and transport patterns arise that show a wide range in temporal and spatial variation. Suitable field data that provide detailed descriptions of water, flow and sediment transport variations on the intra-tidal and intra-event scales with the necessary spatial and temporal detail over the inlet domain are scarce, if not absent. Even at Texel Inlet, one of the most frequently monitored inlets worldwide with high-quality observational datasets of water levels, wind, waves, currents and discharges, bathymetry, bedforms and sediment characteristics present the spatial and temporal data coverage is still limited.

Fundamental understanding of inlet dynamics is obtained by mathematical modelling. Recent advances in process-based modelling techniques include the computation of sediment transport and bed level change fully integrated in the flow module; the Delft3D Online Morphology model. Herein morphologic changes are calculated simultaneously with the flow calculations. One of the major assets of this model is the capability to increase the spatial and temporal resolution of point-oriented field observations. Point-oriented observations are used to force the model quasi real-time 'as realistically as possible' by measured time-series of wind, waves and tides, and the model results provide synoptic, near-realistic data of high spatial and temporal resolution over the inlet domain. Analysis of these data provide valuable information on governing flow and sediment transport patterns both in the instrumented and the un-instrumented areas of the domain, and make identification of the dominant processes and mechanisms for flow and transport possible.

Fundamental understanding of the post-closure inlet dynamics and evolution is obtained by integrating analysis of field and model data, and by formulating a conceptual model describing the post-closure morphological adjustment in different stages of development. Initially, during the adaptation stage following the engineering works the ebb-tidal delta dynamics cannot be described in terms of the natural hydrodynamic processes, such as the ratio of wave versus tidal energy, alone. The asymmetrical ebb-tidal delta development with southward directed main channels was forced by the changed hydrodynamics in the back-barrier basin; the altered tidal characteristics, the northward displacement of the basin centre, the closing of

southward basin channels and the amplification of the tidal prism. In the basin major sedimentation was observed, viz. over 200 Mm^3 of sediment was imported during a period of approximately 40 years.

Tides are identified as the main process for these first-stage developments. Due to the large tidal prism and the corresponding large tidal transports involved, the channels regained equilibrium at a faster rate than the shoal areas (e.g. the abandoned ebb-shield Noorderhaaks), and the present-day ebb-tidal delta development is best described as a second-stage self-organizing process of sediment redistribution, sediment recirculation and sediment exchange to obtain a natural equilibrium state adapted to the changed configuration of the main-ebb channels. Sediment is eroded from the ebb-delta (including adjacent shorelines) and deposited in the basin. Largest erosion prevails on the western margin of Noorderhaaks were tides and waves are important for the landward displacement of sediments. Locally, sedimentation and erosion patterns are governed by channel-shoal interactions; the interaction of the channels Molengat and Noorderlijke Uitlopers of Noorderhaaks induces sediment loss of the Texel coastline, while the Nieuwe Schulpengat-Bollen van Kijkduin channel-shoal-system determines the development of the adjacent North-Holland coast. The presence of large flood-dominant channels along the coast induces a major sediment loss towards the basin. The sediment import in the basin is estimated to range at 5 to 6 Mm^3/year. A number of aspects contribute to this large influx; (1) sediment deficit in the basin caused by the loss of intertidal shoal areas due to closure of the Zuiderzee and relative sea-level rise, (2) availability of a vast amount of sediment in the abandoned ebb-delta front Noorderhaaks, and (3) transport capacity due to the large tidal prisms through the inlet.

The large ongoing sediment import into the basin shows that the effects of closure of the Zuiderzee are far from damped out, and it will take many decades before a new equilibrium will be reached.

Samenvatting

Het grootste zeegat van de Nederlandse Waddenzee, het Zeegat van Texel, heeft na Afsluiting van de Zuiderzee (1926-1932) drastische veranderingen ondergaan in de morfologie van het bekken, de buitendelta en de aanliggende kusten. Grote zandverliezen hebben plaatsgevonden langs de kusten van Texel en Noord-Holland en locaal is er uitschuring opgetreden door de vorming van getijgeulen direct grenzend aan de kustlijn. De grootschalige verliezen zijn gerelateerd aan de zandvraag van het bekken om te compenseren voor de effecten van de Afsluiting, maar ook ten gevolge van relatieve zeespiegelstijging. Alhoewel de Afsluiting van de Zuiderzee al bijna 75 jaar geleden heeft plaatsgevonden behoort ook heden ten dage het kustonderhoud in deze regio tot de meest intensieve binnen het Nederlandse kustsysteem. De processen die de uitwisseling van het sediment tussen de kust, de buitendelta, het zeegat en het bekken bepalen zijn hierbij van groot belang, maar worden echter nog steeds onvoldoende begrepen ondanks intensieve monitoring en analyse. Het onderzoek gerapporteerd in dit proefschrift geeft meer inzicht in deze processen en de morfodynamica van het zeegat in het algemeen.

De morfodynamica van het Zeegat van Texel is bestudeerd op verschillende tijd- en ruimteschalen. De analyses variëren van langetermijn onderzoek, naar de historische ontwikkeling en gedrag van het zeegat (1550 tot heden), tot gedetailleerde analyses van de hydrodynamica en morfodynamica op de processchaal (getij- tot seizoens-invloeden). Alhoewel, het Zeegat van Texel gebruikt wordt als casestudie zijn waar mogelijk de conclusies gegeneraliseerd om bij te dragen in de generieke kennis van zeegat systemen.

Het Zeegat van Texel, met name de buitendelta, is al meer dan 400 jaar intensief bemeten. Deze lange tijdreeks van opnamen van de ligging van de hoofdgeulen en platen is uniek in de wereld en maakt het mogelijk om grootschalige (langetermijn) veranderingen in gedrag en ontwikkeling te beschrijven. De geobserveerde ontwikkeling van het zeegat wordt gedomineerd door de cumulatieve effecten van menselijke ingrepen zoals de stabilisatie van de keel van het zeegat door aanleg van de Helderse Zeewering en reductie van het kombergingsgebied door afsluiting van de Zuiderzee. Aanpassing van de buitendelta aan de effecten van deze ingrepen resulteert in verschillende perioden waarin de topografie gekarakteriseerd wordt door specifieke oriëntaties, ligging en ontwikkeling van de hoofdgeul(en) en platen. In de periode voor de aanleg van de voorlopers van de Helderse Zeewering (rond 1750) kon de keel van het zeegat zuidwaarts migreren. Een noordwaarts gerichte geul-plaat configuratie met een periodiek gedrag in de ontwikkeling, migratie en verheling met de Texelse kust domineerde de buitendelta ontwikkeling (*major shoal bypassing*). Na stabilisatie van de keel van het zeegat vormde zich ook op de buitendelta, in een tijdsbestek van

ongeveer 60 jaar, een stabiel systeem met een westwaarts georiënteerde hoofdgeul. De afsluiting van de Zuiderzee in 1932 verstoorde deze stabiliteit en gedurende een periode van 40 jaar werd de geulontwikkeling gedomineerd door verzanding van de voormalige hoofdgeul Westgat en de zuidwaarts, langs de kust van Noord-Holland, ontwikkelende geulen Schulpengat en Nieuwe Schulpengat. Deze zuidelijk georiënteerde geulconfiguratie is tot op heden stabiel gebleven. Wel verhelen kleinere zandbanken zoals Onrust met de Texelse kust (*minor shoal bypassing*)

De lange tijdsreeksen van bodemmetingen illustreren de respons van de buitendelta ten gevolge van de effecten van grootschalige menselijke ingrepen in de keel en bekken van het zeegat. Een belangrijke conclusie is dat de dynamiek van de buitendelta niet alleen beschreven kan worden door de klassieke beschouwing van getij versus golfenergie. De term *"back-barrier steering"*, letterlijk vertaald bekkensturing, is geïntroduceerd om de additionele (veranderingen in) forcering door bekken en keel te beschrijven.

De analyse van veldmetingen heeft belangrijke inzichten in het gedrag van het zeegat en de ontwikkeling op hogere schalen van aggregatie verschaft. Een tekortkoming is echter dat de onderliggende fysica slechts in geringe mate beschreven is; de geobserveerde morfologische ontwikkelingen en *"expert judgement"* vormen de basis. Fundamentele kennis van de onderliggende processen en mechanismen, de interactie van de stroming met het sediment en complexe sedimentstructuren, is van essentieel belang. Door het niet lineaire gedrag tussen de waterbeweging (een combinatie van getij, wind, golven en/of dichtheidsgedreven componenten) en de zeer variabele geul- en plaatvormen ontstaan er gecompliceerde (residuele) stromingen en transporten. Veldmetingen met voldoende dekking in ruimte en tijd van deze patronen zijn schaars. Zelfs in het geval van het Zeegat van Texel, dat wereldwijd tot de meest intensief bemeten zeegaten gerekend kan worden met beschikbare (hoge kwaliteits)metingen van bodem en bodemvormen, waterstanden, wind, golven, stromingen en sedimentkarakteristieken is de dekking slechts beperkt.

Fundamenteel begrip van de zeegatdynamiek kan worden verkregen door het toepassen van numerieke modellen. Recente ontwikkelingen in het procesgebaseerde model *Delft3D Online Morphology* maken het mogelijk om elke rekentijdstap zowel stroming, sedimenttransport en bodemverandering te berekenen. Door het model realistisch aan te sturen, the kalibreren en te valideren met meetdata kan het model gebruikt worden om gebiedsdekkende data over het gehele domein te verkrijgen; de ruimtelijke resolutie van puntmetingen wordt vergroot. Integratie van de analyse van modeldata en meetdata biedt waardevolle informatie over de maatgevende stromings- en transportpatronen, zowel in de gemeten als ongemeten gebieden. Daarnaast is het mogelijk de dominante processen en mechanismen te kwantificeren door te variëren in modelaansturing.

Fundamentele kennis van de werking van het Zeegat van Texel sinds de afsluiting van de Zuiderzee is verkregen door een dergelijke integrale analyse van model- en velddata. De morfologische ontwikkeling is daartoe beschreven middels een conceptueel model. De basis van dit model ligt in de beschrijving van verschillende stadia van ontwikkeling. Direct na afsluiting ontwikkelen de hoofdgeulen op de buitendelta zich zuidwaarts, geforceerd door de veranderde hydrodynamica van het

bekken en gedurende een periode van zo'n 40 jaar werd er meer dan 200 miljoen m^3 sediment het bekken in geïmporteerd. Getij is geïdentificeerd als het dominante proces voor deze grootschalige veranderingen De gewijzigde getijvoortplanting, de noordwaartse verplaatsing van het zwaartepunt van het komberginsgebied, het afsluiten van de zuidelijk gerichte geulen en de toename van de debieten zijn hierin van essentieel belang. Door het grote getijprisma en de daaraan gerelateerde significante getijstromingen en -transporten hervonden de geulen een nieuw evenwicht sneller dan de platen. De huidige ontwikkeling kan het best omschreven worden als een tweede-stadium aanpassing. Na de veranderingen in het geulenstelsel betreft de aanpassing nu vooral het verhogen van de ondiepwatergebieden en uitbreiding van het plaatareaal in het bekken. Hierbij vindt sedimentherverdeling, circulatie en uitwisseling tussen buitendelta en bekken plaats om een nieuw evenwicht te hervinden. Sediment wordt geërodeerd van de buitendelta (en aanliggende kusten) en gedeponeerd in het bekken. Significante erosie geschiedt op de westelijke rand van Noorderhaaks door landwaarts getij- en golfgedreven sedimenttransport. Locaal worden de sedimentatie-erosie patronen sterk beïnvloedt door circulatiecellen en geul-plaat interacties. Sedimentverliezen langs de Texelse kust zijn nauw verbonden met de interactie tussen en het landwaarts verplaatsen van Molengat en Noorderlijke uitlopers van de Noorderhaaks. Langs de Noord-Hollandse kust is het zandverlies gerelateerd aan de aanwezigheid van een grote (vloed-gedomineerde) getijgeul en de locale interactie van Nieuwe-Schulpengat, Bollen van Kijkduin en Franse Bankje. De huidige sediment import door het Marsdiep de Waddenzee in wordt geschat op 5 tot 6 miljoen m^3/jaar. Een drietal aspecten spelen een grote rol bij deze grote zand verliezen: (1) zandtekort in het bekken ten gevolge van het verlies van intergetijdegebied door afsluiting van de Zuiderzee en relatieve zeespiegelstijging, (2) beschikbaarheid van sediment in de vorm van het afgestoten ebschild Noorderhaaks en (3) transportcapaciteit door het grote getijprisma en stromingen in het zeegat.

De voortdurende significante sedimentimport naar de Waddenzee laat zien dat de effecten van de afsluiting van de Zuiderzee nog verre van uitgewerkt zijn. Het zal waarschijnlijk nog vele decaden duren voordat een nieuw evenwicht wordt bereikt.

Contents

Chapter 1
INTRODUCTION

Approximately one third of the Netherlands is located below sea-level. A major part of the first line of defence against flooding by the sea is formed by the beaches and dunes of the Holland coast, protecting the densely populated and economically important provinces of North-Holland and South-Holland. Good coastal management and maintenance of these beaches and dunes is therefore of prime importance to ensure safety of the hinterland. This maintenance requires large efforts. With the present rate of relative sea-level rise roughly 6 million m^3/year of sand nourishments are needed to maintain the upper shoreface between -6 m and +3 m N.A.P. (the *Basis KustLijn*), and an additional 6 million m^3/year if the deeper coastal zone up to the 20 m depth contour is included (Mulder, 2000). With a greater than expected relative sea-level rise these numbers could increase drastically. Largest sand losses are observed along the coast adjacent to Texel inlet; since 1991 over 25 million m^3 of sand has been nourished. These large losses are plausibly related to the sand demand of the Wadden Sea, and Texel inlet being the first and largest of the Wadden Sea inlets is believed to form a crucial link in the sediment exchange between the Holland coast and the Wadden Sea (Stive and Eysink, 1989; Louters and Gerritsen, 1994; Mulder, 2000).

The processes controlling the sediment exchange between the Texel tidal inlet and the adjacent North-Holland and Texel coasts are insufficiently understood, despite the importance of the inlet in the Dutch coastal sand balance,. The research reported in this thesis aims to acquire more understanding of the dynamics of Texel Inlet, the sediment exchange between ebb-tidal delta and basin, and the interaction with the adjacent coastlines. The core of this thesis consists of six Chapters that treat different aspects of both the short- and long-term evolution of Texel Inlet, and the underlying processes and mechanisms. Combined, these Chapters describe Texel Inlet over a wide range of temporal and spatial scales, ranging from long-term descriptions of historic inlet evolution, 1550 A.D. to present, to detailed analyses of hydrodynamics and morphodynamics on the process scale. Although, the focus is on Texel Inlet, where possible, findings are generalized to contribute to the understanding of generic tidal inlet dynamics.

1.1 Tidal Inlets

1.1.1 General overview

Systems of barrier islands and tidal inlets are found along a major part of the world's coastlines (Glaeser, 1978). Often, the barrier islands are used for recreation and residential development, while the sheltered back-barrier basins form breeding grounds for numerous marine species and birds. The presence of harbours, shipping lanes and recreational activities makes the inlets and basins economically valuable. From a morphodynamic viewpoint inlet systems and the associated tidal deltas are important due to the capacity to store or release large quantities of sand.

Basics

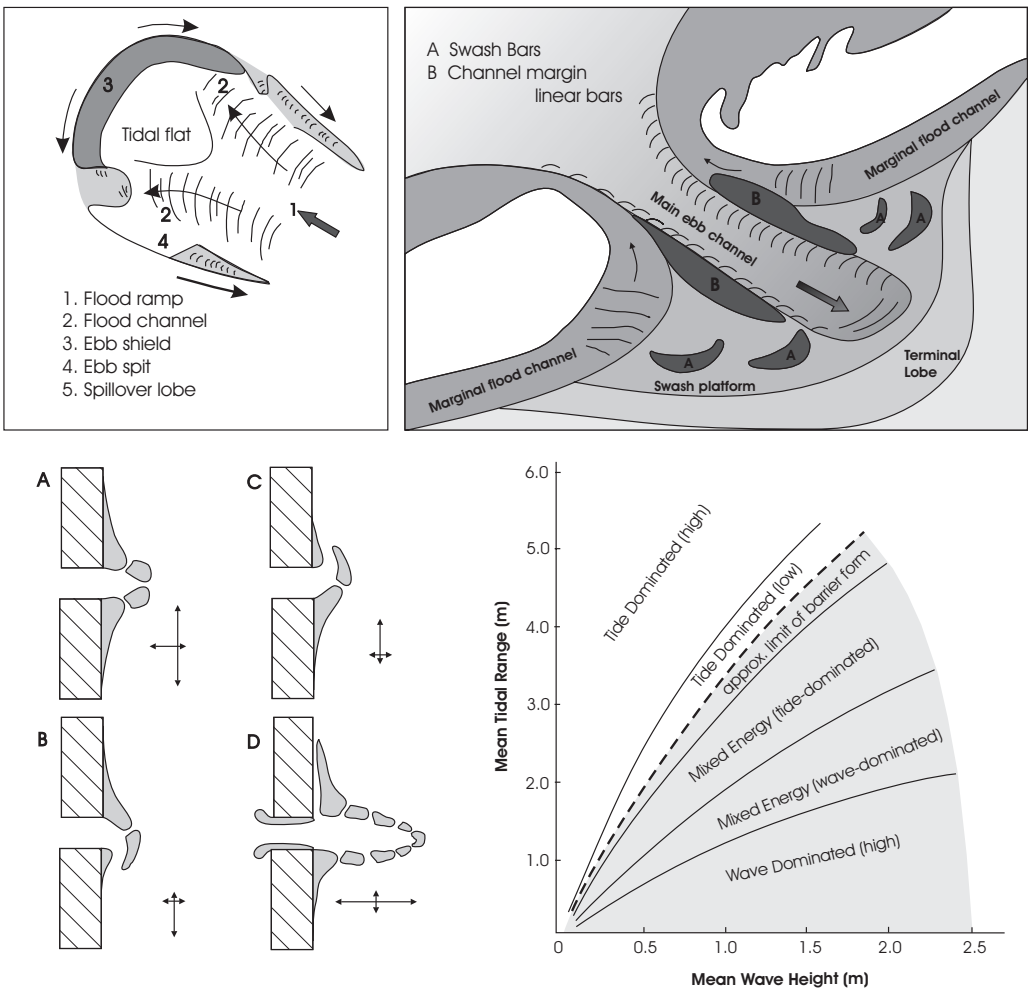

Figure 1-1 top: Hayes inlet model for basin (left) and ebb-tidal delta (right). Bottom left, classification of ebb-tidal delta morphology after Oertel (1975); vectors represent relative forces of cross-shore and longshore currents; A is wave-dominated and D is tide-dominated. Bottom right, relationship between tidal range, wave height and coastal morphology after Davis and Hayes (1984), modified from (Hayes, 1975, 1979).

Principally, a tidal inlet is an interruption of the shoreline through which water (and sediments, nutrients, etc.) is exchanged between the open sea and the back-barrier basin. A dynamically stable inlet channel is maintained by tidal currents (Escoffier, 1940). Sediments eroded from the inlet, and supplied by littoral drift, accumulate in tidal deltas at the seaward and at the landward side (the ebb-tidal and flood-tidal delta respectively) where flow segregates and velocities diminish beyond the sediment transport threshold after passing through the narrow inlet throat (see Fig. 1-1 top panels).

One of the key elements for analyzing inlet evolution and behaviour is the dynamic coupling between ebb-tidal delta, inlet gorge and back-barrier basin, that tends to remain in (dynamic) equilibrium to the large-scale hydraulic forcing, individually as well as collectively (see e.g. Dean, 1988; Oost and de Boer, 1994; Stive *et al.*, 1998; Stive and Wang, 2003). In principle, the geometry of the back-barrier basin, in combination with tidal range, determines the tidal prism (the total volume of water that passes through the inlet per tidal cycle) which in turn determines the size of the inlet (O'Brien, 1931, 1969) and the volume of the ebb-tidal delta (Walton and Adams, 1976).

The geometry of the inlet gorge and the deltas is shown to reflect the ratio of wave versus tidal energy (e.g. Hayes, 1975; Oertel, 1975; Hayes, 1979; Davis and Hayes, 1984). Wave energy tends to move sediment shoreward, therefore wave-dominated ebb-tidal deltas are pushed close to the inlet throat (Fig. 1-1 bottom left, A), while tide-dominated ebb-tidal deltas extend offshore (Fig. 1-1 bottom left, D). Hayes (1975; 1979) was among the first to classify inlet systems on the basis of the ratio of wave versus tidal energy. Additionally, Davis and Hayes (1984) showed that tidal prism is more important than tidal range, large tidal prisms can explain large well-developed ebb-tidal deltas (no direct relation between tidal range and tidal prism was observed). Figure 1-1 (bottom right) shows the Davis and Hayes classification.

FitzGerald (1996) suggests that wave and tidal processes are useful to describe the gross characteristics of inlet systems, but there are many other external controls. These controls include sediment supply, basin geometry, sedimentation history of the back-barrier, regional stratigraphy and occurrence of bedrock, river discharge, and sea level changes. With all these different forcing conditions a wide diversity in inlet morphologies exists.

Ebb-tidal delta

The ebb-tidal delta, sand accumulation seaward of the inlet throat, is formed primary by sediment supplied by the ebb-tidal currents and reworked by wave action and tidal currents. The volume of sand confined in the ebb-tidal delta relates to the tidal prism (Walton and Adams, 1976),

$$V_O = cP^{1.23} \tag{1.1}$$

wherein V_O is the ebb-delta sand volume (m^3), c an empirical constant and P the tidal prism magnitude (m^3).

Studies of mixed-energy tidal inlets have shown that there are common characteristics in the ebb and flood tidal deltas. In this thesis we use the terminology as proposed in the standard inlet model of Hayes (1975); see Figure 1-1 upper panels. The main elements include:

- A main ebb channel dominated by the ebb-tidal currents.
- A terminal lobe located at the distal end of the main ebb channel where the ebb velocities diminishes below the threshold velocity of motion and sediment settles.
- Swash platforms; broad shallow sand platforms located on both sides of the main ebb channel defining the general extend of the ebb delta.
- Channel margin linear bars; levee-like bars flanking the ebb channel and build by the interaction of the ebb-tidal currents and waves
- Swash bars; isolated bars that form and migrate onshore over the swash platform due to wave breaking generated currents and transports.
- Marginal flood channels; channels dominated by the flood tidal currents that may occur between the channel margin linear bars and the updrift and downdrift coasts.

The occurrence of ebb- and flood-dominated tidal channels is of prime importance to the morphology of the ebb tidal delta. Postma (1967) explains their formation as maximum ebb does not occur at midtide but often late in the ebb phase, near low water. Therefore ebb flow is concentrated in the main ebb channel and due to the large velocities and erosive potential this is the largest channel on the ebb-tidal delta. At low water, as the tide turns strong currents are still flowing seaward, out of the main ebb channel, and as the water level rises, the flood currents seek the path of least resistance along the margins of the ebb-tidal delta. Zimmerman (1981) relates the existence of separate ebb and flood channels to the generation of tidal residual (headland) eddies due to interaction between the sloping shoreface and the tidal inlet currents. The main ebb channel may have a preferential updrift or downdrift orientation related to the phase difference between the open-sea (shore-parallel) tidal currents and the inlet currents; the ebb channel orientation follows the steepest gradient in water level (Van Veen, 1936, p. 133; Sha, 1989b,c).

Inlet throat and basin

The ebb-tidal delta and adjacent barriers shelter the inlet throat and flood-tidal delta from open-sea wave penetration. The inlet throat is the narrowest and deepest part of the inlet channel and exhibits the maximum hydraulic radius, while the minimal channel cross-sectional area produces maximum current velocities and greatest potential sediment transport. The correlation between tidal prism and inlet cross-sectional area was first recognized a century ago by LeConte (1905) and later modified by O'Brien (1931; 1969). Their regression relation has the form;

$$A_c = cP^n \tag{1.2}$$

wherein A_c is the cross-sectional area of the inlet (m^2), P (spring) tidal prism (m^3), c and n are empirical coefficients. This relation assumes that adjustments to the inlet cross-

sectional area are a response to the balance in bed shear stress in the inlet and changes in the magnitudes of littoral drift (Oertel, 1988). Hence, an increase in tidal prism enlarges the inlet velocities resulting in enlargement (erosion) of the cross-sectional area, whereas a tidal prism decrease reduces the inlet velocities and cross-sectional area. Eysink (1990) illustrated the approximate empirical validity of this relation for the Dutch Wadden Sea; values of $n = 1$ and $c = 7.0\text{x}10^{-5}$ m^{-1} were suggested if P represents the mean tidal prism. Eysink also showed that the flood basin volume below Mean Sea Level (MSL) is proportional to $P^{1.5}$. Among others, Gerritsen (1990) derived a similar empirical relation between tidal prism and cross-sectional area of the individual basin channels:

$$A_c = 7.16 \times 10^{-5} P + 135 \tag{1.3}$$

where A_c is the cross-sectional channel area (m^2) and P is the tidal prism (m^3/s) in the channel.

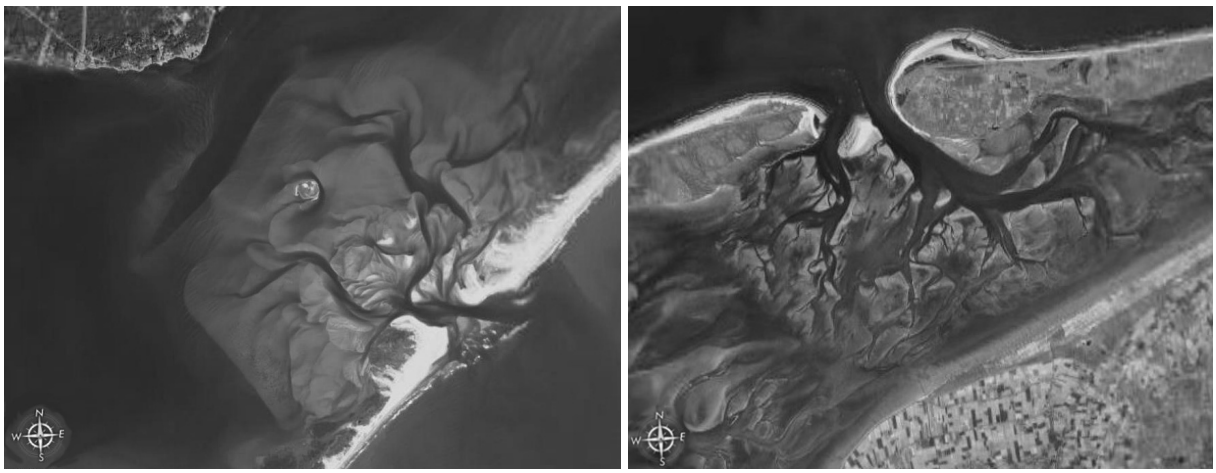

Figure 1-2: (left) underdeveloped flood-tidal delta at Negro Creek Bay inlet (Outer banks at America's east coast), and (right) the fully developed flood-delta of Ameland inlet in the Dutch Wadden Sea.

Following the model of Hayes (1975) the typical elements of the flood-tidal delta include (see Fig. 1-1 top and Fig. 1-2 left):

- Flood ramps; seaward dipping sand surface dominated by flood tidal currents. Sediment movement occurs in the form of sand waves that migrate up the ramp.
- Flood channels; channels dominated by the flood velocities.
- The ebb shield; the high landward margin of the tidal delta.
- Ebb spits; spits formed by ebb currents.
- Spillover lobes, barlike features formed by ebb-tidal current flow over low areas of the ebb shield.

In the Wadden Sea basin such flood tidal deltas are not distinctively observed (Fig. 1-2 right panel and 1-4). The basins all display a well-developed, equilibrium flood-tidal

delta due to the combination of moderate sea-level rise and availability of sediment from the adjacent barrier coasts (Stive and Wang, 2003; Van Goor *et al.*, 2003). The basin bathymetry is characterized by a fractal pattern of channels, separated by shoals and salt marshes, with depths generally decreasing towards the coast (Cleveringa and Oost, 1999).

1.1.2 The Wadden Sea and Texel Inlet

Geological evolution

On the geological time-scale, the Wadden Sea is a young landscape that was formed under the influence of the rise in sea level since the last glacial period (Zagwijn, 1986; Beets and Van der Spek, 2000). Despite the increase in water levels and recent constraining effects of human interventions the characteristic features of the Wadden Sea, the barrier islands, separated by inlets and connecting basins have remained intact (although the size increased due to westward expansion).

In the early Holocene the Wadden Sea, as we know it, was not yet formed. Sea level was still many meters below the present level, but rose rapidly due to melting of ice caps and glaciers and thermal expansion of the seawater resulting from increasing temperatures since the last glacial period. Subsidence of the land surface added to this and the resulting relative sea-level rise is estimated at a rate of about 1.0 m/century. Around 8000 B.P. the North Sea obtained its present configuration. The continuing rise in sea level caused a gradual expansion of the North Sea, and inundation of old river valleys and topographical lows formed during the Weichsel ice age created tidal basins and lagoons. The central and eastern parts of the present Wadden Sea were formed during this interval.

Around 6.500 BP the western part of the Netherlands was transformed into an open coast with lagoons and tidal flats, while the eastern part of the Wadden Sea consisted of several estuaries (Vlie, Borne, and Eems), see Fig. 1-3. The western part of the Wadden Sea was still dry land, due to the presence of glacial tills, a stiff and erosion-resistant deposit from the Saalian, the penultimate ice age (Ter Wee, 1962) which formed the core of a Pleistocene high. Texel's Hooge Berg and the island of Wieringen are till deposits that are still clearly discernable in the present-day landscape. Detailed information on the Holocene-Pleistocene interface at Texel Inlet is presented in Sha (1989d).

Around 5000 BP, the tidal basins had expanded and dominated much of the coastline. The central part of the Holland coastline had shifted landward considerably (east of the coastline position of today). The decreasing rate of sea-level rise (to a rate of 0.3-0.4 m/century) and the availability of vast amounts of sediment (e.g. supplied by rivers and the erosion of capes and former coastal deposits) resulted in decreasing shoreline transgression rates. The tidal basins along the Holland coast filled in with sediments, and the tidal inlets closed. Hence, a closed barrier coastline protecting an extensive peat area had formed in the western part of the Netherlands around 3800 BP (Fig. 1-3). Later on, around 1200 BP, erosion of the peat in the southwest resulted in the formation of the

'Delta' estuaries. The Wadden Sea expanded to the west and south and got its maximum extends. Inland, a large fresh-water lake (Lake Flevo later named Zuider Sea) had formed.

In the Middle Ages, the Wadden Sea was an extensive area of tidal inlets and intertidal flats (Fig. 1-3, 1250 A.D.). During this period Vlie inlet was the only connection to Lake Flevo. Texel Inlet is believed to have evolved from a small local drainage channel that connected to the inland Zuiderzee around the 12th century A.D. after a series of severe storm events (Schoorl, 1973; Hallewas, 1984 [see overview in Oost *et al.*, 2004, p. VII-6]). Up to the Middle Ages the development of the Wadden Sea was relatively undisturbed, but human action such as dike construction, land reclamation, peat excavation, damming of channels and tidal basins (closure of Lauwerszee and Zuiderzee), construction of groins, breakwaters and seawalls (such as Helderse and Pettemer Zeewering) have increasingly influenced the developments ever since (Elias and Van der Spek, 2006, [Chapter 2 of this Thesis]). Detailed descriptions of the palaeographical evolution of the Dutch coastline are presented by Zagwijn (1986), Beets and Van der Spek (2000) and De Mulder *et al.* (2003).

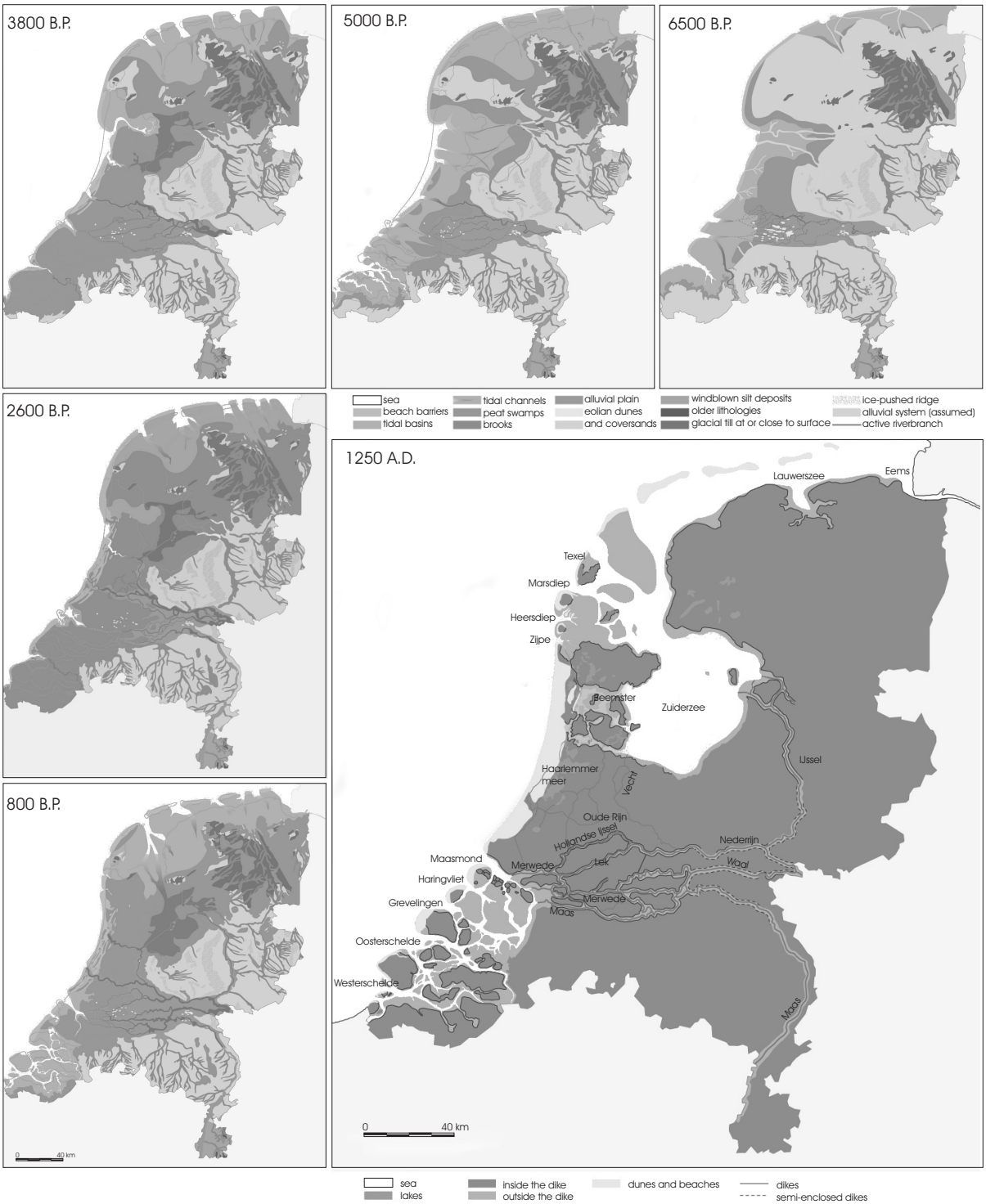

Figure 1-3: Geological evolution of the Netherlands 6500 Before Present (B.P) - 1250 A.D. after De Mulder *et al.* (2003).

Some characteristics of today's Wadden Sea

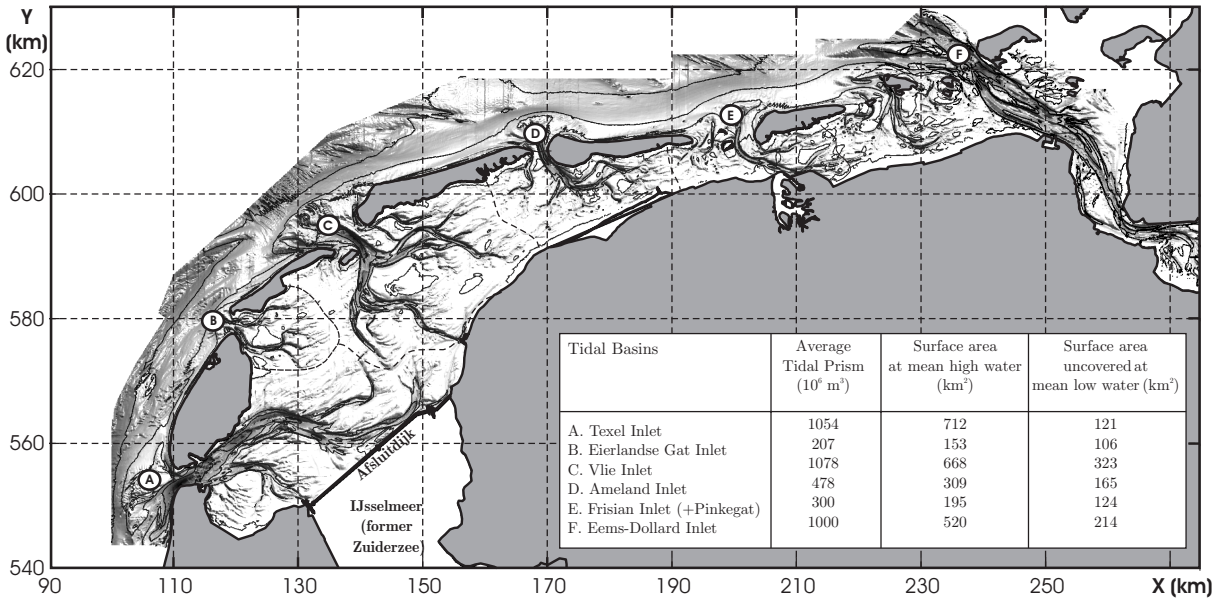

Tidal Basins	Average Tidal Prism (10^6 m^3)	Surface area at mean high water (km^2)	Surface area uncovered at mean low water (km^2)
A. Texel Inlet	1054	712	121
B. Eierlandse Gat Inlet	207	153	106
C. Vlie Inlet	1078	668	323
D. Ameland Inlet	478	309	165
E. Frisian Inlet (+Pinkegat)	300	195	124
F. Eems-Dollard Inlet	1000	520	214

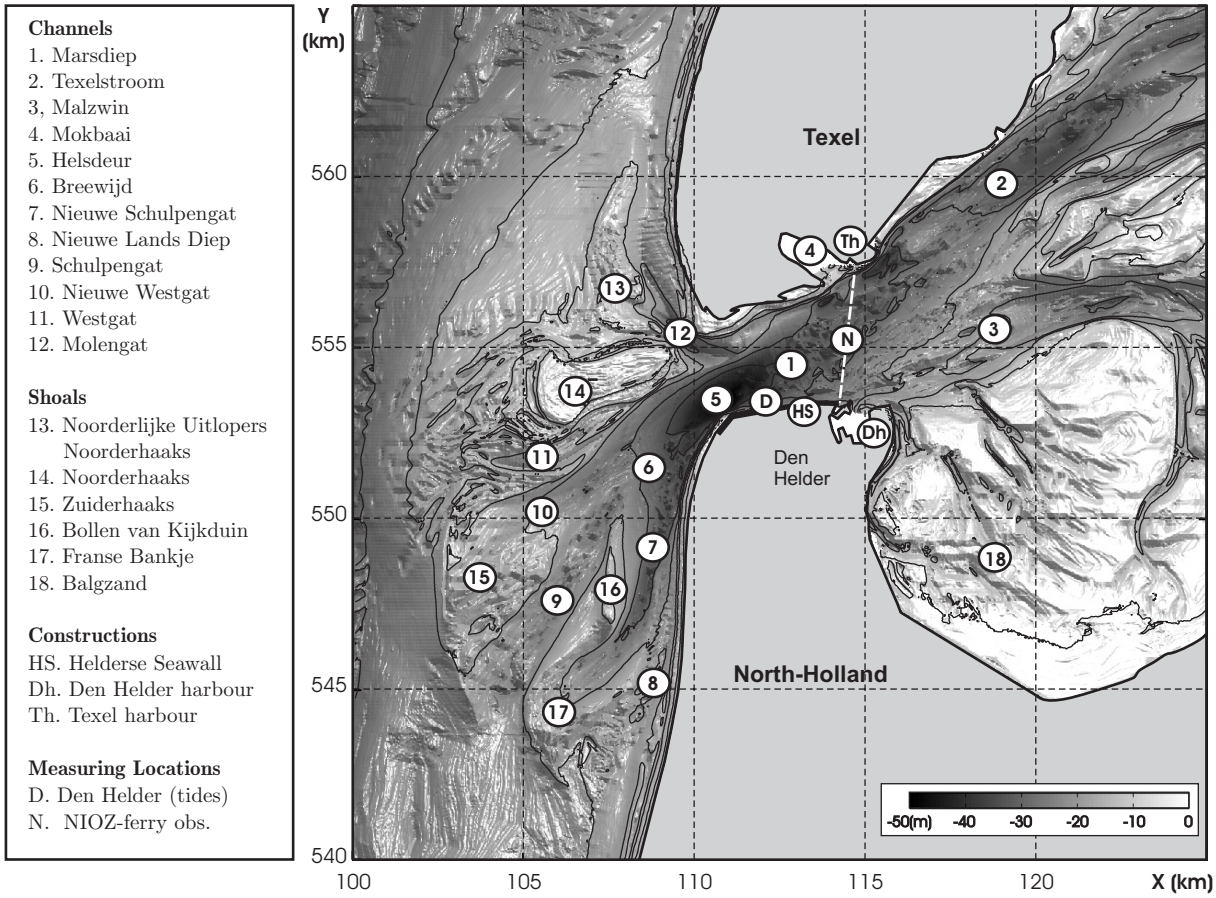

Figure 1-4 top: The barrier island coast of the Wadden Sea and main characteristics of the individual inlet systems based on Louters and Gerritsen (1994). Bottom: present-day configuration of main channels and shoals in Texel tidal inlet (1997 '*Vaklodingen*' depth measurements).

Today, the Wadden Sea system consists of a series of 33 tidal inlet systems extending over a distance of nearly 500 km along the northern part of the Netherlands, the German and Danish coasts. The associated barrier islands separate Europe's largest tidal flat area (~10.000 km^2) from the North Sea. Figure 1-4 (top panel) shows the main tidal inlets for the Dutch part of the Wadden Sea. The Dutch inlets consist of relative large ebb-tidal delta shoals, narrow and deep inlet channels, and extensive systems of branching channels, tidal flats and salt marshes in the back-barrier basins. The change in coastline orientation from South-North to West-East along the Wadden Sea islands relates to the underlying Pleistocene morphology.

A distinct difference is observed between the inlets in western and eastern part of the Dutch Wadden Sea. The back-barrier area of the eastern part (Ameland and Frisian inlet) is relatively shallow, being dominated by large flat areas and small channels; the ratio of intertidal area versus total surface area varies between 0.6 and 0.8 (Oost, 1995, page 50). At Texel and Vlie inlet this value is 0.3 and 0.4 respectively. These latter low values are plausibly related to the construction of the Afsluitdijk separating the shallow Zuiderzee that contained a large portion of tidal flats from the active basin (see Elias *et al.*, 2003b; Elias and Van der Spek, 2006, [Chapter 2 and 3 of this thesis]). Although the channel/shoal ratio suggests that the present western part of the Wadden Sea is still far from an equilibrium state and needs a vast amount of sediment to reach equilibrium, the conclusions about sediment import (or export) and governing processes in Marsdiep are more ambiguous; Sha (1989a), Steijn (1997), Louters and Gerritsen (1994) and Ligtenberg (1998) point to a net import of sediment in the order of 1 to 3 Mm^3/year. Steijn en Jeuken (2000) estimate the transports being 0 Mm^3/year, while Bonekamp *et al.* (2002) conclude to sediment export due to main tidal asymmetries.

Tides and (wind-generated) waves are the dominant processes in the formation, maintenance and evolution of the various morphological elements. Waves are most important on the ebb-tidal deltas. The gross ebb-delta volume might be related to tides or tidal prism (Hayes, 1975; Oertel, 1975; Davis and Hayes, 1984), but waves redistribute the sediments and contribute to the sediment bypassing mechanism (FitzGerald, 1988). Waves drive sediment transports directly via currents due to radiation stress gradients generated by wave breaking of obliquely incident waves, and due to wave asymmetry. Indirectly waves enhance bed-shear stresses and stir-up sediment, allowing more sediment into suspension to be transported by the tidal and wind-driven flow. Wave breaking and refraction on the ebb-delta shoals reduces the amount of wave energy that penetrates the basin from the North Sea. Nevertheless, locally generated waves can play an important role in the tidal flat development; De Vriend *et al.* (1989) indicate that a dynamic equilibrium seems to exist between sediment accumulation on tidal flats by the tidal flood currents and erosion related to locally generated waves.

Tides are the main driving force for the fractal channel patterns in the basin (Cleveringa and Oost, 1999). The tidal movement is generated mainly by the tidal wave from the southern part of the North Sea that enters the Wadden Sea through the inlets. Tides in the North Sea originate from the tidal wave entering from the Atlantic Ocean between Scotland and Norway in the north, and through the Calais Straight in the south. Interference of these two waves, distortion due to Coriolis effects and bottom friction generates a complicated tidal flow pattern in the southern part of the North Sea with anti-

clockwise rotation and propagation around amphidromic points. Along the Dutch coast the result is a combination of a standing and progressive tidal wave propagating from south to north thereby generating maximum tidal velocities in the range of 0.5 to 1.0 m/s. Near Texel inlet this tidal wave meets a second tidal wave that propagates from west to east along the Wadden Sea Islands. Along the Frisian inlets the tidal range increases from 1.4 m at Den Helder towards 2.5 m in the Ems estuary. In the Wadden Sea the tide is distorted due to e.g. bottom friction, topography and geometry.

Tidal divides more or less separate the main inlet systems of the Dutch Wadden Sea (see Figure 1-4 top locations of the tidal divides based on Louters and Gerritsen, 1994). The divides are formed where the tidal waves travelling through two adjacent inlets meet and sedimentation due to near-zero velocities results in tidal flat formation. As the west-east tidal wave propagation is faster in the North Sea, than through the shallow Wadden Sea, the tidal divides are located somewhat eastward of the centre of the barrier islands. The prevailing eastward wind direction contributes to this asymmetry (FitzGerald, 1996). Between Texel and Vlie inlet a tidal divide cannot be distinctively observed. Moreover, studies by Ridderinkhof (1988; 2002) indicate that a throughflow from the Vlie to Texel Inlet exists due to the higher amplitude of the vertical tide in the Vlie basin.

For more detailed overviews of the sedimentology and development of the Dutch Wadden Sea reference is made to e.g. Ehlers (1988), Sha (1990), Eysink (1993) and Oost and De Boer (1994).

Some characteristics of Texel Inlet

This thesis focuses on Texel inlet, the largest and most westerly located inlet of the Dutch part of the Wadden Sea system (see Fig. 1-4, bottom panel). With a mean tidal range of 1.38 m (low mesotidal) and a mean significant wave height of 1.3 m, following the classification of Davis and Hayes (1984), the inlet qualifies as mixed-energy wave-dominated, even under spring tide conditions (~2 m tidal range). However, the morphology of the inlet shows tide-dominated characteristics such as a large ebb-tidal delta resulting from the large tidal prism and the relatively low wave energy.

Texel basin shows a complex pattern of channels and shoals. The main channels being Texelstroom and Doove Balg, extending eastward along the Texel coastline and Afsluitdijk respectively, and the channel Malzwin directed southward towards Balgzand (see Fig. 1-4 bottom). Since its recorded history Texelstroom has remained relative stable in position being located along the south-eastern shore of Texel. Although only limited knowledge is present on the deep subsurface layers, analysis of literature and recent core data (van der Spek, unpublished Personal Communication) renders it likely that the seaward part of Texelstroom channel is bounded by or incised in glacial till and that its stability in dimension and position is governed by this deposit. To the north and to the west, the channel is bounded by the intertidal area Waarden en the island of Texel, respectively. The south-eastern side of Texel, which bounds Texelstroom, has a core of ice-pushed tills, a very stiff and erosion-resistant deposit from the Saalian. Core data from the channel floor along the shore of south-eastern Texel (TNO-NITG; unpublished data) show that the till occurs at depths of 33 m below MSL and more, which is over 8m below

the present-day channel floor. The same deposit is found below the Waarden area at a depth of about 10 to 15 m below MSL. Here, the till is only several meters thick. Although the data are sparse and unevenly distributed, it is likely that the occurrence of the till has limited the mobility of the channel. A channel-perpendicular cross-section that was published by Jelgersma (1961) shows that the most landward part of Texelstroom is situated in a wide paleovalley where the till occurs at depths of over 20m below MSL or is absent. Here, the till was possibly eroded by meltwater fed rivers during the Saalian or by marine erosion during the Eemian, the subsequent interglacial (Van Staalduinen, 1977). Marine deposits of Eemian age and periglacial deposits of the Weichselian, the last glacial period, occupy the paleovalley. This part of Texelstroom is incised into the Weichselian sands. In addition, the coastline defences constructed along the south-eastern coast of Texel contribute to the stability of the channel as well.

Most of the bed sediment in the basin consists of fine sand with a median grain size around 200 μm. Grain size diameter decreases towards the mainland (Eysink, 1979). Near the inlet sediment diameters over 450 μm are observed locally, while at the location of the Afsluitdijk, median grain sizes vary around 120 μm. This sorting of sediment with coarse sand near the inlet and finer fractions along the basin boundaries results from settling lag effects of suspended sediment (Postma, 1954; Van Straaten and Kuenen, 1957; Postma, 1961). Of the sediment that settles within the Wadden Sea, some 70 to 80% consists of sand while the remainder is silt and clay (Oost, 1995). In total about 17% of the basin consists of inter-tidal flats.

The ***inlet gorge***, Marsdiep, is located between the port of Den Helder and the island of Texel. On average tidal prisms through the inlet are $1x10^9$ m^3 and maximum ebb and flood tidal velocities are ranging between 1 to 2 m/s. The location of Marsdiep is fixed in position since the construction of the seawall Helderse Zeewering around 1750 A.D. (location see Fig. 1-4 bottom panel) Scouring at the toe of Helderse Zeewering locally increased the channel depths to over 50 m at the location of Helsdeur. Since 1998 the Royal Netherlands Institute of Sea Research (NIOZ) continuously measures the inlet using an Acoustic Doppler Current Profiler (ADCP) attached to the to the hull of the ferry (ms Schulpengat). During daytime this ferry crosses the 4.5 km wide Marsdiep every 30 minutes, and data on e.g. salinity, surface temperature and flow are transmitted to NIOZ. First results of the flow observations are presented by Ridderinkhof *et al.* (2002) and used by Bonekamp *et al.* (2002).

The inlet channel Marsdiep connects to Texelstroom in the basin and the main channels on the ***ebb-tidal delta***: Molengat, Nieuwe Westgat, Schulpengat and Nieuwe Schulpengat. The ebb-delta shoals protrude approximately 10 km seaward and stretch 25 km alongshore, determining the nearfield bathymetry of the adjacent North-Holland coast in the south and the Texel Island coast in the north. The ebb-tidal delta is asymmetrically shaped. The centre is formed by the supra-tidal part of the Noorderhaaks swash-platform, which faces the inlet gorge Marsdiep. North of Noorderhaaks a large sub-tidal spit (Noorderlijke Uitlopers van de Noorderhaaks) extends along the Texel coastline. The Molengat channel separates this spit from the island of Texel. Interaction of Molengat with the Texel coastline is regarded to play an important role in the sand losses of the adjacent beaches (Cleveringa, 2001). On the southern part of the ebb-tidal delta the two main channels, Schulpengat and Nieuwe Schulpengat, separated by the shoal Bollen van

Kijkduin, extend along the North-Holland coastline. Especially, the growth of Nieuwe Schulpengat after closure of the Zuiderzee locally induced severe erosion of the adjacent North-Holland coastline. Nieuwe Schulpengat remained relative stable in position since 1990, but the large channel velocities still induce major sand losses of the nearby beaches (Elias and Cleveringa, 2003). In front of Nieuwe Schulpengat, Franse Bankje formed as part of the channel's ebb-shield, while the more seaward positioned Zuiderhaaks forms the ebb-shield of the channels Schulpengat and Nieuwe Westgat.

The basic channel configuration on the ebb-tidal delta remained stable over the last decades. The varying bed composition, presence of erosion resistant layers and coastal defence works must have played a role in this stable state. Sha (1990) illustrates the grain size variation the seabed sediment over the ebb-tidal delta. Largest grain diameters are observed in the inlet channel and proximal ebb-delta channels. In Marsdiep and Breewijd, locally, grain diameters exceed 450 μm. In Schulpengat and Nieuwe Schulpengat grain diameters vary between 250 and 350 μm. Generally, in seaward direction the grain size decreases towards values between 150 and 200 μm on the shoals (Sha, 1990). In Nieuwe Schulpengat the alongshore and cross-shore variability in Pleistocene clay/silt and peat content of the bed layers plausibly contributes to the varying alongshore and temporal migration rates of the channel (Van der Spek and Van Heteren, 2004).

In addition to erosion resistant layers the mobility of the North-Holland coastline is restricted due to the presence of groins since the early 20th century. Groins decrease the longshore drift along the coastline; Van Rijn (1995) estimates the blocking effect of groin fields to be in the order of 50%. Most important coastal defence structures in the inlet gorge are the Helderse Zeewering and Den Helder harbour that stabilize the southern embankment (and therefore the position) of Marsdiep. The interaction of tidal flow and Helderse Zeewering has shown to play an important part in the historical inlet evolution (Elias and Van der Spek, 2006, [Chapter 2 of this thesis]).

1.2 Texel Inlet and the Dutch coastal system

1.2.1 The Dutch Coast

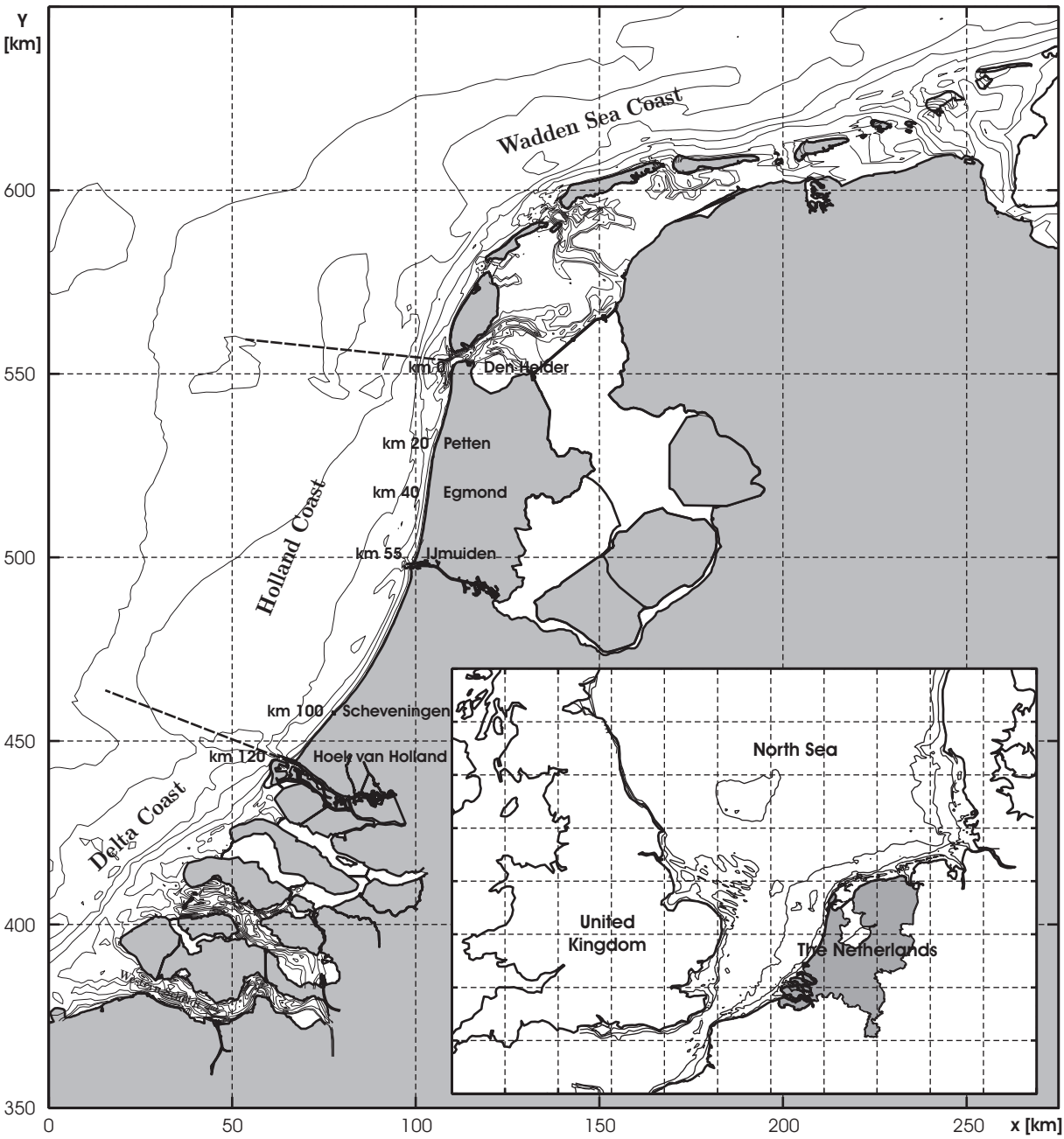

Figure 1-5: Location map of the Dutch coastline and division in three morphologically varying areas; the Delta Coast, the Holland Coast and the Wadden Sea Coast.

The Dutch coastline consists of three areas with distinct morphologic features (Fig. 1-5). The closed Holland coast forms the central part, extending over a length of nearly 120 km. This continued coastline of beaches and dunes is slightly curved with a main orientation of NNE to SSW. In the south the over 4 km long breakwaters near Hoek van Hol-

land and the continuously dredged entrance channel to Rotterdam harbour limit the sand bypassing from the estuary-dominated Delta coast, forming an almost closed boundary (Van Rijn, 1995). The Delta coast consists of a series of islands separated by estuaries. With the exception of the Western Scheldt closed or semi-closed barriers dammed these estuaries during the last decades. In the north, Texel Inlet forms the transition from the Holland coast to the barrier islands of the Wadden Sea.

Table 1-1: Overview most important engineering works along the Holland coast (based on Van Rijn, 1995; Wijnberg, 1995)

	Location	***Period***	***Spatial scale***
Seawalls:			
Helderse Seawall	km 0 - km 1.1	1721	tip of North Holland
		1956	extension
Hondsbossche and	km 20 - km 26	1500/1872/1954	6 km alongshore
Pettemer Seawall		1969	
Scheveningen	km 102	1896 - 1909	140 m alongshore, total length 2.5 km
Groins			
	km 0.4 - km 31	1838 - 1935	
	km 98 - km 118	1776 - 1930	
Harbour Moles			
Ijmuiden	km 55/56	1865 -1879	length 1.5 km
		1962 - 1967	length 2.3 (N) - 2.8 km (S)
Scheveningen	km 102	1900 -1908	0.25 km
		1968 - 1970	0.65 km (N)- 0.5 km (S)
Hoek van Holland	km 118	1864 - 1874	1.8 km
		1968 - 1972	4.2 km
Discharge Sluice			
Katwijk	km 86	1807	
		1984	increased capacity

During the last centuries the natural behaviour of the Holland coast was increasingly distorted by the construction of coastal defence structures such as groins (Hoek van Holland - Scheveningen, Petten - Den Helder), seawalls (Petten, Scheveningen, Den Helder) and harbour breakwaters (Hoek van Holland, Scheveningen and IJmuiden) see Table 1-1. Presently, the behaviour of the Holland coast is best described as naturally undisturbed (no inlets) but largely influenced by man-made structures (Wijnberg, 2002). Since 1990 the coastline is maintained primarily by beach, foreshore and dune nourishments, which requires large efforts. Up to 2000 over 30 million (M) m^3 of sand had been nourished along the Holland coast; in total over 100 Mm^3 along the entire coast (Roelse, 2002). Detailed descriptions of the Holland coast, its development, behaviour and governing processes, can be found in Hoozemans and van Vessem (1990), Van Rijn (1995) and Wijnberg (1995).

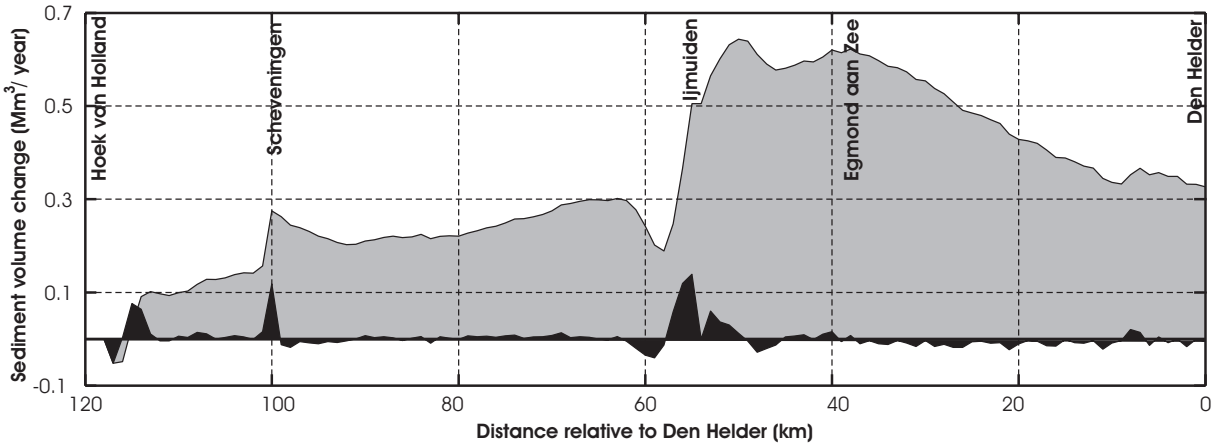

Figure 1-6: Sand volume change of the nearshore (JARKUS zone) over the period 1963 - 1986 in Mm^3/year (black). Gray represent the cumulative contributions. Based on data presented by De Ruig (1989).

To successfully maintain the Dutch coast it was long recognized that monitoring is of the utmost importance. Already in 1850 annual measurements of the mean low waterline, the mean high waterline and the dune-foot position started, and since 1964 yearly cross-shore profiles are surveyed and stored digitally in the JARKUS data-base (Wijnberg, 1995). Analysis of this data using coastline positions and sediment-budget studies (see summary and analysis in Van Rijn, 1995) showed a shoreline progradation at a rate of 0.15 - 0.45 m/yr along the major part of the Holland coast (Fig. 1-6, South of Egmond km 40 - 102). In the North, the stretch of coastline between Den Helder and Egmond (km 0-40) is structurally retreating, at a rate of about 1.5 m/year, even though groins protect this area since 1840. Locally, distortions in the coastline position occur as adaptation to human interventions (e.g. near the harbour moles of IJmuiden and Hoek van Holland, and the sea-wall near Petten). Although more recent studies are available, the nearshore sand-volume changes shown in Figure 1-6, based on De Ruig (1989) provide a clear illustration of the coastal development. Especially the above-average coastline retreat between Egmond and Den Helder is noticeably visible in the decreasing cumulative transport rates. This retreat was first related by Stive and Eysink (1989) to the sediment demand of the Wadden Sea.

Processes along the Dutch coast were intensively studied in the nineties during the Kustgenese studies (Stive *et al.*, 1990; Van Rijn, 1995, 1997). These studies showed that sediment transports along the Holland coast are current-related, when mean currents due to e.g. tides, wind and density differences displace (suspended) sediments, or wave-related, due to e.g. undertow and stokes drift, wave-asymmetry in near-bed orbital velocities or wave-breaking generated long-shore currents. In the middle and lower shoreface area (8 - 20 m waterdepth) transports are dominated by tides and wind, while in the shallower water (dunefoot to 8 m waterdepth) wave-dominated longshore and cross-shore transports prevail. In deep water (-20m) the net landward transport is estimated to range between 5 - 10 m^3/m per year (which equals 3-4 Mm^3/year for the entire coast). The aeolian loss of sediment to the dunes was estimated in the order of 1 Mm^3/year. The net longshore transport ranges between 300.000 and 600.000 m^3/year.

1.2.2 Inlet - Coast interaction

One of the characteristic features of the Wadden Sea is its continuous sedimentation in the tidal basins in order to keep pace with the increase in accommodation due to the relative sea level rise (Louters and Gerritsen, 1994). The sediment demand of the Wadden Sea is fed by sediment supply from the barrier coastlines, ebb-tidal deltas and the adjacent North-Holland coastline. Stive and Eysink (1989) were among the first to note the sand demand of the Wadden Sea basin as a main factor in structural large sand losses from the North-Holland coast. In the previous section we briefly discussed the sand-sharing principle. A tidal inlet consists of three main morphologic elements (basin, inlet and ebb-delta) that are coupled and strive to gain or maintain in (dynamic) equilibrium individually and collectively to the forcing conditions. Changes in the forcing conditions due to e.g. human intervention or natural causes will lead to morphological changes in the elements. First, sediment is redistributed within the elements and sand is exchanged between the elements, but for larger scale permanent distortions a sediment exchange (import or export) with the adjacent coastal sections may take place (Oost, 1995, p. 60; Kragtwijk *et al.*, 2004). In case of sea-level rise, under the assumption that the tidal basin is in dynamic morphological equilibrium and capable of following the rising water levels, Stive and Wang (2003) derived an estimate of the importance of the morphological response of inlets in the coastal sediment budget expressing the shoreline regression via the equation,

$$c_{pr} = \frac{\partial \zeta}{\partial t}\frac{L_p}{H_p} + \frac{\partial \zeta}{\partial t}\frac{A_b}{H_p L_{ac}} \tag{1.4}$$

where, c_{pr} is the rate of profile recession, $\partial\zeta / \partial t$ is the rate of sea-level rise, L_p is the active cross-shore profile length, H_p is the depth of the active cross-shore profile, A_b is the tidal basin area, and L_{ac} is the length of the impacted adjacent coast. In this formulation the first term on the right-hand side expresses the Bruun effect (Bruun, 1962) and the second term expresses the basin effect. The basin effect exceeds the Bruun effect for

$$A_b > L_p L_{ac} \tag{1.5}$$

For typical values of L_p and L_{ac} of 1 km and 10 km respectively, the basin effect exceeds the Bruun effect for basins larger than $O(10\text{km}^2)$. Based on this relation we can expect Texel Inlet with a basin area of approximately 700 km^2 to have significant influence on the long-term sediment budget of the adjacent Holland coast. Based on the gradient in longshore sediment transport, Stive and Eysink (1989) estimated that the effect of sediment import into the Wadden Sea reaches at least as far as Egmond aan Zee, which is 35 km to the south of Texel Inlet (Fig. 1-5 and 1-6). The long-lasting sediment import related to sea-level rise is an important aspect for the long-term sediment budget of the Dutch coastal system (Louters and Gerritsen, 1994; Mulder, 2000).

One of the main aspects making tidal inlet dynamics particularly complex to understand is the wide variety of spatial and temporal scales involved. The inlet system as a whole (*mega-scale*), the morphological elements (*macro-scale*), and the various morphologic features comprising the elements (*meso-scale*) respond differently, spatially and temporally,

to changes in forcing (see De Vriend, 1991 for the scale classification principle). Even if the system and the macro-inlet elements are in a (quasi-)equilibrium state still large fluctuations can occur within the elements. A typical example of such a *meso-scale* phenomenon is sediment bypassing on the ebb-tidal delta in the form of migrating bars (e.g. Bruun and Gerritsen, 1959; FitzGerald, 1988). Tidal inlets disrupt the alongshore continuity of the littoral drift, therefore sediments can be trapped temporarily on the ebb-tidal delta, before being released to the downdrift coastline. The movement of sand from the updrift to the downdrift side of tidal inlets is described as sediment bypassing. Depending on the stage of bypassing we can observe periods (years) of erosion, when the ebb delta is accumulating sand the downdrift shore erodes to make up the sand supply deficit, and deposition due to the merging of bars with adjacent shorelines. Such channel-shoal movements can lead to spatial relocation of the complete inlet system, see e.g. Sha (1989b) and Elias and van der Spek (2006, [Chapter 2 of this thesis]) for Texel inlet and Israel and Dunsbergen (1999) for Ameland inlet, causing large erosion (problems) if channels migrate towards the adjacent coasts, or sedimentation problems if the navigability of channels is hampered.

The channel-shoal movements can result from the systems inherent behaviour, due to local interaction between flow and inlet bathymetry, but can also be imposed due to external forcing such as human intervention. A clear example is the development of the channels Nieuwe Schulpengat and Molengat along the North-Holland and Texel coastlines locally inducing severe erosion. The relocation of these channels is related to the effects of closure of the Zuiderzee (1925-1932 A.D.); see Chapter 3 of this thesis (Elias *et al.*, 2003b). The *meso-scale* analysis of the inherent behaviour on spatial scales of (several) kilometres and time-spans of years to decades has not received much attention (NWO-ALW, 1999; Cleveringa, 2002). Nowadays, morphological models have reached a point where we can begin to analyse these developments in depth (Ribberink and De Vriend, 1995; De Vriend and Ribberink, 1996).

1.3 Research Method and Objectives

1.3.1 Method

Inlet dynamics have long been studied by coastal engineers and geologists due to the dynamic participation in the coastal tract (Cowell *et al.*, 2003). Studies have primarily relied on observation data analysis (De Vriend, 1991), and a range of conceptual models and empirical relations to explain the variety in size, volume, and the distribution of channels and shoals in the inlet system were produced. Well known relations are those of Escoffier (1940), O'Brien (1931; 1969), Hayes (1975; 1979), Oertel (1975; 1988), Walton and Adams (1976), Hubbard (1979) and FitzGerald (1988; 1996), but many more exist. De Vriend (1996) classifies these approaches as data-based, empirical or semi-empirical. Data-based models describe phenomena based on analysis of measured data. Empirical models rely on statistical relations between different state variables that are derived from the field data. Often used relations are those of the equilibrium state of morphological parameters as a function of macro-scale hydrodynamics (e.g. Escoffier, 1940; O'Brien, 1969; Walton and Adams, 1976). Semi-empirical (long-term) models use empirical relationships to represent the effects of smaller-scale process in order to describe the interaction between the large elements of the system. Such semi-empirical models can be a useful tool to predict long-term behaviour as was recently shown by modelling the responses of the Wadden Sea to relative sea-level rise (Stive and Wang, 2003; Van Goor *et al.*, 2003; Kragtwijk *et al.*, 2004).

Conceptual models and empirical relations have significantly contributed to an improved understanding of the inlet behaviour and evolution on higher levels of aggregation. However, their major short-coming is that they lack comprehensive descriptions of the underlying physics. Often, observed morphological changes and expert judgement form the principal source of information for the conceptual specification; detailed descriptions of water, flow and sediment transport variations on the intra-tidal and intra-event scales with the necessary spatial and temporal detail over the inlet domain are scarce (NWO-ALW, 1999, sub-project 3). Flow patterns in the inlet environment are notoriously complex due to the non-linear interaction between water motion (wind, wave, density and tide driven) with variable channel and shoals structures. This interaction leads to compound residual circulation patterns. With the additional non-linear interaction between flow and sediment transport compound morphodynamic behaviour occurs. The necessity of obtaining fundamental understanding of these physics is clearly illustrated in Figure 7-1, showing the complexity of (modelled) tidal flow patterns in the Western Wadden Sea.

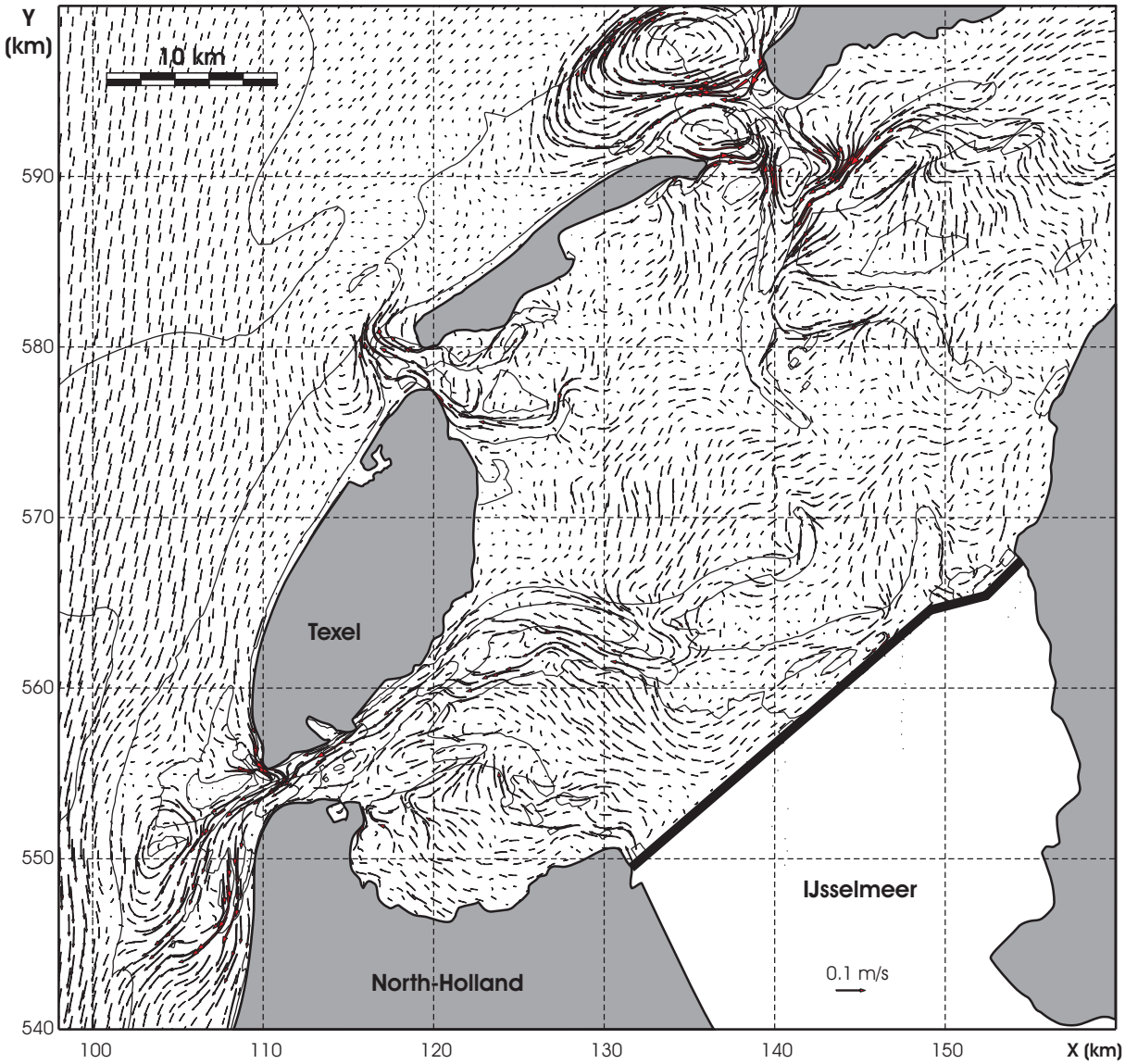

Figure 1-7: Complex residual flow patterns in Texel Inlet resulting from tidal residual eddies and throughflow from Vlie to Marsdiep (Ridderinkhof, 1988). Based on tide- and depth-averaged model results of a mean tide simulation (15-02-1998 08:00-20:20) using the Delft3D Online Morphology model (see Chapters 4 and 6 of this thesis for modelling details).

Nowadays, process-based mathematical models describing the water motion, sediment transport and bottom changes on micro (process) scale by a series of coupled equations for e.g. conservation of mass, momentum and energy can be used to obtain insight into the physical processes. The spatial variability in flow patterns (Fig. 1-7) and sediment transports dictates that sophisticated depth-averaged or full three-dimensional process-based models will have to be used, rather than relative simple one-dimensional coastline of cross-shore profile models, to solve the flow and sediment transports accurately. Since the first morphodynamic application of process-based area models in inlet research (e.g. Wang *et al.*, 1995; Ranasinghe and Pattiaratchi, 1999; Ranasinghe *et al.*, 1999; Cayocca, 2001) there is considerable dissent among researchers whether or not process-based models can be used for simulating the larger scale morphological characteristics and the long-term inlet evolution. Arguments proposed in NWO-ALW (1999, sub-project 2), include:

- Process-based models are designed to represent typical short-term processes and are validated accordingly, against data concerning those processes; long-term developments are governed by other, more subtle processes, which tend to be dominated by the short-term 'noise'.
- Morphodynamic process-models contain various error amplifiers, which may harm the model's ability to reproduce the second-order effects that are important to the long-term behaviour.
- If already at short time-scales the models turn out to be sensitive to input variations and parameter settings, how can a long-term application make sense?
- At first sight, all conditions are met for inherent limitations to the predictability of morphological behaviour: a multi-dimensional, strongly non-linear system with a continuous input, transfer and dissipation of energy, and a variety of modes of free behaviour.

One of our goals in this thesis (see research questions) is to investigate if and how process-based models can be used in inlet research. As a start point we adopt the working hypothesis posed by Roelvink (1999, sub-project 2, page 17):

'If you put enough of the essential physics into the model, the most important features of the morphological behaviour will come out, even at longer time scales'

The recent studies by Hibma (2004) and Van Maren (2004) that have used the Delft3D model system to obtain fundamental understanding of channel-shoal and river-delta dynamics respectively, seem to justify this statement.

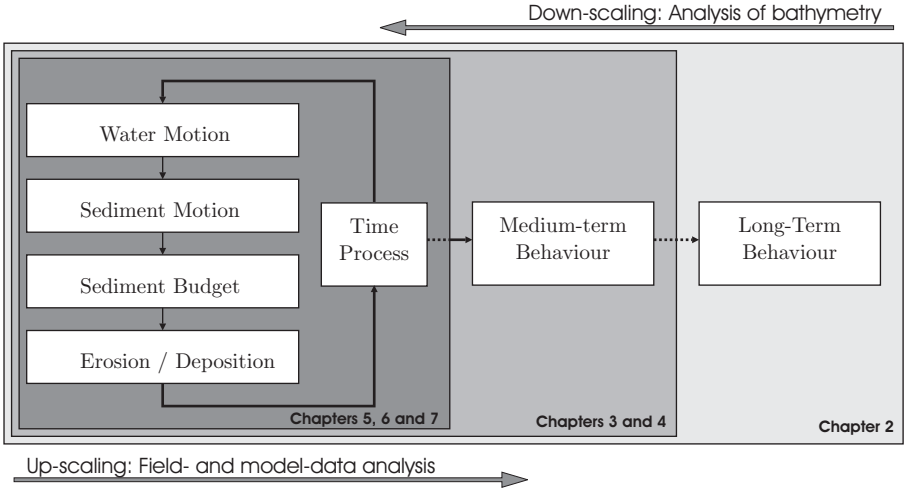

Figure 1-8: Research approach (modified after De Vriend, 1991).

To deal with the uncertainty in model predictions we use an integrated approach of field-data and model-data analysis. By using Texel inlet as a case study a vast amount of field data is available. Texel inlet was and still is intensively monitored by Rijkswaterstaat (Agency of Ministry of Transport, Public Works and Water Management). Extensive datasets of high-quality observations on bathymetry, bedforms, discharges, flow, waves

and water levels over a long period are available. These datasets are an asset in them selves, and can be used for validation and calibration of process-based models.

The research method is presented schematically in Figure 1-8 (modified after De Vriend, 1991). To deal with the wide-variety of spatial and temporal scales in inlet behaviour, we simultaneously use an up-scaling and a down-scaling approach. Down scaling is used to obtain understanding of the large-scale and long-term development of the inlet system based on observational data analysis. Simultaneously, we follow an up-scaling method wherein we use process-based modelling to:

- validate the observation-based conceptual models and hypotheses (Chapter 4).
- provide synoptic, more or less realistic data of high spatial and temporal resolution over the inlet domain. Analysis of this data can provide valuable information on governing flow and sediment transport patterns in the instrumented and the un-instrumented areas of the domain (Chapter 5 - 6).
- provide fundamental understanding of governing processes and mechanisms by simulating short-, medium-, and long-term hydrodynamic and morphodynamic change (Chapters 4 - 6).

1.3.2 Objectives

The objective of this thesis is to increase the fundamental understanding of the behaviour, evolution and physical processes underlying the dynamics of tidal inlets. Texel Inlet is used as a study object because of the abundant data as well as its crucial role in the sand exchange between the Holland coast and the Wadden Sea. We aim to answer the following questions: - what are the natural dynamics of channels and shoals on the ebb-tidal delta (How was Texel Inlet formed?), - what are the processes driving the inlet and ebb-delta development, - what are the transport paths along the shorelines, over the ebb-tidal delta and into the basin, and, - what causes the erosion of the North-Holland coastline near the inlet? These questions are expressed in three basic research objectives:

1– **Determine the characteristics of the 'natural' ebb-tidal delta evolution of the Texel inlet system, and determine the (cumulative) effects of human intervention.**

2– **Determine the present inlet behaviour, the governing processes and dominant physical mechanisms responsible for the flow and sediment fluxes. The following sub-questions may be specified:**

   - What are the characteristics of the water motion and which mechanisms are most dominant?
   - What are the characteristics of the sediment transports and which mechanisms are most dominant?
   - How does the current field contribute to a net, tidally-averaged, transport of sediments in the tidal inlet: what is the contribution of tidal asymmetries, estuarine circulation, residual currents and waves?

3– **Determine the potential of 'state of the art' process-based models in inlet research; e.g. how can process-based models be used in inlet research?**

1.4 Research Approach and Outline

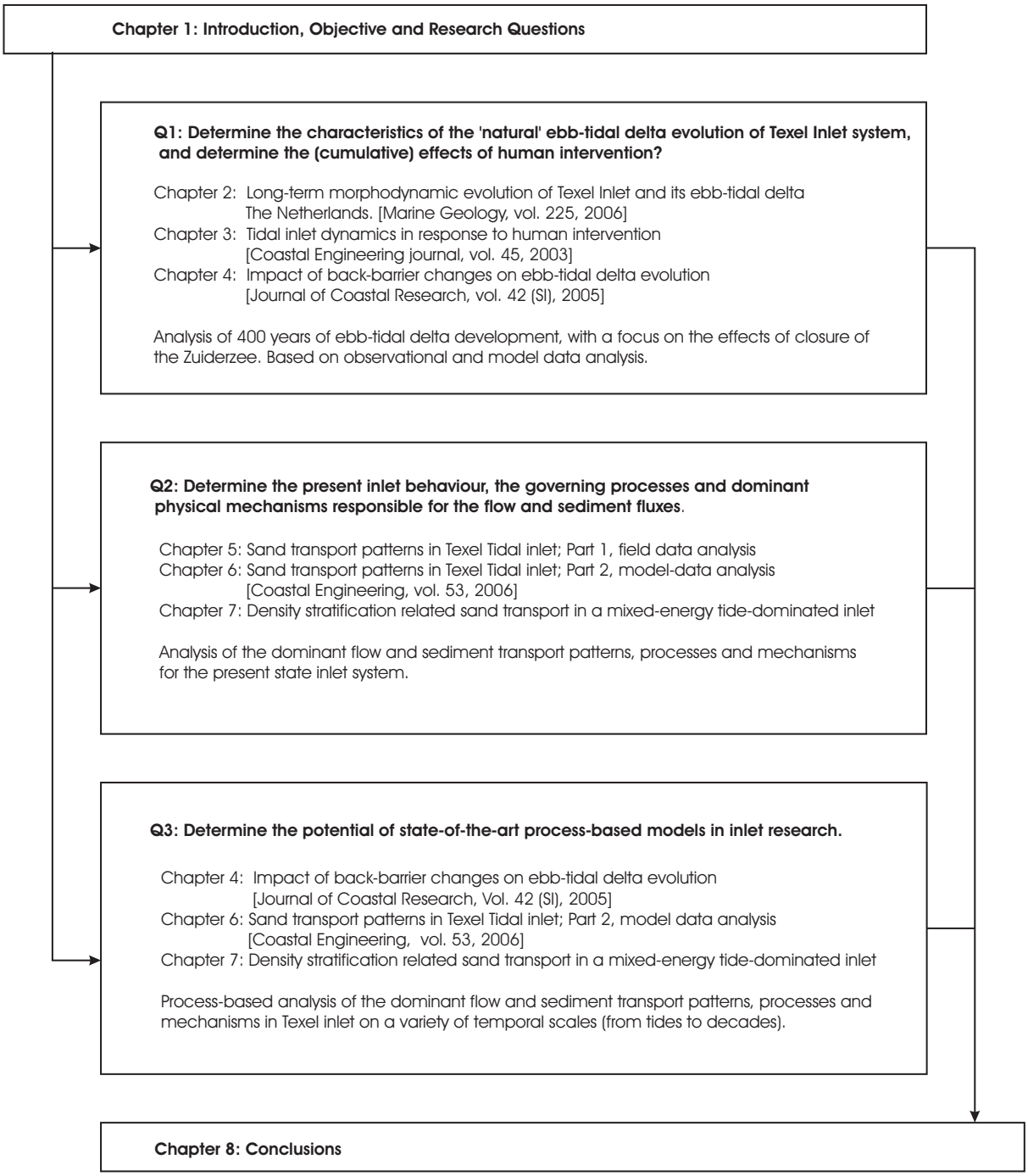

Figure 1-9: Thesis outline

The research questions formulated in the previous section cover a wide range of temporal and spatial scales that require a range of methodologies, varying from morphological interpretation of maps to understand long-term morphological developments, to numerical process-based modelling and detailed analysis of field measurements to obtain fundamental understanding of inlet processes. Figure 1-9 summarizes the thesis outline; a detailed description is given below. Five scientific papers (presented in six Chapters) that have

been submitted or published in peer-reviewed international journals form the core of this thesis (see References).

Chapters 2, 3 and 7 are near-duplicates of these papers (some minor changes in format and Figures are made for clarity). Chapters 4, 5 and 6 are adapted (expanded) versions. Although the papers are not followed completely, the thesis is written in such a manner that all Chapters can be read individually. Therefore, some repetition in sections as introductions or model descriptions occurs.

In order to understand the dynamics of the present-day inlet system we need to identify the (natural) behaviour underlying this system. The inlet behaviour has changed considerably over time, partly due to natural causes and partly as a result of man-induced interventions. Human interventions played a dominant role during the last century after closure of the Zuiderzee. ***Chapter 2*** describes the long-term evolution of the inlet system. Over 400 years of regular bathymetric measurements of Texel Inlet's ebb-tidal delta forms a globally unique morphodynamic dataset. The substantial changes in ebb-tidal delta evolution provide a clear example of the response of the inlet system to the cumulative effects of human intervention. Analysis of the evolution of the ebb-tidal delta morphology shows different stages each characterized by specific orientations of the main channels and shoals. The well-monitored large-scale changes on the ebb-tidal delta which were initiated by the construction of the coastal defence works (Helderse Zeewering, 1750 A.D.) and closure of the Zuiderzee (1925-1932 A.D.) show that incorporation of inlet modifications and back-barrier processes is vital for a correct description of the ebb-tidal delta dynamics and processes at Texel Inlet. A conceptual model is introduced to describe the process-response relation between intervention and ebb-tidal delta change.

One of the eye-catching characteristics of the present-day bathymetry of Texel Inlet is the distinct asymmetrical shape of the ebb-tidal delta with the main channels being updrift orientated (updrift with respect to the direction of littoral drift along the Holland coast and tidal-wave propagation). This asymmetric shape formed in response to the closure of the Zuider Sea. ***Chapter 3*** describes the effects of the closure on the inlet dynamics based on the re-analysis of field observations. A conceptual model is postulated that describes the morphologic adjustment of tidal inlets due to large-scale human intervention. The kernel of this model is a two-stage morphological adjustment towards a new overall equilibrium, related to the existence of more than one temporal response scale.

The Delft3D model system, developed by WL|Delft Hydraulics in close cooperation with Delft University of Technology, has proven to be capable of simulating the hydrodynamics and morphodynamics of complex sedimentary systems. In ***Chapter 4*** model data are used to validate the observation-based conceptual ideas on post-closure inlet evolution (see Chapters 2 and 3). The results of a 'semi-realistic' Delft3D Online Morphology model application have been used to generate synoptic data of high spatial and temporal resolution over the inlet domain during various stages of the morphological adjustment process. Model results indicate that the back-barrier changes in tidal characteristics have triggered the observed ebb-tidal delta developments. Sediment import into the basin is explained to result from spatially uneven sediment availability due to an imbalance between flow and bed on the ebb-tidal delta and a balance in the upper part of the basin.

With the ongoing morphological adaptation of the ebb-tidal delta the imbalance between flow and bathymetry and the related sediment import into the basin diminishes.

Chapter 5 and Chapter 6 concern detailed (process) analysis of the present state of the inlet. ***Chapter 5*** describes the flow and sand transport patterns based on field-data analysis. Observations of water levels, flow, sedimentation and erosion patterns, bathymetric features and bedforms are analyzed and conceptual descriptions of the dominant sand transport patterns on the ebb-tidal delta and the interaction with the adjacent coastlines are given. Additionally, the field data is used to validate and calibrate a Delft3D Online Morphology model (***Chapter 6***). It is shown that this model is capable of the quasi real-time simulation of the dominant flow, transport and sedimentation-erosion patterns over a 10-month period on the scale of the inlet. The high-resolution numerical model results prove to be a valuable tool in identifying the main transport patterns and mechanisms in the inlet domain. Qualitative transport patterns in Texel Inlet and its associated ebb-tidal delta are derived by integration of the high-resolution observations and model results.

Chapter 7 focuses on the three-dimensional structure of flow in the inlet on the intra-tidal time scale. The effects of density-stratification of the water column on flow and sand transport during a period of high fresh-water discharge in the basin are investigated. High-resolution flow data obtained from three simultaneously executed 13-hour Acoustic Doppler Current Profiler(ADCP) observations in the inlet gorge and main ebb-delta channels are studied and used to validate a 3D application of the process-based model. The model is capable of reproducing the dominant features of the residual flow patterns accurately when fresh-water discharge in the basin is included. The model results show that local density stratification plays an important role in the residual flow patterns of inlet gorge and ebb-tidal delta during (after) periods of major fresh-water discharge in Texel basin. Density differences are essential to tilt the residual flow distribution from a horizontal to the observed vertical shear. As a result ebb flow and flood flow are more distinctively separated; flood flow concentrates in the near-bed regions along the coast due to larger salinities, and ebb flow of smaller density prevails in the upper layers along Noorderhaaks. The altered residual flow patterns and magnitudes have potential large impact on the residual sand transport in the inlet gorge and proximal ebb-delta channels

Finally, ***Chapter 8*** summarizes the results, answers the research questions and provides recommendations for further research. An important section is the translation from 'scientific' research to relevant coastal maintenance practice.

Chapter 2
LONG-TERM MORPHODYNAMIC EVOLUTION OF TEXEL INLET AND ITS EBB-TIDAL DELTA (THE NETHERLANDS)

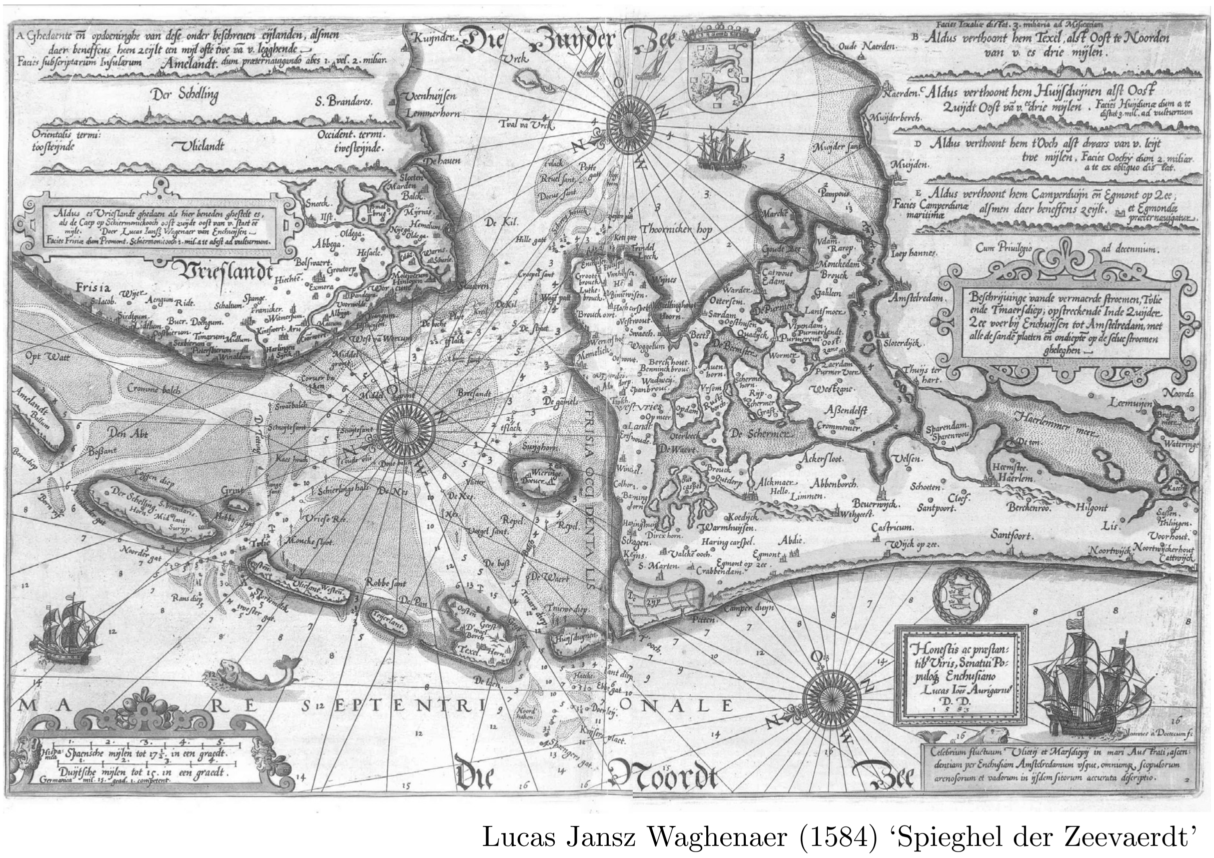

Lucas Jansz Waghenaer (1584) 'Spieghel der Zeevaerdt'

Abstract:

A series of regular bathymetric surveys of Texel Inlet and its ebb-tidal delta spanning a period of over 400 years forms a unique long-term morphodynamic dataset of this largest inlet of the Wadden Sea. The substantial changes in ebb-tidal delta evolution provide a clear example of the response of the inlet system to the cumulative effects of human intervention.

Analysis of the evolution of the ebb-tidal delta morphology shows different stages, each characterized by specific orientations of the main channels and shoals. Prior to construction of extensive coastal defence works on the southern shore of the inlet in 1750 A.D., the ebb-tidal delta showed a downdrift asymmetry. Periodic shoal breaching and downdrift channel relocation were the dominant mechanisms for sediment bypassing (major shoal bypassing). After construction of the coastal defence works, a stable ebb-tidal delta with a westward stretching main ebb-channel developed over a period of c. 60 years. Damming of the Zuiderzee, separating the major part of the back-barrier basin and completed in 1932 A.D., distorted this stable state and over a period of about 40 years the main channel switched to a southward course, remaining in position ever since. During the pre- and post-damming stable states the sediment bypassing took place as minor shoal bypassing; the main channel remained in position and smaller parts of the swash platform (periodically) migrated landward over the ebb-tidal delta.

The well-monitored large-scale changes on the ebb-tidal delta which were initiated by the construction of the coastal defence works and closure of the Zuiderzee show that incorporation of inlet modifications and back-barrier processes is vital for a correct description of the ebb-tidal delta dynamics and processes of Texel Inlet. A conceptual model is introduced to describe the process-response relation between intervention and ebb-tidal delta change.

© Elias and van der Spek (2006); Marine Geology 225 (1-4), 5-21

2.1 Introduction and Objective

Tidal inlets occur along a major part of the world's sediment coastlines. They are increasingly influenced by human interventions such as maintenance dredging, jetty construction and land reclamation in the basin. Knowledge of the intervention-induced effects on inlet dynamics is crucial for a successful coastal management. Nevertheless, the study of the consequences of large-scale human interventions (e.g. engineering works) on the long-term behaviour of inlet systems is a relatively unexplored field of research, mainly due to the absence of datasets comprising frequent observations over a long period.

Texel Inlet's ebb-tidal delta has been monitored over the last 400 years. This series of regular bathymetric observations allows the description of its long-term morphodynamic evolution. This evolution has been governed by an increasing impact of major engineering works (e.g. seawall construction, damming of a major part of the basin). The well-monitored changes in ebb-tidal delta development show the impact of inlet modification and anthropogenic changes in the back-barrier basin. A conceptual model is introduced to describe the process-response relations between these interventions and changes in ebb-tidal delta morphology.

2.1.1 Tidal inlet morphodynamics

Principally, a tidal inlet is an opening in the shoreline through which water (and sediments, nutrients, etc.) is exchanged between the open sea and the back-barrier basin. The inlet channel is maintained by tidal currents (Escoffier, 1940). Sediments eroded from the inlet, and supplied by littoral drift, accumulate in tidal deltas at the seaward and at the landward side (the ebb- and flood-tidal delta respectively) were flow segregates and decreases after passing through the narrow inlet throat.

One of the key elements for analyzing inlet evolution and behaviour is the dynamic coupling between ebb-tidal delta, inlet gorge and back-barrier basin, that tend to remain in (dynamic) equilibrium to the large-scale hydraulic forcing, individually as well as collectively (see e.g. Dean, 1988; Oost and de Boer, 1994; Stive *et al.*, 1998; Stive and Wang, 2003). Distortion of the equilibrium state in one of the components will result in sand exchange between the components as other parts of the system will (temporarily) deliver or store sand to compensate. Larger scale permanent distortions due to natural causes (such as accelerated sea-level rise) or human intervention (e.g. damming of a part of the back-barrier basin, construction of breakwaters and jetties) can cause the entire inlet system to shift towards a new equilibrium state. Unfortunately, long-term datasets covering the ebb-tidal delta, inlet and basin in sufficient accuracy and resolution are scarce. Nevertheless, due to the dynamic coupling of the ebb-tidal delta, inlet and basin valuable clues on the (changing) dynamics of the complete inlet system can already be obtained from the analysis of one of the elements, for example the ebb-tidal delta in this study.

Various conceptual models and empirical relations have been proposed to explain the variety in size, volume and distribution of channels and shoals on the ebb-tidal delta (e.g. Hayes, 1975; Oertel, 1975; Hayes, 1979; Hubbard *et al.*, 1979; FitzGerald, 1988; Kana *et*

al., 1999). Most studies agree that the morphology of the ebb-tidal delta is essentially determined by the relative importance of wave versus tidal energy. Wave-dominated ebb-tidal deltas are pushed close to the inlet throat, while tide-dominated ebb-tidal deltas extend offshore (Oertel, 1975). Bruun and Gerritsen (1959) were among the first to recognize the importance of sediment bypassing, the sand exchange over the ebb-tidal delta from the updrift to the downdrift beaches, for the channel-shoal distribution on the ebb delta. They related sediment-bypassing to the ratio between longshore sediment transport by waves and tidal inlet currents. For high ratios wave-induced sand transport along the periphery of the ebb delta dominates. For low ratios sediment transport through channels and migration of tidal channels and bars prevails. Based on this pioneering work, various other researchers have further elaborated on models of sediment bypassing mechanisms. FitzGerald (1982; 1988) and FitzGerald *et al.* (2000) proposed various conceptual models to explain sediment bypassing under mixed-energy conditions. These models are based on the relation between stability of the inlet throat and the movement of the main ebb channels, and have shown to be valid for a wide range of mixed-energy tide-dominated inlets. We have illustrated the mechanisms most relevant for this paper in Figure 2-1 (based on FitzGerald *et al.*, 2000).

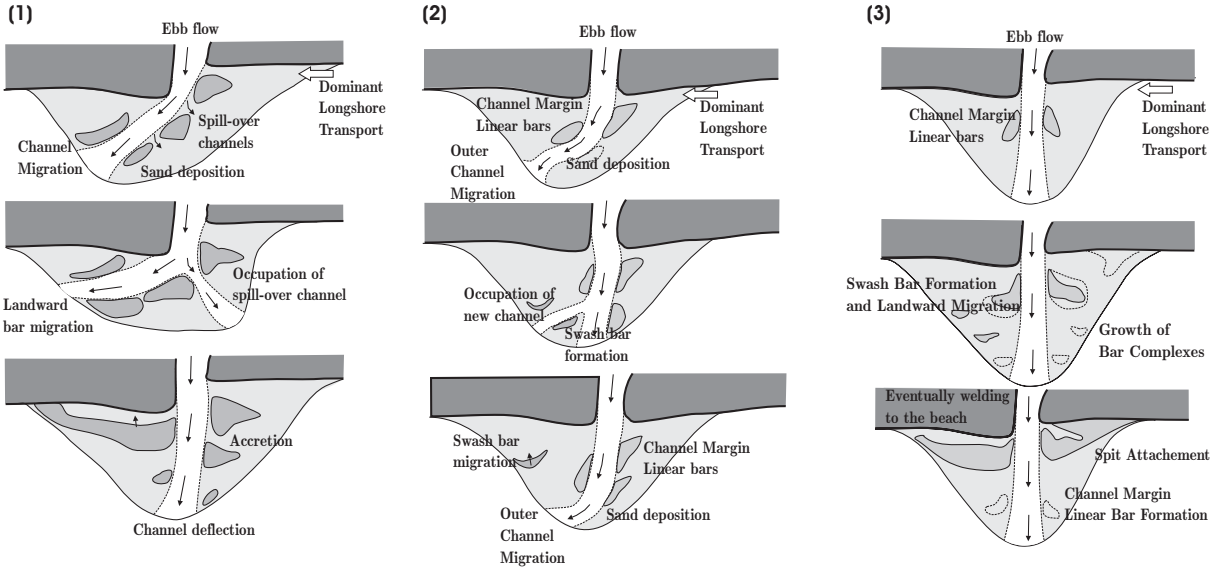

Figure 2-1: Models of sediment bypassing (1) Cyclic ebb-tidal delta breaching, (2) Outer channel shifting, (3) Stable inlet processes, Redrawn after FitzGerald *et al.* (2000).

(1) cyclic ebb-tidal delta breaching; The main ebb channels periodically migrate downdrift due to sediment accumulation at the updrift side of the ebb-delta. These shoals deflect the main ebb-channel in downdrift direction. The curved channel is hydraulically less efficient and a more competent, seaward-directed pathway through the ebb-tidal delta forms.

(2) outer channel shifting; Similar to cyclic ebb-tidal delta breaching, but the channel migration is limited to the distal part of the channel while the proximal part remains stable.

(3) stable inlet processes; The main ebb channel remains stable in position often related to the presence of erosion resistant layers. Bar complexes, formed by stack-

ing and coalescence of swash bars on the delta platform, migrate onshore due to the dominance of landward flow created by wave swash.

With ongoing research it has become obvious that on smaller, decadal, time scales the ebb-tidal delta dynamics cannot be described in sufficient detail by a general classification based on wave versus tidal energy. There are many secondary external controls that influence inlet behaviour, including sediment supply, basin geometry and sedimentation history, regional stratigraphy (e.g. presence of resistant layers like bedrock) and freshwater discharge by rivers (FitzGerald, 1996).

2.2 Texel Inlet

2.2.1 General characteristics

Texel Inlet is the largest tidal inlet of the Dutch Wadden Sea, and is located in the north-western part of The Netherlands between Den Helder and the barrier island of Texel (Fig. 2-2). With bathymetric data of the inlet and ebb-tidal delta being available since the 16th century, the inlet is probably the longest regularly monitored inlet worldwide.

Tides and wind-generated waves are the dominant (natural) processes governing the morphological developments. The tide has a mean tidal range of nearly 1.4 m in Marsdiep, increasing to 2.0 m during spring tide, while during neap tide it drops to about 1.0 m. Measurements show an average tidal prism through the inlet of 1x10^9 m^3, with maximum ebb and flood tidal velocities ranging between 1.0 and 2.0 m/s (Ridderinkhof *et al.*, 2002). An important characteristic of the present-day Texel basin is that it does not form a closed system but the basin connects to the neighbouring Vlie basin allowing an exchange between the two systems (Fig. 2-2). Due to the higher amplitude of the vertical tide in the Vlie basin, the residual flow through Texel inlet of about 115 million (M) m^3/tide is seaward directed.

Detailed overviews of the governing wind and wave conditions along the Holland coast and Texel Inlet are presented by Roskam (1988) and Wijnberg (1995). Analysis of the wave data from the nearby measuring station Eierlandse Gat (location see Fig. 2-2). shows that the mean significant wave height is 1.3 m from the west-southwest, with a corresponding mean wave period of 5 seconds. During storms wind-generated waves can reach heights of over 6 m and water level surges of more than 2 m have been measured.

Following the classification of Hayes (1979) the inlet qualifies as mixed-energy wave-dominated, even under spring tide conditions. However, the morphology of the inlet shows tide-dominated characteristics such as a large ebb-tidal delta. This is caused by the large tidal prism and the relatively low wave energy (Davis and Hayes, 1984). Figure 2-2 shows the present-day geometry and bathymetry of the inlet including its back-barrier drainage area.

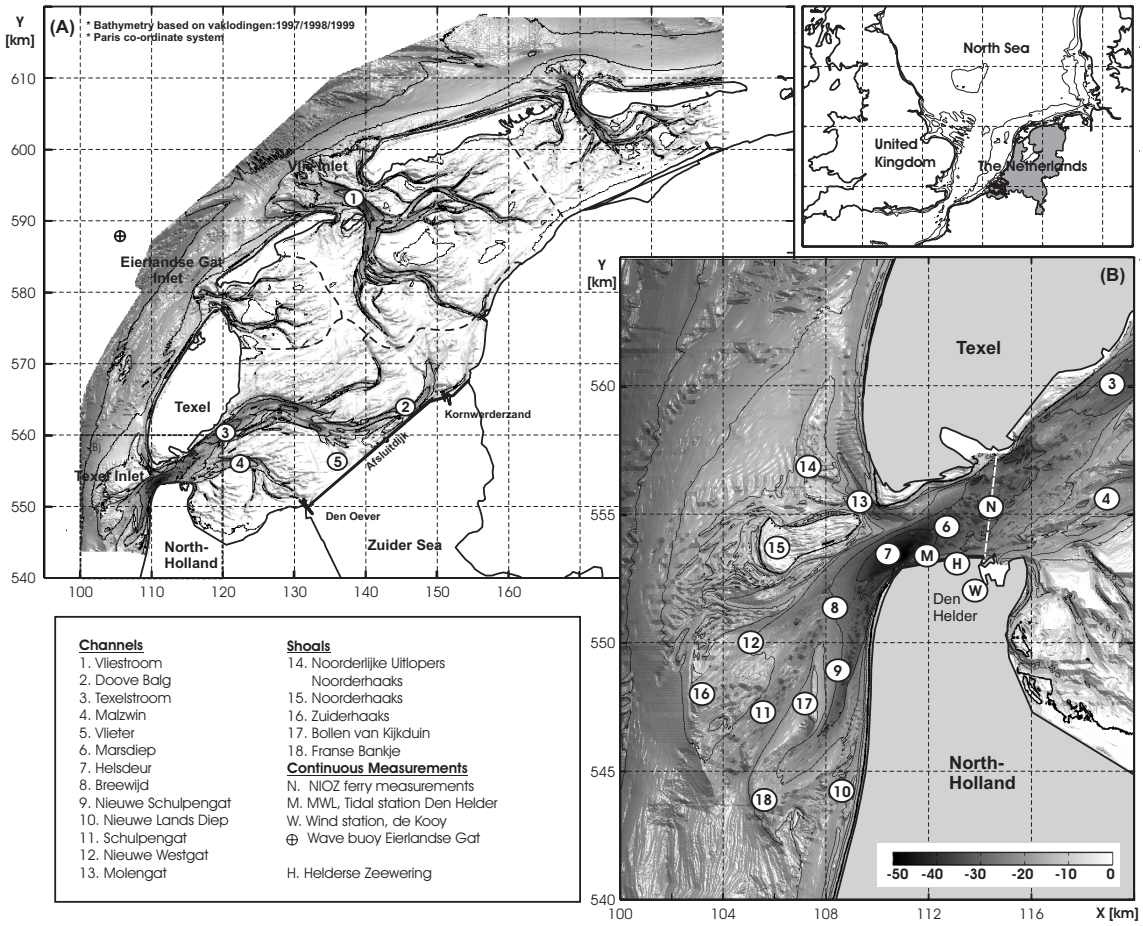

Figure 2-2: Location map of the Texel Inlet (dashed lines indicate approximate locations of the tidal divides separating the basins of Texel, Eierlandse Gat and Vlie inlet).

2.2.2 Bathymetric data

The dataset of more than 400 years of bathymetric observations from Texel Inlet is unique. Due to the presence of harbours and important shipping lanes in the basin and the Zuiderzee (to e.g. the port of Amsterdam), nautical and hydrographical charts describing the location and depth of the main channels and shoals in the inlet system dating back to the 16th century A.D. are available. Obviously, the resolution and accuracy of the older maps (16th, 17th, 18th century A.D.) cannot be compared to present standards, but they nevertheless allow for geomorphologic reconstructions of the main channel and shoal distributions on the ebb-tidal delta. Ongoing progress in surveying techniques and methods increased the resolution and accuracy of the bathymetric maps and since the 19th century A.D. the detailed maps include depth contours. After the closure of the Zuiderzee, completed in 1932 A.D., monitoring campaigns by Rijkswaterstaat (Ministry of Transport, Public Works and Water Management) further intensified. Nowadays, Rijkswaterstaat surveys the ebb-tidal delta every three years.

These bathymetric observations form the basis for the description of the long-term evolution that follows below. Where relevant, process interpretations of the channel and shoal evolution will be given in association with the descriptions.

2.2.3 Historic development of Texel Inlet; tidal prism and inlet dimensions

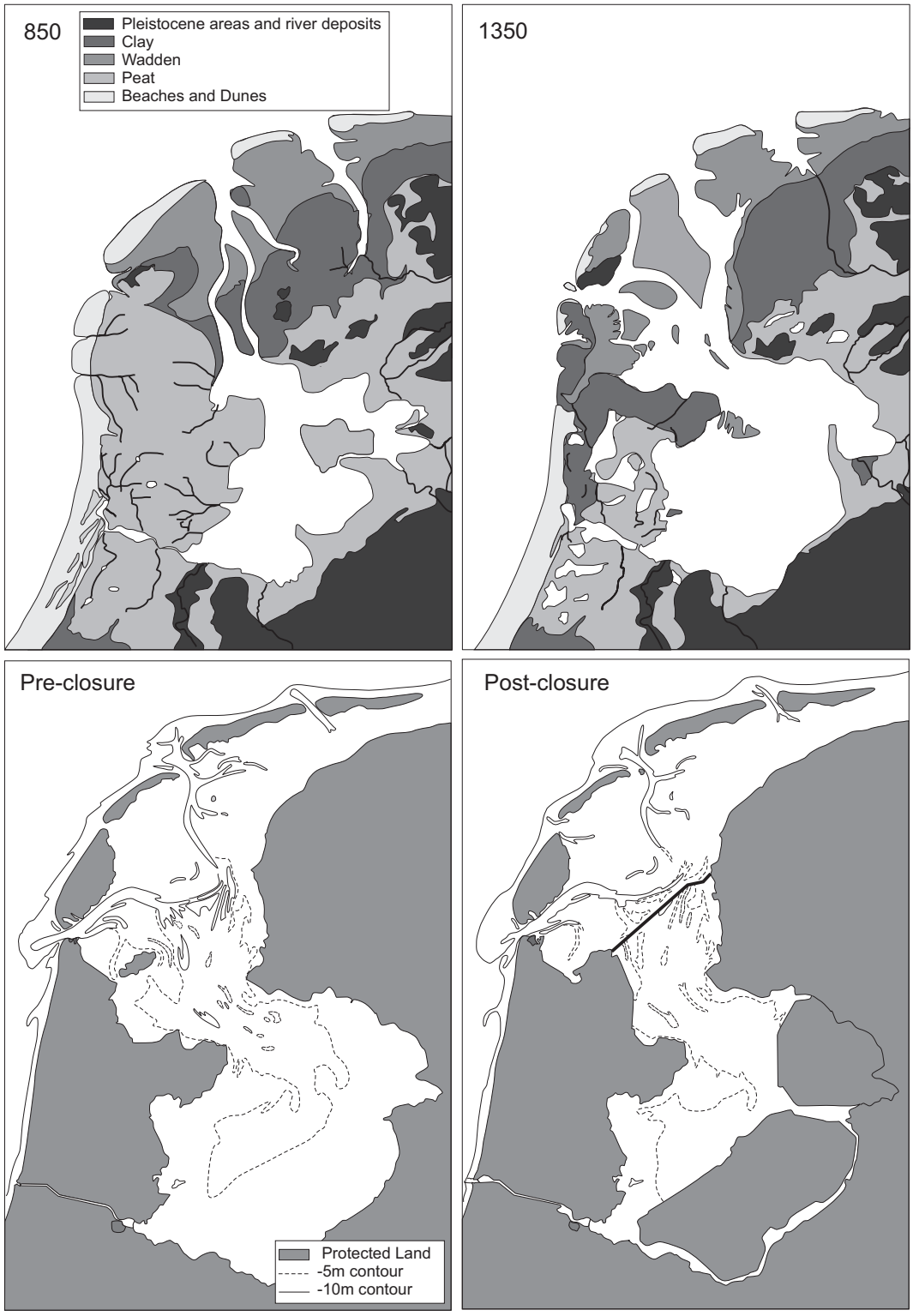

Figure 2-3: Development of the basin through time. Upper left: Paleografic map for the situation in 850 A.D., before development of the inlet. Upper right: Paleografic map for the situation in 1350 A.D. (both based on maps presented by Lenselink and Koopstra, 1994). Lower left: Texel Inlet before closure of Zuiderzee in 1932 and (lower right) after closure.

Texel Inlet is believed to have evolved from a small local drainage channel that connected to the inland Zuiderzee around the 12th century A.D. after a series of severe storm events (Schoorl, 1973; Hallewas, 1984 [see overview in Oost *et al.*, 2004, p. VII-6]). Prior to breaching the Vliestroom (east of Vlieland, Fig. 2-2) was the only connection between Zuiderzee and North Sea.

The size of the inlet increased with time as a result of subsidence of the surface level due to excavation and drainage of low-lying peat areas bordering the inlet's initial basin for agricultural use; see Eisma and Wolff (1980) summarizing Schoorl (1973), Westenberg (1974), Pons and Van Oosten (1974). This subsidence is estimated to be in the order of magnitude of 1 m per century. The basin expansion was further enhanced during storm surges as larger areas were flooded, and even more peat was eroded. With increasing basin volume the tidal prism through the inlet increased considerably causing the inlet channels to scour and increase in depth and width. Up to c. 1600 A.D. this natural feedback mechanism of erosion and increasing tidal prisms governed the development of the inlet system. The basin expansion was constrained by the increasing influence of human activities, such as construction of dykes, embankments and coastal protection works (Schoorl, 1973). It is to be expected that the tidal prism and inlet dimensions followed the increase and subsequent stabilisation of back-barrier dimensions (Fig. 2-3 and 2-4 respectively).

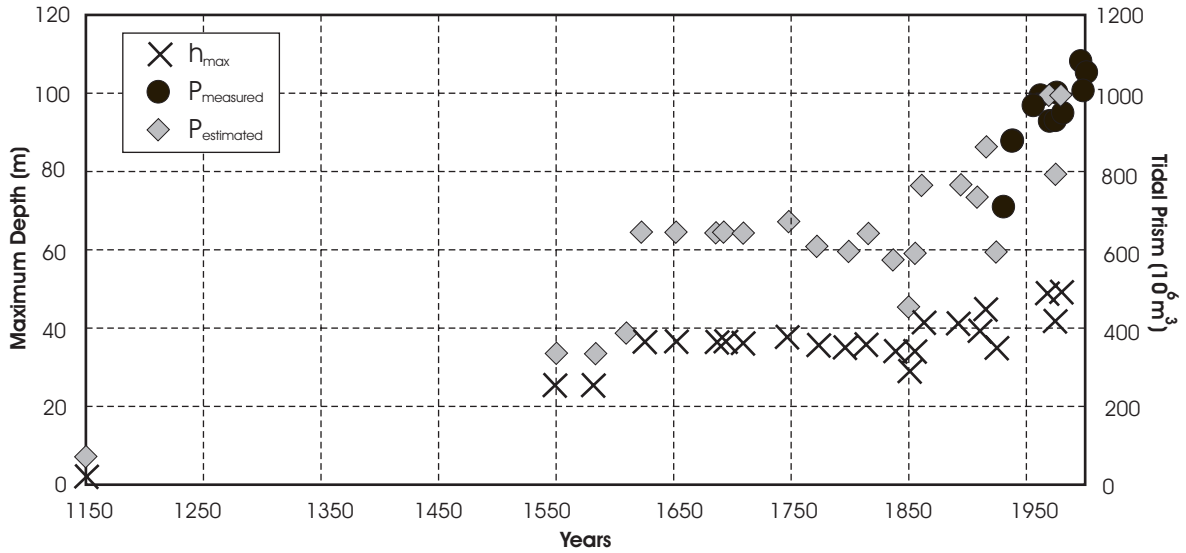

Figure 2-4: Development of the maximum depth of the inlet throat (h_{max} in m), measured tidal prisms ($P_{measured}$ in 10^6 m^3) and estimated tidal prism based on the relation: $P_{estimated} = (h_{max} - 13)//37*10^{-9}$, (Van der Spek, 1994, 1995).

Unfortunately, discharge measurements in the inlet throat are only available since the 20th century A.D. after closure of the Zuiderzee (indicated by black circles in Fig. 2-4). The relative large scatter is due to inaccuracies in the measurements. Discharge measurements are based on 13-hour observations and e.g. meteorological variations can cause relative large differences between successive measurements. A rough estimate of the tidal prism evolution since breaching of the inlet is obtained through the relationship between tidal prism and maximum depth of the inlet throat (Fig. 2-4).; depth values are indi-

cated on most of the historic maps. Sha (1990) and Van der Spek (1994; 1995) propose linear relationships linking maximum inlet depth and tidal prism, based on the relationships between tidal prism and the cross-sectional area of the inlet throat that were quantified by O'Brien (1931; 1969) and Escoffier (1940), and for the Dutch Wadden Sea by Gerritsen and De Jong (1985) and Eysink (1990). The tidal prisms remained more or less constant from the 17th to the early 19th century. The increase in tidal prism during the mid 19th century is possibly related to an increase in relative sea-level rise to ~ 0.2 m/year in this period (Van Veen, 1945, 1954; Oost, 1995, pages: 203-207). Analysis of the tidal water-level records of Amsterdam over the period 1682 A.D. -1930 A.D. shows a relatively constant sea level up to about 1870 A.D. and a rise ever since.

One of the characteristic features of the Wadden Sea is the continuous sedimentation in the tidal basins in order to keep pace with the increase in accommodation due to the relative sea level rise (Stive and Eysink, 1989). Hence, more sediment must be supplied from the adjacent coastlines and ebb-deltas to fulfil the sea-level rise related sediment demand in the basin. The large increase in tidal prism during the 20th century resulted from closure of the Zuiderzee (Fig 2-4. bottom panels). This increase was approximately 26% (Rietveld, 1962; Thijsse, 1972).

Note that the estimated tidal prisms only provide a rough qualitative indication as the correlation between maximum inlet depth and tidal prism is relatively weak (Van der Spek, 1994, 1995) and inaccuracies are expected in the indicated depths. For navigation only minimum channel depths are relevant, so, particularly in older maps, maximum channel depths cannot be considered accurate. Furthermore, the scour around constructions (such as the Helderse Zeewering) may have increased maximum depths beyond what would be derived from natural scouring processes.

An important element forms the presence of erosion-resistant layers in the basin. Comparing Figures 2-3b, c and d it can be observed that the southwest-northeast outflow from Texelstroom to Marsdiep remained remarkably stable. Even following closure of the Zuiderzee, there was hardly any change in position and geometry of the channel; the channel rotated slightly to align with the Texel coastline. Although, only limited knowledge is present on the deep subsurface layers, analysis of literature and recent core data (TNO-NITG; unpublished data) indicates that the seaward part of Texelstroom channel is bounded by or incised into glacial till and that its stability in dimension and position is governed by this stiff deposit. In addition, defence structures that have been constructed along the south-eastern coast of Texel since approximately 1750 A.D. (Schoorl, 1999) must have contributed to the stability of Texelstroom as well.

2.2.4 Ebb-tidal delta evolution

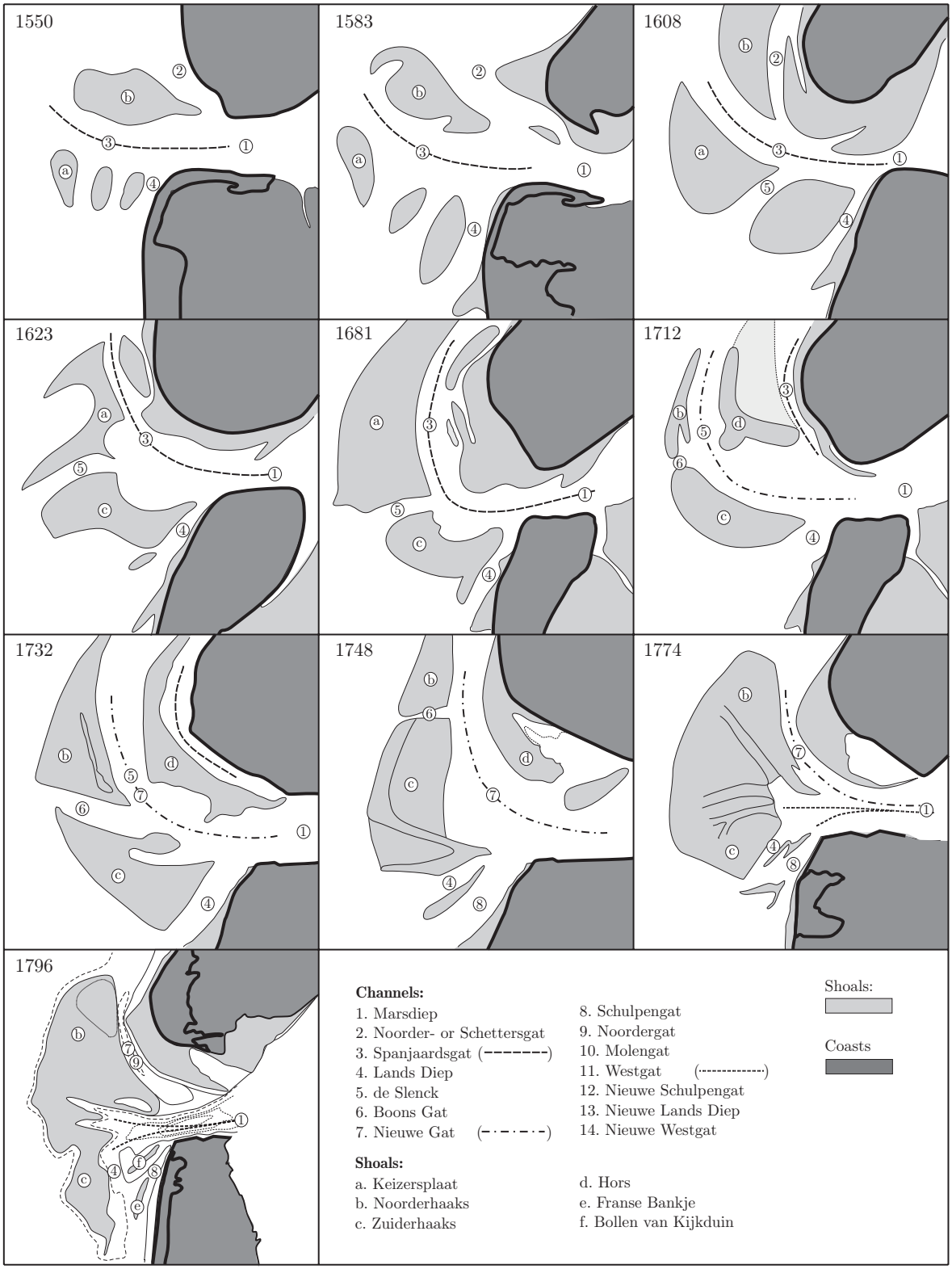

Figure 2-5: Ebb-tidal delta development Texel Inlet from 1550 A.D. to 1796 A.D. Redrawn after original maps presented in Schoorl (1973) and Sha (1990). Maps not to scale.

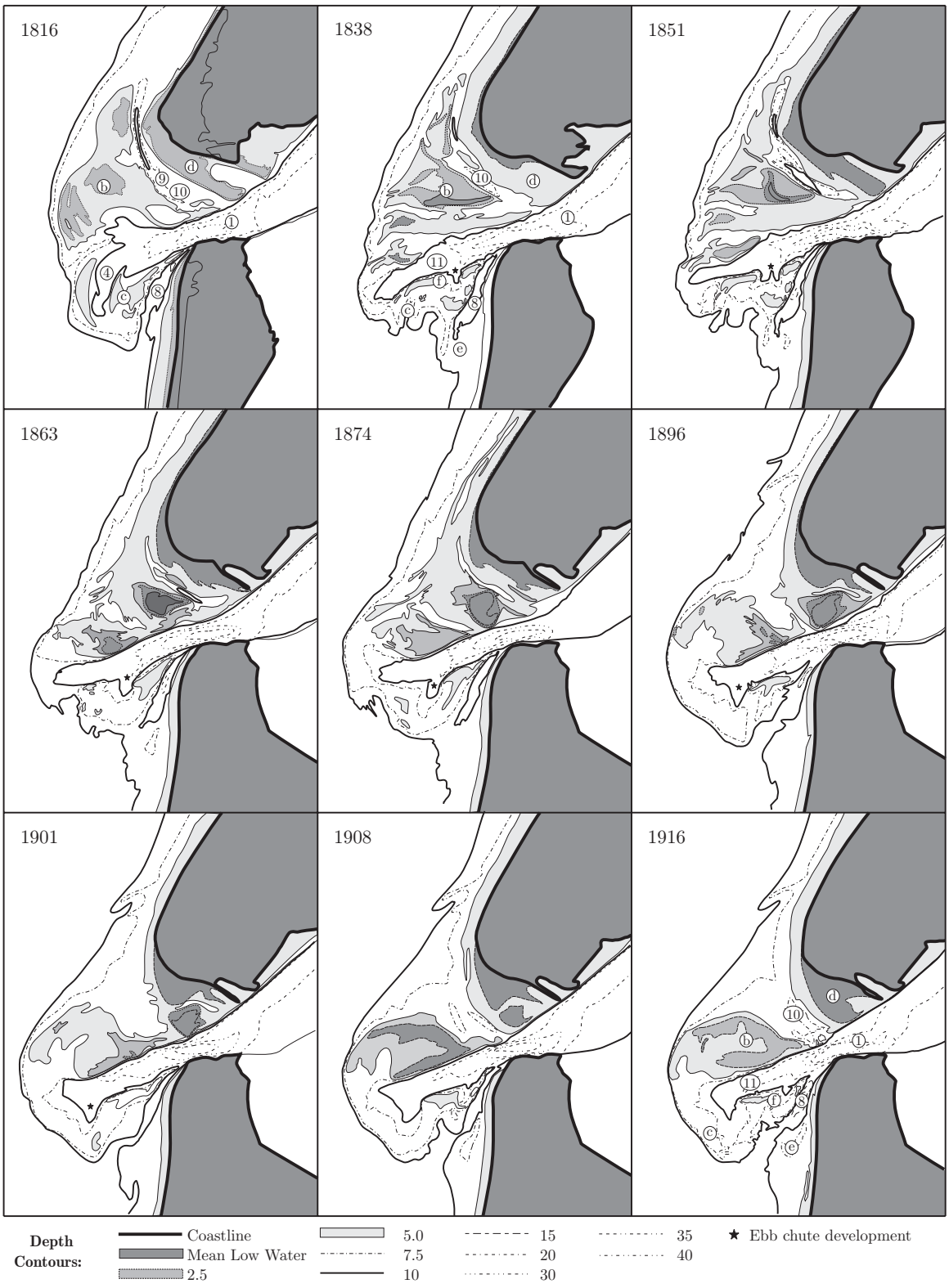

Figure 2-6: Ebb-tidal delta development Texel Inlet from 1816 A.D. to 1916 A.D. Redrawn after original bathymetric maps presented in Rijzewijk (1986). Legend numbers see Fig. 2-5.

The 16th, 17 th and 18 th century: channel and inlet migration

During the 16th, 17th and 18th century A.D. the ebb-tidal delta was asymmetric with a predominant downdrift-oriented (relative to the direction of littoral drift and tidal propagation, which is to the north in this case) main channel (Fig. 2-5). In the northern part of the delta, periodic, possibly cyclic migration of the main channel and shoals occurred during this period (Joustra, 1973; Sha, 1990; Van Heteren *et al.*, 2004). The migration can be described with the cyclic ebb-tidal delta breaching mechanism (see Fig. 2-1; mechanism 1). Possibly cyclic, as two sequences of clockwise rotation, migration and eventually merging with the Texel coastline of the main channel and shoals with a period of 100 to 160 years are observed (indicated by the dashed and dash-dot line in Fig. 2-5).

Several processes contribute to the cyclic ebb-tidal delta breaching mechanism. Firstly, updrift shoal development is augmented as the ebb channel forms a hydrodynamic obstacle for the northward directed littoral drift causing a preferential sedimentation at the updrift side of the channel (FitzGerald, 1988). Building up of shoals enhances wave breaking and associated wave-driven flow, that increasingly influences shoal behaviour. Shoals migrate downdrift due to the residual north-eastward directed wave-driven flow and transports, thereby not only exerting a lateral force on the channel, but also deflecting the ebb currents to the north. As a result, the main channel and adjacent shoals rotate clockwise and migrate in downdrift direction. Channel over-extension in downdrift direction reduces the hydraulic efficiency of the channel, and eventually ebb discharges will find a new (seaward-located) pathway through the ebb delta, following a steeper gradient in water level (Van Veen, 1936, p. 133).

A second mechanism that plausibly contributed to the downdrift channel migration is the interaction of strong, northward directed flood-dominated flow (through Lands Diep and Schulpengat), with the ebb dominant flow through Marsdiep. Due to the segregation of flow, separate ebb- and flood-dominated channels can exist in tidal systems (Van Veen, 1950; Postma, 1967). Postma explains; maximum ebb does not occur at midtide but late in the ebb phase, near low water. Therefore ebb flow is concentrated in the main ebb channel and due to the large velocities and erosive potential this is the largest channel in the ebb-tidal delta. At low water, strong currents are still flowing seaward, out of the main ebb channel, and as the water level rises, the flood currents seek the path of least resistance along the margins of the ebb-tidal delta (Lands Diep and Schulpengat).

Thirdly, updrift migration of the inlet throat. In contrast to the downdrift migration of the main channel on the ebb delta, the inlet throat migrated updrift; it is estimated to have migrated 1500 meters to the south between 1600 A.D. and 1750 A.D., opposite to the dominant longshore transport direction. This southward migration of the inlet throat probably resulted from the obliquely approaching channel Texelstroom (Fig. 2-2 and 2-3) scouring the updrift embankment. The latter was further enhanced by the flood-dominated flow trough the channels Lands Diep and Schulpengat. Other mechanism that might have contributed include the periodic attachment of swash bars to the downdrift shoreline of Texel and secondary flow (Aubrey and Speer, 1984). Secondary flow, across-channel flow due to channel-curvature, promotes erosion of the inlet throat's outer bank (shore of North Holland) and accretion of the inner bank (shore of Texel).

Beginning in the early 17th century, the first defensive works such as wooden groins and underwater willow mattresses were placed on this embankment to retard the erosion and to protect the toe of the dikes. Nevertheless, it was not until the 18th century before the continuous scouring of the updrift embankment was permanently halted by the construction of stone revetments, predecessors of what is now known as Helderse Zeewering (zeewering = sea defence).

The 19th and early 20th century: stable channels, migrating bars

Advances in surveying techniques and mapping accuracy which resulted in more accurate hydrographic charts from the 19th century A.D. allow for a detailed reconstruction of the channel and shoal evolution (Fig. 2-6).

Toward the end of the 18th century A.D. the previously observed clock-wise rotation and downdrift migration of the main channels and shoals no longer occurred. In contrast, the main channel Westgat migrated to a westward, slightly updrift-directed, position flanked on either side by large shoal areas: Noorderhaaks and Zuiderhaaks (see map of 1796 A.D.; Fig 2-5). The channel remained stable in position (Figs. 2-6, 2-7) until the closure of the Zuiderzee (over the period 1925 A.D. - 1932 A.D.). Marginal flood channels extended along the adjacent coastlines; initially Noordergat and later Molengat bounded the Texel coastline, and Schulpengat the North-Holland coast.

The evolution of Westgat and Lands Diep initially was a case of outer channel shifting (Fig. 2-1; mechanism 2), until around 1816 A.D. By then a straight, stable, slightly updrift-directed channel had formed (Fig. 2-1; mechanism 3). In stable inlet systems, parts of the swash-platform (often episodically) shift within the inlet domain, eventually leading to bar or shoal welding with the downdrift coastline (FitzGerald, 1982, 1988). Such a 'minor' shoal bypassing event (the main ebb channel and the shoals keep their positions) occurred on the Noorderhaaks swash platform between 1838 A.D. - 1916 A.D. A large linear bar that formed on top of Noorderhaaks, deformed, migrated landwards, and attached to the Texel coastline.

The shift in channel orientation from a downdrift to an updrift orientation is remarkable. It indicates a change in the forcing of the ebb-tidal delta dynamics. Since we did not observe significant changes in the tidal prism (Fig. 2-4), this shift is likely to be caused by the construction of Helderse Zeewering. The westward, slightly updrift-oriented direction of the channel corresponds with the westward-directed Helderse Zeewering that realigns the southwest-directed ebb flow from Texelstroom. Oertel (1975) suggested that the magnitude of flow acceleration at constricted inlets, bounded by bedrock, sediment composition, or human interventions, is generally greater than that for (broad-mouthed) natural inlets. The Helderse Zeewering prevented migration of the updrift embankment, while the southward outbuilding of the downdrift shore continued. Southward migration of this shoreline was counteracted by seaward flushing of sediment through the inlet throat, and eventually, a balance between minimal cross-sectional area and maximum inlet velocities established. The deep scour hole which was formed at the tip of Helderse Zeewering since 1796 A.D. is an indication for these larger velocities. The erosive poten-

tial of larger flow velocities creates a deeper tidal channel, and plausibly this channel scoured into semi-consolidated layers (Sha, 1989d) which contributes to its stability.

In detail:

Formation, migration and merger of the shoal *Onrust*

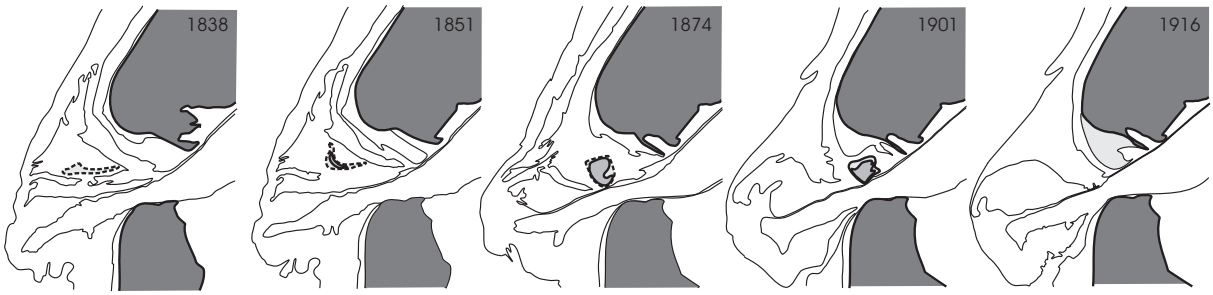

Figure I-1: Formation, migration and attachment of *Onrust*

In stable inlet systems parts of the swash-platform (often episodically) shift within the inlet domain, eventually leading to bar or shoal welding with the downdrift coastline (FitzGerald, 1982, 1988). Such a "minor" shoal bypassing event (the main ebb channel and the shoals keep their positions) occurred on the Noorderhaaks swash platform (1838 A.D. - 1916 A.D.). This process can be sub-divided into four stages: formation, deformation, migration and finally attachment of the bar (see Fig. A-1).

Phase 1, Formation: The first stage shows the formation of a large linear bar on top of Noorderhaaks (situation 1838 A.D.). Commonly, linear bars are formed along the flanks of the main tidal channels in tidally-dominated parts of ebb deltas. They are ascribed to the presence of ebb- and flood-dominated zones that are separated by the crest of the peripheral shoal complex (Van Veen, 1950; Postma, 1967; Hubbard *et al.*, 1979).

Phase 2, Deformation: As the bar builds up to intertidal heights, wave breaking and the associated wave-driven currents and transports increase. This results in deformation of the linear bar into a crescent shape with 'tails' pointing shoreward due to wave refraction (see situation 1851 A.D.). The shielded, wave-sheltered area behind this shoal favours deposition, further increasing the size and height of the shoal up to supratidal level.

Phase 3, Migration: With net landward directed wind- and wave-generated currents, the shoal started to migrate onshore between 1851 A.D. and 1908 A.D. thereby decreasing the width of the flood-dominated channel Noordergat.

Phase 4, Attachment: Wind and waves continuously pushed the shoal shoreward, further reducing the hydraulic efficiency of Noordergat. Meanwhile, more seaward the former spill-over channel Molengat developed into a new flood-dominated channel, taking over the role of Noordergat and allowing *Onrust* to attach to the island of Texel in 1916.

The 20 th century after the closure: updrift channel migration

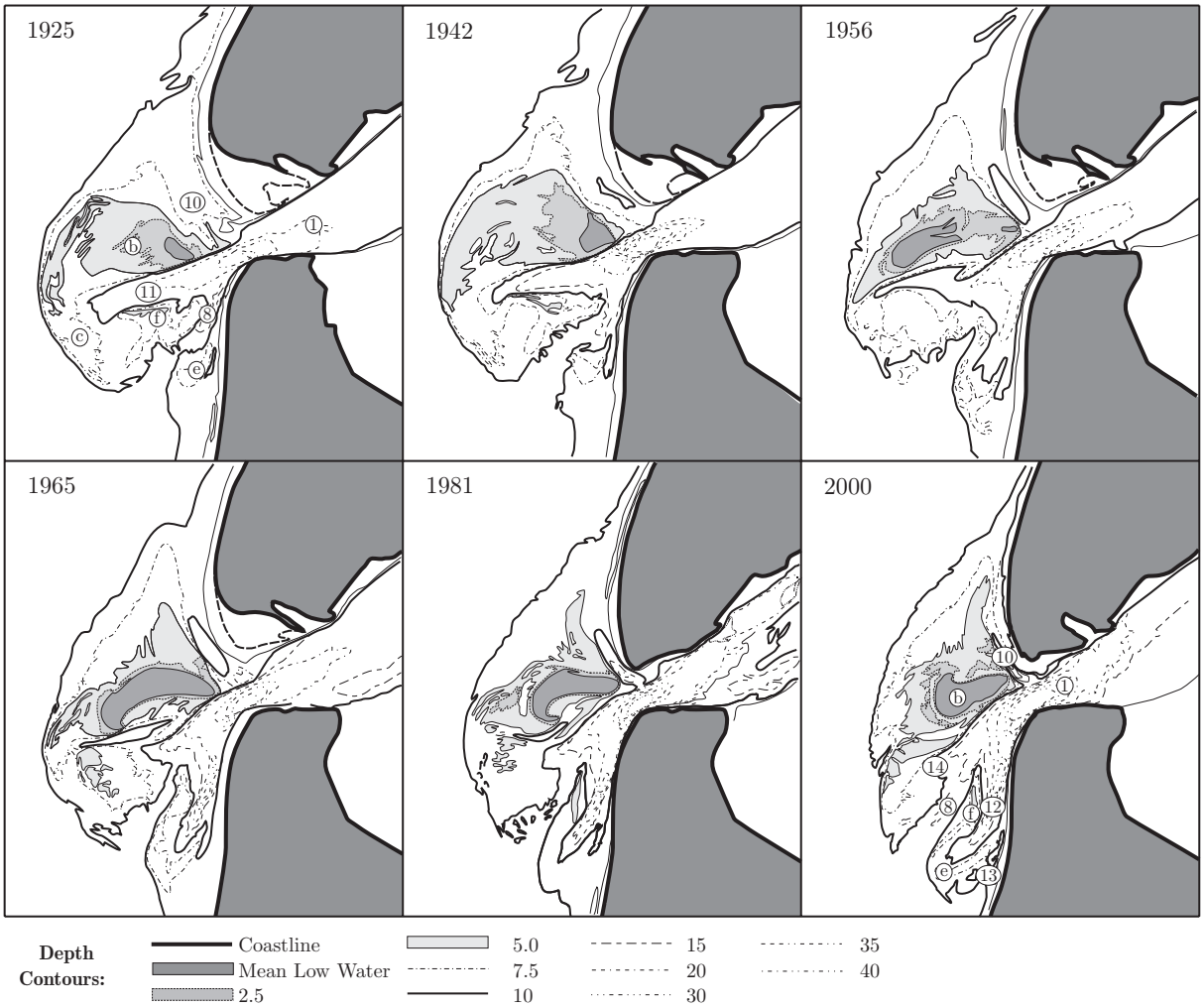

Figure 2-7: Ebb-tidal delta development Texel Inlet from 1925 A.D. to 2000 A.D. based on the maps presented by Rijzewijk (1986) and De Kruif (2001). Legend numbers see Fig. 2-5.

The basin dimensions remained more or less equal until closure of the Zuiderzee between 1925 A.D. and 1932 A.D. (Fig. 2-3). Preceding the closure the Texel and Vlie tidal basins covered the south-western part of the Wadden Sea and the former Zuiderzee (Fig. 2-3, lower left panel). In total, the basin covered a surface area over 4000 km^2 with a basin length of 130 km. Pre-closure there were smaller-scale land-reclamation works in the basin, but the effects of these were minute compared to the major reduction of basin area following the damming (Elias *et al.*, 2003b; Rietveld, 1962; Thijsse, 1972). The closure dam reduced the basin length from about 130 km to 30 km, and the drainage area to roughly 712 km^2 (Fig. 2-3, lower right panel). The tidal characteristics in the remaining active part of the basin changed from a propagating to a standing tidal wave, and the large decrease in basin length caused greater tidal wave reflection at the closure dam resulting in a drastic increase in tidal range from approximately 1.1 to 1.4 m in Marsdiep. Tidal prism through Marsdiep increased with approximately 26% after 1932 (Rietveld, 1962; Thijsse, 1972). These large changes in hydrodynamics and particularly in geometry, caused pronounced changes in the morphodynamic evolution of the remaining basin, such

as a large sedimentation, ~200 Mm^3 (Van Marion, 1999), by filling in of the cut-off channels near the closure dam (Eisma and Wolff, 1980; Berger *et al.*, 1987).

With the exception of an approximate 40 year period after closure of the Zuiderzee the ebb-tidal delta remained in a stable state, only the main channels relocated to a distinct southward orientation (see the upper panels of Fig. 2-7). Elias *et al.* (2005) showed that after closure the increased ebb outflow was more southward directed (due to the changes in tidal propagation and basin geometry) towards Schulpengat, triggering the change of this former flood-dominated channel into the main ebb channel[(1)]. Initially, Schulpengat developed as a single channel but since 1956 A.D. two separate channels (Schulpengat and Nieuwe Schulpengat) formed in an updrift direction aligned along the North-Holland coastline (Fig. 2-7, 1965 A.D. - 2000 A.D.). The gross changes took about 40 years to complete and a maximum channel length was reached in approximately 60 years. During the same period the ebb-tidal delta showed a southward and northward growth. In the south sediment supplied by the main tidal channels develops a new ebb-delta front, while wave-driven transports contribute to landward and northward directed redistribution of sand from the abandoned ebb-delta front (western margin of Noorderhaaks). This northward transport contributes to the elongate outbuilding of the ebb-delta along the Texel coastline.

The re-orientation of the main channels and shoals has had large consequences for coastal maintenance; over 200 Mm^3 of sand was eroded from the ebb-tidal delta and adjacent coastlines (Van Marion, 1999). Both, the Texel as the North-Holland coastline are still subject to structural erosion (Cleveringa, 2001; Elias and Cleveringa, 2003) and maintenance of these coastal stretches belongs to the most intensive of the entire Dutch coastal system (Mulder, 2000; Roelse, 2002).

(1) A discussion remains whether the ebb-tidal delta wouldn't have shown a similar southern development without Closure of the Zuiderzee. Schulpengat already showed a southward development along the North-Holland coast prior to damming (see Fig. 2-6). Closure of the Zuider Sea might not be responsible for the southward development, but has accelerated and increased the changes. It is questionable if without the Closure Westgat would have become abandoned, as the channel remained stable in the forgoing period. The pre-closure rotation might possibly be related to smaller-scale land reclamation works in the basin such as closure of Amsteldiep connecting the former island Wieringen to North-Holland (just south of the inlet).

2.2.5 Summary of back-barrier evolution and its impact on the ebb-tidal delta

The different stages of ebb-tidal delta evolution and the main features of the inlet throat and basin are summarized in Fig. 2-8. It is clear that the major changes in ebb-tidal delta evolution are related to changes in the tidal basin and in the inlet throat.

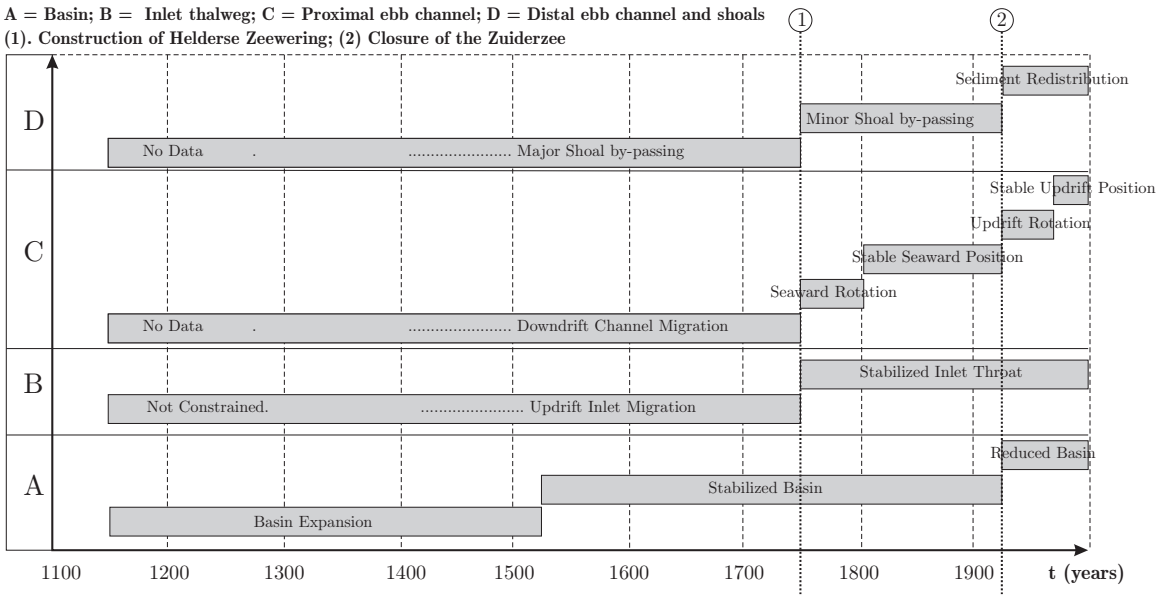

Figure 2-8: Observed behaviour of the Texel Inlet system over the period 1100 A.D. - 2000 A.D., sub-divided in the elements basin (A), inlet throat (B), proximal ebb channel (C) and distal ebb-channel and shoals D).

Evolution of the back-barrier basin can be summarized as; (1) expansion, partly related to human activities such as the excavation of peat and subsidence of the surface level due to drainage, (2) stabilization, due to construction of dykes, embankments and coastal protection works in the basin, and (3) reduction, due to damming. It is to be expected that the tidal prism and inlet dimensions followed the increase and subsequent stabilisation in back-barrier dimensions. Unfortunately no bathymetric data are available to describe the ebb-tidal delta evolution prior to 1550 A.D. Although little information is present, we assume that the stable inlet state was established around 1600 A.D.

Prior to 1750 A.D. the inlet throat was relatively unconstrained, and migrated to the south. Meanwhile, the ebb-tidal delta showed a downdrift skewness due to periodic ebb-delta breaching and downdrift migrating channels and shoals. With a relative stable basin we can assume that this behaviour is fairly representative for the 'natural' state. After stabilization of the inlet throat, by formation of Helderse Zeewering, a westward-directed, main ebb channel formed (1750 A.D. - 1810 A.D.). With the exception of an approximate 40 year period after closure of the Zuiderzee the ebb-tidal delta remained in this stable state, only the channels relocated to a distinct southward orientation. The gross change took about 40 years to complete and a maximum channel length was reached in approximately 60 years. Ever since sediment is redistributed from the abandoned ebb-delta front (western margin of Noorderhaaks) into the basin (major part), and to the new ebb-delta front formation in the south (minor).

2.3 Conceptual model for the evolution of mixed-energy inlet systems

The well-monitored large-scale changes on the ebb-tidal delta initiated by construction of Helderse Zeewering and closure of the Zuiderzee show that in addition to the wave-energy/tidal-energy ratio inlet modifications and back-barrier processes are vital for a correct description of the ebb-tidal delta dynamics and processes of Texel Inlet. Therefore, a conceptual model is proposed to describe the evolution of the inlet (Fig. 2-9) that takes into account the constraining effects of the inlet throat and back-barrier. We introduce the term 'back-barrier steering' as the sum of all possible constraints that might influence the outflow onto the ebb-tidal delta, such as tidal prism, oblique basin-channel orientation, composition of the subsurface, and anthropogenic forcing.

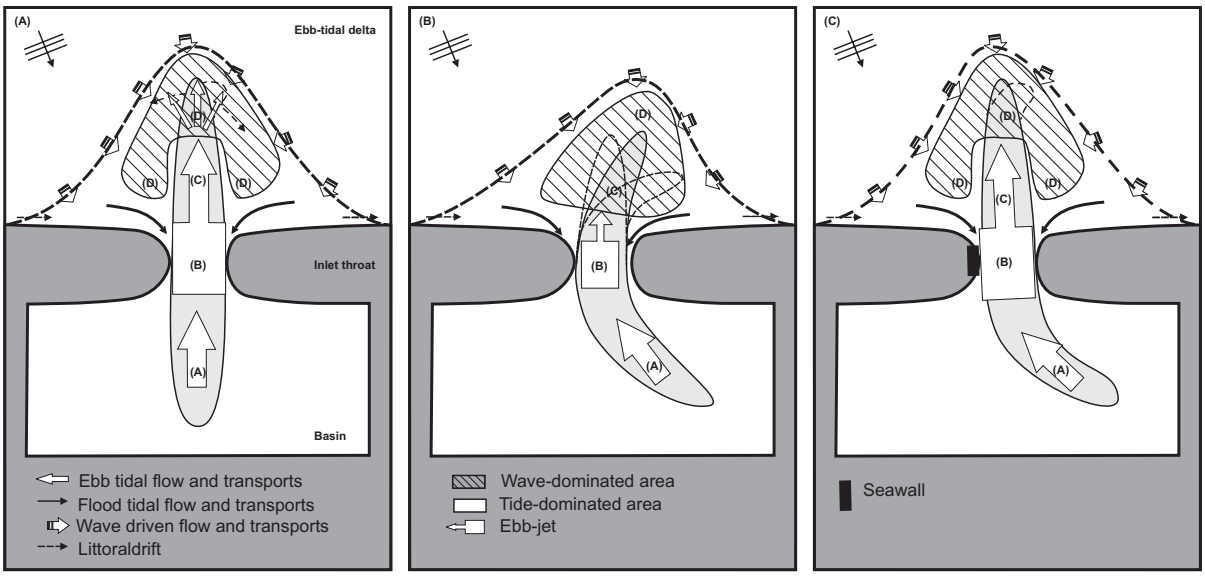

Figure 2-9: Conceptual model description based on the wave- versus tide-dominated areas and back-barrier steering.

Our model description elaborates on the concepts of e.g. FitzGerald (1982; 1988), Kana *et. al.* (1999), Dean (1988), Oost and de Boer (1994). The morphological system consists of the three basic elements; basin, inlet throat and ebb-tidal delta. These elements are coupled through a main ebb-channel comprising four coupled domains, to represent the contributions of the separate elements (Fig. 2-9). These domains are;

A. basin channel
B. inlet throat
C. proximal ebb-channel (tide-dominated part of the ebb-tidal delta)
D. distal ebb-channel including the ebb-shield (wave-dominated part of the ebb-tidal delta).

During ebb the basin is primarily drained by flow through the (main) basin channel (domain A). The maximum tidal prism magnitude is determined by tidal range and maximum basin storage area. For inlet systems with well-developed channels and shoals in the

back-barrier (common to most of the Wadden Sea inlets) or systems having constrained inlet throats (e.g. due to seawalls, jetties or bedrock) it is not only tidal prism that is important, but also the configuration of the basin and inlet throat can exert an additional constraint in or forcing on the ebb-tidal delta behaviour. The importance of back-barrier steering controlling ebb-tidal delta configuration was illustrated by FitzGerald *et. al.* (1984) for the East Frisian Islands, while Hicks and Hume (1996) showed the importance of bedrock controlled ebb-jet realignment for inlets in New Zealand.

The orientation of the main channel in the basin dictates the initial direction of the ebb outflow into the inlet throat. In the limited cross-sectional area of the constricted inlet throat (Domain B) the ebb flow is confined and accelerates, forming an ebb-jet outflow onto the ebb-tidal delta (see e.g. Oertel, 1975). The ebb-jet magnitude determines the seaward protrusion of the ebb channel; larger ebb flows have a greater sand carrying capacity and are capable of transporting sand further seaward onto the ebb-tidal delta (e.g. Oertel, 1975; Kana *et al.*, 1999; Gaudiano and Kana, 2001). Ebb-jet flow is characterized by maximum axial flow velocities and a large erosive potential. Due to this erosive potential the proximal channels are deep (Domain C) and in The Netherlands often scoured into semi-consolidated layers which contributes to the stability of the channel (Sha, 1989d). In Domain C, the proximal ebb-channel, the large axial flow velocities are capable of retarding lateral sediment inflow (due to littoral drift or shoal migration) by flushing sediment seaward during ebb or towards the basin during flood. In a seaward direction, the strength of the ebb-jet diminishes due to bottom friction and segregation of flow. Meanwhile, wave-driven currents increase due to waves breaking on the terminal lobe of the ebb-tidal delta. Consequently, wave-driven currents become increasingly important in channel development. Tidal flow tends to develop the main channel in the direction of the largest, tide-averaged, water surface gradient (Van Veen, 1936)[2], but shoal migration and deflection of tidal flow by these shoals can induce channel migration. Domain D is described as the area where the terminal lobe and channel are governed by the dynamic balance between landward-directed wave-driven transports and seaward-directed tidal transports.

Waves redistribute sediment landward and on the shoals a landward residual transport prevails. An important element completing the inlet circulation is the presence of flood channels, often along the adjacent coastlines. The ebb-jet generates vortexes on its side and near the coast a flood surplus prevails. Postma (1967) shows that also the phase difference between the horizontal and vertical tide is of importance for the formation of separate ebb and flood channels. The flood channels are of major importance for transporting sediments back into the basin and often these channels induce erosion of the coastlines.

The ebb-tidal delta evolution, which is basically the evolution of domain C and D, can be described by existing concepts such as the models of sediment bypassing of FitzGerald (1982; 1988) and FitzGerald *et al.* (2000), the meso-scale model of Kana *et al.* (1999) and

[2] A major difference with the US inlets described in the work of e.g. Oertel, Kana and FitzGerald is the open-sea tidal wave propagation at the Dutch Wadden Sea inlets. As a result at a phase difference exists between the inlet and open-sea currents, and a preferential updrift orientation of the main channel is observed (Van Veen, 1936; Sha 1989c).

the descriptions of e.g. Hayes (1975), Hubbard *et al.* (1979), Oertel (1975). For systems in which wave energy is small compared to tidal energy, the ebb flow is capable of removing the lateral sediment supply from the shoals which results in a stable channel (domain C) that extends seaward (e.g. Fig 2-1c; stable inlet process). In inlet systems where waves dominate, the cross-shore and lateral wave-driven transports are capable of filling in or deflecting the ebb-channel causing periodic and/or cyclic movements of the channels and shoals (e.g. Fig 2-1a or b; cyclic or outer channel shifting sediment bypassing mechanisms). These inlets exhibit ebb-tidal deltas that are pushed close to the inlet throat. In this type of system domain C is small and the major part of the ebb-delta channel falls in domain D.

Such an ebb-tidal delta existed prior to the formation of Helderse Zeewering. A southward migrating inlet throat and northerly longshore transport system resulted in northward migration of the channel and shoal system. Periodic shoal breaching and channel relocation are the dominant mechanisms for sediment bypassing (major shoal bypassing); see Figure 2-9(B). A stable channel (Domain C), developed after construction of Helderse Zeewering, limiting migration of the tidal channels and minor shoal bypassing occurred on the large swash platforms; see Figure 2-9(C). This stable state remained after closure of the Zuiderzee, although the imbalance between the augmented, southward directed ebb-jet and the ebb-delta bathymetry shifted the large tidal channels to a southward direction.

2.4 Discussion

The substantial changes in ebb-tidal delta evolution of Texel Inlet provide a clear example of the responses of an inlet system to the cumulative effects of human intervention. Human interventions are important in the initial stage of inlet and basin enlargement; the basin area increased due to subsidence, excavation and drainage of low-lying peat areas bordering the inlet's initial basin for agricultural use. This might have expanded the inlet system beyond a size that would normally be expected for the given tidal prisms as storm surges flood these low-lying areas and increase flow velocities and scour considerably. Nevertheless, during this period human interventions directly influencing the ebb-tidal delta behaviour are limited, and therefore we describe the ebb-tidal behaviour during this period being in a 'natural' state. Ever since, the influence of human activities, such as construction of dykes, embankments and coastal protection works in the basin and at the inlet throat increasingly constrained and affected the natural inlet behaviour.

Among others Oertel (1975) and Kana *et al.* (1999) showed that the ratio between tidal prism and wave energy primary controls the gross-scale distribution of the channels and shoals on the ebb-tidal delta. Such classifications have proven valid in situations where flood deltas are absent and the predominant sand bodies associated with the inlet are confined to the ocean side of the system (as defined in Kana *et al.*, 1999). One of the main findings of this study is the significant effect of back-barrier processes on the development of the ebb-tidal delta. The evolution of Texel Inlet shows that in inlet systems with well-developed channels and shoals in the back-barrier (common to most of the

Wadden Sea inlets) or systems having constrained inlet throats (e.g. due to seawalls, jetties or bedrock) the basin and inlet throat can exert an additional important constraint or forcing (e.g. back-barrier steering) on the ebb-tidal delta behaviour.

The response of the ebb-tidal delta to closure of the Zuiderzee illustrates that engineering works can significantly influence the inlet dynamics and can cause the inlet to develop differently from what would be derived from the generally accepted equilibrium relations and conceptual inlet models. Although the tidal prisms in the inlet increased considerably (~ 26%) due to the changed tidal characteristics, the ebb-tidal delta volume did not increase (Walburg, 2001; Elias *et al.*, 2003b), as would be expected from empirical relations (e.g. Walton and Adams, 1976). Possibly, due to a dominant sand demand of the basin and only a limited sand source (adjacent coastline), no sand is available for the ebb-tidal delta growth. An alternative explanation for this inconsistency is that the ebb-tidal delta volume exceeded the equilibrium volume prior to the closure due to storm surge related deposits (Kragtwijk, 2001). During storms, the associated set-up in the entire Zuiderzee basin could have caused the effective tidal prism through the Texel inlet to increase considerably. The resulting greater than average ebb-currents and transport may have contributed to an ebb-tidal delta that expanded beyond the equilibrium size, that would otherwise be correlated to the mean tidal prism, but that corresponds with the equilibrium volume related to the increased tidal prism after the closure.

Two aspects which have not been considered in detail are the lithology of the ebb-tidal delta's subsurface and possible constraints imposed by the adjacent coastlines. Analysis of literature and core data (Sha, 1989d; Van der Spek and Van Heteren, 2004) shows the presence of erosion resistant layers. These layers must have contributed to the stability of the larger tidal channels and the inlet throat. The second aspect concerns the influence of changes in sediment supply by the adjacent coastlines on inlet development. Coastal protection works along the Holland coast date back to the Middle Ages, but especially during the last century numerous groins, breakwaters and seawalls were constructed that limited the landward retreat of the coastline and possibly the sediment transport towards the inlet.

2.5 Concluding Remarks

A series of regular bathymetric surveys of Texel Inlet and its ebb-tidal delta spanning a period of over 400 years forms a unique long-term morphodynamic dataset of this largest inlet of the Wadden Sea. The substantial changes in ebb-tidal delta evolution provide a clear example of the response of the inlet system to the cumulative effects of human intervention.

Analysis of the evolution of the ebb-tidal delta morphology shows different stages, each characterized by specific orientations of the main channels and shoals. Prior to construction of the Helderse Zeewering (extensive coastal defence works on the southern shore of the inlet in 1750 A.D.) the ebb-tidal delta showed a downdrift skewness. Periodic shoal breaching and downdrift channel relocation are the dominant mechanisms for sediment

bypassing (summarized as major shoal bypassing). After construction of the Helderse Zeewering a stable ebb-tidal delta with a westward stretching main ebb-channel developed over a period of c. 60 years. Closure of the Zuiderzee, the major part of the back-barrier basin, which was completed in 1932 A.D., temporarily distorted this stable state and over a period of about 40 years the main channel switched to a southward course, remaining stable ever since.

The well-monitored large-scale changes on the ebb-tidal delta which were initiated by the construction of the Helderse Zeewering and closure of the Zuiderzee show that incorporation of inlet modifications and back-barrier processes is vital for a correct description of the ebb-tidal delta dynamics and processes of Texel Inlet. Therefore the concept of back-barrier steering, which is the sum of all possible constraints that might influence the outflow onto the ebb-tidal delta, viz. tidal prism, oblique basin-channel orientation, throat constriction and composition of the subsurface, is introduced. A conceptual model is proposed as a framework to account for back-barrier steering on the evolution of the inlet systems with well-developed channels and shoals in the back-barrier (common to most of the Wadden Sea inlets) or systems having constrained inlet throats. The model couples the basic morphological elements basin, inlet throat and ebb-tidal delta through a main ebb-channel comprising the domains: 'basin channel', 'inlet throat', 'proximal ebb-channel' and 'distal ebb-channel'.

2.6 Acknowledgements

The work herein was carried out as co-operation between Delft University of Technology, the Netherlands Institute of Applied Geoscience TNO - National Geological Survey and RIKZ (Dutch National Institute for Coastal and Marine Management). Funding was provided by the Dr. Ir. Cornelis Lely Foundation. Data were made available by the Directorate-General of Public Works and Water Management (Rijkswaterstaat). The authors thank Prof. M.J.F. Stive, dr. J. Cleveringa, Prof. D.M. FitzGerald (reviewer) and an anonymous reviewer for their constructive comments and contributions to the manuscript.

Chapter 3
Tidal inlet dynamics in response to human intervention

Impressions of the Zuiderzee works

Abstract:

The effects of large-scale human intervention on inlet dynamics are studied. In particular, the response of the largest of the Wadden Sea inlets (Texel Inlet) to the closure of a major part of its inner basin is re-analysed. The re-analysis is based on datasets of bathymetry, discharges and water levels that have been obtained by intensive monitoring of both the inner basin and the ebb-tidal delta. Based on this re-analyses and modern theoretical knowledge a conceptual model is postulated that describes the morphologic adjustment of tidal inlets due to large-scale human intervention. The kernel of this model is that the morphological adjustment towards a new overall equilibrium is split into two stages related to the existence of more then one temporal response scale.

©Elias *et al.* (2003b), Coastal Engineering Journal 45(4), 629-658

Awarded the Coastal Engineering Award 2003 for excellent research achievement by the Japanese Society of Civil Engineers

3.1 Introduction

Tidal inlets and their ebb-tidal deltas play a substantial role in the coastal evolution of the adjacent shorelines. Several studies, (e.g. Bruun and Gerritsen, 1960; FitzGerald, 1988; Oertel, 1988; Stive *et al.*, 1998) have considered the long-term development of aggregated features. Various empirical relations describing the morphological properties of the inlet, ebb-tidal delta and back-barrier basin have been developed. These relations have recently been summarized by Buonaiuto and Kraus (2003). However, due to the complexity of physics involved, still many aspects of inlet processes are not fully understood. In the meantime, large-scale interventions have taken place or are planned for these environments.

Further understanding can be obtained from process-based modelling (e.g. Wang *et al.*, 1995; De Vriend and Ribberink, 1996; Cayocca, 2001). However, process-based models need comprehensive validation and calibration before being applied in the complexity of the inlet domain, especially if one aims to predict the response of an inlet system to (large-scale) interventions. Detailed datasets of measurements are required for validation and calibration. The fact that these datasets are not only useful for validation and calibration, but are a value in themselves is nowadays often overlooked by coastal engineers. A thorough analysis of measurements can provide valuable understanding of inlet behaviour.

To illustrate the above statement, this paper aims to provide insight in the responses of a tidal inlet system to the effects of closure of a major part of the basin. The paper concerns the behaviour of the Texel tidal inlet in the Netherlands. Through the construction of the 30 km long closure dam, the Afsluitdijk, completed in 1932, the Texel Inlet basin area reduced considerably. The closure drastically distorted the autonomous behaviour of the inlet system and large-scale effects in the hydrodynamics and consequently the morphodynamics were observed. In hindsight, previous studies on Texel Inlet do not give a univocal answer on the behaviour of the inlet since this closure. Fortunately, after the closure, the inlet was and still is intensively monitored by the Rijkswaterstaat (Agency of the Ministry of Transport, Public Works and Water Management). The availability of high-quality observational data of bathymetry, discharges and water levels forms a unique opportunity to evaluate inlet and in particular ebb-tidal delta dynamics under the influence of this large-scale human intervention.

The initial focus of this paper is on the description of the morphological development of the tidal basin since the closure, mainly based on the analysis of bathymetric data. The final focus is on the behaviour of the ebb-tidal delta. The paper starts with a description of the physical setting of Texel Inlet and a re-analysis of observations. This is followed by new results of the analysis of the morphodynamic changes in the basin and on the ebb-tidal delta since the closure. We subsequently discuss the changed dynamics of the ebb-tidal delta, present a conceptual model for Wadden Sea inlets impacted by large-scale interventions and specify this model for the development of Texel Inlet. We conclude by generalizing some of our findings that contribute to our understanding of tidal inlet behaviour under human intervention.

3.2 The Texel Tidal Inlet

3.2.1 Setting of the study area

Texel Inlet is the largest tidal inlet of the Dutch Wadden Sea, and is located in the North of the Netherlands between Den Helder and the barrier island Texel. Figure 3-1 shows the present-day geometry and bathymetry of Texel inlet including its drainage area. Following the classification of Hayes (1979) the inlet qualifies as mixed-energy wave-dominated, even under spring tide conditions. However, the morphology of the inlet shows tide-dominated characteristics such as a large ebb-tidal delta. This is caused by the large tidal prism and the relatively low wave energy (Davis and Hayes, 1984). A small supply of fresh water through the discharge sluices at Den Oever and Kornwerderzand is present.

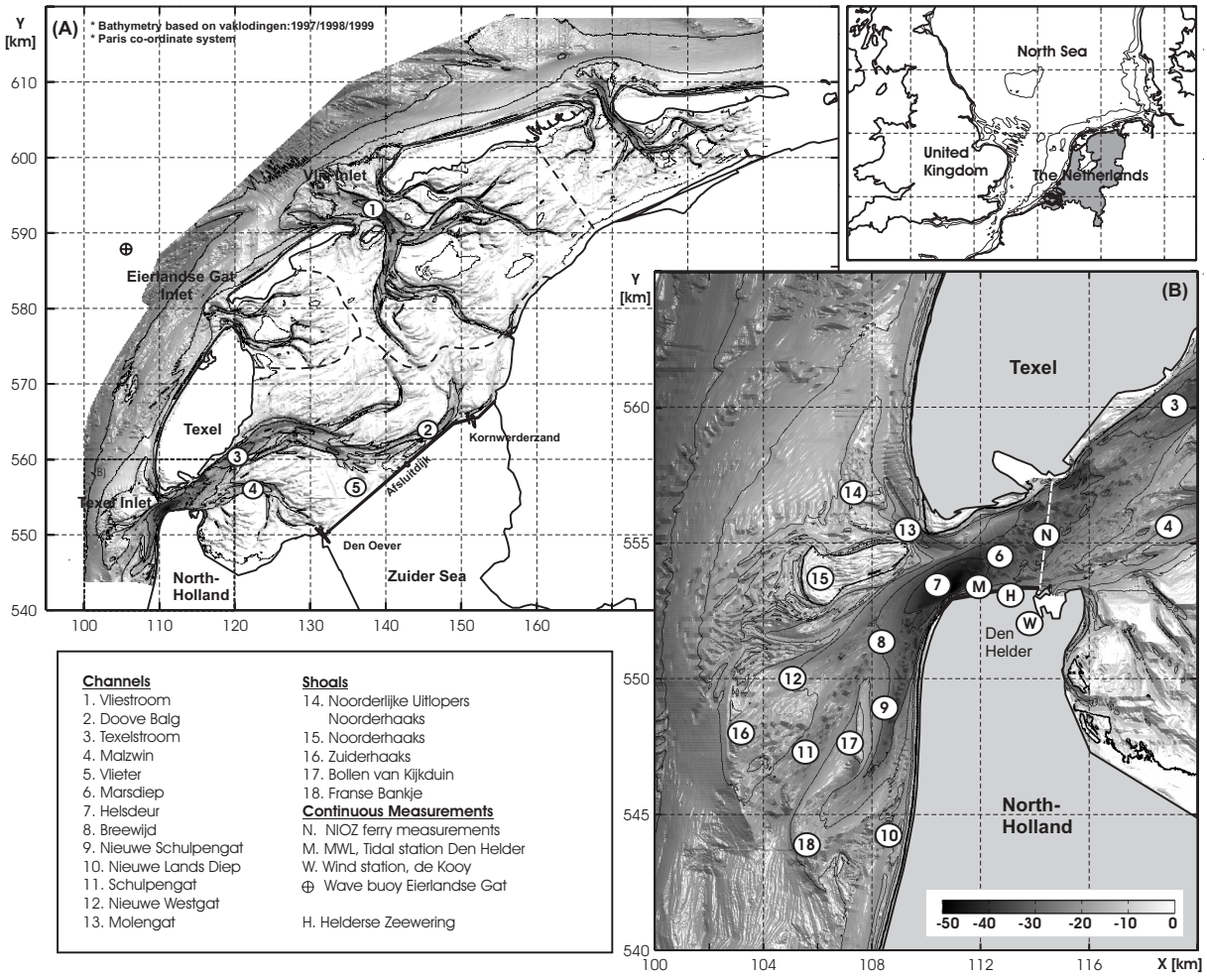

Figure 3-1: Location map of the Texel Inlet.

The inlet gorge is formed by the Marsdiep that has a minimum width of about 2.5 km and a maximum depth of 53 meters. The Marsdiep gorge forms the connection between the main channel in the basin, Texelstroom, and the main-ebb channels, Schulpengat and Nieuwe Schulpengat, on the ebb-tidal delta. Since 1998 flow through the inlet has been

continuously measured using an Acoustic Doppler Current Profiler (ADCP) attached to the hull of the ferry from Den Helder to Texel island, the *ms* Schulpengat of the TESO company (Ridderinkhof *et al.*, 2002). On average the tidal prism through the inlet is $1x10^9$ m^3, with both ebb and flood tidal velocities between 1 and 2 m/s. Based on harmonic analysis of the flow measurements, Ridderinkhof *et al.* (2002) observed a volume transport through the inlet that is dominantly tidally driven, with the semi-diurnal M_2 and S_2 and their higher harmonics being the largest constituents. The net discharge is seaward directed, with a magnitude of about 4% of the amplitude of the semi-diurnal tide.

The ebb-tidal delta protrudes approximately 10 km seaward and 25 km along-shore, determining the nearshore bathymetry of the adjacent North-Holland coast in the south and the Texel Island coast in the north. The ebb-tidal delta contains a large supra-tidal shoal area (Noorderhaaks) facing Marsdiep. On the southern part of the ebb-tidal delta, along the North-Holland coastline, the two main channels (Schulpengat and Nieuwe Schulpengat) are updrift orientated, with respect to the direction of tidal wave propagation. Along Texel Island, a smaller channel (Molengat) separates the coastline and the Noorderhaaks shoal.

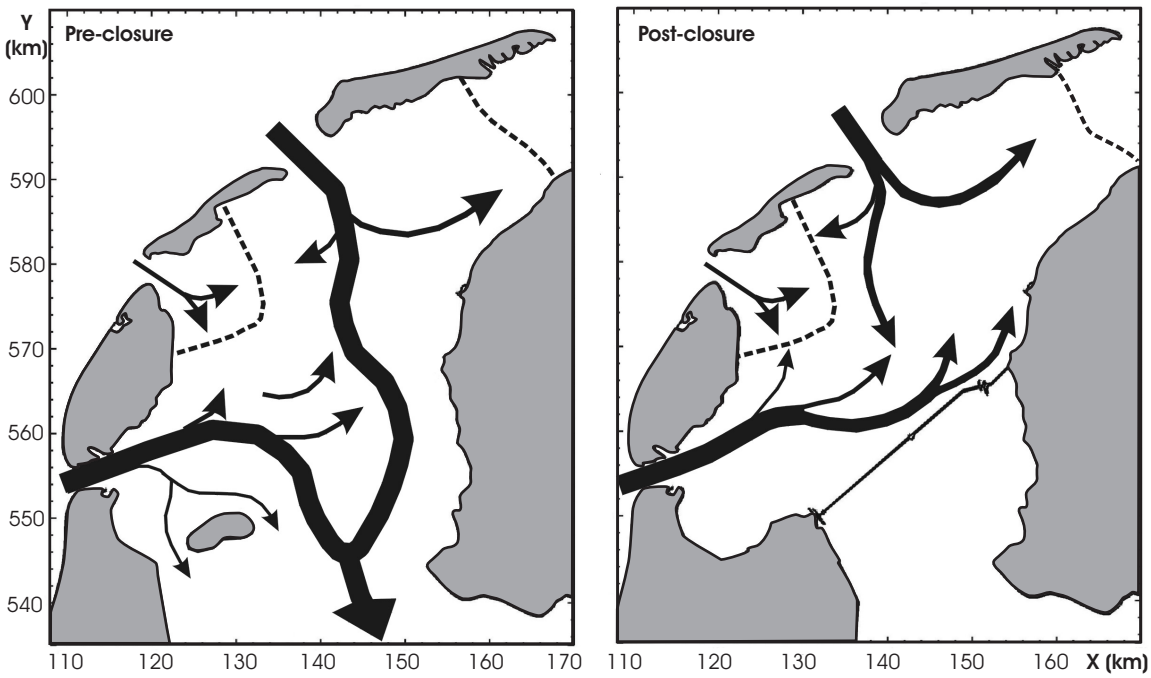

Figure 3-2: Impression of the tidal wave propagation prior (left) and after closure (right); redrawn after Thijsse (1972).

Preceding the closure in 1932, the Texel and Vlie inlet tidal basin covered the southwestern part of the Wadden Sea and the former Zuiderzee (Fig. 3-2, left panel). In total, the basin covered a surface area over 4.000 km^2 with a basin length of 130 km. After the closure, the basin area reduced substantially to an area of 712 km^2 (Fig. 3-2, right panel) and a length of about 30 km. The two basins, Texel and Vlie, are now separated by a tidal divide (see Fig. 3-1) with only a minor residual transport between the two basins

remaining. The magnitude of this exchange is estimated being 1% of the transport amplitude in the inlets (Ridderinkhof, 1988).

About 17% of the basin consists of inter-tidal flats. Most of the seabed sediment consists of fine sand with a median grain size around 200 μm. Coarser sand is found on the channel floors near the inlet (> 300 μm), and the grain size distribution decreases towards the mainland. At the location of the Afsluitdijk, median grain sizes vary around 180 μm. Of the sediment that settles within the Wadden Sea, some 70 to 80% consists of sand while the remainder is silt and clay (Oost, 1995).

3.2.2 Tidal conditions

The tidal movement along the Dutch coast and the Texel inlet is mainly determined by the tidal wave entering the North Sea from the Atlantic Ocean between Scotland and Norway. In the North Sea the tidal wave is distorted, and this results in a Kelvin wave that propagates along the Dutch coast from the south to the north. At Texel Inlet, the tidal movement is the main driving force for the horizontal water flow, with the semi-diurnal M_2 constituent being the dominant component. The tide has a mean range of 1.38 m in Den Helder that increases up to 2.0 m during spring tide, while during neap tide it reduces to about 1.0 meters. The tidal curve is asymmetrical mainly due to distortion of the M_2 tide by the M_4 constituent. This distortion results in a faster rise than fall of the tide.

3.2.3 Wind and wave conditions

Overviews of the governing wind and wave conditions along the Holland coast and Texel inlet are presented by, e.g. Roskam (1988), De Ronde *et al.* (1995) and Wijnberg (1995). In brief, the wave height distribution at the ebb-tidal delta is dominated by wind-generated waves in the North Sea basin with only a minor contribution of swell. The yearly mean wind direction is west-southwest, which corresponds to the direction of the mean wave height on the ebb-tidal delta. Wave measurements at the nearby Eierlandse Gat, located at a water depth of 26 m (co-ordinates X: 106.514, Y: 587.985 m), are representative for the Texel Inlet. A mean significant wave height of 1.3 m with a corresponding mean significant wave period of 5 s is observed. During storms, wind-generated waves can exceed 6 m, and additional water level set-ups of over 2 m have been measured at Texel Inlet.

3.3 Re-analysis of observations

Texel Inlet has been well monitored over a long period. Historic reconstructions have been made that describe the inlet since the 16th century (Sha, 1990; Schoorl, 1999; Elias and Van der Spek, 2006, [Chapter 2 of this thesis]). Navigational charts are available from 1796. After the closure monitoring campaigns by Rijkswaterstaat intensified. This has resulted in the availability of large, detailed datasets of digitally available echo-sounding based maps, discharges, water levels, wind, waves, current velocities and sediment observations.

3.3.1 Hydrodynamics of the basin

Hydrodynamic studies of the basin have extensively used the available data. Clear descriptions of the consequences of the closure on the tidal flow patterns in the basin are presented in the studies of e.g. Battjes (1962); Rietveld (1962); Thijsse (1972); Klok and Schalkers (1980); Doekes (1985); Ligtenberg (1998) and Kragtwijk (2004).

The closure of the Zuiderzee (or Zuider Sea) has decreased the Texel Inlet basin area substantially, whereas the tidal prism increased about 20%. This apparent contradiction mainly results from the changed characteristics of the tidal wave in the basin. Preceding the closure, the tidal wave in the Zuiderzee consisted of the combined tidal waves of the Texel and Vlie inlets. These two tidal waves propagated separately through the Wadden Sea and merged into one tidal wave in the Zuiderzee area (as illustrated in Fig. 3-2, left panel). The tidal wave reflected at the southern boundary of the Zuiderzee basin, about 130 km inland from the Texel inlet. The basin length (L) equals about half the tidal wave length (λ) and, in a hypothetical situation without bottom friction and the wave propagating at an oblique angle to the shore, a standing wave would form in the basin. In such case, at the location $L \approx 0.5\lambda$ from the southern boundary an anti-node in water level occurs at which discharges are zero and all exchange of water south of this boundary takes places in the basin.

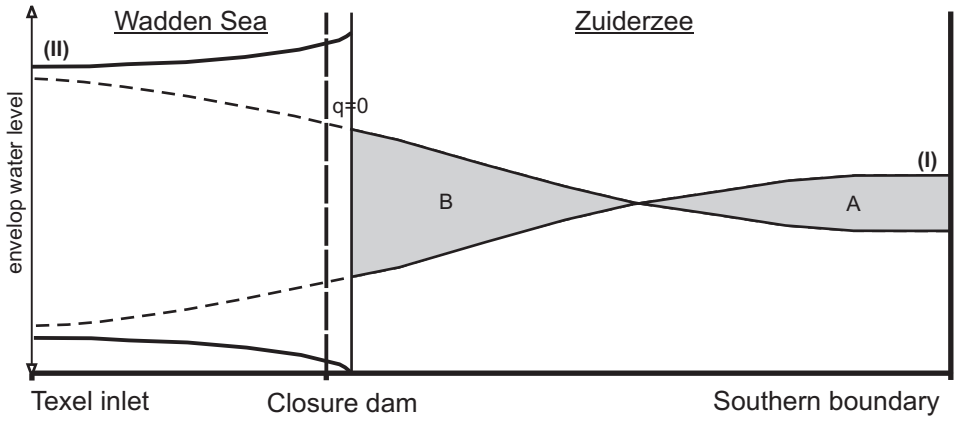

Figure 3-3: Schematization tidal wave envelop prior (I) and after the closure (II).

In reality, the tidal wave propagating through the Zuiderzee, that is limited in depth, decreased and deformed by bottom friction. The reflected tidal wave is considerably smaller in amplitude than the incoming tidal wave. The interference of the two waves results in the formation of a damped tidal wave with a propagating character at the inlet and a standing character near the southern boundary. A schematization of the resulting tidal wave envelop is indicated by (I) in Figure 3-3 (after Kragtwijk, 2001).

The no-exchange boundary (indicated by $q = 0$ in Fig. 3-3) is no longer located at $L \approx 0.5\lambda$, but is formed at the location where the areas indicated by (A) and (B) balance. This location is closer to the southern boundary. The actual location of the closure dam is north of the no-exchange line because the tidal ranges in the basin were predicted to increase substantially. Due to the closure dam the basin length reduced to about 30 km (Fig. 3-2, right panel) that is small compared to the tidal wave length ($L \approx 0.2\lambda$), and a tidal wave is formed with a standing wave character. This strong decrease in basin length reduced the damping of the tidal wave due to friction and with more reflection at the closure dam the tidal ranges increased drastically (tidal wave envelope after the closure indicated by (II) in Fig. 3-3). This is the reason that the location of the closure dam was chosen seaward of the no-exchange location, i.e. to minimize the changes in flow velocities through the inlets (Lorentz, 1926).

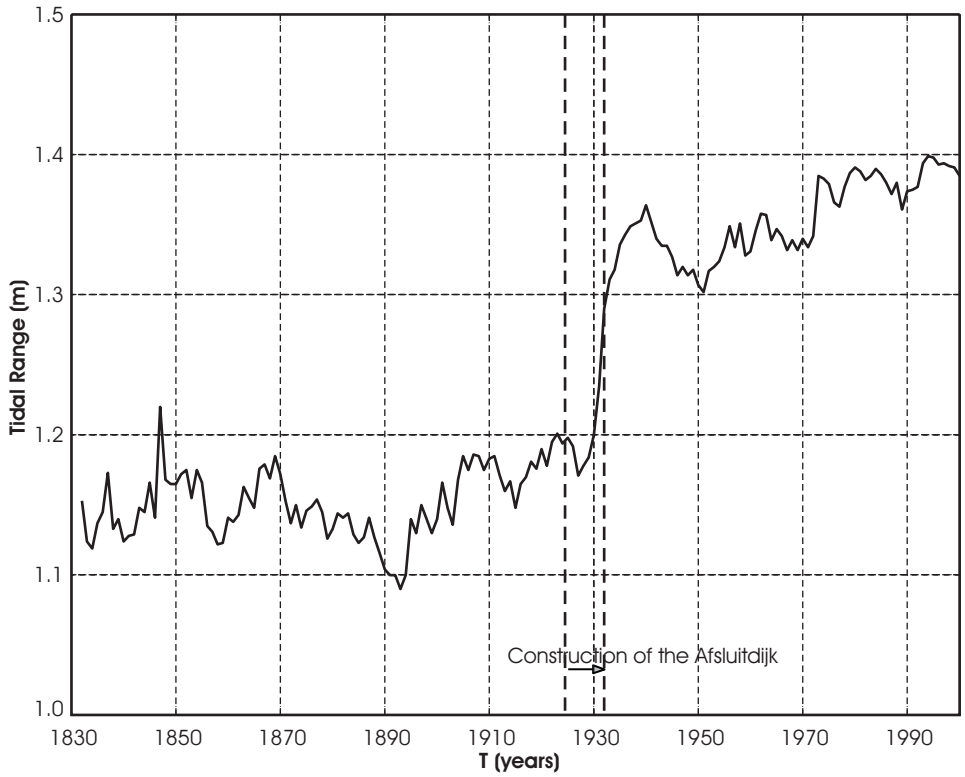

Figure 3-4: Tidal range station Den Helder measured over the period 1830 - 2000.

Alterations in tidal range and tidal volumes were predicted and have occurred. The increase in tidal range is clearly reflected in Figure 3-4 by the water level observations of the measuring station Den Helder, located in the Texel inlet gorge. The tidal ranges increased nearly instantaneous with approximately 15%. This corresponds reasonably with

the 21% increase predicted by Lorentz *et al.* (1926). At the location of the Afsluitdijk in Den Oever, the increase in tidal range was even more dramatic as an increase of nearly 100% was observed and predicted (Thijsse, 1972).

In addition to this increase in tidal range, the changed flow patterns in the basin must have contributed to the large changes in hydrodynamics and morphodynamics of the basin. The closure resulted in closing of the southward flow channels. Consequently, these channels lost their effective function, while flow through eastward channels increased. This latter flow was further enhanced by the eastward deflection of the tidal wave at the closure dam (Fig. 3-2, right panel). The two tidal waves originating from Texel and Vlie inlet now meet east of the original meeting point, at the location of Harlingen, forming a tidal divide. This eastward extension resulted in an actual drainage area that is slightly larger than the active part of the drainage area prior to the closure (Klok and Schalkers, 1980).

The analysis shows that most of the former Zuiderzee did not actively take part in the water exchange with the Wadden Sea. The basin area after the closure is at least comparable with the active basin area prior to closure. Combined with the enlargement of the tidal range an increase in tidal prism of about 26% was observed (and predicted).

3.3.2 Morphodynamic interactions

With these large changes in hydrodynamics and particularly in geometry, pronounced changes in basin morphology have occurred. This cause and effect can be deducted from empirical relations. Prior to the closure, it is plausible that the basin was in an equilibrium state and the size of the intertidal shoal area was related to the drainage area (Eysink *et al.*, 1992; Louters and Gerritsen, 1994). With the closure, the back part of the basin (Zuiderzee) that contained a relative large portion of shoals was separated from the basin. The remaining shoal area was too small relative to the area of the channels; therefore, a morphologic adjustment of the basin was to be expected during the initial stage of non-equilibrium after the closure.

The basin forms part of a coherent morphological system (De Vriend, 1996). The changes in hydrodynamics and morphodynamics of the basin must have had effects on the other parts of this system (e.g. the ebb-tidal delta and adjacent coastlines). For instance, Walton and Adams (1976) showed the direct correspondence between an inlets tidal prism and the volume of sand comprising the ebb delta shoals. The observed changes in tidal prism must have influenced the ebb-tidal delta. The morphological system can also be described as a sand-sharing system. By definition, all parts of such a system are coupled, and in dynamic equilibrium with each other under constant forcing. Changes in forcing or geometry of any part of the system results in sediment transport to or from other parts of the system (Oost, 1995).

Although various studies have analyzed the morphodynamic adjustment of the entire inlet system or its separate morphological units (basin or ebb-tidal delta), many questions remain. The basin has been analyzed by, e.g. Battjes (1962); Eysink *et al.* (1992); Eysink (1993); Biegel (1993) and Van Marion (1999). Although these studies all confirm

that sedimentation occurred after the closure, the conclusions about the observed morphological response time and present state of the basin (equilibrium or non-equilibrium, sedimentation or erosion) are more ambiguous.

The ebb-tidal delta was analyzed by Battjes (1962), Sha (1990), Van Marion (1999) and Walburg (2001), but no clear univocal conclusions are reached about morphological adaptation time and present state. A clear description of the interaction between basin and ebb-tidal delta is only presented by Battjes (1962). With the ongoing measurements, the analysis of longer time series contributes to an increased understanding of the ebb-tidal delta behaviour and its interaction with the basin.

Our morphodynamic investigations are based on analysis of bathymetric maps that are systematically constructed through weighted interpolation of the measurements onto a rectangular grid (50x50m resolution), where the weights are proportional to the reciprocal of the distance to the grid point. Basin and ebb-tidal delta bathymetry are considered separately as not all bathymetric measurements cover both units simultaneously. Basin measurements for the years 1933, 1951, 1965, 1972, 1977, 1982, 1986, 1991 and 1997 (see De Kruif, 2001) are used to estimate the basin's morphologic adaptation time based on volume changes. The volumes are determined with respect to a fixed reference height and area. The separation of the Texel, Vlie and Eierlandse Gat basins is based on the location of minimal water depth (as displayed in Fig. 3-1). The resulting computational area used covers 680 km^2, which is slightly smaller than the basin area of 712 km^2 as defined by Louters and Gerritsen (1994). The difference is mainly caused by not accounting for the utmost eastern part of the basin at the location of the watershed[(1)]. For each year, a correction for sand removal due to mining is applied. These gave only minor corrections.

The ebb-tidal delta is analyzed using measurements for the years 1925, 1933, 1950, 1975, 1981, 1986, 1991, 1994, 1997 and 2000 (see De Kruif, 2001). Complete bathymetric maps, covering the entire ebb delta domain including the adjacent coastlines, are derived for the years 1925, 1975, 1981, 1986 and 2000. In the years 1991, 1994 and 1997 the supratidal shoal area of the Noorderhaaks is not measured. The 1933 and 1950 measurements only contain the ebb-tidal delta and are bounded roughly by the –20 m contour at the seaward side. Sand volumes of the ebb-tidal delta are determined with respect to a fixed reference depth. The balance area is bounded at the seaward site by the –20 m depth contour, the landward boundary is formed by the 0 m contour, and the northern and southern boundaries are fixed and located outside the ebb-tidal delta perimeter. Correction for dredging, beach nourishments, and sea level rise are negligible relative to the total sand volume of the ebb-tidal delta (which is estimated to be in the order of $450x10^6$ m^3).

(1) Analysis of the present state ebb-delta and basin evolution indicates that a clear separation of the Texel and Vlie basins does not exist. Therefore recent sediment budget studies focuses on the entire western Wadden Sea (see Chapter 5 Appendix A of this thesis).

3.3.3 Re-analysis of morphodynamic basin changes

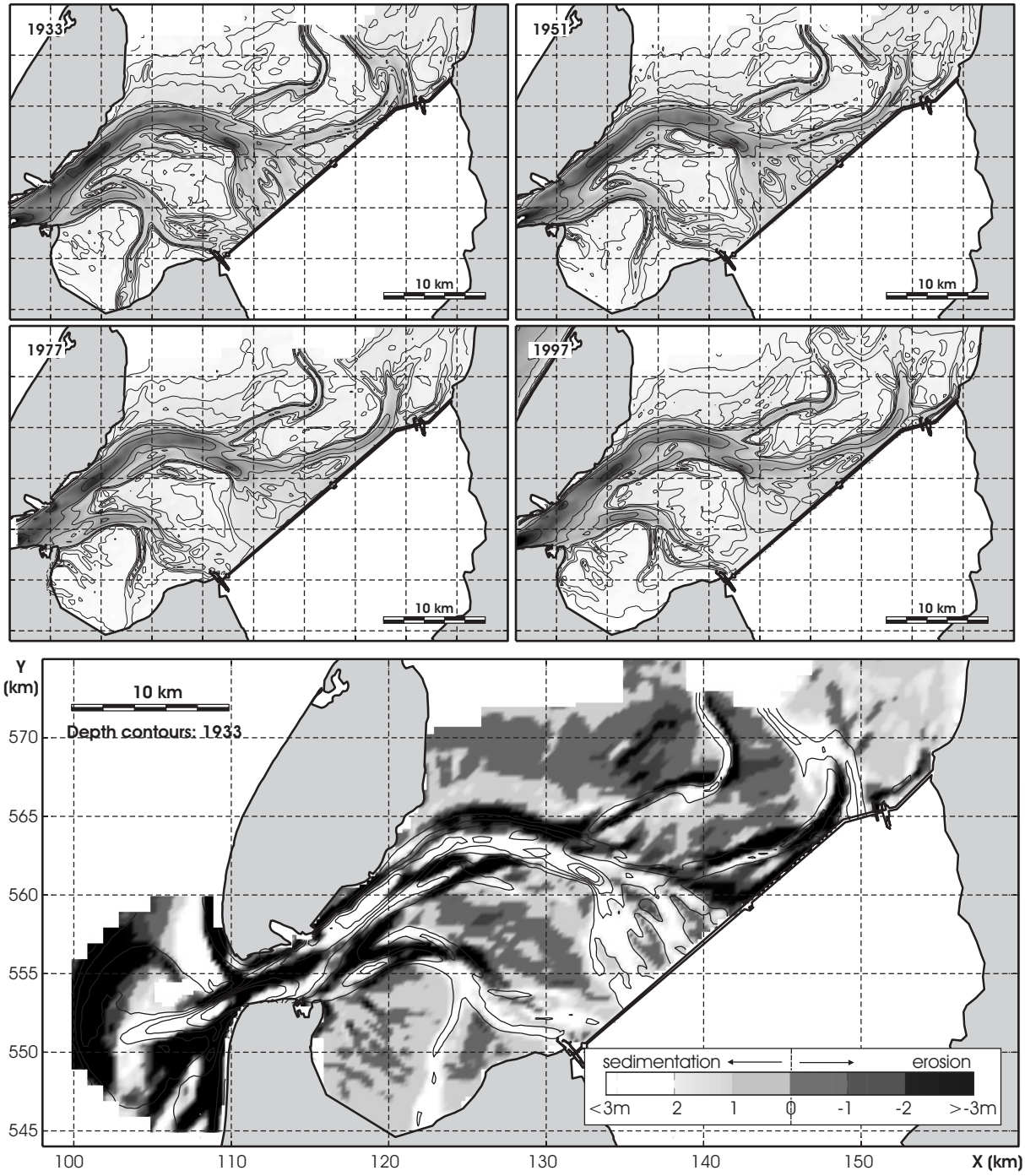

Figure 3-5: Upper four panels: bathymetric maps for the years 1933, 1951, 1977 and 1997. Lower panel: Sedimentation- erosion pattern over the period 1933 - 1997.

The analysis of the basin hydrodynamics indicates an increase in tidal prism and change in flow patterns after the closure. Comparison of the inlet bathymetry in 1932, just after the closure, with the 1997 bathymetry (Fig. 3-5, lower panel) shows the resulting drastic changes in basin and ebb-tidal delta morphology. Large sedimentation areas were observed in the terminal parts of channels (see, e.g. the Vlieter, Vliestroom and Tex-

elstroom) where tidal currents reduced to almost zero and the loss of discharge caused the channels to accrete rapidly (Berger *et al.*, 1987; Oost and de Boer, 1994).

Changes were also observed in the upper part of the Texelstroom (lower panel of Fig. 3-5). The alterations in flow patterns resulted in an increasing importance of this channel. A prominent feature is the lateral channel migration (Oost and de Boer, 1994) indicated by the alternating pattern of sedimentation and erosion areas. In addition, the Texelstroom migrated northward aligning along the Texel island back barrier shoreline. The inertia of the increased discharge and resulting increased flow through the channel extended the upper part of the channel in eastward direction. Such an eastward extension and increasing channel depth also occurred at the Doove Balg channel due to the eastward deflection of the flow at the closure dam.

The time development of the basin is illustrated in the upper 4 panels of Figure 3-5 based upon bathymetric maps for the years 1933, 1951, 1977 and 1997. The main changes in bathymetry occurred between the years 1933-1951 and 1951-1977, whereas changes between 1977 and 1997 were relatively small. This strengthens the impression that the basin had already completed the internal adjustment process by 1977 and regained an equilibrium or near equilibrium situation.

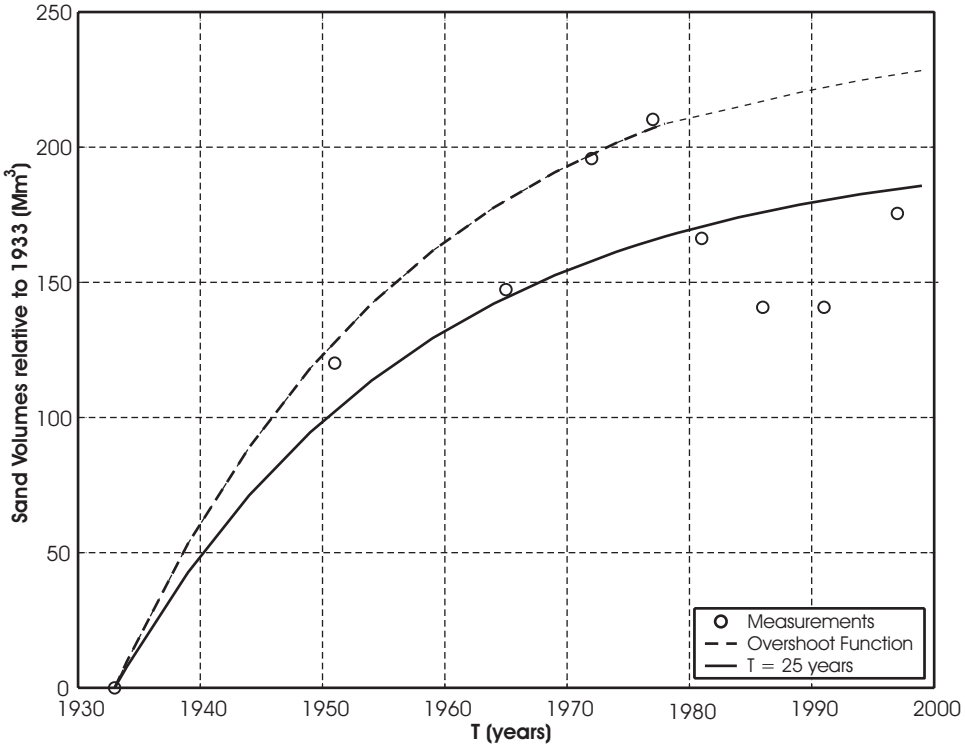

Figure 3-6: Sediment volume change in the basin with respect to 1933 volume.

To quantify the development of changes in the basin, we determined the sediment volume change (Fig. 3-6). A strong increase in sediment volume of the basin is observed after the closure. The sedimentation rate decreases towards a maximum sedimentation volume in 1977. Since 1977, alternating periods of increasing and decreasing sediment volumes suggest that a new equilibrium situation was reached. These results confirm the

conclusions of Van Marion (1999). In addition to the work of Van Marion (1999), we incorporate the observations to derive the morphodynamice adjustment time-scale for the developments in the basin. An exponential response function

$$V_t = V_{1988} + V_e\left(1 - e^{\left(\frac{1933-t}{T}\right)}\right) \tag{3-1}$$

is fitted in which V_t is the sand volume in year t, V_e the equilibrium sand volume (additional to the volume of 1933), and T is the response or adjustment time-scale. Applying this to the measurements, with an estimate of the additional equilibrium sediment volume of 200x10^6 m^3 (based on Fig. 3-6), a 25-year response time-scale is discerned. According to Eq. (3-1) in the year 2000, 93% of the total change should have occurred and it would take another 50 years to reach 99%. Although the basin volumes indicate a state that is close to a new equilibrium in the basin, the total inlets system (including ebb-tidal delta and adjacent coastline) may still be far from actual equilibrium (Gerritsen, 1990)[(2)].

This latter observation is further elaborated using the model results of Kragtwijk (2001) and Kragtwijk *et al.* (2004). In this study, different time-scales in the morphological response of the inlet to the closure are derived, based on linearization of the ASMITA equations (Stive *et al.*, 1998). It is shown that in this morphological system unequal timescales interact. These timescales differ in order of magnitude (years, decades, and centuries) due to the interaction between morphological units. For example, the interaction of a single channel and shoal acts on a short timescale of *O(years)*; interaction of the total basin acts on a medium timescale of *O(decades)*, and the adaptation of the entire morphological system of basin (channels and shoals), ebb-tidal delta (channels and shoals) and adjacent coastlines acts on a long-term timescale, *O(centuries)*.

In this respect, the large sediment volume change up to 1977 represents the response of the yearly and decadal time-scale causing the rapid filling in of the basin. The sediment volume in 1977, significantly higher than the values afterwards, might indicate an sedimentation surplus due to an overshoot of the interaction on the medium, decadal, timescale that is corrected afterwards (see Fig. 3-6, indicated by overshoot function). Kragtwijk (2001) explains this overshoot as a system of which the elements evolve towards an equilibrium state (given sufficient time); however, this evolution is not necessarily monotonous. It is possible that an element initially overshoots its equilibrium value and returns to equilibrium afterwards.

Since 1977, the adaptation of the entire inlet (ebb-tidal delta, basin and coastlines) dominates the sedimentation-erosion patterns that is estimated to act on a scale *O(centuries)*. The related changes on this time-scale of centuries are small relative to the yearly fluctuations. We assume these fluctuations to be due to seasonal fluctuations in

[2] This latter statement is illustrated by looking at the ratio between channels and shoals. In Texel basin this ratio is approximately 0.3, while in the eastern Wadden Sea the ratio lies between 0.6 to 0.8. This discrepancy indicates that the Western Wadden Sea has not reached its final equilibrium state and a lot of sediment is still needed to reach it.

wind and wave climate, which might explain the variations in sediment volume since 1977.

In conclusion, the large changes in hydrodynamics and morphodynamics of the basin must have had a significant effect on the ebb-tidal delta and adjacent coastlines. The changed flow patterns in the basin, the increased tidal prism and the sand demand of the basin have contributed to a changed morphologic forcing from the basin on the ebb-tidal delta, that contributed to the large changes in hydrodynamics and morphodynamics of the ebb-tidal delta. In the following sections, the changes in hydrodynamics are re-analyzed by analysis of discharges through the dominant channels, and the effects on morphodynamics are re-analyzed based on the bathymetric measurements[3].

[3] In hindsight the changes in the basin are much more complex. Recent reanalysis of the Wadden Sea (Chapter 5, Appendix A) shows a large continuous sediment import; hence a basin that is far from equilibrium. It is the hypothesis that nowadays Texel inlet and Vlie form a coupled system and the recent morphodynamics are governed by sediment exchange between the two inlets. Similar to the ebb-tidal delta change this second-order adaptation acts on a higher order time-scale and it is expected to take many decades (or even centuries) to complete if sufficient sediment availability enables such equilibrium to be formed.

3.3.4 Re-analysis of hydrodynamic and morphodynamic ebb-tidal delta changes

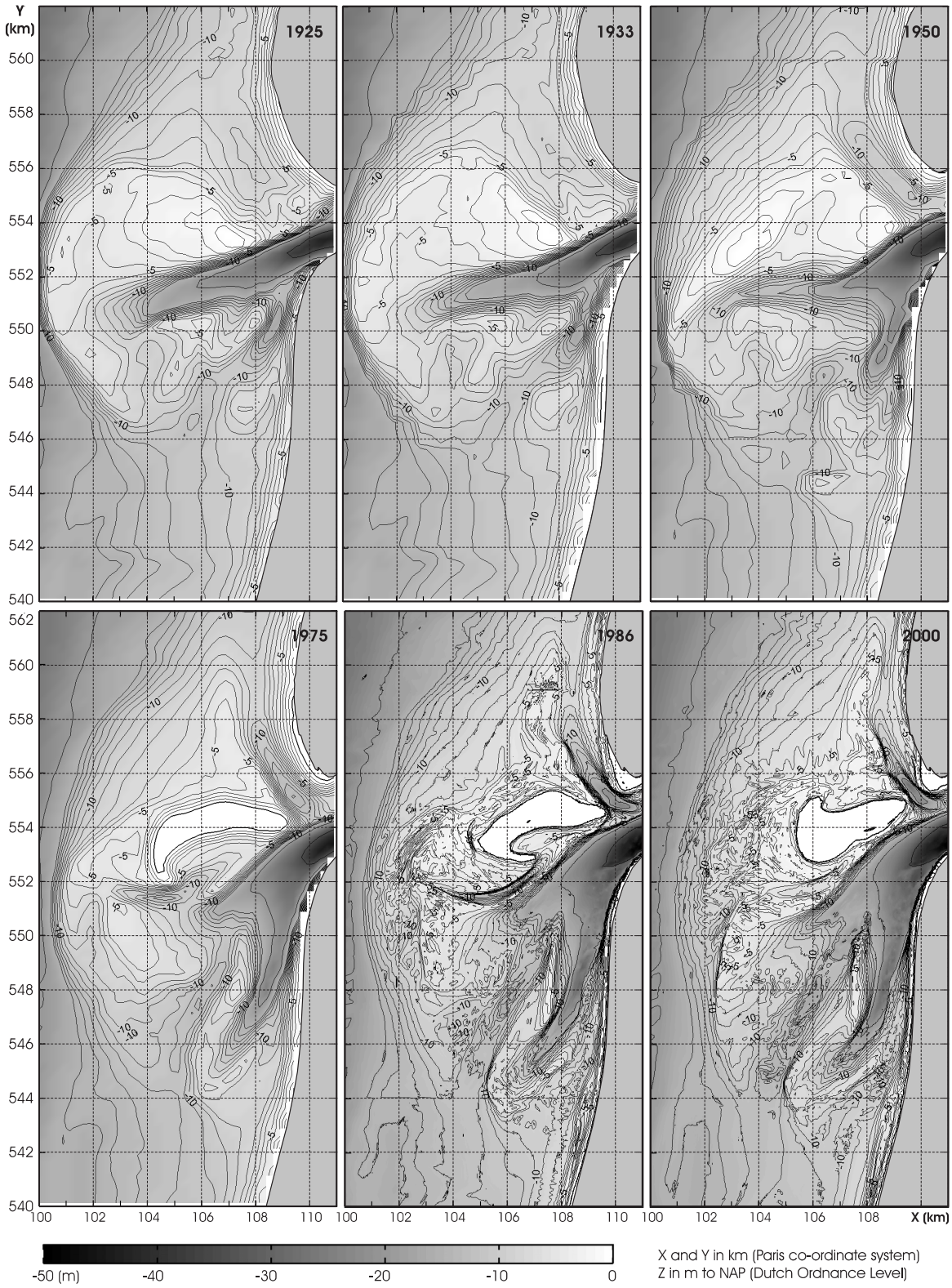

Figure 3-7: Bathymetry of the Texel Inlet ebb-tidal delta for the years 1925 to 2000. Complete maps are compiled by filling in missing data with the nearest measurements available.

The development of the ebb-tidal delta is illustrated by analysis of several bathymetric surveys over the period 1925 to 2000 (Fig. 3-7). The stable position of the ebb-tidal delta preceding the closure indicates the existence of an equilibrium state prior to closure (Sha, 1990; Louters and Gerritsen, 1994; Van Goor *et al.*, 2003). The arrangement of channels and shoals exhibited by the 1925 bathymetry is representative for this equilibrium state and can be described by standard ebb-tidal delta models such as the model of Hayes (1975) or Kana (1999). The channels are dominated by tidal currents and wave-driven transports prevail over the shoals. The main ebb-channel (Westgat) protrudes seaward, with marginal flood channels along the adjacent shoreline on both sides. In front of, but mainly north of the Westgat, the main shoal area (Noorderhaaks) is formed where ebb-tidal currents and incident wave-generated currents balance.

Since the closure, large changes are observed on the ebb-tidal delta. The relations between ebb-tidal delta shape, volume, and protrusion with the governing morphologic forcing (tidal prism and wave climate) have been recognized in many studies in the past (see e.g. Oertel, 1975; Hayes, 1979; FitzGerald, 1996; Kana *et al.*, 1999). Consequently, the altered morphologic forcing of the basin on the ebb-tidal delta must be related to these changes on the ebb-tidal delta. Not only the sand demand of the basin has had a large effect on the ebb-tidal delta and adjacent coastlines, but the closure also increased the outflow to the ebb-tidal delta that is more southward orientated due to the increased importance of the Texelstroom. The significance of the outflow orientation for the ebb-tidal delta development was recognized by Beckering Vinkers (1951), Ringma (1953), Battjes (1962) and Sha (1990). In these studies, the updrift development of the main channel on the ebb-tidal delta was related to the orientation of the Helsdeur (most western part of the inlet gorge that determines the outflow orientation, see Fig. 3-1), although different theories as to the cause of the rotation apply. Battjes (1962) and Ringma (1953) relate the rotation of the Helsdeur to changes in the basin, whereas Sha (1990) and Beckering Vinkers (1951) relate the rotation to the onshore movement of the main shoal area and the development of a three-channel system on the ebb-tidal delta.

Re-analysis of the data showed that a small rotation of the inlet gorge occurred prior to the closure that was followed by a large rotation rate directly after the closure (Elias and Cleveringa, 2003). This large rotation rate, prior to the development of the main shoal area in front of the inlet, indicates that the dominant alteration in Helsdeur orientation is related to the hydrodynamic changes in the basin, rather than the morphodynamic change of the ebb-tidal delta.

The main channel in the basin (Texelstroom) connects to the inlet gorge Marsdiep. Therefore, the orientation of the inlet gorge is related to the orientation of the Texelstroom as they have a tendency to align due to inertia of flow. The observed increase in discharge and (small) rotation of the Texelstroom by alignment along the Texel coastline after the closure (Fig. 3-5) most likely has contributed to the southward rotation of the inlet gorge and Helsdeur. Secondly, the North-Holland coastline facing the Marsdiep is fixed in position by the Helderse Zeewering. At the location of the Helsdeur, the northwestern tip of the seawall interacts with the main channel, and the channel deforms (rotates southward and increases in depth) due to contraction of flow streamlines and secondary flow. As a result, the southward-orientated Schulpengat developed as an ebb channel, thereby decreasing the discharges through the main-ebb channel Westgat. The

balance between ebb-tidal currents and incident wave-generated currents that had formed the terminal lobe (Noorderhaaks) in front of the Westgat was distorted. With wave-generated currents dominating over tidal (ebb-)currents the terminal lobe was pushed landward silting up and reducing the hydraulic efficiency of the channel. Eventually, as a result of this feedback system, the Westgat channel silted up and disappeared and, meanwhile, the Schulpengat expanded as the new main-ebb channel. Initially, the Schulpengat developed as a single channel, but since 1956 two separate channels (Schulpengat and Nieuwe Schulpengat) were formed in updrift direction (i.e. direction of littoral drift along the Holland coast and tidal wave propagation), aligned along the North-Holland coastline.

Coincident with the evolution of the channels, the main shoal area Noorderhaaks was also subject to large morphologic changes. The re-orientation and development of the main-ebb channel in southward direction caused a dominance of the shoreward-directed wave-driven transports over the seaward-directed ebb transports on the western wing of the Noorderhaaks. In brief, the development is governed by a strong landward migration of the seaward part of the Noorderhaaks that decreased the sub-tidal shoal area, while increasing the supra-tidal shoal area and height. On the landward side of this supra-tidal area, a shallow, wave-sheltered region developed that is preferable for deposition. As a consequence, the shoal strongly developed in front of the inlet thereby increasingly contributing to the southward deflection of the flow and updrift development of the Schulpengat channel.

The hydrodynamic development of the main channels (Westgat and Schulpengat) is quantified by the measured discharges, illustrated in Fig. 3-8. Initially, the discharges in both the Schulpengat and Westgat increased, related to the amplified tidal prism through the inlet after the closure. This initial increase is followed by a strong reduction of the discharges through the Westgat and an enlargement of the discharges through the Schulpengat channels. The Schulpengat channels became the dominant ebb-channels on the ebb-tidal delta around 1955 and strongly developed up to 1977.

The hydrodynamic development of the Schulpengat channels showed a character similar to the morphologic development of the basin (Fig. 3-6). This correspondence gives rise to the assumption that, analogous to the basin development, we can distinguish a fast response, *O(decades)*, resulting from an internal adaptation of the ebb-tidal delta (channel-shoal interactions) to the changed boundary conditions. This rapid change is followed by a response smaller in magnitude that is related to the long-term adaptation of the overall equilibrium of the entire inlet system through interaction of basin, ebb-tidal delta and adjacent coastlines.

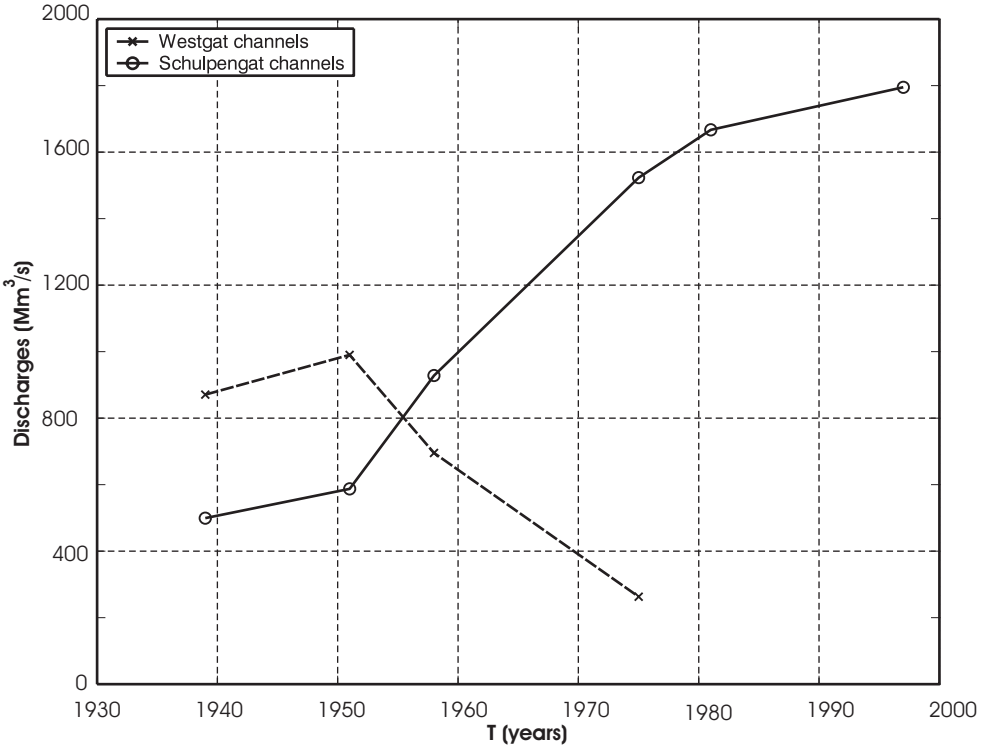

Figure 3-8: Measured (tide-averaged) discharges through Westgat and Schulpengat channels.

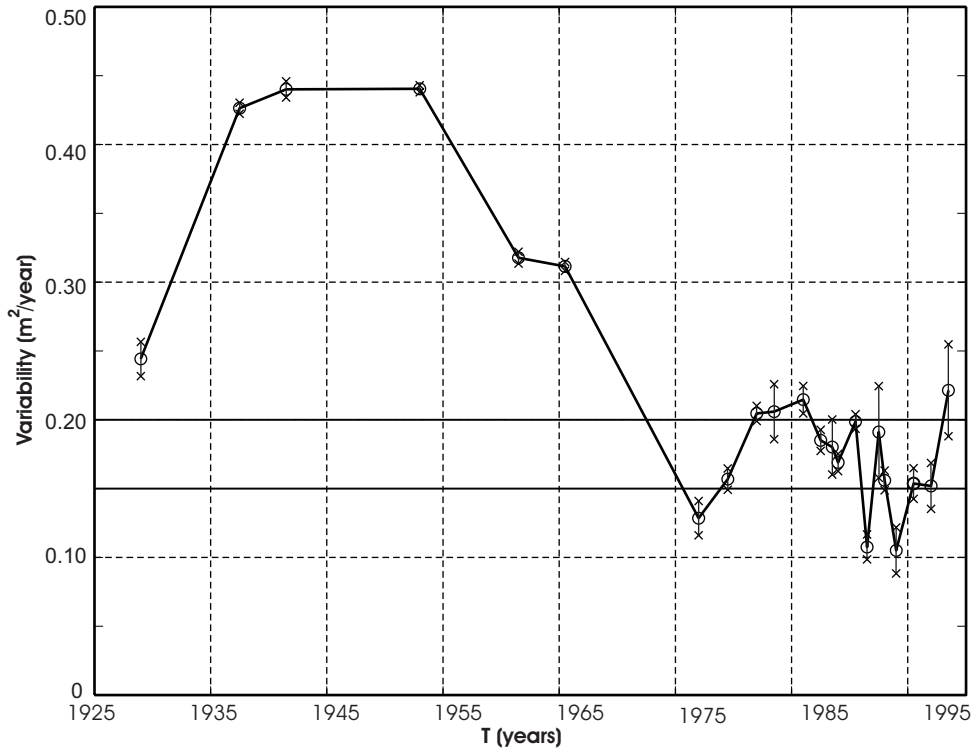

Figure 3-9: Variability of the ebb-tidal delta.

A clear indication of the time span in which the ebb-tidal delta behaviour is dominated by the internal adaptation to equilibrium is obtained by statistical analysis of the variability (in m^2/yr) of the channel and shoal sedimentation–erosion patterns (Fig. 3-9). The following expression of variability is applied to the bathymetry data for the years 1925, 1933, 1950, 1975, 1981, 1986, 1991, 1994, 1997, and 2000:

$$Variability = \sum_{i=1}^{n} \frac{\left(z_{year2}(x_i - y_i) - z_{year1}(x_i - y_i)\right)^2}{n\left(year_2 - year_1\right)} \tag{3.2}$$

in which $t = (year_1+year_2)/2$, $z_{year1}(x_i,y_i)$ and $z_{year2}(x_i,y_i)$ are the measured bottom depths for $year_1$ and $year_2$ respectively, where n discrete locations (co-ordinates x_i, y_i) covering the ebb-tidal delta are taken.

Prior to 1925, no measurements are digitally available to determine the variability preceding the closure. An estimate for the pre-closure magnitude of the variability is based on the value of 0.25 m^2/yr in 1929, derived from the depth variation between 1925 and 1933. In 1933 limited effects of the closure are expected to have occurred. Therefore, the variability value representing the equilibrium situation prior to the closure is estimated to be on the order of 0.15 to 0.20 m^2/yr (indicated by the solid lines in Fig. 3-9). The development of the variability in erosion and sedimentation suggests that the ebb-tidal delta obtained a new dynamic state after a time period of 40 to 50 years. The scatter that dominates the plot since 1975 probably results from natural developments such as seasonal fluctuations in wind and wave climate that are superimposed on the small net overall sediment volume change related to the long-term morphodynamic response.

In addition to the variability, the morphodynamic development of the ebb-tidal delta is quantified by the changes in sand volumes as illustrated in Figure 3-10. The results of the sand volume computation for the Texel ebb-tidal delta based on a fixed spatial balance area (ETD) are similar to the studies of Glim *et al.* (1988) and Van Marion (1999). Although magnitudes differ slightly depending on selection of the balance area, a coherent volume development is observed. Initially, the volume of the ebb-tidal delta increased[4], followed by a strong decrease in volume until 1970, ever since the erosion rate decreases. Because the basin gained sand at a similar rate, it was concluded that the sand lost from the ebb-tidal delta was transported to the basin (Van Marion, 1999).

[4] This initial increase plausibly results from erosion of the main channels and inlet gorge. These are to small to accommodate the increased tidal prisms after closure. Therefore initially sediment is removed from the main channels and deposited in the basin and on the ebb-delta.

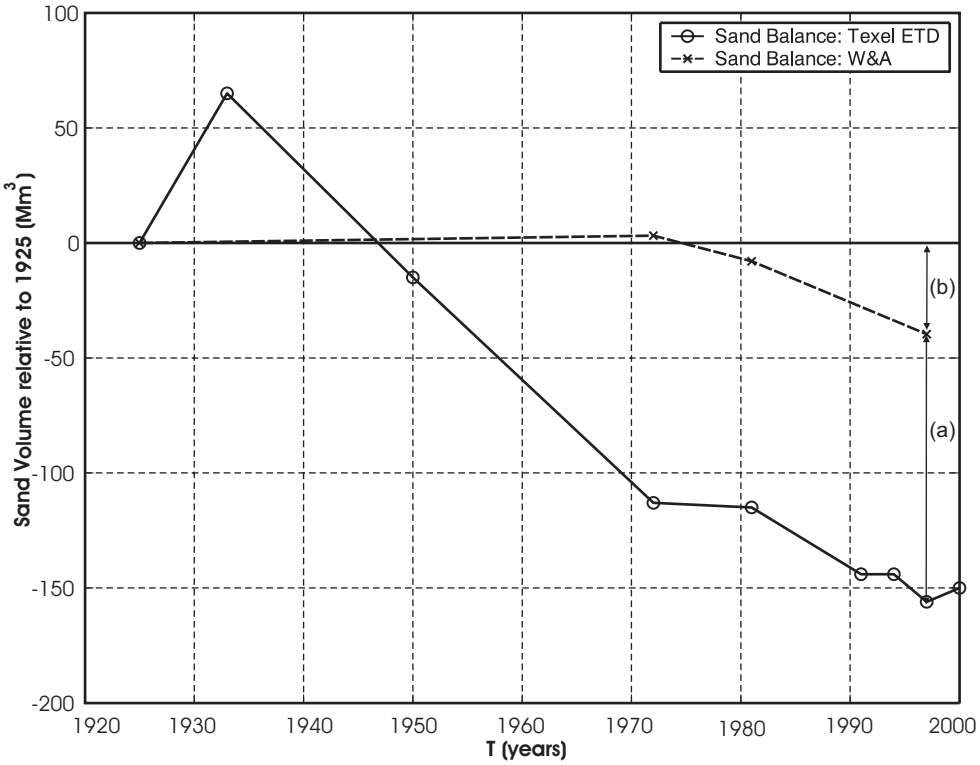

Figure 3-10: Sand volume of the ebb-tidal delta with respect to the 1925 sand volume.

The main conclusion following from the W&A sand balance is that the ebb-tidal delta volume remained relative stable after the closure, despite the increase in tidal prism. With the 26% increase in tidal prism an increase in ebb-tidal volume is expected ($V_o \sim P^{1.23}$). We hypothesize that this inconsistency is caused by an ebb-tidal delta volume that exceeded the equilibrium volume prior to the closure due to storm surge related deposits. During storms, the associated set-up in the entire Zuiderzee basin could have caused the effective tidal prism through the Texel inlet to increase considerably. The resulting greater than average ebb-currents and transports may have contributed to an ebb-tidal delta that expanded beyond the equilibrium size, that would otherwise be correlated to the mean tidal prism, but that corresponds with the equilibrium volume related to the increased tidal prism after the closure. An alternative hypothesis is that due to a dominant sand demand of the basin and only a limited sand source (adjacent coastline), no sand is available for the ebb-tidal delta growth.

The decrease in ebb-tidal delta volume as observed in the W&A sand balance, see (b) in Figure 3-10, is difficult to interpret as a trend. The erosion is based on a single value that is relative small in magnitude compared to the total sediment volume of the ebb-tidal delta (less then 10%), whereas the variability (Fig. 3-9) indicates that large yearly changes can occur on the ebb-tidal delta due to seasonal fluctuations in wind and wave climate[(5)].

The corresponding time-scales of basin and ebb-tidal delta development indicate that the major effects of closure of the Zuiderzee have occurred in a time span from 1932 to about

[(5)] See Chapter 5 Appendix A for an update with recent insights

1975. During this period, large changes took place that are related to the adaptation of the short and medium time-scales due to the internal interaction of channels and shoals. The resulting sand demand of the basin is fulfilled by erosion of the adjacent coastlines. Since about 1975, the internal state of both basin and ebb-tidal delta is quantified as a dynamic, plausibly near equilibrium. It was shown by Kragtwijk *et al.* (2004) that it takes *O(centuries)* for the entire inlet system to fully adapt to the effects of the closure and to regain a new (dynamic) equilibrium state. However, yearly changes on this long-term time-scale are small and the observed basin and ebb-tidal delta development during the last decades clearly shows that the dominant changes on a yearly scale are related to natural developments such as seasonal fluctuations in wind and wave climate superimposed on the relatively slow evolving long-term effects of the closure.

3.4 Discussion

3.4.1 Conceptual model of a Wadden Sea inlet impacted by large-scale intervention

Based on available theoretical knowledge and re-analysis of bathymetric survey data, supplemented by observations, a conceptual model is postulated that describes the morphologic development of a Wadden Sea inlet, that had to respond to large-scale human intervention in the basin. The entire inlet system is assumed to be a sand-sharing system. By definition, all parts of such system are coupled, and, under constant forcing, in dynamic equilibrium, individually and with each other. Changes in forcing or geometry of any part of the system results in morphological adjustments to regain equilibrium. The adjustments are not instantaneous; regaining equilibrium takes a certain time as governed by the availability of sediment and the sediment transport capacity. It has been observed that the rate of adjustments is often proportional to the magnitude of the disruption (Louters and Gerritsen, 1994), and it was shown by Kragtwijk *et al.* (2004) that the morphological response of tidal basins consists of a complex combination of interactions on several time-scales that may differ by an order-of-magnitude. Our conceptual model uses these findings and describes the morphologic response of an inlet in four stages of development (Fig. 3-11).

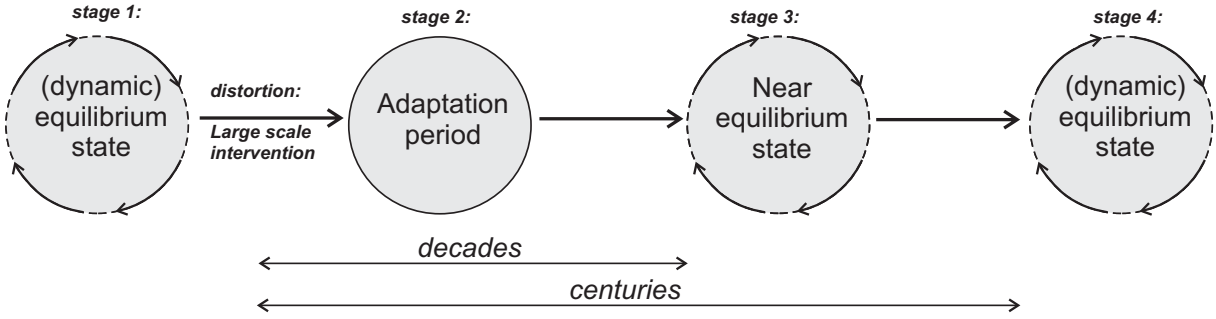

Figure 3-11: Conceptual model for Wadden Sea inlets impacted by large-scale intervention.

Stage 1 concerns the equilibrium behaviour of the natural inlet preceding the human intervention. For the Wadden Sea inlets, this is a system-wide dynamic equilibrium state due to a long-lasting balance between a moderate and approximately constant rate of sea level rise and a sufficient supply of sediment that enabled the basin to develop towards an equilibrium (Van Goor *et al.*, 2003). On different levels of aggregation the various morphologic elements of the natural inlet system can be described with empirical relations. For example, the channel volume of the basin and the sediment volume of the ebb-tidal delta have been quantified in relation to the tidal prism (e.g. Walton and Adams, 1976; De Vriend and Ribberink, 1996; Buonaiuto and Kraus, 2003), whereas on smaller scale relationships for individual channels in the basin have been derived (e.g. Gerritsen, 1990; Eysink *et al.*, 1992; Louters and Gerritsen, 1994).

This first stage abruptly ends with the large-scale intervention that drastically changes the hydrodynamics and morphodynamics of the basin. Because the basin forms part of a coherent morphological inlet system, these changes must be manifested in the other parts of the system such as the ebb-tidal delta and adjacent coastline.

Stage 2 describes this period of large changes. We can no longer speak of natural behaviour of the inlet system because the human intervention dominates the development. The inlet behaviour (the complete system) can no longer be described by straightforward application of empirical relationships, although there is an adjustment of the individual morphological units (basin, ebb-tidal delta and adjacent coastlines). Morphological equilibrium is sought on the smaller scale of these units rather than on the large-scale of the entire inlet.

In Stage 3 we consider the adaptation of the entire inlet system through sediment exchange between the morphological units. Kragtwijk *et al.* (2004) has shown that this adaptation occurs on the long-term time-scale. The associated yearly changes involved are small, but with potentially large impact on this long-term. We postulate that the behaviour of the inlet system during this stage can be described by application of empirical relations, and we call this stage the near-equilibrium period.

Stage 4 describes the new dynamic equilibrium state. Due to the changed external conditions this state is likely to differ from the equilibrium state of Stage 1.

3.4.2 Specification of the model for the Texel inlet ebb-tidal delta development

A generally adopted conceptual model describing the morphologic evolution of channels and shoals on the Texel inlets has been postulated by Sha (1989b). Sha describes a cyclic morphologic behaviour of the channels and shoals on the ebb-tidal delta (Fig. 3-12). The cycle starts with (1) a maximum extension of the main-ebb channel, (2) formation of a large shoal downdrift of the channel, (3 and 4) onshore migration of this shoal due to prevalent eastward-directed wind and wave conditions, and clockwise flood channel rotation. Meanwhile, the ebb channel develops updrift in response to southward deflection of the ebb current by the shoal. The cycle ends with the attachment of the shoal to the downdrift coastline of Texel (5).

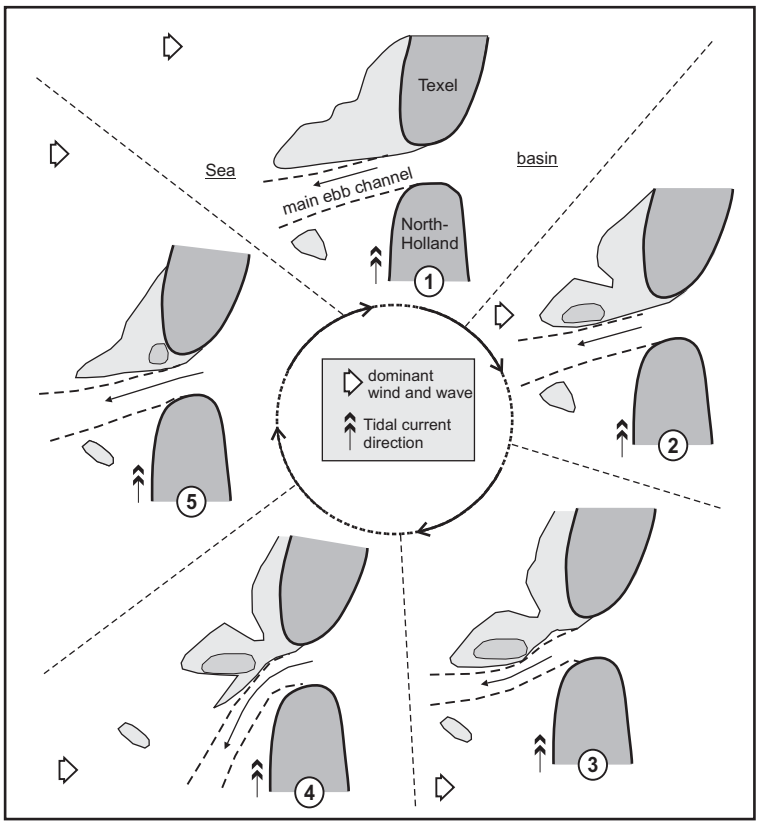

Figure 3-12: Model of Cyclic Morphologic development; redrawn after Sha (1989b).

Our major critique on this model description is that it is mainly based on analysis of historical data, prior to the closure. The impact of the changed hydrodynamic and morphodynamic characteristics of the inner basin and the resulting changes in hydrodynamic and morphodynamic forcing on the development of the ebb-tidal delta are ignored. In contrast to Sha (1989b), we postulate that the changes in the basin cannot be neglected. The changed morphologic forcing of the basin must have considerably altered the ebb-tidal delta processes, while the sand demand of the basin has affected the sand balance of the adjacent coastlines and the ebb-tidal delta. Even more importantly, the changed flow patterns in the basin changed the outflow to the ebb-tidal delta. The increased outflow that is more southward orientated is considered to be a trigger for the observed developments. These are amplified by the feedback mechanism of channel-shoal interaction between the Noorderhaaks shoal and main-ebb channels (first Westgat and later Schulpengat).

The development of the main shoal area Noorderhaaks resulted in a drastic change in the morphodynamic character of this shoal. Prior to the closure, the (mainly sub-tidal) Noorderhaaks formed the ebb-shield of the Westgat. After the closure, the shoal developed into a large supra-tidal shoal facing the inlet gorge. This large, supra-tidal Noorderhaaks shoal is considered to be a barrier or perhaps even a barrier island in its initiation that prevents a direct interaction between the ebb-tidal delta area north and south of the Noorderhaaks. In addition, due to its location directly in front of the inlet gorge, the barrier shoal contributes to the diversion of tidal flow in predominantly southward direction. Combined with the distinct updrift orientation of the main-ebb channels, transporting the majority of the discharges through the southern part of the ebb-tidal

delta, it seems justified to describe the recent behaviour of the northern and southern part of the ebb-tidal delta separately, i.e. on a decadal time-scale. Discharge measurements (De Reus and Lieshout, 1982; Blok and Mol, 2001) indicate that over 90% of the total discharge through the inlet is transported through the southern part of the ebb-tidal delta, while less than 10% is transported through the northward-orientated Molengat.

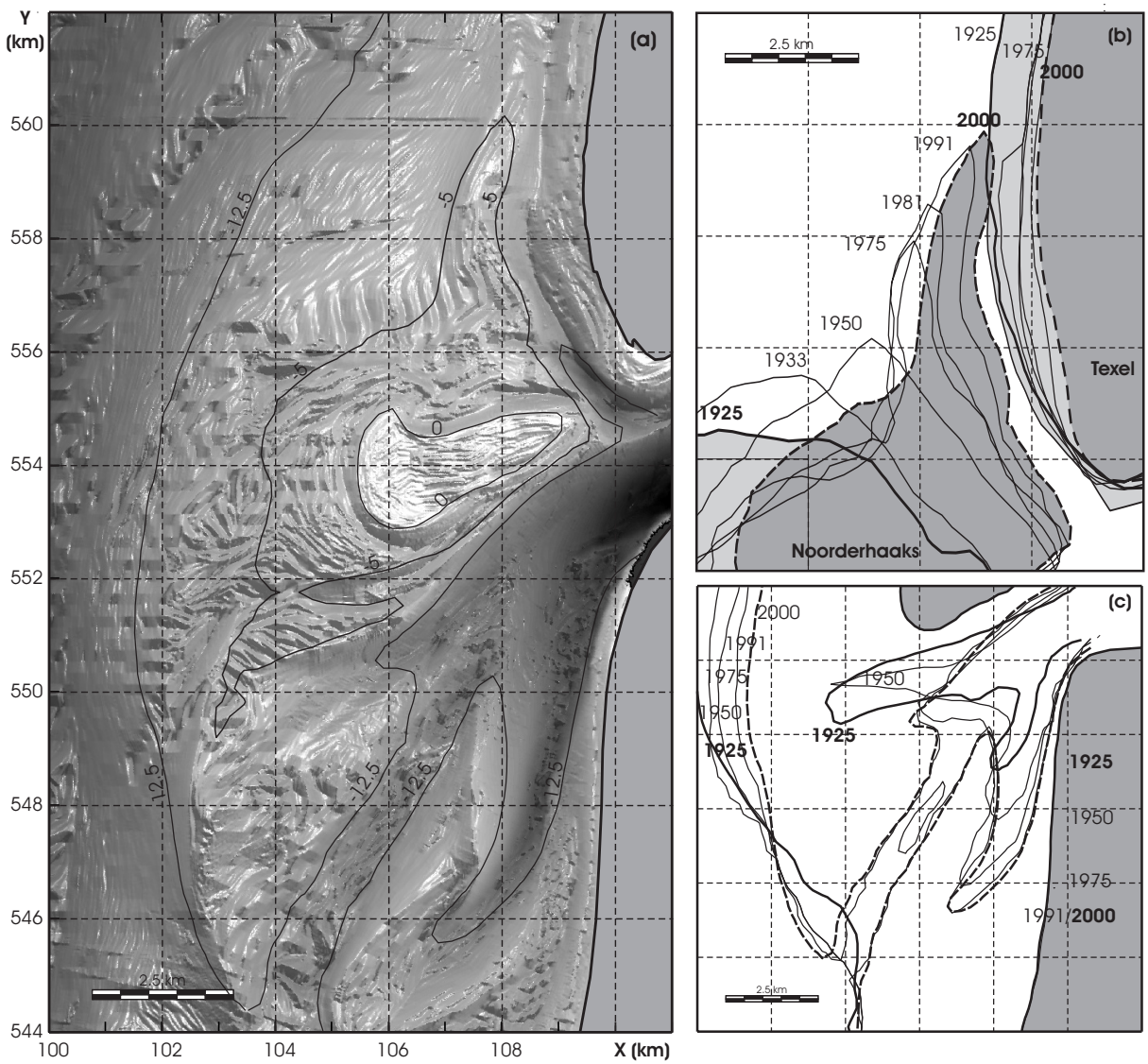

Figure 3-13 (a): Details of the 2003 ebb-delta bathymetry, (b) development of the northern sub-system illustrated by the 5 m depth contour, and (c) development of the southern sub-system illustrated by the 12.5 m depth contour over the period 1925 - 2000.

The development of the northern sub-system is dominated by the landward migration and northward extension of the shallow Noorderhaaks shoal in the form of a large cuspate spit, extending along the Texel coastline. The spit development is illustrated in Figure 3-13b and results from spit accretion on the seaward side by the net east-north-eastward directed wind and wave driven currents (Steijn, 1997; Steijn and Jeuken, 2000). Furthermore, the ripple formation and the large number of saw-tooth bars separated by

runnels along the seaward northern part of the Noorderhaaks shoal (Fig. 3-13a) and the dynamic character of this subsystem, observed by the relatively large, yearly variations in bathymetry, are typical for wave dominated environments. Therefore, it appears reasonable to describe the behaviour of this sub-system as wave dominated.

In contrast to the observed dominant shoal development of the northern sub-system, the behaviour of the southern sub-system is dominated by the evolution of large, deep tidal channels in updrift direction along the North-Holland coastline (Fig. 3-13c). In front of the channels, the ebb-shields (southern part of the Zuiderhaaks and Franse Bankje) show a southward outbuilding. The channels strongly developed up to about 1975, and thereafter annual changes in this part of the ebb-tidal delta are small.

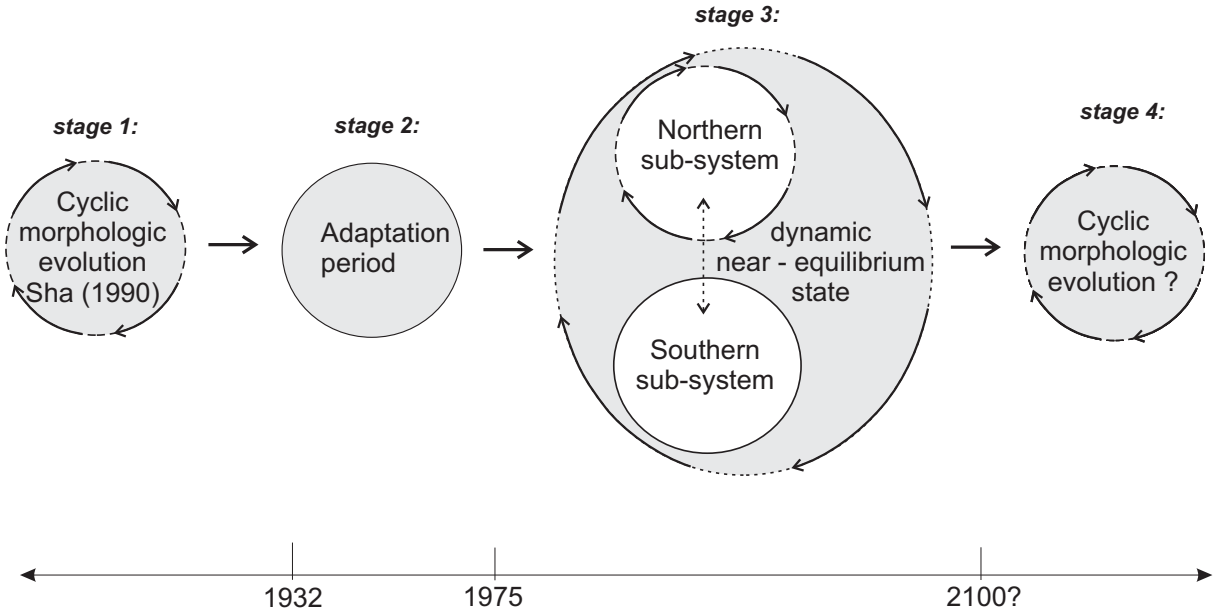

Figure 3-14: Conceptual model of the Texel inlet.

Based on the observed morphologic evolution after the closure, we suggest a refinement of our conceptual model to describe the behaviour of the Texel inlet (Fig. 3-14). In addition to our previously introduced model description a sub-model is proposed to describe the near equilibrium behaviour of the ebb-tidal delta during stage 3.

Stage 1 of the conceptual model describes the dynamic equilibrium state of the ebb-tidal delta preceding the closure. This is a dynamic equilibrium state, due to a long-lasting balance between a moderate and approximately constant rate of sea level rise and a sufficient supply of sediment that enabled the basin to develop towards an equilibrium (Van Goor *et al.*, 2003). Main changes occurred in the form of migrating channels and shoals, possibly, as described by the conceptual model of cyclic morphologic development of Sha (1989b)[(6)].

[(6)] In Elias *et al.* (2006), Chapter 2, of this thesis it is shown that two cycles of morphologic evolution occurred during the period 1583-1730 A.D., while the main channels and shoals on the ebb-tidal delta remained relative stable during the 19th century.

The altered morphologic forcing of the basin on the ebb-tidal delta resulting from the closure abruptly ended this dynamic equilibrium state, which is clearly reflected by the retreat of the coastline and the morphological variability of the ebb-tidal delta that significantly exceeded the equilibrium value up to about 1975. We find the conceptual model of Sha (1989b) unable to describe the ebb-tidal delta behaviour since the closure.

In Stage 2 the adaptation of the basin and ebb-tidal delta to the effects of the closure resulted in large changes in morphology. The development of the variability in erosion and sedimentation suggests that the ebb-tidal delta obtained a state of (internal) dynamic near-equilibrium behaviour (Stage 3) after a time period of approximately 40 years. During this period, channel-shoal interactions induced an updrift development of the main ebb-channels, while the supra-tidal part of the main shoal increased considerably. The increase in supra-tidal shoal area has resulted in a segregation and diversion of tidal flow mainly through the southern part of the inlet, while the shoal acts as a barrier, preventing a direct interaction between the northern and southern component. Therefore, it seems justified to describe the behaviour of the northern and southern part of the ebb-tidal delta separately on a decadal time-scale. This sub-division of the ebb-tidal delta in a northern and southern sub-system separated by the large supra-tidal shoal area of the barrier Noorderhaaks forms the kernel of our conceptual sub-model that describes the internal behaviour of the ebb-tidal delta during the near equilibrium state of Stage 3.

The northern sub-system is dominated by the development of the shoals (wave dominated), with only a small contribution of tidal currents through the Molengat channel. The behaviour can best be depicted as reworking of the existing sand volume of the Noorderhaaks by the wind and wave driven currents and transports. The development is described by the conceptual model of spit development and breaching as introduced by FitzGerald (1988).

A contrasting behaviour is observed in the evolution of the southern sub-system that is dominated by the interaction of the tidal channels and the associated shoals. The tidal channels transport over 90% of the inlets tidal prism. As a result the southern sub-system forms the active part of the ebb-tidal delta.

This conceptual sub-system model describes the behaviour as observed during the preceding three decades (since approximately 1975) and is expected to remain valid to describe the future (decadal) development during the near equilibrium state (stage 3). This latter assumption is not based on hard evidence, but rather our interpretation and integrated prediction of future development.

On the long-term, one cannot neglect the interaction between the two sub-systems. We expect that the ongoing northward extension of the Noorderhaaks continues. With each cycle of spit development and breaching, the sand volume of the main shoal area decreases, thereby reducing the segregation and southward deflection of the tidal flow. The reduced segregation and deflection possibly allows the main-ebb channel to return to its original westward orientated position and eventually an ebb-tidal delta situation is formed, with a morphology that satisfies the equilibrium conditions, but differs from the original morphology, prior to the closure, as the external boundary conditions changed (Stage 4).

An additional problem in the case of the Texel inlet is that, to obtain a new equilibrium, both ebb-tidal delta and basin need a vast amount of sediment, and this sediment demand increases with the ongoing rate of relative sea-level rise (Louters and Gerritsen, 1994). The only sediment sources available are the adjacent coastlines (restricted due to coastal protection works) and a small supply of sediment due to the net northward directed longshore drift. This limited supply of sediment can further extend the time span of the near equilibrium stage.

3.5 Conclusions

We have studied the morphological response of the largest of the Wadden Sea inlets to the most far-reaching intervention ever constructed in it. Intensive monitoring of the Texel tidal inlet since the closure of a major part of the basin resulted in a high-quality dataset of bathymetry, discharges, and water levels that provides a unique opportunity to evaluate inlet dynamics under the influence of large-scale human intervention.

Re-analysis of the drastically changed hydrodynamics and morphodynamics of the basin and ebb-tidal delta indicates that the behaviour of Texel Inlet during seven decades after the closure cannot be described by an often assumed morphological adaptation with a single morphological time-scale.

Based on this re-analysis of observations and modern theoretical knowledge, a conceptual model is postulated describing the morphologic adjustment of tidal inlets due to large-scale human intervention. The kernel of this model is the distinction of four stages of development, acknowledging the likely existence of different morphological time-scales. The first and the last stage concern the equilibrium behaviour of the total natural inlet system respectively preceding and after the human intervention. In between we distinguish two adjustment stages (Stages 2 and 3). Stage 1 abruptly ends with the intervention. Stage 2 describes the period in which large intervention related internal changes dominate the development. These changes are related to the individual adjustment of the distorted morphological units ebb-tidal delta, basin and adjacent coastlines on the short and medium time-scales. The large-scale adaptation of the entire inlet system through global sediment exchanges between the morphological units is described by Stage 3. The associated yearly changes involved are small, but with potentially large impact on this long-term. Finally, in Stage 4 the new dynamic equilibrium state is reached.

The conceptual model is illustrated for Texel Inlet with a focus on the ebb-tidal delta development. The conceptual model of cyclic morphologic evolution of Sha (1989b) is found invalid to describe the ebb-tidal delta development after the closure. The changed hydrodynamic and morphodynamic forcing of the basin on the ebb-tidal delta considerably impacted and modified the ebb-tidal delta processes. The time-span on which this changed hydrodynamic and morphodynamic forcing dominated the ebb-tidal delta behaviour (Stage 2) is estimated by the variability in erosion and sedimentation. The variability suggests that the ebb-tidal delta obtained a state of internal dynamic near-equilibrium behaviour (Stage 3) in approximately 40 years. During Stage 2, the large,

supra-tidal, Noorderhaaks shoal developed directly in front of the inlet gorge and is considered to be a barrier or perhaps even a barrier island in its initiation that prevents direct interaction between the ebb-tidal delta area north and south of the Noorderhaaks. Combined with the distinct updrift development of the main-ebb channels, it seems justified to describe the recent behaviour (Stage 3) of the northern and southern part of the ebb-tidal delta separately, i.e., on a decadal time-scale. The northern sub-system is wave-dominated and can best be described as reworking of the existing sand volume of the Noorderhaaks by the wind and wave driven currents and transports. A contrasting behaviour is observed in the evolution of the southern sub-system that is dominated by the interaction of the tidal channels and the associated shoals. The measured period is too small to describe the equilibrium State 4 in more detail, but based on expert judgment and integration of modern process knowledge, we expect it to take many decades before this stage is finally reached

3.6 Acknowledgements

The work herein was carried out as cooperation between RIKZ (Dutch National Institute for Coastal and Marine Management) and Delft University of Technology. Funding was provided by the Dr. Ir. Cornelis Lely Foundation and the Delft Cluster Project: Coasts 03.01.03. Data were made available by the Directorate-General of Public Works and Water Management (Rijkswaterstaat). The authors thank Dr. A.J.F. van der Spek and the reviewer Dr. N.C. Kraus for their constructive comments.

Chapter 4
Impact of back-barrier changes on ebb-tidal delta evolution

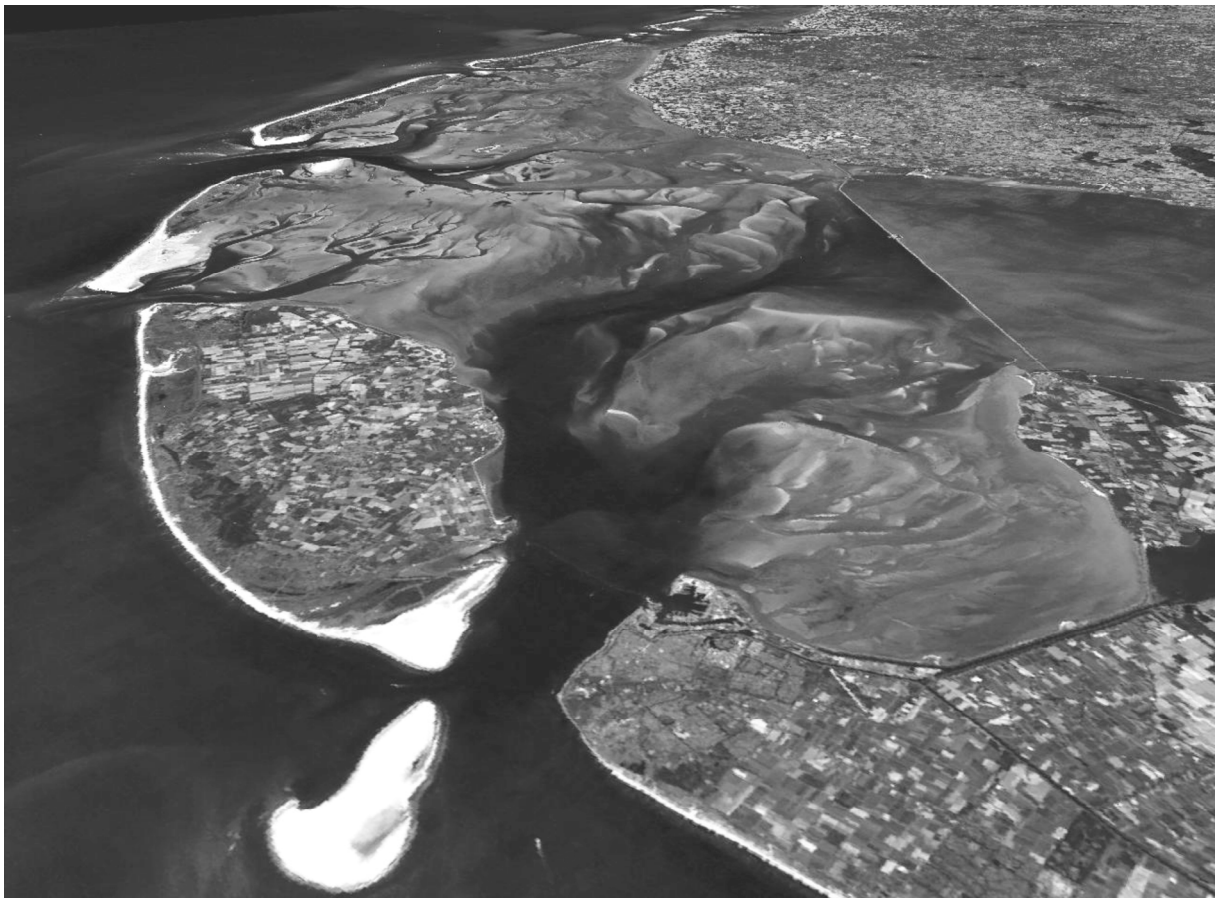

Satellite view of Texel Tidal Inlet (www.earth.google.com)

Abstract:

Texel inlet, the largest inlet in the Dutch Wadden Sea, has undergone drastic changes in the morphology of its basin, ebb-tidal delta and adjacent coastlines after closure of the Zuiderzee. Despite intensive monitoring and analysis, present observation-based conceptual models lack the subtle physics necessary to explain the observed transient developments, such as channel relocation on the ebb-tidal delta and large sediment import into the basin. Fundamental understanding of the inlet dynamics and evolution is obtained by integrating field- and model-data analysis. The state of the art process-based model Delft3D Online Morphology has been used to generate synoptic data of high spatial and temporal resolution over the inlet domain during various stages of the morphological adaptation process in order to validate the observation-based conceptual ideas on inlet evolution. Model results indicate that the back-barrier changes have triggered the observed ebb-tidal delta developments. Sediment import is explained to result from spatially uneven sediment availability due to an imbalance between flow on the ebb-tidal delta and a balance between the bathymetry in the upper part of the basin after closure. With the ongoing morphological adaptation of the ebb-tidal delta the imbalance between flow and bathymetry, and the sediment import into the basin diminishes.

4.1 Introduction

Traditionally, much inlet research efforts have been put into the analysis of observations of morphological changes; the large spatial and temporal scales involved of tens to hundreds of kilometers in space and time scales of centuries left little room for other approaches. The analysis of field data has resulted in a range of conceptual models and empirical relations to explain the variety in size, volume, and gross-scale distribution of channels and shoals in the inlet system. Well known relations are the inlet cross-sectional area versus tidal prism relations by O'Brien(1931; 1969), inlet stability by Escoffier (1940), the tidal prism versus ebb-shoal volume relation of Walton and Adams (1976), inlet morphology classifications based on the relative importance of wave versus tidal-energy by Hayes (1975; 1979), Oertel (1975; 1988) and Hubbard(1979), and sediment bypassing models of Bruun and Gerritsen (1960) and FitzGerald(1988; 1996). These studies have significantly contributed to an improved understanding of inlet behavior and evolution but lack the subtle physics necessary to explain observed transient developments, e.g., when inlets are impacted by large-scale human intervention (Elias *et al.*, 2003a; Elias *et al.*, 2003b).

Texel inlet, the largest inlet in the Dutch Wadden Sea, has undergone drastic changes in the morphology of the basin, ebb-tidal delta and adjacent coastlines after closure of a major part of its back-barrier basin (Closure of the Zuiderzee completed in 1932). Intensive monitoring of the inlet by Rijkswaterstaat (Ministry of Transport, Public Works and Water Management) has resulted in the availability of long-term datasets of water levels, wind, waves, currents and discharges, bathymetry, bedforms and sediments. These observations provide a unique opportunity to study inlet evolution under the influence of human intervention. Observation-based conceptual models and hypotheses on the governing processes and mechanisms for the ebb-tidal delta alterations and the sediment exchange between basin and ebb-tidal delta were proposed by Sha (1989a,b) and Elias *et al.* (2003b, [Chapter 3 of this thesis]). Elias *et al.* recognized that the initial response to the closure on the ebb-tidal delta (erosion and channel relocation) and in the basin (sedimentation) appeared in a time span of approximately 40 years. Nevertheless, basic questions such as how sand exchanges between inlet and ebb-tidal delta, and which processes determine this exchange are still not satisfactory understood.

In this Chapter we aim to expand insight into the main mechanisms responsible for the large changes in ebb-tidal delta morphology after closure. We use process-based model results to validate the existing observation-based conceptual models and hypotheses. The Chapter starts with a short description of the physical setting of Texel Inlet and the morphodynamic changes in the basin and ebb-tidal delta since closure. Recent insights and conceptual model descriptions of the inlet behavior are summarized and research questions formulated. Short-term, process-based model simulations in combination with the simple transport relation of Groen (1967) and the comprehensive VanRijn (1993) formulation are used to obtain fundamental understanding of the mechanisms responsible for the changes in inlet morphology.

4.2 Texel Inlet

4.2.1 Physical setting

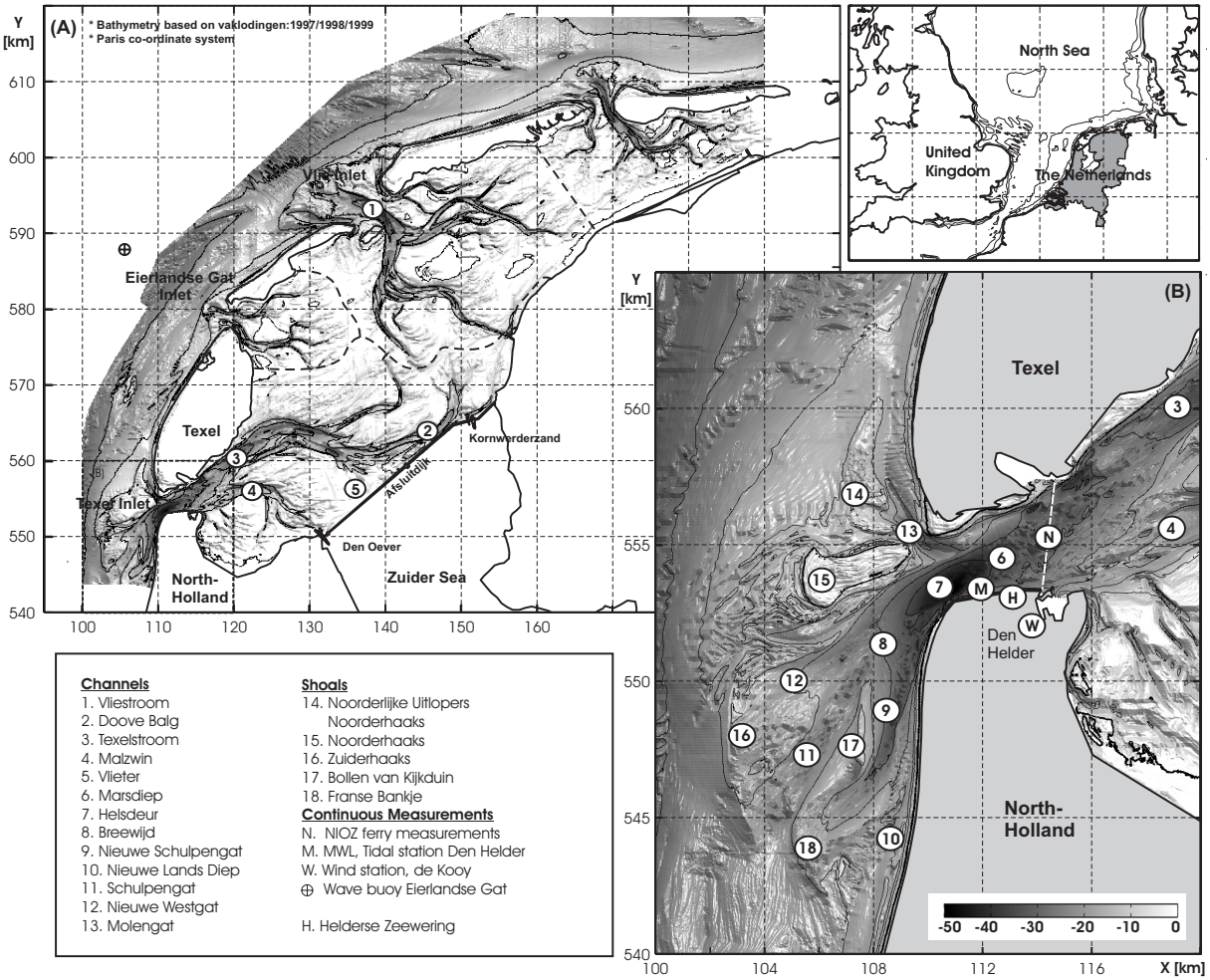

Figure 4-1: Location map of (a) the Western part of the Dutch Wadden sea and (b) Texel Inlet in detail (co-ordinates are based on the Paris co-ordinate system).

Texel Inlet is the largest tidal inlet of the Dutch Wadden Sea and is located in the northwestern part of the Netherlands between Den Helder and the barrier island of Texel (Fig. 4-1a). With bathymetric data of the inlet and ebb-tidal delta being available since the 16th century, the inlet is probably the longest regularly monitored inlet worldwide.

Fig. 4-1b shows the present-day geometry and bathymetry of the inlet including its back-barrier drainage area. The inlet gorge is formed by Marsdiep that is about 2.5-km wide with a maximum depth of 53 m. Marsdiep forms the connection between the main channel in the basin, Texelstroom, and the main-ebb channels, Schulpengat and Nieuwe Schulpengat, on the ebb-tidal delta. The ebb-tidal delta protrudes approximately 10 km seaward and 25 km alongshore, determining the nearshore bathymetry of the adjacent North-Holland coast in the south and the Texel Island coast in the north. The ebb-tidal delta contains a large supra-tidal shoal area (Noorderhaaks) facing Marsdiep. On the

southern part of the ebb-tidal delta, along the North-Holland coastline, the two main channels (Schulpengat and Nieuwe Schulpengat) are updrift orientated, with respect to the direction of tidal propagation and littoral drift. Along Texel Island a smaller channel (Molengat) separates the coastline and the Noorderhaaks shoal.

At Texel Inlet tides are the main driving force behind the horizontal water flow with the semi-diurnal M_2 constituent being the dominant component. The tide has a mean tidal range of 1.38 m in Den Helder, increasing to 2.0 m during spring tide, while during neap tide it drops to about 1.0 m. Recent measurements show an average tidal prism through the inlet of $1x10^9$ m^3, with maximum ebb and flood tidal velocities ranging between 1.0 and 2.0 m/s. The wave height distribution at the ebb-tidal delta is dominated by wind-generated waves in the North Sea basin with only a minor contribution of swell. The mean significant wave height at the nearby Eierlandse Gat wave buoy is 1.3 m from the west-southwest, with a corresponding mean wave period of 5 seconds.

Following the classification of Hayes (1979) the inlet qualifies as mixed-energy wave-dominated, even under spring tide conditions. However, the morphology of the inlet shows tide-dominated characteristics such as a large ebb-tidal delta. This is caused by the large tidal prism and the relatively low wave energy (Davis and Hayes, 1984).

4.2.2 Closure of the Zuiderzee

The closure of the Zuiderzee (1925-1932) is the largest single intervention ever constructed in the Wadden Sea. Preceding the closure the Texel and Vlie tidal basins covered the southwestern part of the Wadden Sea and the former Zuiderzee (Fig. 4-2, left panel). In total, the basin covered a surface area over 4000 km^2 with a basin length of 130 km. The major part of the former Zuiderzee coast was protected by dykes and during storm surges breaching occurred frequently, flooding large areas. The closure dam ensured safety by reducing the Zuiderzee coastline from approximately 250 km of dykes to 30 km of dam. Additionally, land reclamation in the enclosed basin was facilitated and the basin formed a large fresh-water reservoir also reducing salt intrusion into the hinterland.

After the closure, the basin area reduced substantially to an area of roughly 712 km^2 (Fig. 4-2, right panel) and a length of about 30 km. The closure considerably altered the hydrodynamics and morphodynamics in the remaining active part of the basin (Rietveld, 1962; Elias *et al.*, 2003b, [Chapter 3]). The tidal characteristics changed from predominantly propagating to a more standing tidal wave resulting in an increase of the tidal range and tidal prism through Marsdiep by approximately 26%. With these large changes in hydrodynamics and particularly in basin geometry, pronounced changes in the morphology of Texel inlet have taken place. The closure separated the back part of the basin (Zuiderzee) that contained a relative large portion of shoals. In the remaining active part of the basin the remaining shoals area was too small compared to the channel area, therefore, a morphologic adjustment of the basin was to be expected (Eysink, 1990). Large sedimentation was observed, over 200 million (M)m^3 of sediment, during a period of approximately 40 years (Elias *et al.*, 2003b, [Chapter 3, Fig. 3-6]).

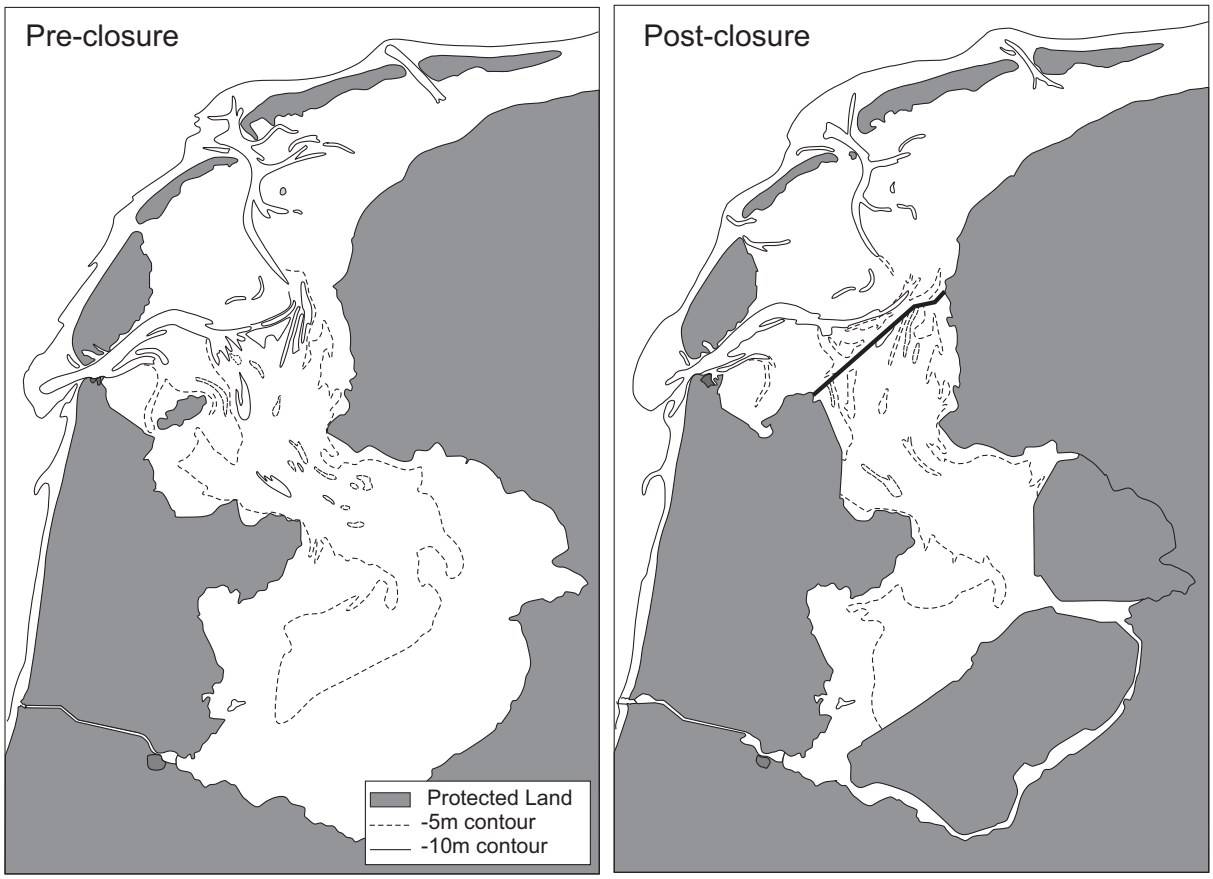

Figure 4-2: Impression of the western Wadden Sea prior and after closure of the Zuiderzee (redrawn after Thijsse, 1972).

The corresponding rates of sedimentation in the basin and erosion of the adjacent ebb-tidal delta and coasts point to sand exchange between these elements (Van Marion, 1999). Hence, sediment import into the basin through Marsdiep must have dominated after closure. The governing mechanisms for these transports have long been and still are a matter of debate. A number of important mechanisms, e.g. tidal asymmetry, gravitational circulation, large-scale residual circulations, wind and wave effects, have been identified in literature (Postma, 1981; Dronkers, 1984, 1986; Ligtenberg, 1998). Postma (1954) was among the first to recognize the essential role of tidal asymmetry in generating residual sediment transport in Texel inlet. Also the studies by Dronkers (1998), Ligtenberg (1998), Ridderinkhof (1997) and Van de Kreeke and Robaczewska (1993) point to the importance of tidal asymmetry for the sediment exchange between the Wadden Sea basins and ebb-tidal deltas. Ligtenberg (1998) suggested that after closure tidal asymmetry induced a large sediment import into the Texel basin. As the morphology of the basin adapted to the effects of closure, tidal asymmetry and the related sediment import into the basin reduced. Possibly the reduced tidal asymmetry is an explanation why in the recent study of Bonekamp *et al.* (2002) a sediment export was observed (and modeled) due to the large ebb residual (M_0M_2) related transports and minor tidal asymmetry (M_2M_4) driven flood transports.

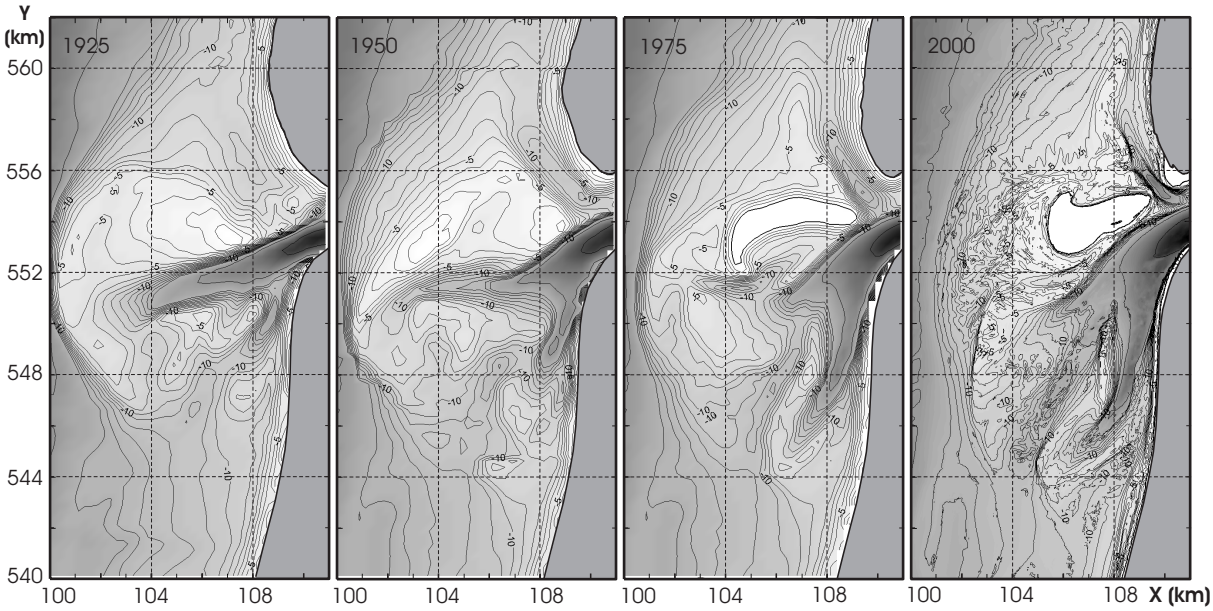

Figure 4-3: Ebb-tidal delta bathymetry of the Texel Inlet for the years 1925, 1950, 1975 and 2000 (complete maps are compiled by filling in missing data with the nearest measurements available).

The changes in hydrodynamics and the sediment demand of the basin contributed to an altered morphologic forcing by the basin on the ebb-tidal delta, and large changes in the ebb-delta morphology were observed. Elias *et al.* (2003b) and Elias and Van der Spek (2006, [see Chapter 2 and 3]) conclude that during the adaptation stage following the engineering works the ebb-tidal delta dynamics cannot be described in terms of natural hydrodynamic processes, such as the ratio of wave versus tidal energy, alone. Moreover, these authors hypothesize that the ebb-tidal delta evolution after closure was triggered by the changed hydrodynamics in the basin. The changed tidal characteristics, the northward displacement of the basin centre, the closing of southward channels and the amplified tidal prism increased the discharges through Texelstroom. Texelstroom determines the ebb outflow into the inlet gorge that re-orientated resulting in a more southward-directed outflow onto the ebb-tidal delta. The expression back-barrier steering was introduced to describe this 'forcing' induced by the basin on the ebb-tidal delta. The altered ebb outflow triggered the development of the former flood-dominated Schulpengat as main ebb channel, while the original westward-oriented main ebb channel Westgat filled in and disappeared (Fig. 4-3, 1925-1950). Initially, Schulpengat developed as a single channel but since 1956 two separate channels (Schulpengat and Nieuwe Schulpengat) formed in an updrift direction aligned along the North-Holland coastline (Fig. 4-3, 1950-1975).

The re-orientation of the main channels on the ebb-tidal delta has had large consequences for the coastal maintenance of the adjacent coasts. Over 200 Mm^3 of sand was eroded from the ebb-tidal delta and coastlines (see Fig. 4-3b). Both, the Texel as the North-Holland coastline are still subject to structural erosion (Cleveringa, 2001; Elias and Cleveringa, 2003; Elias *et al.*, 2003b) and maintenance of these stretches of coast belongs to the most intensive of the entire Dutch coastal system (Mulder, 2000; Roelse, 2002).

4.2.3 Research Questions

Analysis of literature points to the importance of tidal sediment transports for the development of Texel Inlet since closure of the Zuiderzee. The changes in tidal wave characteristics (e.g. increased tidal range and outflow orientation) were identified to trigger the southward development of the main channels on the ebb-delta. Back-barrier steering was used to describe this mechanism.

Tides were also identified as main transport mechanism for the large sediment transports into the basin. An interesting contradiction arose by the analysis of recent flow observations and model results in combination with the Groen (1967) transport formulation (Bonekamp *et al.*, 2002). Bonekamp points to a net sediment export due to the main tidal asymmetries; sediment export prevails due to the large ebb residual (M_0M_2) transports and a minor tidal asymmetry (M_2M_4) driven influx. Ligtenberg's (1998) research suggests that this apparent contradiction results from the changes in tidal asymmetry since closure; directly after closure tidal asymmetry induced a large sediment import into the Texel basin, but as the morphology of the basin adapted to the effects of closure, tidal asymmetry and the related sediment import into the basin reduced.

In this chapter we aim to identify the importance of tidal sediment transports for the evolution of Texel inlet since closure using process-based model results. We focus on the importance of back-barrier steering for ebb-delta development, and on the importance of tidal asymmetries for (reduced) sediment transports between ebb-delta and basin.

4.3 Method and Models

4.3.1 Method

Process-based models, describing the water motion, sediment transport and bottom change by a series of mathematical formulations, have been applied in the modeling of coastal processes since the early days of computer technology. Recent studies by e.g. Wang *et al.* (1995), Ribberink and De Vriend (1995), Cayocca (2001), Bonekamp *et al.* (2002), Van Leeuwen (2002), Hibma *et al.* (2003) and Van Maren (2004) have shown that such models can be used successfully to study complex morphological evolution in tidal inlet systems. The studies of Wang *et al.* (1995), Cayocca (2001) and Hibma *et al.* (2003) used a more-or-less '*traditional*' approach. The model consists of a number of coupled modules that compute waves, currents, sediment transport and bed-level changes sequentially (Fig. 4-4a). By applying larger time-steps for the computation of bed-level updates then for the computation of flow and sediment transports morphodynamic simulations over larger time spans could be made. As the frequency of bed-level update is typically in the order of (several) tides to days these models were forced by representative steady boundary conditions rather than randomly varying input conditions (Latteux, 1995; De Vriend and Ribberink, 1996; Cayocca, 2001). The construction of representative conditions, but also the correct coupling of the various modules made such model simulations complicated and results sometimes unpredictable. This might be one of the reasons why

still only a limited number of quasi-realistic process-based model applications have been conducted for complex areas such as tidal inlet systems.

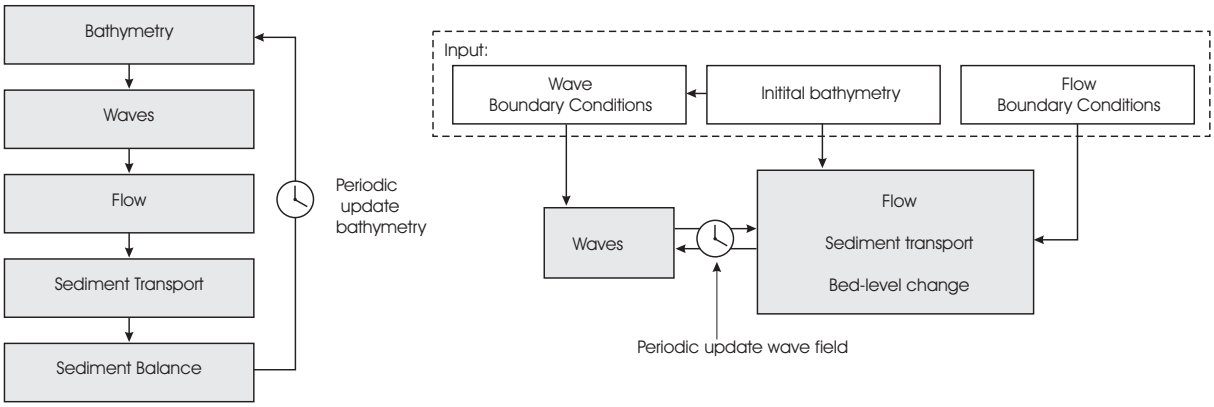

Figure 4-4: Schematic representation of the Delft3D-MOR model (a, left) and Delft3D Online Morphology model (b, right)

Recently the computation of sediment transport and bed level change has been fully integrated in the Delft3D flow module; Figure 4-4b illustrates the Delft3D Online Morphology model principle. As the morphologic changes are calculated simultaneously with the flow calculations only the fairly straightforward wave-flow coupling has to be specified, minimizing the change on coupling errors, and large exchange (communication) files between the modules are not required. Similar to the traditional approach long term simulations can be made by using schematized boundary conditions and a morphological acceleration factor (Lesser *et al.*, 2004; Van Maren, 2004 provides an example of a river delta application).

One of the major assets of this *'modern'* model approach is the capability to increase the spatial and temporal resolution of point-oriented field observations. Observations are used to force the model as-realistically-as-possible (quasi real-time by measured time-series of wind, waves and tides) and as sediment transports and flow are resolved simultaneously the model results provides synoptic more-or-less realistic 'field-data' of high spatial and temporal resolution over the entire inlet domain (also see Chapters 6 and 7 of this Thesis). In this manner spatial variations in velocities and concentrations are fully resolved. Analysis of the model data can provide valuable information on governing flow and sediment transport patterns in the instrumented and the un-instrumented areas, and allows to perform sensitivity analyses for identification of the dominant processes and mechanisms by varying the forcing conditions. This information is needed for correct boundary (forcing) schematizations if one aims to perform long-term morphodynamic simulations.

A major drawback of such a quasi real-time model approach is that identification of the basic mechanisms and processes is complicated due to the compound model output. Identification of basic mechanisms usually requires simplification, a method used in the so-called class of idealized models. Idealized models use governing equations based on physical principles, but simplify and/or schematize for instance the equations of sediment transport, basin geometry, and/or principal forcing constituents. Using these models ba-

sic mechanisms for the formation of inlet morphologies can be identified and described through linear and nonlinear stability analysis, see the recent studies of Van Leeuwen (2002) and Van der Vegt (2006) for basin and ebb-delta formation in the Wadden Sea. A disadvantage of such an approach is that results are not easily translated to field observations. A sort of intermediate approach is to use the complex flow model results in combination with a simple sediment transport relation (Bonekamp *et al.*, 2002; Van Leeuwen, 2002 [Chapter 5 pages: 105-128]). Bonekamp *et al.* (2002) obtained as-realistic-as-possible flow patterns for Texel Inlet by running the Deflt3D-FLOW model with a measured bathymetry under tidal forcing (validated and calibrated using the NIOZ ferry measurements). The relatively simple transport model of Groen (1967) was afterwards used to compute sediment transports and to determine the separate contributions of the main tidal asymmetries.

First, we adopt the '*local Bonekamp approach*' to investigate the importance of tidal asymmetry for sediment import (or export) into the basin. One-month flow simulations are made on the 1925 and 2000 bathymetry and residual sediment transports are determined afterwards using the Groen (1967) model.

Second, back-barrier steering is investigated by running the Delft3D Online Morphology Model (in combination with the Van Rijn 1993 transport formulation). Residual flow and transport patterns obtained from 1-month model simulations on the 1925, 1950, 1975 and 2000 bathymetry provide snap-shots during various stages of the inlet development. By studying the changes in residual patterns insight is obtained in the dominant processes and mechanisms for ebb-delta development and sediment exchange between basin and ebb-delta.

4.3.2 Models

Delft3D-Flow

The Delft3D-Flow model (Version 3.43.01.00) was used in depth-averaged mode to solve the interaction of the alongshore-propagating open-sea tidal wave with the compound inlet bathymetry and the cross-inlet currents. In this study the focus is on tides. Waves and density differences due to non-uniform salinity distributions were neglected. Wave-driven transports are investigated in Chapter 6, while Chapter 7 deals with density stratification and it effects on flow and transport during a high-discharge period.

Delft3D-FLOW solves the unsteady shallow-water equations, that consist of the continuity equation, the horizontal momentum equations, the transport equation under the shallow water and Boussinesq assumptions. Vertical accelerations are assumed minor compared to gravitational acceleration (shallow water assumption) reducing the vertical momentum equation to the hydrostatic pressure relation. By specifying boundary conditions for bed (quadratic friction law using a Chézy coefficient of 61 $m^{½}/s$), free surface (no wind stress) and lateral boundaries (water levels due to tidal forcing on the open-sea boundaries and closed boundaries with free-slip conditions at the coasts) the equations can be solved on a staggered grid using an Alternating Direction Implicit method (1984;

Leendertse, 1987). The specific model application for Texel Inlet (*Texel Outer Delta model*) uses a well-structured curvilinear grid (38311 points) with a maximum resolution of 80x120 m at the location of the inlet (Fig. 4-5a). The Eierlandse Gat and Vlie inlet are included in the model domain to enable the simulation of the important internal residual volume transport between Vlie and Texel inlet (Ridderinkhof, 1988a). Depending on the simulation the bathymetry of the nearshore, the inlets and the basin is based on bathymetric data of 1925, 1950, 1975 and 2000 (Fig. 4-3). Depth measurements were grid-cell averaged or triangularly interpolated to the curvilinear grid depending on the resolution of the observations. Depths in the deeper region are based on Dutch Continental Shelf data supplied by TNO-NITG (Frantsen, 2001). The initial bathymetry was smoothened to reduce the small-scale disturbances (~ 0-0.1 m) in the bathymetry. In this manner unrealistically high sediment transports due to the 'noise' in the bathymetry are prevented.

The North-Holland coastline, the landward coastline in the back-barrier basin, and the island coastlines form closed boundaries (free- slip conditions). The northern basin periphery is chosen on the Terschelling tidal divide (as present in 2000) and set as a Neumann boundary (Roelvink and Walstra, 2004). The location of this tidal divide might not be entirely representative for the 1925 situation. Comparison of the 1925 and 2000 bathymetry shows that the tidal divide has migrated slightly westward estimated at 0.5 – 1 km. Sensitivity studies by varying the boundary location and conditions (zero-velocity gradient, velocity versus water level boundary, zero velocity, estimated velocity and estimated water levels) shows that the exact choice of this boundary condition and location does not affect the transport model results for Texel Inlet. The open-sea boundaries are located 'far away', outside the direct sphere of Texel inlet's influence and prescribed as representative harmonic constituents (frequencies, amplitudes and phases) of the water level elevations (Fig. 4.5b)

The time step for the flow computations is 60 seconds to fulfill the maximum courant number criterion of 15. Simulations were run over a 1-month period, which includes two spring-neap tidal cycles (see Fig. 4-5b for a water-level time series of Den Helder tidal station) and therefore, due to the periodicity of tides, provides a fairly representative depiction of the long-term tidal residual transport patterns. Default settings of 1.0 m^2/s and 1.0 m^2/s for the uniform horizontal eddy viscosity and eddy diffusivity coefficients have been applied.

Computations start from a uniform water level. A two-day spin up and 60 minutes smoothing time prior to the actual computations is sufficient to dissipate the errors in hydrodynamics induced by the discrepancy between boundary conditions and initial state.

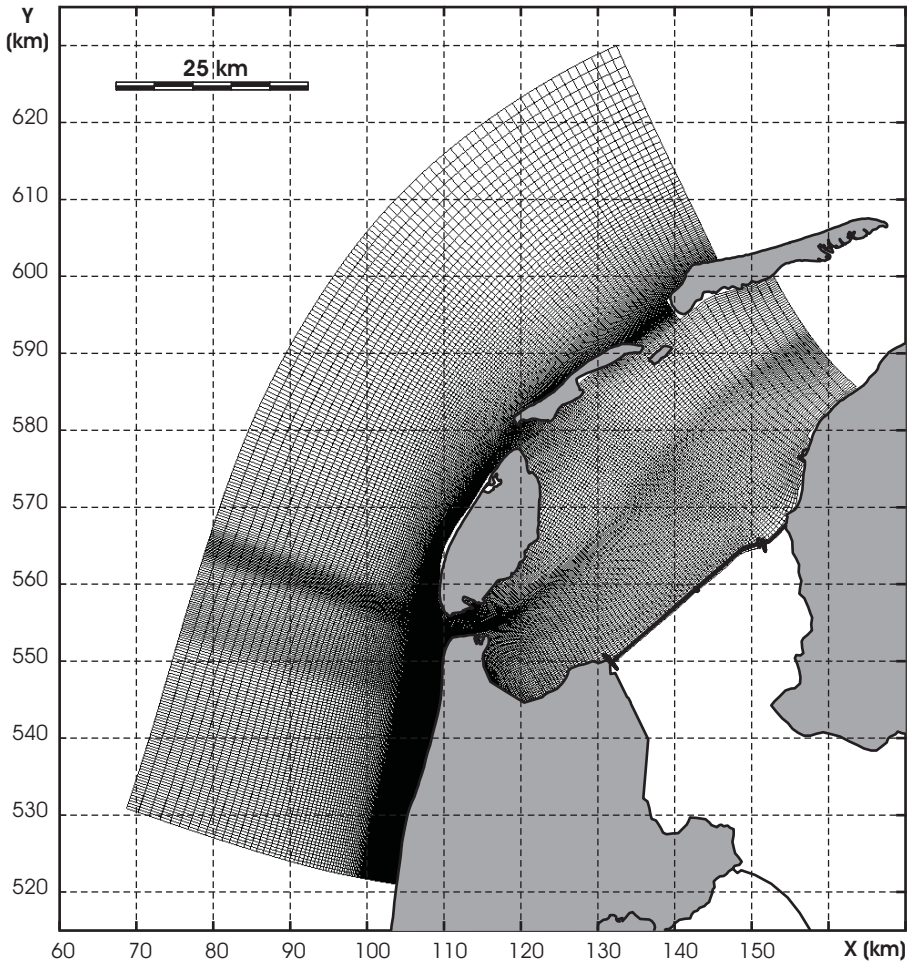

Figure 4-5a: Texel Outer Delta model grid

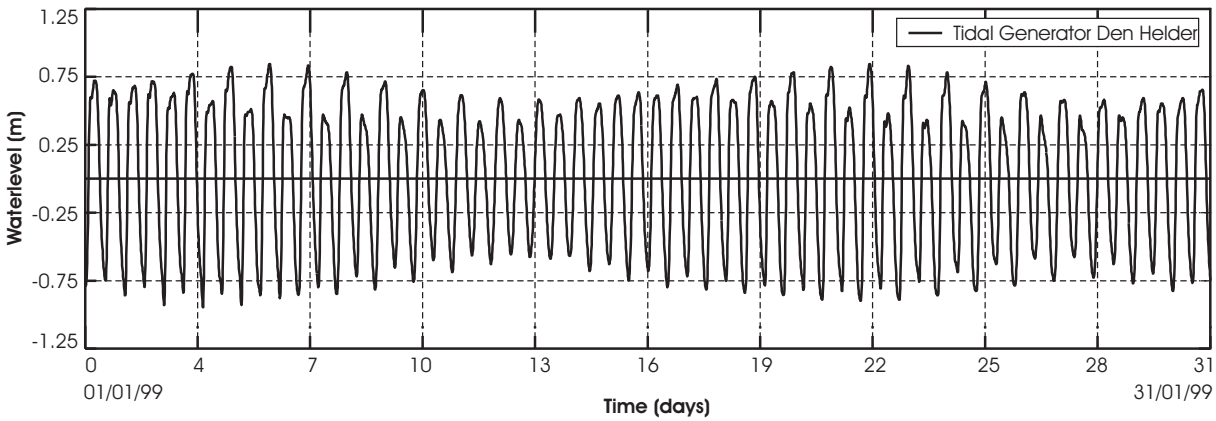

Figure 4-5b: Tidal water levels for the month of January 1999 at Den Helder tidal station (location see Fig. 4-1)

Sediment transport formulation of Groen (1967)

Recently in the work of Bonekamp *et al.* (2002) process-based flow model results were combined with a relative simple transport formulation (Groen, 1967) to obtain insight in the possible correlation between tidal asymmetry and sediment transport in Marsdiep. Groen uses the concept of an equilibrium total load of suspended matter, and assumes that the rate of increase or decrease of the suspended sediment concentration is proportional to the deficit or excess of the instantaneous concentration (C) with respect to the equilibrium concentration (C_e). The Groen formulation for the concentration reads,

$$\begin{aligned} \beta \frac{\partial C}{dt} &= \omega\left(C_e - C\right) \\ C_e &= A\left(u^2 + v^2\right) \end{aligned} \tag{4.1}$$

where the settling lag time factor β (-) determines the lag between C and C_e (which is a measure of the settling velocity), C and C_e represent the instantaneous and equilibrium depth-averaged sediment concentration (kg/m^3) respectively, w is the angular frequency of the main tidal constituent (M_2), A is a proportionally constant depending on e.g. sediment and bed characteristics (s^2/m^2) and (u, v) are the depth-averaged velocities (m/s).

For coarse-grained sediments (sand) it is often assumed that the sediment particles respond instantaneously to the local flow velocities; the concentration adjusts instantaneously to the flow ($\beta = 0$) and the Groen formula for the transport reduces to the basic approximation:

$$\vec{S} = C\vec{u} = A\left|\vec{u}\right|^2 \vec{u} \tag{4.2}$$

wherein the sediment transports (S) are proportional to the depth-averaged flow velocity (u) by a power 3. Such assumption is considered representative for coarse-grained sediment dominated by bed-load transport.

After harmonic analysis of the tidal flow model results (obtained with the Delft3D flow module) the Groen sediment transport formulation allows for the analytical approximation of the tidally averaged transports, only considering the residual current, the M_2 and M_4 constituents of flow (see Van de Kreeke and Robaczewska, 1993; Van der Molen and de Swart, 2001; Bonekamp *et al.*, 2002). Using M_2 and M_4 as main forcing the velocity field can be written as equation

$$u = u_0 + u_2 \cos(\omega t) + u_4 \cos(2\omega t - \varphi) \tag{4.3}$$

where u_0 is the eulerian residual current, u_2 and ω are the amplitude and frequency of the M_2 tide and u_4 and φ are the amplitude and phase (relative to the M_2 phase) of the M_4 tide. The net (tide-averaged) sediment transport ($<S>$) is obtained from substitution of equation 4.3 in 4.2,

$$\langle S \rangle = \frac{3}{2} A u_2^2 u_0 + \frac{3}{4} A u_2^2 u_4 \tag{4.4}$$

the first term expresses the contribution of the M_0M_2 (stirring of sediment by the leading tidal constituent which is subsequently transported by the residual current, and the second term the M_2M_4 transports due to the asymmetrical behavior of the maximum current velocity (deformation of the tidal curve due to tide-bathymetry interaction results in a longer duration of the flood or ebb-period and differences between peak velocities).

The advantage of the Groen model over a simple velocity to the power n transport relations is that lag effects can be accounted for. Lag effects have shown to play an important role for fine-grained suspended sediments (<100 μm), as these sediment particles do not respond instantaneously to the local flow velocities and a hysteresis between velocity and corresponding concentration arises (Postma 1961). As a result the sediment transport is not only determined by the magnitudes of the ebb and flood velocities, but also by the velocity variation during high and low water slack. In the Groen formulation an estimate of settling lag is obtained by specifying the β coefficient. ($\beta = 1$ is indicated by Groen as reference for the Wadden Sea).

Delft3D Online Morphology using Van Rijn (1993)

The method using the Groen transport formulation can be considered a *local approach*; all grid points are treated individually as time-series to determine the sediment transports. This means that diffusive transports due to concentration differences, or adjective transports due to spatially varying concentrations and velocities are not accounted for. Ridderinkhof (1997) resolved some of these aspects by addressing the Lagrangian velocities rather then the Eulerian velocities for suspended sediment transport.

In this study we use the Delft3D Online Morphology model (*online approach*) to resolve the sediment transport patterns dynamically. The Online Morphology version supplements the flow model results with sediment transport computations. Each computational time-step sediment transports of in this case non-cohesive sediment are computed within the flow simulation. Default settings for the calculation of sediment transports and morphological change are used (Van Rijn 1993 transport formulation).

Sediment transport computations are initiated after a 1440 minutes spin-up time. A morphological scale factor of 1 is applied (no morphological acceleration, see Lesser *et al.*, 2004). Bottom sediments characteristics for the morphological computation include: the use of a single-fraction of non-cohesive sand (d_{50}= 250 μm), no hindered settling, a sediment density of 2650 kg/m^3, a dry bed density of 1600 kg/m^3 and an initial sediment mass at the bed of 16000 kg/m^2.

A brief description of the governing formulations and (depth-averaged) implementation of the Van Rijn 1993 transport formulas is presented in Appendix A. Complete overviews of the basics, testing and validation of the Delft3D Online Morphology has been reported in Lesser (2000), Lesser *et al.* (2004). See Walstra and Van Rijn (2003), and Van Rijn (1993; 2000; 2002) specifically for the transport formulations.

4.4 Model Validation

4.4.1 Tidal asymmetry in the inlet gorge

Previous studies point to the importance of tidal asymmetry for the sediment exchange between basin and ebb-tidal delta after closure (Dronkers, 1998; Ligtenberg, 1998). The focus is on the M_2 and M_4 as in literature it is shown that the long-term residual (coarse) sand transport essentially depends on the interaction of the fundamental constituent and the Eulerian mean current, and the interaction of the fundamental constituent and its even over-tides (Van de Kreeke and Robaczewska, 1993). Since the M_2 is dominant in Texel inlet, to first order, tidal sediment transport essentially depends on the M_0M_2 tidal residual transport and the M_2M_4 tidal asymmetry.

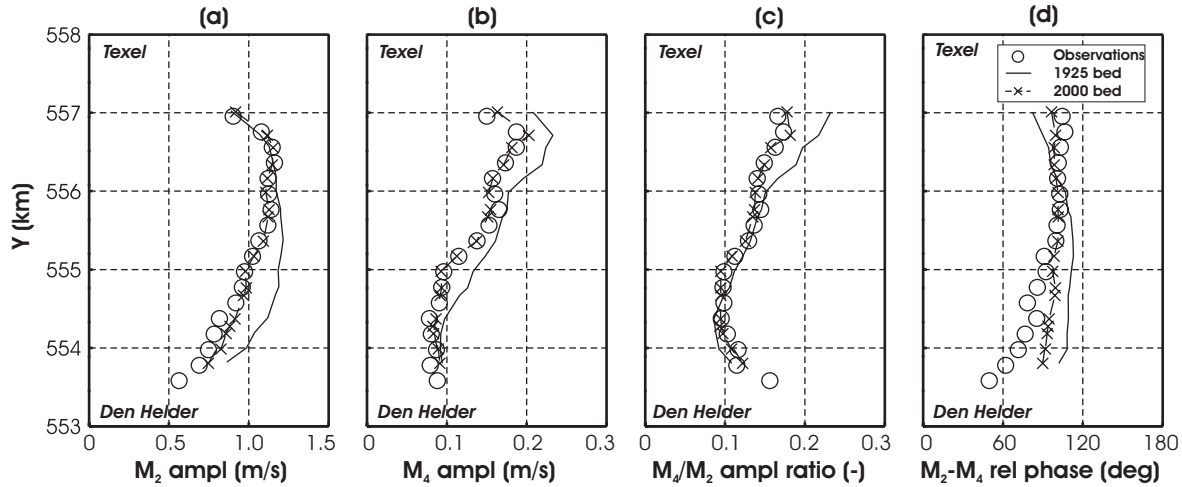

Figure 4-6: From left to right, comparison of (a) M_2 velocity amplitude, (b) M_4 velocity amplitude, (c) M_4/M_2 amplitude ratio and (d) M_4 phase relative to the M_2 for the modeled and observed tidal flow in the NIOZ-ferry transect (see Fig. 4-1 for location).

The tidal model is calibrated on the correct representation of the main tidal constituents for flow at a cross-section between Den Helder and Texel. Since 1998 an ADCP attached to the hull of the ferry from Den Helder to Texel (location see Fig. 4-1b) is used to measure current velocities in the inlet gorge (Ridderinkhof *et al.*, 2002). Preliminary results of the ongoing measurements have been made available by NIOZ for analysis (Bonekamp *et al.*, 2002). Flow data have been used to calculate time-series of depth-averaged flow at eighteen equidistantly distributed aggregation points between Den Helder and Texel. Harmonic analysis has been applied to these time series, and to the simulated flow output in the nearest grid cells, to derive the tidal mean flow conditions and amplitudes and phases of the main tidal flow constituents.

The correspondence in amplitude ratio and the relative phase difference between model and NIOZ ferry observations (Fig. 4-6c and d compare crosses and dots) indicate that the model is capable to reproduce the tidal asymmetry for the present situation reasonably well; only near the North Holland coast the relative phase difference is overestimated.

To our knowledge there is no evidence that the closure of the Zuiderzee has distorted the tidal wave propagation in the North Sea outside the sphere of inlet influence. The model boundaries are located well outside the ebb-tidal delta domain, and we therefore assume that the closure of the Zuiderzee has had no effect on the external forcing conditions. Changes in the tidal characteristics in the inlet domain result from the local interaction between bathymetry and tides only. Under this assumption we can apply similar tidal and quasi real-time boundary conditions on the different model bathymetries (1925, 1950, 1975 and 2000).

No validation could be performed on the accuracy of the simulated transport magnitudes due to a lack of suitable field data. The ongoing analysis of NIOZ-ferry measurements might provide an impression of the transport of suspended matter through Marsdiep in the near-future (Merckelbach and Ridderinkhof, 2006). Such datasets would provide an indispensable tool for model validation. For the moment, the simulated transport patterns must be considered in a qualitative sense rather than in a quantitative exact sense. Sensitivity analysis of model forcing and model parameters by variations in e.g. boundary conditions, bathymetry, bottom friction and wave parameters showed that the qualitative flow and transport patterns are relative insensitive to small-scale changes. This provides confidence in the modeled transport patterns. In addition Figure 4-9 (see Model results section) shows the general good agreement between transport vectors based on harmonically analyzed observations (gray vectors) in combination with the Groen model and similarly analyzed model results (black vectors), although the M_2M_4 bed load transports are somewhat underestimated and magnitudes of the bed load are slightly larger than the suspended load.

4.4.2 Tidal distortion of the flow

The dominant features of tidal distortion in shallow estuaries can be represented by the non-linear growth of the compound constituents and harmonics of the principal tidal components (Aubrey and Speer, 1984; Friedrichs and Aubrey, 1988). In principal the M_4/M_2 amplitude ratio of water levels (a) or velocities (u) can be used as an indicator for the non-linear tidal distortion (Aubrey and Speer, 1984), expressed as,

$$M_4 / M_2 = a_{M_4} / a_{M_2} \quad and / or \quad M_4 / M_2 = u_{M_4} / u_{M_2} \tag{4.5}$$

which reflects the combined effects of energy transfer from the M_2 to M_4 and frictional dissipation of both components. The relative phase difference between the M_2 and M_4, expressed as,

$$2M_2 - M_4 = 2\theta_{M_2} - \theta_{M_4} \tag{4.6}$$

determines the nature of the tidal asymmetry. For water levels, a relative phase difference in the vertical tide between 0 and 180 degrees indicates that the duration of the falling tide exceeds the rising tide and a flood-dominant flow occurs. Ebb-dominance is observed for relative phase-differences between -180 and 0 degrees. In a similar manner, for velocities it can be derived that sediment import occurs for $-90^\circ < 2\varphi_{M2} - \varphi_{M4} < 90^\circ$ and sediment export for $90^\circ < 2\varphi_{M2} - \varphi_{M4} < 270^\circ$.

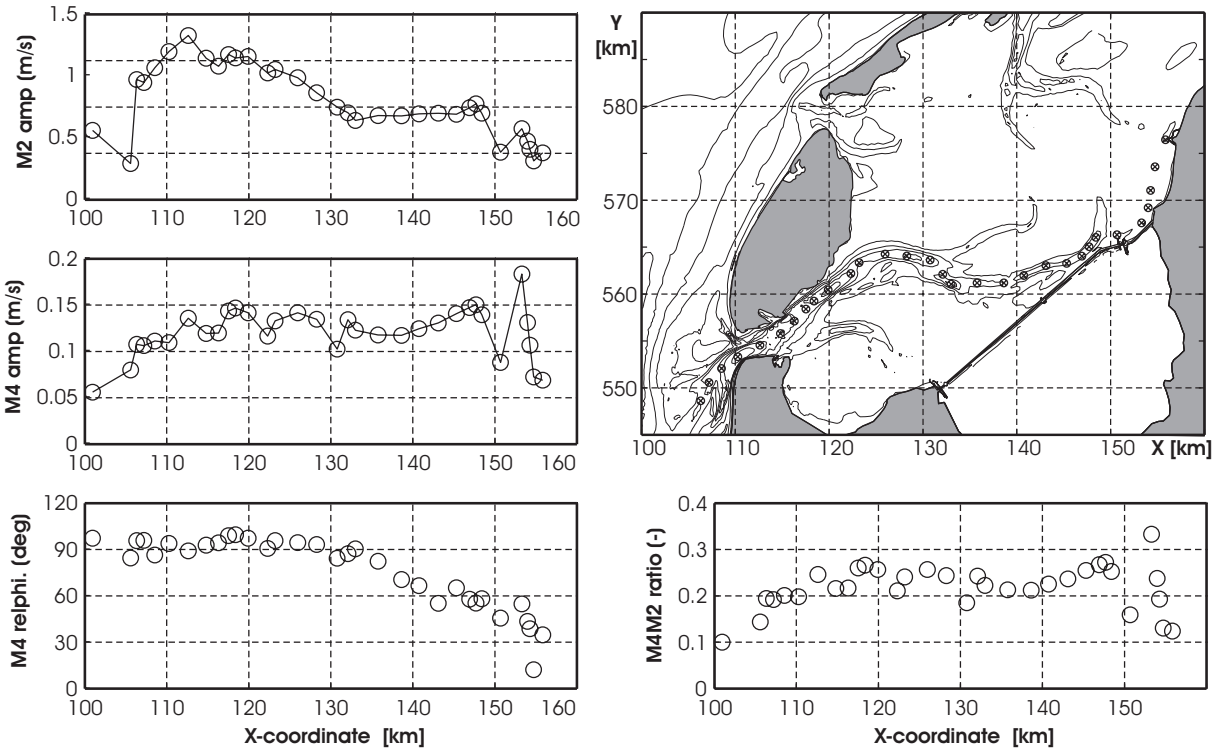

Figure 4-7: Tidal flow characteristics following Texelstroom (2000 bathymetry); black circles in the upper right plot indicate location of the observation point used in the harmonic analysis.

Measurements of flow in the basin are absent, however to obtain insight in the tidal distortion in the basin observation points were placed in the centre of the main inlet and basin channels; from ebb-delta to Harlingen following Breewijd, Marsdiep, Texelstroom and Doove Balg respectively. The focus is on the channel centre as this enables to define a major and minor axis of the tidal ellipses due to uni-directional (along-channel) flow. In each observation point a harmonic analysis was applied to the velocities in the major axis. Results for the velocities are plotted in Figure 4-7.

Maximum velocity amplitudes are observed in the confined margin of the inlet gorge due to the local acceleration of flow. In the basin and on the ebb-tidal delta velocities reduce considerably due to directional spreading and bottom friction. The fluctuations near Harlingen (X: 150-160 km) are due to the absence of a well-defined channel at this location.

In the middle of the inlet throat (X: 110-115 km) the $2M_2$-M_4 relative phases fluctuate around 90 degrees. In more detail it can be observed that the relative phase difference varies strongly over the cross-section increasing from 60 degrees near the southern embankment towards 100 degrees near Texel (Figure 4-6). Relative constant M_4/M_2 velocity amplitude ratios, but a substantial decrease in relative phase points to the increasing importance of tidal asymmetry in the basin. The modeled tidal distortion in the basin corresponds to what would be expected from on literature. Among others, Boon and Byrne (1981), Aubrey and Speer (1985), Friedrichs and Aubrey (1988) have shown that in addition to asymmetrical open-sea tidal forcing, basin morphology can affect the tidal asymmetry due to local generation by non-linear bottom friction, non-linear advection of momentum or tidal interaction with the morphology inside the basin such as the hypsometry effect leading to asymmetric flooding and drying of the inter-tidal shoals (e.g.

Boon and Byrne, 1981), and bathymetry-related residual flow circulations (e.g. Ridderinkhof, 1988; Van de Kreeke and Robaczewska, 1993).

In the proximal part of the basin (near the inlets) residual transport vectors dominate over the tidal asymmetry. In the central and back part of the basin the residual vectors of similar magnitude and smaller to the tidal asymmetry but in opposite direction (Fig. 4-8 e,f). The ebb-residuals induce a net westward (towards Marsdiep) directed transport plausibly related to the net throughflow from Vlie to Texel Inlet, whereas the tidal asymmetry transports are eastward directed towards Harlingen.

By specifying a Dominance Index (I_D) the relative contribution of the residual (S_{res}) versus the tidal asymmetry driven transports (S_{asym}) can be quantified (Van der Molen and de Swart, 2001). The dominance index reads,

$$I_D = \frac{|S_{res}| - |S_{asym}|}{|S_{res}| + |S_{asym}|} \tag{4.7}$$

The dominance index ranges between -1 and 1. Sediment transport due to residual currents prevails if $I_D > 0$, and tidal asymmetry prevails if $I_D < 0$. The dominance index (Figure 4-8g) illustrates the prevailing eastward-directed transports in the back, shallow, part of the basin. The tidal asymmetry driven transports plausibly play a role in the large observed sedimentation near Harlingen and along the Frisian coast.

Transports in the inlet gorge

An important observation is the ebb-dominant character of the sediment transports in the inlet gorge (see details in Fig. 4-9). The model results for the 2000 simulation reproduce the NIOZ measurements (see gray vectors) and observations by Bonekamp *et al.* (2002) well. An export in the northern part of the inlet and a smaller influx along the Den Helder coastline is modeled (Fig. 4-9, right). Both bed load and suspended load transports are dominated by the residual component (M_0M_2). In the bed load the M_2M_4 enhances the sediment export. In the suspended load the settling lag increases the sediment import in the south and reduces the sediment export in the north. The modeled sediment import is underestimated as the relative phase difference is close to 90 degrees over the entire cross-section. In reality the phase difference varies over the inlet gorge from 40° in the south to 100° near Texel (Fig. 4-6).

The modeled sediment transport patterns on the 1925 bathymetry shows similar characteristics to the 2000 bathymetry. The dominant M_0M_2 transports induce a net sediment export in the basin for both the suspended and bed load component. Transport magnitudes are slightly larger than in the present situation. As a result of the closure the tidal prism increased approximately 26%. The pre-closure bathymetry is not yet adapted to accommodate the increased discharges and velocities and the 1925 velocities in the inlet gorge are larger. The larger velocities in combination with small changes in relative phase difference and M_2M_4amplitude ratio (Fig. 4-9) enlarge the sediment transports. Relatively the largest differences occur in the M_2M_4 bed load transports. In 1925 these are twice the magnitude of the 2000 transport rates, due to the ebb dominance this increase cannot explain the large sediment import into the basin.

4.5 Model Results

Model results for the Groen (1967) and the Van Rijn (1993) sediment transport relations are presented. The Groen model is used to investigate the importance of the separate contributions of the main tidal asymmetries following the *local method* of Bonekamp *et al.* (2002) for the 1925 and 2000 bathymetry. Analysis of this data provides insight in the (changes in) importance of the tidal sediment transport mechanisms for the large sediment influx since closure of the Zuiderzee.

The second part of the model results presents the sediment transports derived from the Online Morphology model using the Van Rijn 1993 formulation. This section addresses the transports in the inlet gorge, while analysis of the flow and transport patterns for (different bathymetries) provide information on the back-barrier steering mechanism. Only results for the 1925 and 2000 simulation are presented in detail.

4.5.1 Model Results using the Groen Formulation

Transport patterns

Sediment transport patterns have been obtained by running the flow model for a 1-month period under tidal forcing. Harmonic analysis of the flow results was applied to derive the amplitudes and phases of the 15 main tidal flow constituents (e.g. M_2, O_1, K_1, $2N_2$, mu_2, N_2, nu_2, M_2, L_2, S_2, K_2, M_4, MS_4, $2MN_6$, M_6, $2MS_6$). The M_0, M_2 and M_4 were substituted in the Groen formula (see method) and residual transport patterns for the combined and individual contributions of the M_0M_2 and M_2M_4 were determined on the 2000 bathymetry. Residual transports in the inlet gorge are an order of magnitude larger then in the basin therefore we have made separate plots for clarity. Figure 4-8 presents the results for the bed-load transports ($\beta = 0$) on the ebb-delta (top panels a,b,c) and in the basin (d-g). The large-scale patterns for the suspended load transports ($\beta = 1$) are similar but smaller in magnitude (these are discussed for the inlet gorge only). As the interest is in the relative importance of the interactions rather than obtaining accurate estimates of magnitudes, and for comparison with the Bonekamp results transport rates are expressed as a velocity cubed.

Near the inlet, in the inlet gorge and on the ebb-delta the sediment transports are dominated by the M_0M_2 residual transports. Large sediment transports prevail at the locations of the main channels Schulpengat and Nieuwe Schulpengat. The presence of a large ebb-shield facing Nieuwe Schulpengat is an indication of the ebb-dominant character of this channel. Sediment transports related to the M_2M_4 tidal asymmetry induce a small net sediment import into the basin. In the inlet gorge results are similar to Bonekamp *et al.* (2002). Sediment export prevails as ebb transports, M_0M_2 driven, are larger then the flood dominant transports along the North-Holland coast (due to $M_0M_2 + M_2M_4$ forcing).

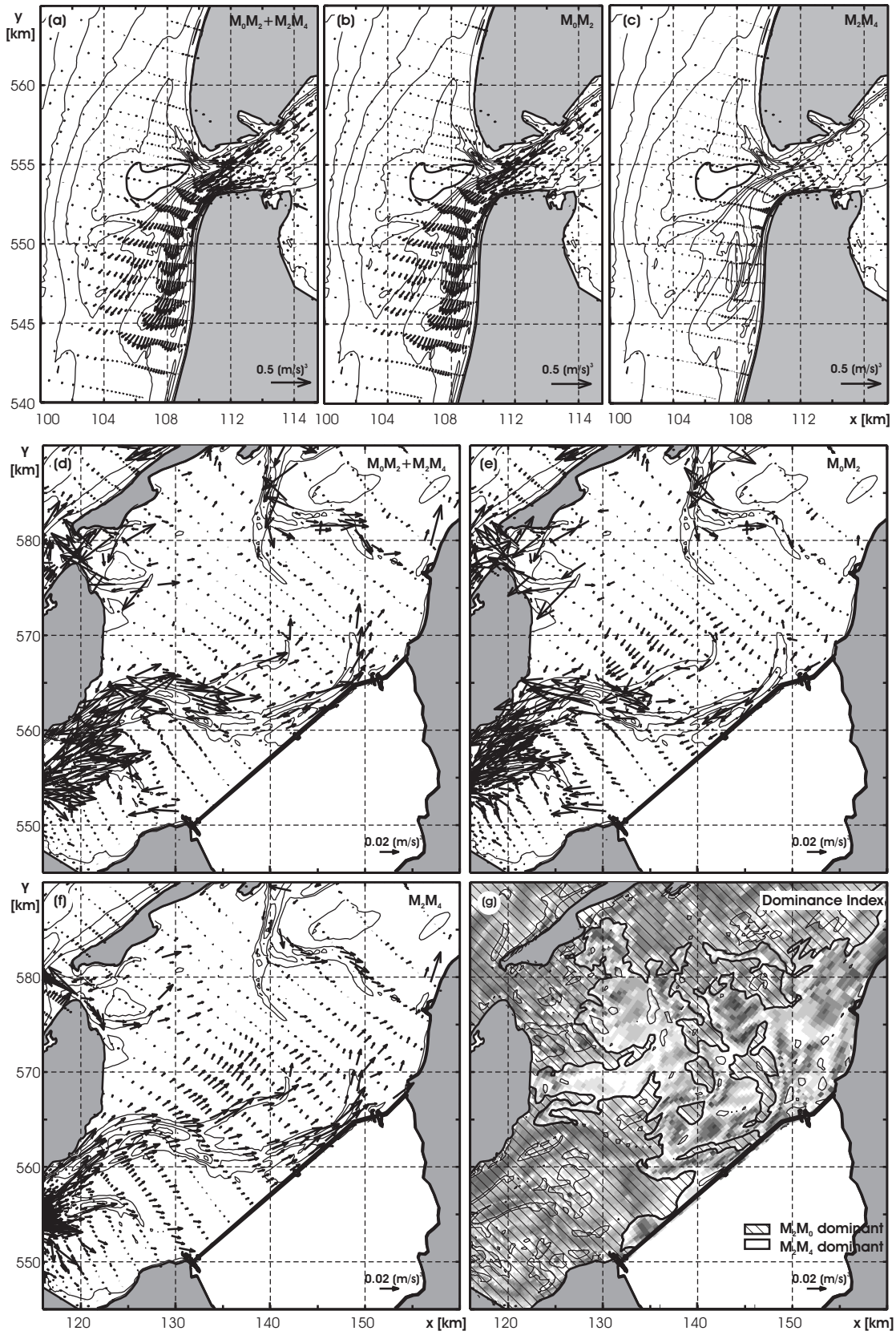

Figure 4-8: Bed-load transport patterns for ebb-tidal delta (top panels) and basin based on tidal flow in combination with the Groen (1967) transport formulation. Ebb delta transports for (a) M_0M_2 , (b) the M_2M_4 and (c) M_0M_2 + M_2M_4. Basin transport vectors for (d) M_0M_2 + M_2M_4, (e) M_0M_2, (f) M_2M_4 and (g) the dominance index

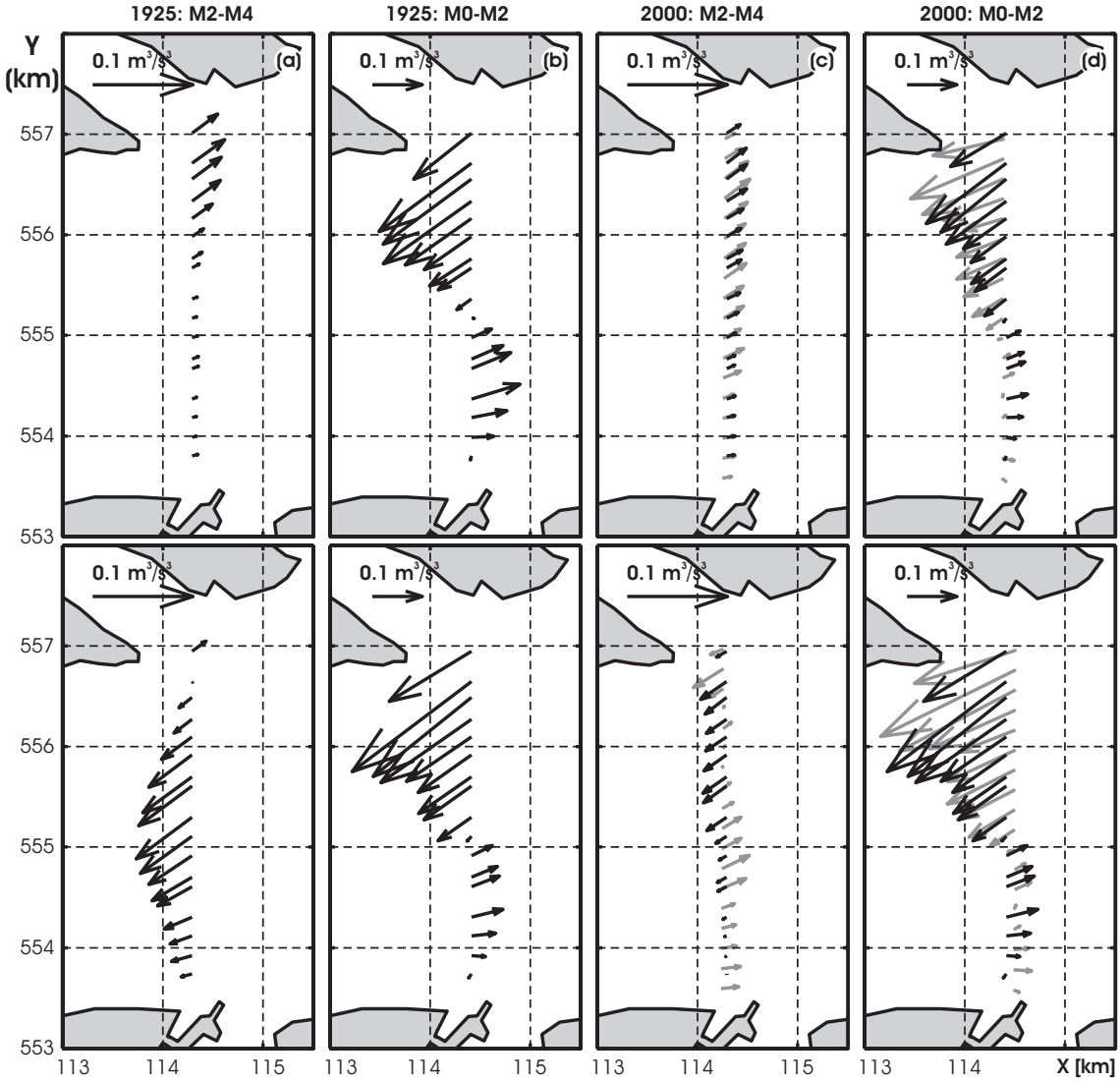

Figure 4-9: Suspended load (top) and bed-load sediment transport (bottom) due to and M_2M_4 and M_0M_2 asymmetry based on the Groen (1967) sediment transport formulation for the 1925 (a,b) and 2000 bathymetry(c,d) respectively. The gray vectors in the 2000 plots (c,d) represent the transport vectors based similarly analyzed NIOZ-ferry observations.

Table 5-1: Depth-averaged transport magnitudes averaged over the Marsdiep transect (m^3/s^3).

Transport	***1925***	***2000***	***Observations***
Suspended load			
M_0-M_2	-0.92	-0.89	-1.05
M_2-M_4	0.25	0.24	0.36
Bed load			
M_0-M_2	-1.37	-1.32	-1.54
M_2-M_4	-0.60	-0.28	0.15
Total :	-2.64	-2.25	-2.08

A major shortcoming of this *local* approach is that neither for the 2000 and 1925 bathymetry sediment import is predicted due to the dominance of the ebb-dominant tidal residual transports. Also, including the single interaction between M_6 and M_2 does not give a net transport of sediment as the flood and ebb velocity curves are equal but opposite directed. The interaction between the M_2, M_4 and the M_6 however gives an extra contribution to the net transport, which is of similar magnitude to the M_2, M_4 contribution. Applying a threshold velocity of motion reduced the (residual) sediment transports but also did not result in a sediment import. In reality bathymetric observations indicate a net sediment import in the order of 3-6 Mm^3/year.

4.5.2 Model Results using Delft3D Online Morphology (Van Rijn 1993)

Sediment transport patterns

Tide-averaged flow and transport patterns obtained from running the Online Morphology model using the Van Rijn (1993) transport option are presented in Figure 4-10 for the 1925 and 2000 bathymetry. The tidal residual flow field (Fig. 4-10a,b) illustrates the distortion of the alongshore propagating tidal wave due to interaction with the complex bathymetry of the ebb-tidal delta and the cross-shore inlet currents. Flood enters the ebb-delta from the south increasing substantially towards the inlet gorge (Fig. 4-11a). Maximum flood velocities occur at the western tip of Helderse Zeewering where flow accelerates around the sharp curvature of the seawall. This acceleration is larger during flood than during ebb. Ebb-tidal currents through Texelstroom accelerate in the narrow constriction of the inlet gorge (Fig. 4-11b) and the ebb outflow dominates the updrift part of the ebb-tidal delta.

Despite similar tidal forcing conditions on the open-sea boundaries difference in discharge and flow magnitudes in Texel inlet are observe. The 1925 maximum ebb and flood velocities, and residual discharges exceed the 2000 values by approximately 10-15%; the net outflow on the 1925 bathymetry is 110 Mm^3/tide compared to 97 Mm^3 in 2000. This difference plausibly relates to the larger storage area of the basin in 1925 and the presence of connecting channels near Harlingen in 1925 enabling a more efficient throughflow.

The larger 1925 tidal prism is one of the causes for the substantial larger flow and transports in the inlet gorge directly after closure (also see Fig. 4-6a). An interesting characteristic is the imbalance between the location of the largest residual flow and transports, and the position of the main channels (Fig. 4-10a,c). The main channel orientation is westward, whereas largest instantaneous and residual flow velocities and transports are directed southwestward towards Schulpengat. Major gradients in residual transport rates are observed at the locations where Molengat and Nieuwe- Schulpengat developed (erosion) and in Westgat (sedimentation). This inequality between flow and bathymetry, directly after closure before morphological updating, is interpreted as a manifestation of the back-barrier steering effect.

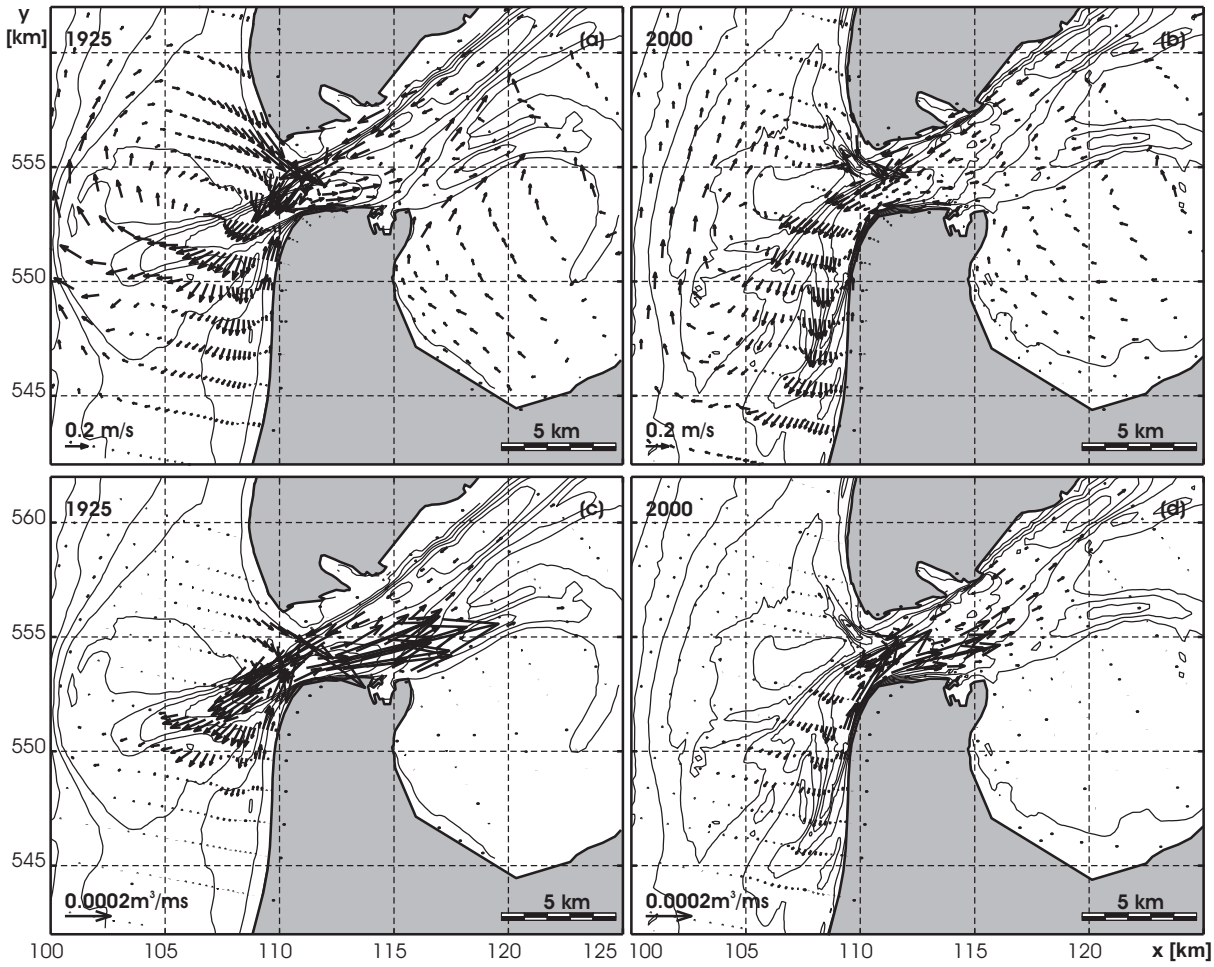

Figure 4-10: Residual flow and transport vector fields for the 1925 (a,c) and 2000 (b,d) Online Morphology simulation.

With ongoing morphological adaptation of the bathymetry, filling in of Westgat and the scouring of Schulpengat and Molengat, the imbalance between transports and bathymetry and the residual transport rates decrease (1950 and 1975 patterns, not shown). In 2000 the residual flow and transport patterns are smaller and correspond reasonably well with the location of the main channels (Fig. 4-10b and d).

Detailed analysis of the concentration and transport fields in Marsdiep provides more understanding of the dominant mechanisms behind the large sediment influx since closure (Fig. 4-12). Model results are presented for concentration fields (during spring tide as differences are most pronounced) averaged over the ebb (Fig. 4-12a), averaged over the flood (Fig. 4-12b) and tide-averaged for the 1925 bathymetry. During flood the major part of the sediment is picked up at the location of Nieuwe Schulpengat and Molengat resulting in a large sediment influx through Marsdiep. During ebb the majority of the flow is directed from Texelstroom towards Marsdiep, despite large flow velocities sediment concentrations in Texelstroom are relative minor; most of the sediments are picked up in the inlet gorge along the Texel coastline where flow accelerates. The resulting tide-averaged concentration field shows distinct flood orientated concentrations along the North-Holland coastline, through Marsdiep towards Texelstroom. The ebb-dominant counterpart in Marsdiep (at the location of the NIOZ transect) is small.

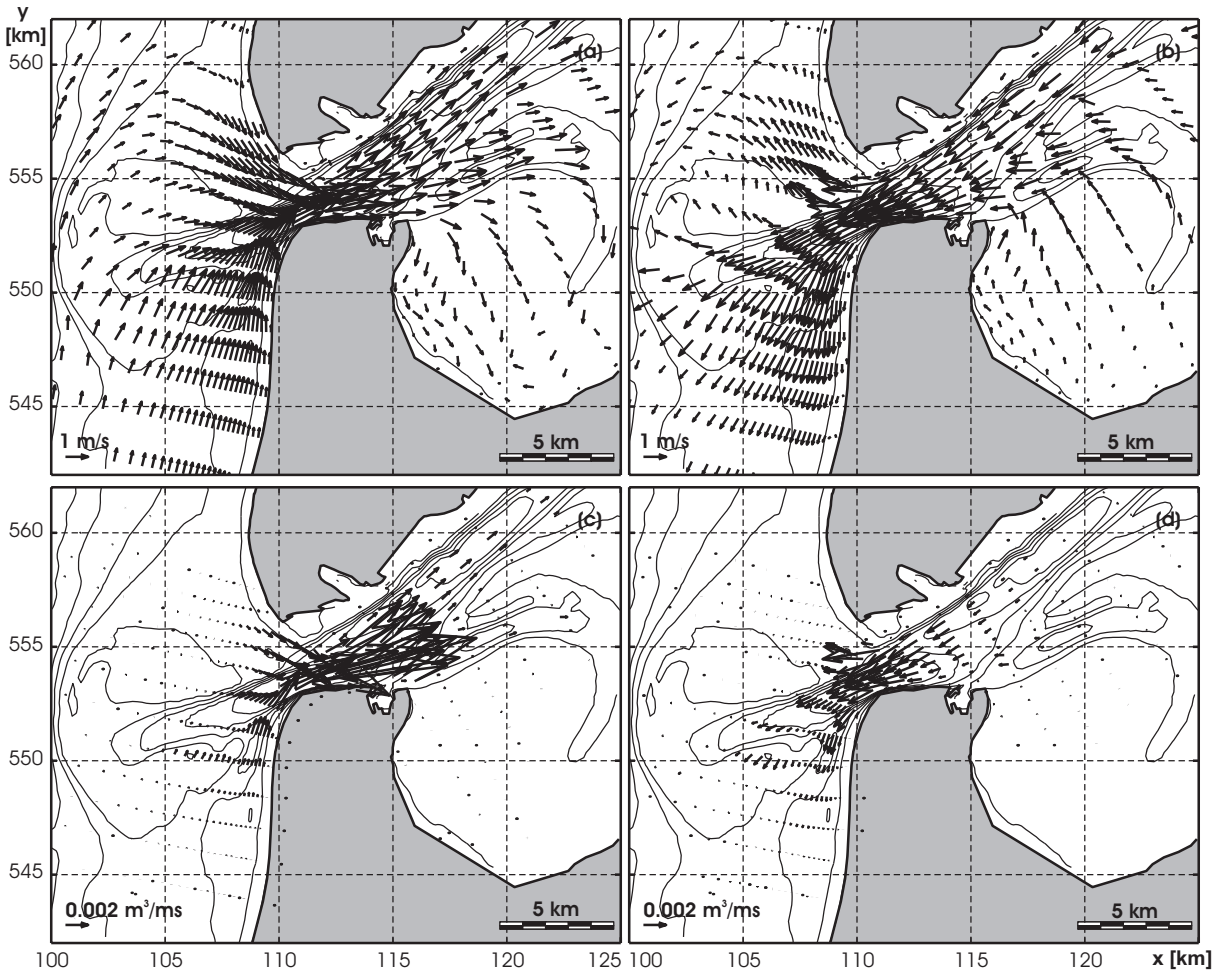

Figure 4-11: Maximum ebb and flood flow (top) and transports (bottom) for the 1925 (a, c) and 2000 (b,d) Online Morphology simulation. For clarity only a limited number of vectors have been plotted in x- and y-direction.

Details of the flow, concentrations and sediment transports along the NIOZ ferry transect confirm this analysis (Fig. 4-12 d to g); the middle panels show results for the 1925 bathymetry, the lower panels for the 2000 simulation. Sediment import is mainly caused by the suspended transports (note the difference in scaling in Figure 4-12f and g) and results from the asymmetry between maximum ebb and flood velocities. This asymmetry is largest along the North-Holland coast where maximum flood velocities (of nearly 2 m/s during spring tide) induce a large import. These large flood velocities are related to the acceleration of flow around the tip of Helderse Zeewering. The accelerating flow is capable of transporting a vast amount of sediment into the basin.

Along the Texel coast peak ebb and peak flood velocities are near-equal. During flood the modeled (depth-averaged) concentrations exceed the equilibrium concentrations (Fig. 4-12e), while during ebb sediment transport rates and sediment concentrations in Texelstroom are below the equilibrium concentration. This suggests that during ebb sediments transported from the basin partly settle in Texelstroom and only a limited amount of sediment is transported from the basin seaward. It is only in the inlet gorge and on the ebb-tidal delta that sediment is picked-up and transported seaward (Fig. 4-10b).

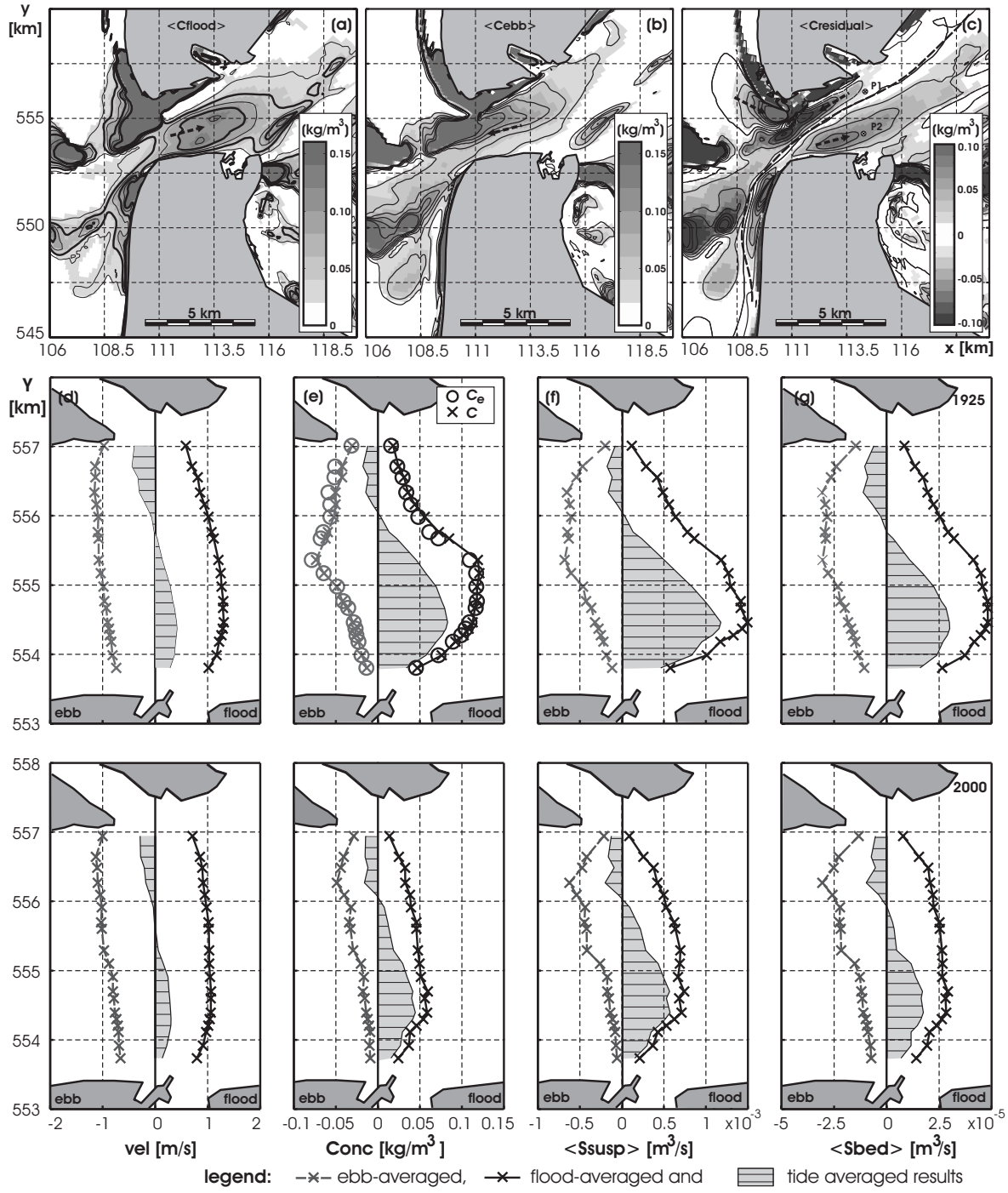

Figure 4-12: (top) Modeled concentration fields averaged over the flood (a), ebb (b) and tide-averaged (c) for spring tide conditions (20-01-1999 16:40 - 05:30). Model results for flow (d), concentration and equilibrium concentration (e), suspended and bed-load transports (f and g) for the 1925 (middle) and 2000 (bottom) bathymetry in the NIOZ transect.

With ongoing adaptation of the basin the asymmetry between ebb and flood transports reduces (Fig. 4-12e 1925-2000) and sediment import rates diminish; sediment import rates exceed 3.5 Mm^3/year in 1925, diminish towards 0.2 Mm^3/tide in 2000 (sediment volumes corrected for pores). Note that these sediment transport rates are strongly determined by the selected grain diameter (relative change in sediment transports in inlet gorge for d_{50} = 150 μm +20%, d_{50} = 400 μm -26%, d_{50} = 600 μm -62 %).

4.6 Discussion

4.6.1 Tidal sediment transport mechanisms

One of the major unresolved aspects for Texel Inlet are the main mechanisms responsible for the observed large sediment import into the basin after closure. Sediment import for the present situation could not be explained by locally applying the Groen (1967) transport relation to the modeled tidal flow fields; the ebb-residual sediment export dominates over the flood-dominant tidal-asymmetry driven import (in correspondence to Bonekamp *et al.*, 2002). Similar results were obtained by analysis of the sediment transports for the 1925 bathymetry, while in reality bathymetric observations indicate a net sediment import in the order of 3-6 Mm^3/year.

Sediment import is predicted by running Delft3D Online Morphology computing the sediment transport dynamically (each time-step) using the Van Rijn (1993) transport formulation. The sediment influx is dominated by the large flood-dominant transports along the North-Holland coastline that exceed the minor ebb transports along the Texel coastline. The suspended-load component dominates over the bed-load. The main factors for the discrepancy between *local* and *complex* model results can be obtained from Figure 4-13 illustrating time-series for flow, concentration and sediment transport in two representative points covering the spring tide cycle presented in Fig. 4-12.

Point 1 is representative for the ebb dominant part of the channel (for flow). Tidal asymmetry between maximum ebb and flood velocities is minimal, but due to the longer duration of the ebb a net outflow of water occurs. As maximum ebb and flood velocities are near-equal also the equilibrium concentrations during maximum ebb and flood are of similar magnitude. However, the modeled sediment concentrations during flood exceed the equilibrium concentration due to lag effects related to the large sediment influx from Molengat and Nieuwe Schulpengat (settling lag). During ebb an opposite behavior is observed with sediment concentrations below the equilibrium value (scour lag). This opposite behavior of the concentration curves results in larger flood then ebb concentrations, and in contrast to the predicted large sediment export in the *local model*, averaged over the tidal period a near-zero sediment export is modeled.

Point 2 shows a time-series representative for the tidal asymmetry related sediment import along the Den Helder coast. The considerable difference between the maximum ebb and flood velocities results in large sediment import into the basin (note that suspended sediment import due to tidal asymmetry was also predicted by the *local model*).

As the Online Sediment simulation is capable of reproducing the observed sediment import only by tidal forcing it must be concluded that tides (tidal asymmetries) play an important role in the sediment influx into the Wadden Sea. The *local model* formulation (or in a more general context a simple model formulation based on local transports only) is not suited for complex areas such as tidal inlet systems, where large gradients in velocities and transports are present.

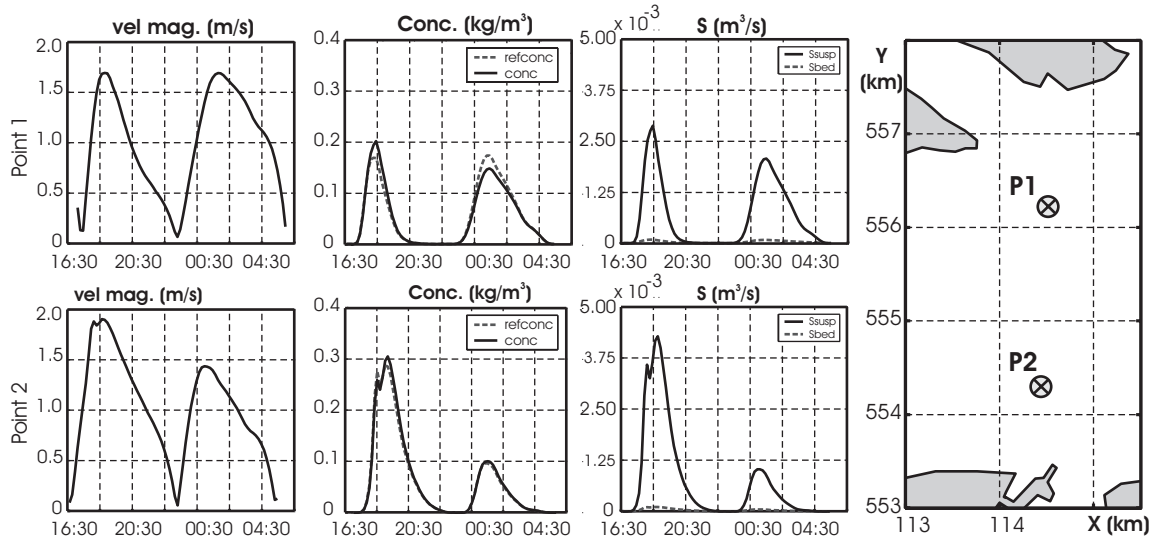

Figure 4-13: Modeled time series for flow, sediment concentration and transports in Point 1 (top) and Point 2 (bottom).

Two main actors are identified for the observed discrepancy between *complex* and *simple* model:

(1) the dominance of the suspended load transports.

The Groen formulation is basically a power 3 relation (bed load representative) to the velocities wherein changes in the suspended sediment concentration are caused by local erosion and deposition. Spatial variations in concentrations and velocity are neglected and therefore the important mechanisms of settling lag and scour lag (Van Straaten and Kuenen 1957) are not accounted for. Settling lag can be important when considering the fall velocity and depth difference between ebb-delta and inlet gorge. Assuming that a particle is brought into suspension on the ebb-delta shoals (at -5 m water depth) and is supplied to the deep main inlet channel (on average 20 m deep). Then assuming a fall velocity of 0.001 m/s it takes this particle over 4 hours to reach the bottom. With horizontal velocities peaking over 1 m/s it would travel km's during its settling period. To effectively account for settling lag in the Groen model a Lagrangian in stead of an Eulerian description of the velocity field must be applied (Ridderinkhof, 1997).

(2) spring-neap modulations in suspended load transports.

An aspect which needs further investigation is the spring-neap modulation in sediment import rates. Time-series of the sediment transports in Marsdiep show increasing transport towards spring-tide, and near-zero import during neap tides. In theory for (bed-load) transport only the interaction between the leading tidal constituent and its even-overtides leads to a net import of sediment (Van de Kreeke and Robaczewska, 1993). In the complex environment of Texel inlet where flow interacts with the ebb-delta bathymetry and accelerates around the Helderse Zeewering during flood, the considerably larger spring tidal prisms can lead to differences in the residual flow and transport patterns. Additionally a variation in tidal asymmetry is observed in the velocity and water level time-series; a larger asymmetry is present during spring tide compared to the neap tide.

4.6.2 Sediment demand, transport capacity and availability

Using the complex model results, and basic principles of sediment demand, sediment transport capacity and sediment availability we can hypothesize on the mechanisms governing the large sediment import since closure.

Sediment demand; As a result of the closure both the basin and the ebb-tidal delta require sediment. The basin needs sediment to restore the distorted balance between channel and shoal areas; due to the Closure the relative shallow Zuiderzee was separated from the deep Wadden Sea. Hence, the remaining shoals area is too small relative to the volume of channels (e.g. Eysink, 1990). But also the ebb-tidal delta needs sand. Based on empirical relations (Walton and Adams, 1976) the ebb-tidal delta sand volume was expected to enlarge as the tidal prism increased after closure.

Sediment transport capacity; The large tidal prisms and associated tidal currents are capable of transporting vast quantities of sediment during flood from the ebb-tidal delta to the basin and vice versa during ebb. The residual ebb discharges exceed the residual flood discharges. Ebb flow dominates Marsdiep along the Texel coast and flood dominates Marsdiep along the North-Holland coastline.

Sediment availability; In principle when a system is forced out of equilibrium the adaptation rate is dependent on the size of the distortion. After closure, on the ebb-tidal delta an imbalance between flow and bed is observed; e.g. large flow velocities are directed onto a relative shallow area. This denotes a large scouring capacity of the tidal currents on the ebb-tidal delta. In the upper part of the ebb-tidal delta new channels are formed (Molengat and Schulpengat) and during ebb a vast amount of sediment is redistributed seaward and deposited. Consequently a large quantity of sediment is available for transport into the basin with the flood tidal currents. Largest (residual) flood transport rates are observed along the North-Holland coastline. In the sheltered environment of the basin sediment partly settles.

The majority of the ebb outflow from the basin onto the ebb-tidal delta is concentrated in Texelstroom. Alterations in the size and position of Texelstroom have been minor compared to the large changes on the ebb-tidal delta (Elias *et al.*, 2003b). Hence, the upper-part of the basin remained in near-equilibrium state after closure and only a limited amount of sediment is available to be transported seaward during ebb. Fig. 4-10 (maximum ebb) shows that the majority of the ebb-outflow originates from Texelstroom that contains only limited sediment concentrations and sediment transport rates.

In conclusion, both basin and ebb-tidal delta require sediment. More sediment is available during flood to be transported from the ebb-tidal delta into the basin than during ebb. The spatially uneven sediment availability in combination with the distinct separation of ebb-dominant transport along the Texel coast and flood-dominant transport along the North-Holland coast plausible explains why sediment is imported into the basin despite the residual export of flow. With the ongoing morphological adaptation of the ebb-tidal delta the imbalance between flow and bathymetry, and the (tidal) sediment import into the basin diminish.

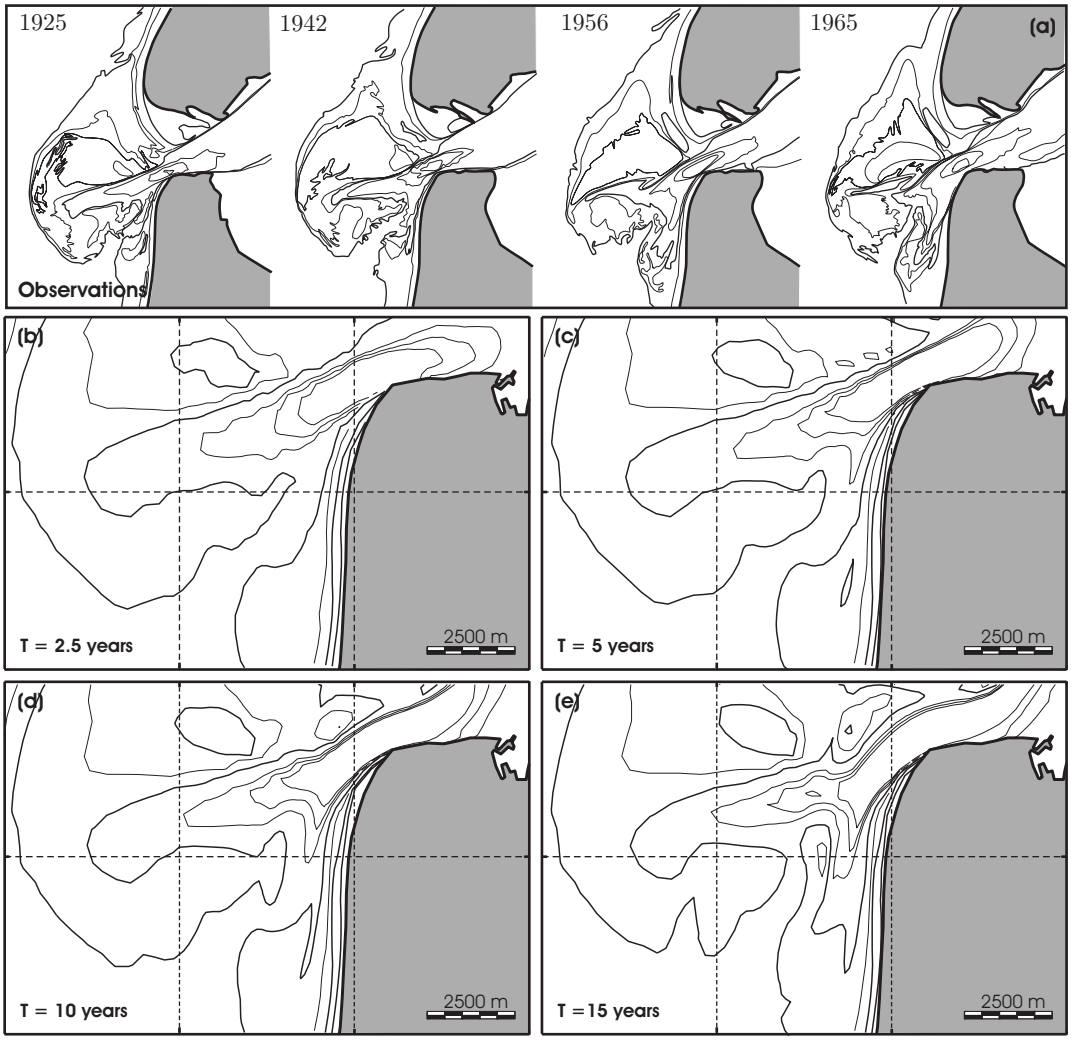

Figure 4-14: Development of a two-channel system on the ebb-tidal delta after closure. Top: observations and (bottom) modeled bathymetries after 2.5, 5, 10 and 20 years of simulation

Wind and waves have not been investigated in detail, but model results indicate that these processes are dominant on the major shoal areas of the ebb-tidal delta. On the ebb-tidal delta wave breaking, enhancement of bed shear stresses and stirring-up of sediment allows more sediment into suspension to be transported by the tidal flow. In the deep proximal part of the basin waves are less important due to the sheltering effects of the ebb-tidal delta and Texel.

4.6.3 Back-barrier steering mechanism

A second aspect studied is the back-barrier steering mechanism. Under the assumption that the closure of the Zuiderzee did not impact the open-sea boundary conditions (that are placed far-away outside the sphere of inlet influence) we applied similar tidal forcing time-series on the 1925 and 2000 bathymetries. The 1925 bathymetry is representative for the pre-closure state, whereas the hydrodynamics respond instantaneously to the presence of the Closure dam.

Model results illustrate that after closure the majority of the ebb-flow was directed from Marsdiep onto the southern part of the ebb-tidal delta and in 1925 an imbalance between the location of the largest (residual) flow velocities and the presence of tidal channels occurred (Fig. 4-10). The modeled imbalance between flow and bathymetry, directly after closure before morphological updating, is a manifestation of the back-barrier steering effect.

This latter statement is confirmed by continuing the tidal simulation over a 25-year period (using a morphological acceleration factor of 25). Figure 4-14 illustrates the modeled bathymetries for selected years. This tidally forced model is capable of reproducing the major developments on the southern part of the ebb-delta (although time scales differ).

Nieuwe Schulpengat enlarges and extends along the North-Holland coastline. Similarly to the observations (1942,1956) first an ebb-chute develops along the coastline (see T = 10 years) that gradually increases in depth and length forming the main ebb channel. After 15 years of simulation a two-channel system arises separated by a linear shoal (similar to the 1975 in the observations). The formation of the two-channel system is due to the segregation of ebb and flood flow. Ebb currents dominate the main channel and form a hydrodynamic obstacle for the flood currents. Flood currents are pushed seaward along the ebb-shield front. Already Van Veen (1950) showed the formation of separate ebb and flood channels separated by shoals due to the evasive action of the ebb and flood flow.

Although the scouring of the channels in the southern part of the ebb-delta is predicted, the landward migration and deformation of Noorderhaaks is not reproduced. This deficit indicates that Noorderhaaks developments are dominated by wave-driven processes that are not included in the present model.

4.7 Conclusions

Inlet research has long relied on expert-judgment based interpretations of observations. However, due to the spatial extent of inlet systems and the temporal and spatial variety of the forcing processes it is practically impossible to obtain field data with sufficient resolution and accuracy over the entire inlet domain. This makes identification of the dominant processes and mechanisms difficult; especially if the inlet is subject to large morphological change due to human intervention, and existing conceptual models and empirical relations cannot explain the observed developments.

An integrated approach of field- and model-data analysis can help to understand inlet dynamics and evolution as was shown in this study by making initial tidal simulations during various stages of the morphological adaptation process. The back-barrier steering mechanism is revealed to trigger the observed morphological developments on Texel Inlet's ebb-tidal delta. After closure, the imbalance between the location of the largest residual tidal flow and the presence of tidal channels on the ebb-tidal delta and the balance in the upper part of the basin provide a larger sediment availability during flood than during ebb. This spatially uneven sediment availability plausibly explains why sediment is imported into the basin despite the residual export of flow. With the ongoing morphological adaptation of the ebb-tidal delta the imbalance between flow and bathymetry and the sediment import into the basin diminish.

This study illustrates the necessity of *'complex'* process-based model simulations in a compound inlet environment. The *'local'* model approach showed that even an intermediate method using complex flow model results and a simple transport formulation (assuming that the transports can be expressed as a cubic expression of the flow velocity) leads to spurious results. Observed sediment import could not be explained as the ebb-residual sediment export dominates over the flood-dominant tidal-asymmetry driven import in both the 1925 as 2000 simulation. This discrepancy with observations results from the suspended load dominance. The applied Groen sediment transport formulation is basically a velocity to the power 3 relation wherein settling lag (spatial variations in the concentration field due to accelerating or decelerating flow) and scour lag effects are not accounted for. In addition it is questionable if analysis based on M_0, M_2, M_4 and M_6 only is valid, but this aspect needs further investigation.

Wind and waves have not been investigated in detail, but model results indicate that these processes are dominant on the major shoal areas of the ebb-tidal delta. On the ebb-tidal delta wave breaking, enhancement of bed shear stresses and stirring-up of sediment allows more sediment into suspension to be transported by the tidal flow. In the deep proximal part of the basin waves are less important due to the sheltering effects of the ebb-tidal delta and Texel. The importance of these processes are the focus of further research [presented in Chapter 6 of this Thesis].

4.8 Acknowledgements

The work herein was carried out as co-operation between RIKZ (Dutch National Institute for Coastal and Marine Management) and Delft University of Technology. Funding was provided by the Dr. Ir. Cornelis Lely Foundation and the Delft Cluster Project: Coasts 03.01.03. Data were made available by the Directorate-General of Public Works and Water Management. The Delft3D model was made available by WL | Delft Hydraulics. Tidal analysis tools were provided by dr. J.G. Bonekamp. The authors thank dr. J. Cleveringa, ir. J. de Ronde and Prof. J. van der Kreeke for their constructive comments and contributions to the manuscript.

Appendix A : DELFT3D ONLINE MORPHOLOGY (2DH IMPLEMENTATION)

The physical and numerical implementation, testing and validation of the Delft3D Online Morphology has been reported in detail by Lesser (2000), Lesser *et. al.* (2004) and WL| Delft Hydraulics (2005). Therefore only a short description of the model basics (largely based on Lesser *et. al.* 2004) is presented with an additional section on the depth-averaged implementation of the Van Rijn (1993) transport formulation (Roelvink 2006, Personal Communication).

Hydrodynamics

The Delft3D-FLOW module (Version 3.43.01.00 is used in this thesis) forms the core of the Delft3D Online Morphology model, simulating water motion due to tidal and meteorological forcing by solving the unsteady shallow-water equations. The system of equations consists of the continuity equation (A.1), the horizontal momentum equations (A.2), the transport (advection-diffusion) equation (A.3) and a turbulence closure model (by default the k-ε model for 3D simulations):

$$\frac{\partial \xi}{\partial t} + \frac{\partial \left[h\bar{U}\right]}{\partial x} + \frac{\partial \left[h\bar{V}\right]}{\partial y} = S \tag{A.1}$$

$$\frac{\partial U}{\partial t} + U\frac{\partial U}{\partial x} + v\frac{\partial U}{\partial y} + \frac{\omega}{h}\frac{\partial U}{\partial \sigma} - fV = -\frac{1}{\rho_0}P_x + F_x + M_x + \frac{1}{h^2}\frac{\partial}{\partial \sigma}\left[v_V \frac{\partial u}{\partial \sigma}\right]$$

and (A.2)

$$\frac{\partial V}{\partial t} + U\frac{\partial V}{\partial x} + v\frac{\partial V}{\partial y} + \frac{\omega}{h}\frac{\partial V}{\partial \sigma} - fU = -\frac{1}{\rho_0}P_y + F_y + M_y + \frac{1}{h^2}\frac{\partial}{\partial \sigma}\left[v_V \frac{\partial v}{\partial \sigma}\right]$$

$$\frac{\partial [hc]}{\partial t} + \frac{\partial [hUc]}{\partial x} + \frac{\partial [hVc]}{\partial y} + \frac{\partial [\omega c]}{\partial \sigma} = h\left[\frac{\partial}{\partial x}\left(D_H \frac{\partial c}{\partial x}\right) + \frac{\partial}{\partial y}\left(D_H \frac{\partial c}{\partial y}\right)\right] + \frac{1}{h}\frac{\partial}{\partial \sigma}\left[D_V \frac{\partial c}{\partial \sigma}\right] + hS \tag{A.3}$$

Wherein ζ and h are water level and depth (m), U, V are flow velocity components (m/s) consisting of the Eulerian flow velocities and stokes drift components if waves are included (Walstra *et al.*, 2000), S represents the contributions per unit area due to e.g. discharge or evaporation of water (m/s), w is the vertical velocity component (s^{-1}), eddy diffusivities and viscosities need to be prescribed (D_H, D_V and v_H, v_V), c is the mass con-

centration of sediment (kg/m^3), M_x and M_y represent the contributions due to external sources or sinks of momentum (e,g structures, discharge of withdrawal of water, wave stresses), f is the Coriolis parameter (1/s). See Lesser *et al.* (2004) for details on how the horizontal pressure gradients (P_x and P_y), horizontal Reynold stresses (F_x and F_y) are solved.

A basic assumption in Delft3D is that vertical accelerations are minor compared to gravitational acceleration ('shallow water assumption') reducing the vertical momentum equation to the hydrostatic pressure relation:

$$\frac{\partial P}{\partial \sigma} = -\rho g h \tag{A.4}$$

To solve this set of equations boundary conditions for bed, free surface and lateral boundaries have to be specified; see Deft3D manual for a complete overview (WL| Delft Hydraulics, 2005).

The continuity and horizontal momentum equations are solved on a staggered grid (Arakawa C-grid) by default using an Alternating Direction Implicit method (Leendertse, 1987) extended with the Cyclic Method of Stelling (1984).

Sediment transport

The Online Morphology version supplements the flow results with sediment transports. In this thesis TRANSPOR1993 is used. The Delft3D implementation of this formulation follows the principle description of Van Rijn (1993). Van Rijn distinguishes between bed load (S_b) and suspended load (S_s) transports.

Sediment exchange with the bed is implemented through a source (D) and sink (E) relations following the Van Rijn (1993) approach. This approach is based on the calculation of a reference sediment concentration (c_a see A.12) at a reference height (a) determined by bed roughness (based on Van Rijn 1984):

$$D = c_a \left(\frac{D_V}{\Delta z} \right) \text{ and } E = c_{kmx} \left(\frac{D_V}{\Delta z} + w_s \right) \tag{A.5}$$

where D_v is the vertical diffusion coefficient at the bottom of the reference cell (first cell above the reference height), Δz the vertical distance from the reference level a to the centre of the reference cell (Van Rijn, 1993), and c_{kmx} the mass concentration in the reference cell (see Lesser, 2000 for implementation), w_s is the sediment settling velocity (m/s).

The sediment concentration at the reference height (c_a) is specified as,

$$c_a = f_{SUS} \eta 0.015 \rho_s \frac{d_{50}}{a} \frac{T_a^{1.5}}{D_*^{0.3}} \tag{A.6}$$

Here f_{sus} is a calibration coefficient, η is the relative availability of the sediment fraction at the bed T_a and D_* are the dimensionless bed shear stress and particle diameter (Van Rijn, 1993, 2000).

Suspended sediment transport is computed by the advection-diffusion solver (A.3). To describe sediment characteristics additional formulations are included to account for: density effects of sediment in suspension (Eckart, 1958), settling velocity (Van Rijn, 1993), vertical diffusion coefficient for sediment, suspended sediment correction vector and sediment exchange with the bed. See Lesser *et al.* (2004) for details on implementation.

For depth-averaged applications (as presented in this Chapter) the 3D advection-diffusion equation is approximated by the depth-integrated advection-diffusion equation (Roelvink, Personal Communication):

$$\frac{\partial h\overline{c}}{\partial t}+\overline{u}\frac{\partial h\overline{c}}{\partial x}+\overline{v}\frac{\partial h\overline{c}}{\partial y}-D_H\frac{\partial^2 h\overline{c}}{\partial x^2}-D_H\frac{\partial^2 h\overline{c}}{\partial y^2}=h\frac{\overline{c}_{eq}-\overline{c}}{T_s} \tag{A.7}$$

Here h is the water depth, $\overline{u}$ and $\overline{v}$ are the depth-averaged velocity components in x- and y-directions, D_H is the horizontal dispersion coefficient, $\overline{c}$ is the depth-averaged sediment concentration, $\overline{c}_{eq}$ is the depth-averaged equilibrium concentration and T_s is an adaptation time-scale.

The depth-averaged equilibrium concentration $\overline{c}_{eq}$ is defined as:

$$\overline{c}_{eq}=\frac{\left|S_{sus,eq}\right|}{\left|\overline{\vec{u}}\right|h} \tag{A.8}$$

Here, $S_{sus,eq}$ is the depth-integrated suspended sediment transport for steady and uniform conditions. There are two ways of specifying this transport rate, depending on the type of formulation used. In using a formulation developed for depth-averaged simulations, the existing algorithms provide $S_{sus,eq}$ directly and no further action is required. For formulations developed for 3D simulations, such as Van Rijn 1993 or 2004, $S_{sus,eq}$ has to be determined by (1DV) numerical integration:

$$S_{sus,eq}=\int_{z_b}^{z_s}u_{eq}(z)\,c_{eq}(z)\,dz \tag{A.9}$$

The equilibrium velocity profile is assumed to be logarithmic:

$$u_{eq}(z)=\overline{u}\frac{\ln\left(1+\frac{z}{z_0}\right)}{\ln\left(1+\frac{h}{ez_0}\right)} \tag{A.10}$$

The equilibrium concentration profile is computed by numerically integrating Schmidt's equation:

$$wc_{eq}(z)+D_v(z)\frac{\partial c_{eq}(z)}{\partial z}=0 \tag{A.11}$$

Here $D_v(z)$ is the vertical dispersion coefficient as prescribed by Van Rijn (1993); the boundary condition is taken as $c_{eq}(z_{ref}) = c_{ref}$, where the reference concentration is a function of the local bed shear stress.

Te adaptation time is a function of water depth, fall velocity and shear velocity, according to the Galappatti formulations (Gallappatti, 1983):

$$T_s = \frac{h}{w} T_{sd} \tag{A.12}$$

The dimensionless adaptation time is given by the following approximation:

$$T_{sd} = w_* \exp\begin{bmatrix} (1.547 - 20.12u_r)\, w_*^{\,3} \\ +\left(326.832 u_r^{\,2.2047} - 0.2\right) w_*^{\,2} \\ +(0.1385 \ln(u_r) - 6.4061)\, w_* \\ +(0.5467 u_r + 2.1963) \end{bmatrix} \tag{A.13}$$

with $u_r = u_* / \overline{u}$ and $w_* = w / u_*$

Bed load transports represent the transport of sand particles in the wave boundary layer in close contact with the bed surface (below the reference level a) and are calculated following the Van Rijn (1993) approach.

For simulations without waves the bed-load sediment transport rate ($|S_b|$ in kg/m/s) is calculated by:

$$|S_b| = f_{BED}\, 0.5 \eta \rho_s d_{50} u_*' D_*^{-0.3} T \tag{A.14}$$

herein f_{BED} is a calibration coefficient, η is the relative availability of the sediment fraction in the mixing layer (-), u_*' is the effective bed shear velocity, D_* is the dimensionless bed shear stress and dimensionless particle diameter (Van Rijn, 1993).

For completeness the formulations for simulations including waves, are presented below as these are solved slightly different. The approximation method of Van Rijn (2002) is used to include an estimate of the effect of wave orbital velocity asymmetry. The bed-load transport (kg/m/s) is solved by:

$$|S_b| = f_{BED}\, 0.006 \eta \rho_s w_s M^{0.5} M_e^{0.7} \tag{A.15}$$

herein η is the relative availability of the sediment fraction in the mixing layer (-), w_s sediment settling velocity (m/s), M and M_e are the sediment mobility number due to waves and currents and the excess sediment mobility number respectively. The sediment and excess sediment mobility number are formulated by

$$M = \frac{v_R^2 + U_{on}^2}{(s-1)gd_{50}} \tag{A.16}$$

and

$$M_e = \frac{(\sqrt{v_R^2 + U_{on}^2} - v_{cr})^2}{(s-1)gd_{50}} \tag{A.17}$$

where v_{cr} is the critical depth averaged velocity for initiation of sediment (m/s), v_R is the magnitude of the depth-averaged velocity computed from the velocity in the bottom computational layer assuming a logarithmic profile (m/s), g is gravitational acceleration (m^2/s) and U_{on} is the high-frequency near-bed orbital velocity due to short waves in the direction of wave propagation (m/s), s is relative density of sediment fraction (-). See Walstra and Van Rijn for details (2003).

The direction of the bed-load transport vector is determined by the relative contributions of a current- and a wave-related contribution acting in the direction of the near-bed current and the direction of wave propagation respectively. These are given by

$$|S_{b,c}| = \frac{|S_b|}{\sqrt{1 + r^2 + 2|r|\cos\varphi}} \quad \text{and} \quad |S_{b,w}| = r|S_{b,c}| \tag{A.18,A.19}$$

where φ the angle between current and wave direction and,

$$r = \frac{(|U_{on}| - v_{cr})^3}{(|v_R| - v_{cr})^3}, \; S_{b,c} = 0 \text{ if } r > 100 \text{ and } S_{b,w} = 0 \text{ if } r < 0.01. \tag{A.20}$$

An additional wave-related suspended transport ($|S_{s,w}|$ in kg/m/s), to account for the effects of asymmetric wave orbital velocities, is calculated by:

$$|S_{s,w}| = \gamma U_A L_T \tag{A.21}$$

where γ is a phase lag coefficient (0.2), U_A represents velocity asymmetry $\left(\frac{U_{on}^4 - U_{off}^4}{U_{on}^3 + U_{off}^3}\right)$ and $L_T = 0.007\rho_s d_{50} M$; approximation method of Van Rijn (Van Rijn, 2002). The different transport components are combined assuming that $S_{b,c}$ is in de direction of the eulerian near-bed current and $S_{b,w}$ in the direction of wave propagation.

After an upwind shift from the bed-load transport vectors to the velocity points, transports are corrected for bed-slope effects (see Lesser *et al.* 2004).

Morphodynamic updating

The elevation of the bed is dynamically updated at each computational time-step by calculating the change in mass of the bottom sediment resulting from the sediment gradients. This mass change is then translated into a change in bed elevation. A morphological acceleration factor (f_{MOR}) can be applied for reduction of computational time achieved by simply multiplying the erosion and deposition fluxes by f_{MOR} at each computational time-step. The f_{MOR}- factor can be used as the time scales related to the morphological changes are several orders of magnitude larger than the time scales of the water motion (Latteux, 1995).

Chapter 5
Sand transport patterns in Texel Inlet; Part 1, Field Data Analysis

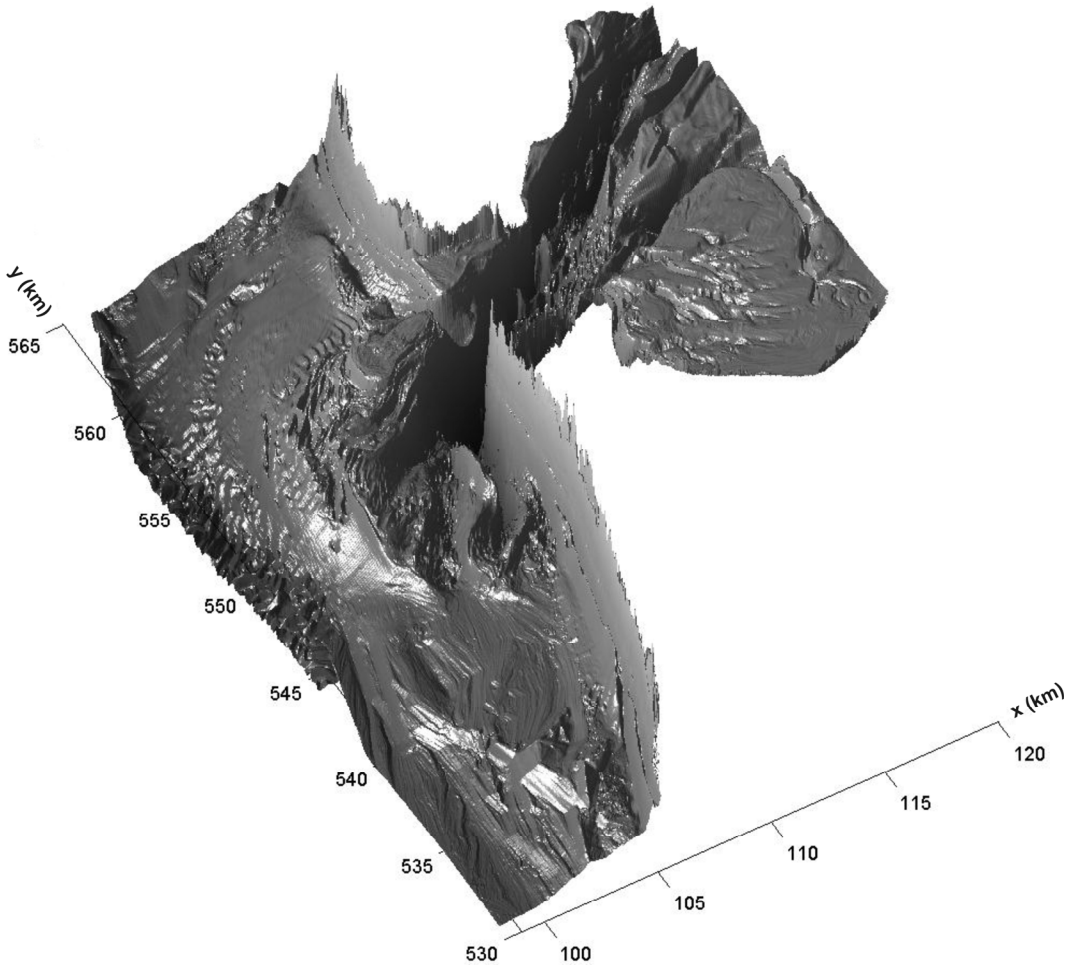

3D impression of Texel Tidal Inlet bathymetry based on 1997 and 2000 *Vaklodingen* data

Epilogue to Chapter 5 and 6:

Traditionally, ebb-tidal delta research has primarily relied on observation data analysis. Empirical relations were proposed to explain the relation between forcing conditions (e.g. waves and tides) and ebb-tidal delta shape and volume (Hayes, 1975; Oertel, 1975; Walton and Adams, 1976; Hayes, 1979; FitzGerald, 1988; Oertel, 1988; De Vriend, 1996; FitzGerald, 1996; Buonaiuto and Kraus, 2003). Also knowledge on distribution and behaviour of channels and shoals on ebb-tidal deltas largely relied on conceptual descriptions (Bruun and Gerritsen, 1959; FitzGerald, 1982; Sha, 1986b; FitzGerald, 1996; FitzGerald *et al.*, 2000). These empirical relations and conceptual models have significantly contributed to an improved understanding of the inlet behaviour and evolution on higher levels of aggregation. However, their major shortcoming is that they lack comprehensive descriptions of the underlying physics. Observed morphological changes and expert judgement form the principal source of information.

Knowledge of the underlying physical processes, and their interaction with sediments and sediment bodies is important for understanding ebb-tidal delta behaviour. Due to the non-linear interaction between water motion (wind-, wave-, density- and tide-driven) with variable channel and shoals structures compound (residual) flow and transport patterns arise, that can show a wide range in temporal and spatial variation, sediment transport processes and mechanisms on the ebb-tidal delta are therefore notoriously complex. Suitable field data that provides detailed descriptions of water, flow and sediment transport variations on the intra-tidal and intra-event scales with the necessary spatial and temporal detail over the inlet domain are scarce, if not absent. Even at Texel Inlet, being one of the most frequently monitored inlets worldwide, with the presence of high-quality observational datasets of water levels, wind, waves, currents and discharges, bathymetry, bedforms and sediment characteristics, there is only limited spatial and temporal data coverage (**Chapter 5**).

Nowadays, fundamental understanding of inlet dynamics can be obtained by mathematical modelling. Recent advances in process-based modelling techniques include the computation of sediment transport and bed level change fully integrated in the flow module; the ***Delft3D Online Morphology model*** (Lesser *et al.*, 2004). Herein morphologic changes are calculated simultaneously with the flow calculations. One of the major assets of this type of model is the capability to increase the spatial and temporal resolution of point-oriented field observations. Point-oriented observations are used to force the model 'as realistically as possible' (quasi real-time by measured time-series of wind, waves and tides) and the model results provide synoptic, more or less realistic data of high spatial and temporal resolution over the inlet domain. Analysis of this data can provide valuable information on governing flow and sediment transport patterns in the instrumented and the un-instrumented areas of the domain, and make identification of the dominant processes and mechanisms for flow and transports possible (**Chapter 6**).

5.1 Introduction

5.1.1 Problem description

In the north of the Netherlands Texel inlet forms the transition of the closed Holland coast to the barriers of the interrupted Wadden Sea coast. One of the characteristics of the Wadden Sea is it continued sedimentation to keep in pace with sea-level rise (Louters and Gerritsen, 1994), and to regain equilibrium after large-scale human distortion, e.g. due to closure of the Zuiderzee completed in 1932 (Elias *et al.*, 2003; Elias and Van der Spek, 2006, [Chapter 2 and 3]). Large changes in the morphology of the basin, the ebb-tidal delta and the adjacent coastlines were observed after closure, and even though the major closure-induced effects on the ebb-tidal delta and in the basin have appeared in a time span of approximately 40 years (Elias *et al.*, 2003, [Chapter 3]), the adjacent coastlines still belong to the most erosive sections of the Dutch coast. Maintenance requires large efforts as since 1991 over 25 million (M)m^3 of sand has been nourished (Roelse, 2002). It is assumed that the majority of these sand losses results from the interaction of the coastline with Texel Inlet. Especially, the ebb-tidal delta channels Molengat and Nieuwe Schulpengat locally induce severe erosion (Cleveringa, 2001; Elias and Cleveringa, 2003). How the sand exchange between inlet, ebb-tidal delta and adjacent coast occurs, and which processes determine this exchange are still not fully understood even though many studies have been conducted in the past.

Our research goal is to gain fundamental understanding of the present-day inlet–coast interaction and dominant transport patterns by detailed analysis of the Texel Inlet and the neighbouring coastlines of North-Holland and Texel (the Netherlands). We present an up-to-date conceptual sand transport model for the inlet and adjacent coasts based on an integrated approach of field- and model-data analysis (described in Chapters 5 and 6 respectively).

5.1.2 Method

Texel Inlet has been intensively monitored by Rijkswaterstaat (Ministry of Transport, Public Works and Water Management) over a long period. Regular bathymetric observations of Texel Inlet's ebb-tidal delta have been conducted since the 16th century B.C.; see overviews presented in Sha (1990), Schoorl (1999) and Elias and van der Spek (2006). After the closure of the Zuiderzee monitoring campaigns by Rijkswaterstaat intensified, and the recent use of state of the art monitoring techniques (such as Acoustic Doppler Current Profilers and Multi beam surveys) has formed a globally unique dataset of water levels, discharges and bathymetries. Analysis of this data can yield valuable insights in the sediment balance of Texel inlet, and improve insight in inlet-coast dynamics in general. Additionally, the long-term datasets provide an unique opportunity to study inlet evolution in response to large-scale human intervention as was shown in Chapters 2 to 4 of this thesis. However, these datasets have two major drawbacks: (1) the accuracy of the older measurements is unknown and (2) the local measurements taken during the adaptation period preceding the closure might not be representative for the present state due

to the large effects of the Closure. This latter drawback might explain why still no conclusive description of the dominant flow and transport patterns on the ebb-tidal delta and through the inlet exists even though many studies have been conducted (e.g. Beckering Vickers, 1951; Battjes, 1962; Sha, 1986a, b, 1989b; Louters and Gerritsen, 1994; Steijn, 1997; Van Marion, 1999; Steijn and Jeuken, 2000).

The research presented in this Chapter focuses on the analysis of measurements that were obtained recently. The measurements were made with modern techniques and are considered to be quite accurate compared to earlier measurements. Flow is analyzed using high-frequent ADCP flow observations in the inlet gorge and main channels on the ebb-tidal delta. The analysis of bathymetric changes, using three-yearly echo-sounding based surveys over the period 1986-2000, and bedform analysis of multi-beam survey data of seafloor bathymetry provide insight in the dominant sediment transport directions in parts of the ebb-tidal delta.

5.2 General Overview of Study Area

5.2.1 Bathymetry

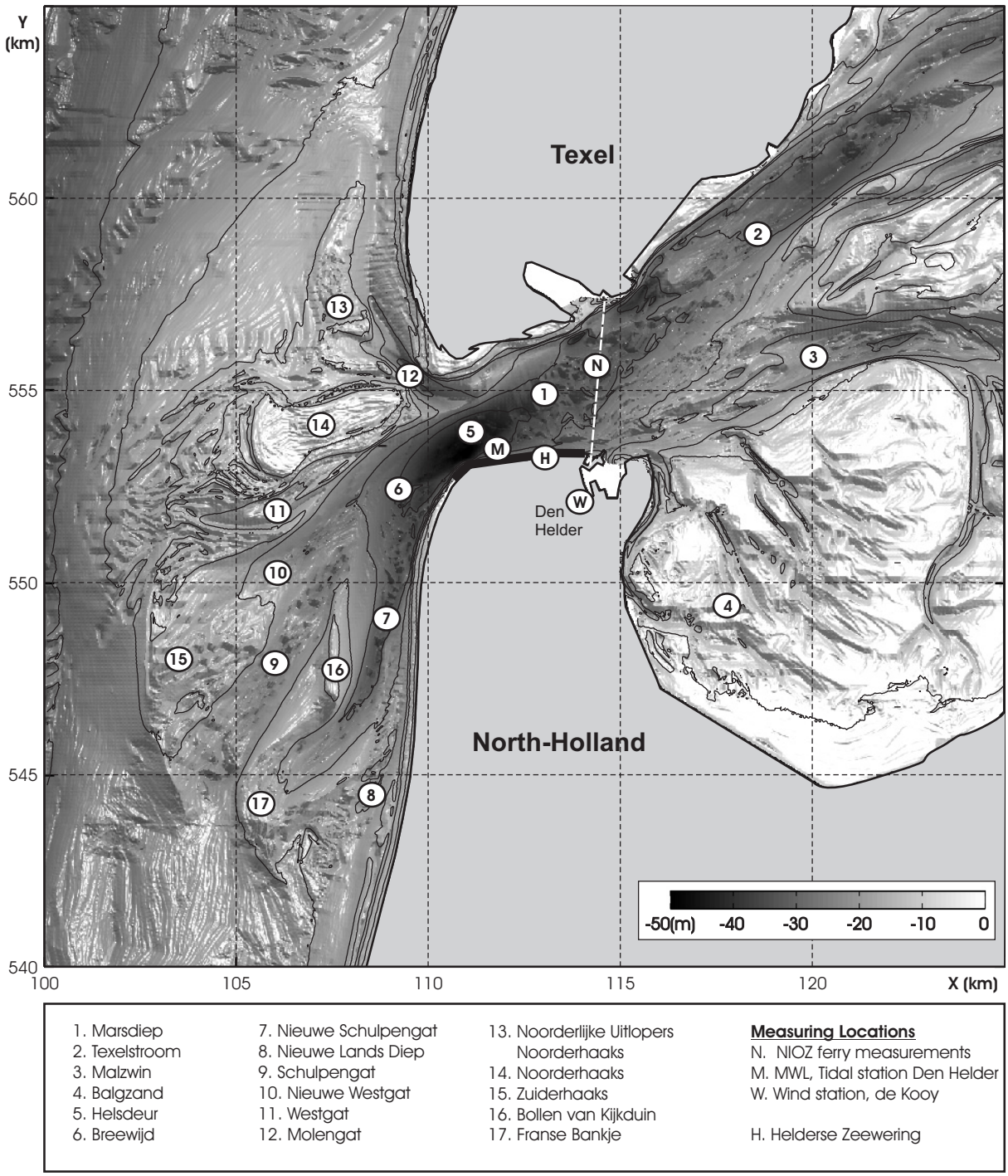

Figure 5-1: Detailed representation of the channel-shoal configuration of Texel Inlet. Based on the 1997 *Vaklodingen* data (Paris co-ordinate system).

Texel Inlet is the largest tidal inlet of the Dutch Wadden Sea being located in the north-western part of The Netherlands between Den Helder and the barrier island Texel (Fig. 5-1). According to the classification of Davis and Hayes (1984) the inlet belongs to the group of the mixed-energy tide-dominated (METD) inlets. Following the classification of Hayes (1979) the inlet qualifies as mixed-energy wave-dominated, even under spring tide conditions. However, the morphology of the inlet shows tide-dominated characteristics such as a large ebb-tidal delta and a deep entrance channel. This is caused by the large tidal prism and compared to this the relatively low wave energy.

The Marsdiep inlet gorge has a minimum width of 2.5 km and a maximum depth of 53 m. On average the tidal prism through the inlet is $1x10^9$ m^3, with both ebb- and flood-tidal velocities ranging between 1 and 2 m/s. Marsdiep forms the connection between the main channel in the basin, Texelstroom, and the main channels, Schulpengat and Nieuwe Schulpengat, on the ebb-tidal delta. The upper part where Schulpengat and Nieuwe Schulpengat still form a single channel is called Breewijd. The ebb-tidal delta is asymmetrically shaped protruding approximately 10 km seaward and 25 km alongshore, hereby determining the nearfield bathymetry of the adjacent North-Holland coast in the south and the Texel Island coast in the north. The large partly supra-tidal Noorderhaaks shoal facing the inlet gorge Marsdiep forms the centre of the ebb-tidal delta. North of Noorderhaaks, a large spit-shaped sub-tidal shoal (Noorderlijke Uitlopers van de Noorderhaaks) extends along the Texel coastline. The Molengat channel separates this shoal from the coast. Interaction of Molengat with the coast is regarded as a main factor in the structural sand losses of the adjacent beaches (Cleveringa, 2001). On the southern part of the ebb-tidal delta the two main channels, Schulpengat and Nieuwe Schulpengat, are distinctly updrift orientated with respect to the northern directed tidal wave propagation and net littoral drift along the Holland coast. Nieuwe Schulpengat locally induced severe erosion of the North-Holland coastline (Elias and Cleveringa, 2003).

Sha (1989a) proposed a conceptual sand transport model to explain the asymmetrical ebb-tidal delta shape based on the analysis of bedforms, sedimentary structures, geomorphology and current data. In brief, sand is transported to the seaward margin of the ebb-tidal delta by the ebb flow through the channels and is then carried further north by converging tidal currents along the delta front. Part of the sediments is deposited on the sub-tidal Noorderhaaks shoals due to the weak circular character of the currents. The predominant waves from the north redeposit the sediments shoreward, forming swash bars and channel-margin bars that produced Noorderhaaks. Recent studies (Elias *et al.*, 2005; Elias and Van der Spek, 2006, [Chapters 2 and 4]) show that the present asymmetrical ebb-tidal delta shape formed as a result of adaptation to the effects of the closure of the Zuiderzee in 1932. The major closure-induced effects on the ebb-tidal delta appeared in a time span of approximately 40 years after closure (Elias *et al.*, 2003, [Chapter 3]). Ever since relative stability exists in the position and orientation of the main channels and shoals on the ebb-tidal delta.

5.2.2 Bed composition

Important factors that contribute to the stability of the tidal channels in Texel Inlet are the bed composition and the presence of erosion resistant layers and of coastal defence works. The south-eastern side of Texel, which bounds Texelstroom, has a core of ice-pushed tills, a stiff and erosion-resistant deposit from the Saalian (Ter Wee, 1962), while Nieuwe Schulpengat cuts deep into the Pleistocene deposits (Sha, 1989c). The presence of Weichselian clay (Van der Spek and Van Heteren, 2004) plausible explains the steep channel slopes observed in the landward channel embankment of Nieuwe Schulpengat (see Fig. 5-1 for details). The longshore and cross-shore variability in pleistocene clay/silt and peat content of the bed layers contributes to the varying alongshore and temporal migration rates of the channel (Elias and Cleveringa, 2003; Van der Spek and Van Heteren, 2004).

In addition to erosion resistant layers, mobility of the North-Holland and Texel coastline is also limited due to the presence of groins since the early 20^{th} century. In addition groins decrease the longshore drift along the coastline. Van Rijn (1995) estimates the blocking effect of groin fields to be in the order of 50%. The most dominant coastal defence structure is Helderse Zeewering (including Den Helder harbour) that stabilizes the southern embankment of the inlet gorge. The interaction of tidal flow and Helderse Zeewering has shown to play an important part in the historical inlet evolution (Elias and Van der Spek, 2006). Acceleration of flow around the western tip of Helderse Zeewering increased the channel depths to over 50 meters at the location of Helsdeur (Fig. 5-1).

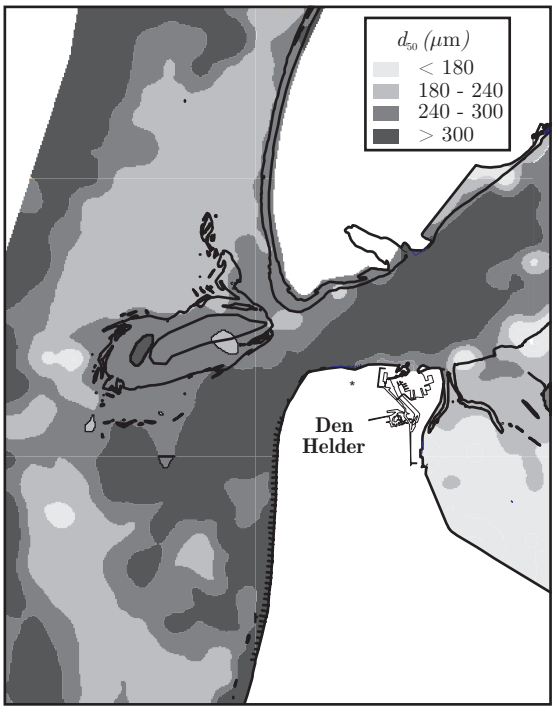

Figure 5-2: Grain size diameters Texel ebb-tidal delta and inlet gorge (source: Sedimentatlas Wadden Sea 1998, RWS-RIKZ Haren)

Grain sizes of the seabed sediment vary over the ebb-tidal delta (Fig. 5-2). Largest grain diameters are observed in the inlet channel and proximal ebb-tidal delta channels. In Marsdiep and Breewijd grain diameters locally exceed 450 μm. In Schulpengat and Nieuwe Schulpengat grain diameters vary between 250 and 350 μm. Generally, in seaward direction the grain size decreases towards values between 150 and 200 μm. This finer sand is also observed on the Noorderlijke Uitlopers of Noorderhaaks. Sha (1990, pages 95-115) concludes that generally sediment diameters on the shallow shoal areas are below 200 μm, while in the channels sediments are above 200 μm.

In the basin the grain size distribution decreases towards the mainland. At the location of the Afsluitdijk, median grain sizes vary around 120 μm. Of the sediment that settles within the Wadden Sea, some 70 to 80% consists of sand while the remainder is silt and clay (Oost, 1995).

5.2.3 Tides

The tidal motion along the Dutch coast and in the Wadden Sea is generated by the tidal wave entering the North Sea from the Atlantic Ocean between Scotland and Norway in the north, and through the Calais Straight in the south. Interference of these two waves, distortion due to Coriolis effects and bottom friction generates a complicated tidal flow pattern in the southern part of the North Sea with anti-clockwise rotation and propagation around amphidromic points. Along the Dutch coast the result is a composition of a standing and progressive tidal wave propagating from the south to the north, generating maximum tidal velocities in the range of 0.5 to 1.0 m/s. Near, Texel inlet this tidal wave meets a second Kelvin-type tidal wave that propagates from west to east along the Wadden-Sea Islands. At Texel Inlet the semi-diurnal tidal movement is the main driving force behind the horizontal water flow through the inlet, with the M_2 constituent being the dominant tidal component. Ebb- and flood-tidal velocities in Marsdiep range between 1.0 and 2.0 m/s. The tidal curve is asymmetrical mainly due to distortion of the M_2 tide by the M_4 constituent, resulting in a faster rise than fall of the tide. The vertical tide has a mean tidal range of 1.38 m in Den Helder, increasing up to 2.0 m during spring tides, while decreasing to about 1.0 m during neap tides (Fig. 5-3b). In the Wadden Sea the tidal wave propagation is damped due e.g. bottom friction and distorted by reflection.

The tidal signal only partly represents the measured water levels (Fig. 5-3a). Several meteorological factors such as air pressure and the air pressure induced wind fields contribute to the tidal distortion. The wind-generated set-up or set-down forms the major component as due to the funnel shape of the North-Sea this set-up can reach significant heights along the Dutch coast (see Fig. 5-3c). At the Den Helder tidal station set-ups of nearly 2 meters are measured sporadically during major onshore-directed storm events (Fig 5-3c). In the Wadden Sea with its complex bathymetry set-up-gradients can drive complicated residual wind-driven flow fields, generate shore-parallel velocities and throughflow between adjacent basins. In addition the volume of water stored in the Wadden Sea due to the larger set-up can considerably enlarge the outflow velocities in the inlets, thereby effecting the ebb-tidal delta development and adjacent beaches.

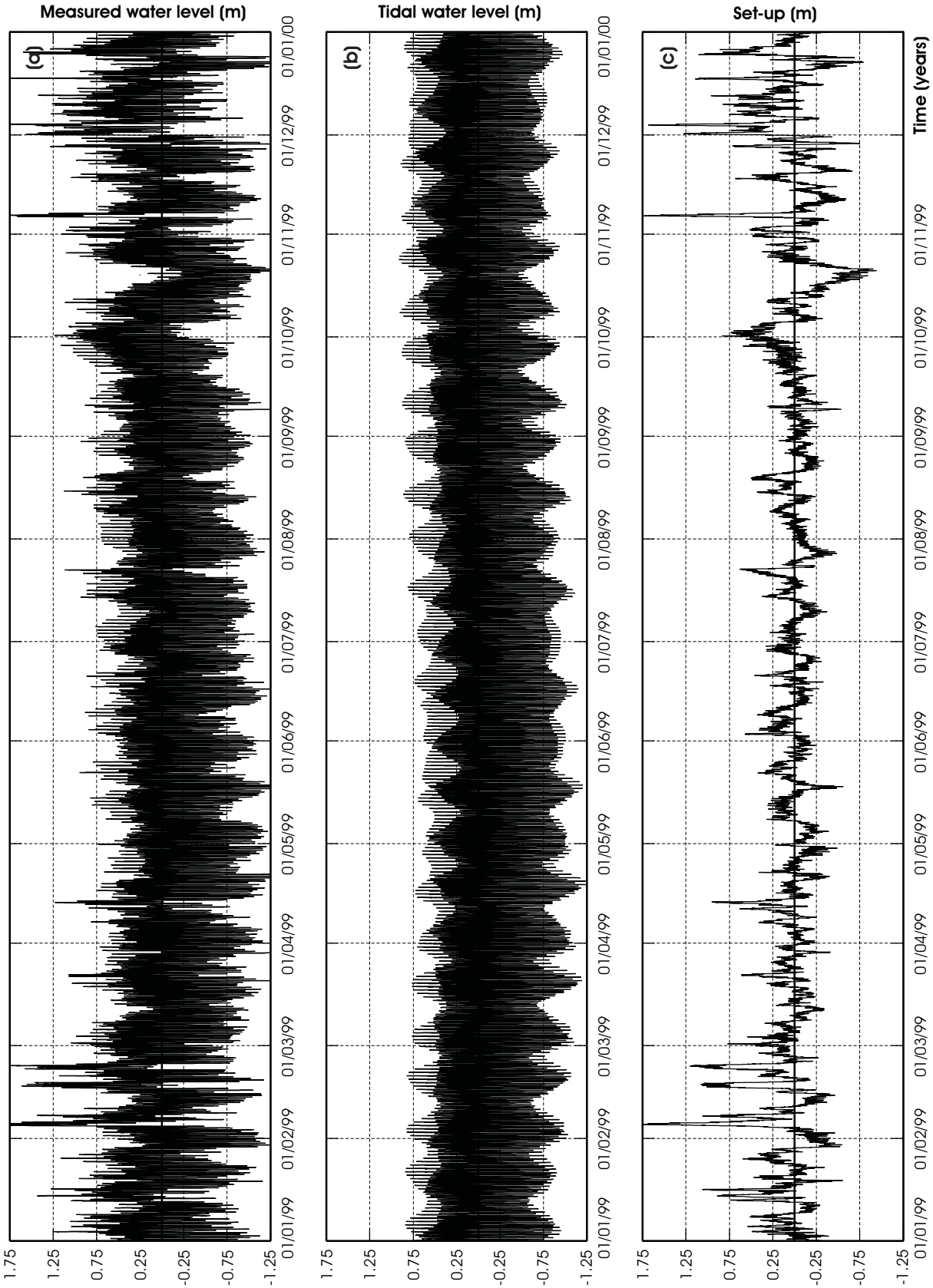

Figure 5-3: Overview of (a) measured water levels, (b) tidal water levels (estimated by the Tide Generator 1999) and (c) water level set-up (= measured - tidal water levels) for the Den Helder tidal station over the period 1-1-1999 / 1-1-2000.

5.2.4 Wind and waves

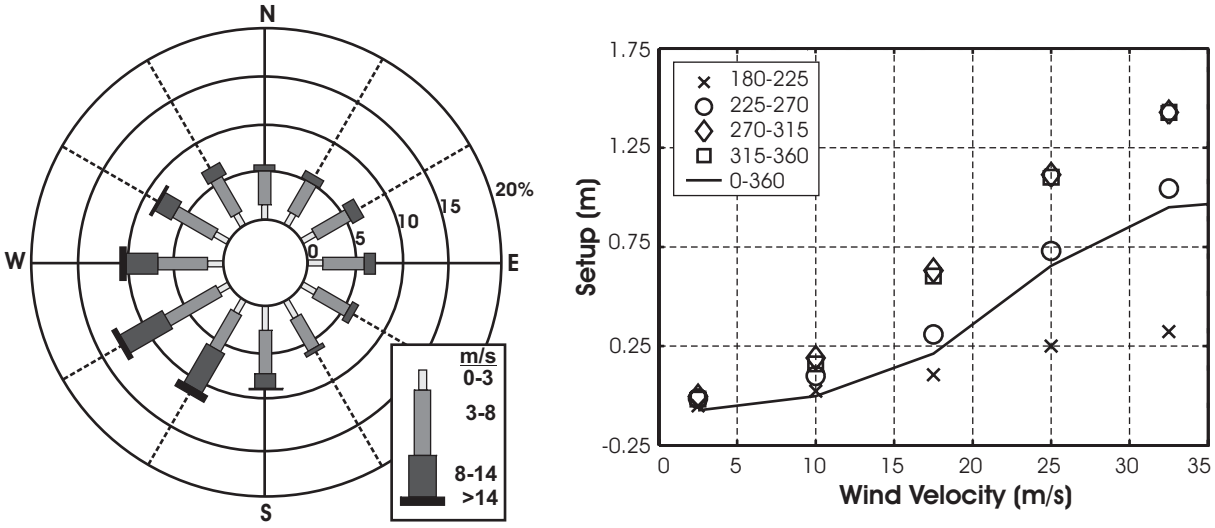

Figure 5-4 left: Wind rose station De Kooy near Den Helder (see Fig. 5-1 for location) based on data 1971-2000 from Royal Netherlands Meteorological Institute. Right: relation between wind velocity, direction and set-up derived from the Eierlandse Gat wave buoy dataset (www.golfklimaat.nl).

Overviews of the governing wind and wave conditions along the Holland coast and Texel Inlet are presented by e.g. Roskam (1988), De Ronde *et al.* (1995), Wijnberg (1995) and Coelingh *et al.* (1996). The wind rose of Fig. 5-4 summarizes the observations for station De Kooy near Den Helder (location see Fig. 5-1) over the period 1971 - 2000. Winds from the sector southwest to northwest prevail. The yearly averaged wind speed is 7 m/s from the west-southwest. These prevailing west-south-westerly winds are the main driving force for the north-eastward residual velocities (5 to 10 cm/s) on the lower shoreface of the Holland coast (Roelvink *et al.*, 2001). Additionally, wind is important for the generation of storm surges (Fig. 5-3 and Fig. 5-4 right), wave growth, and eolian sand transport on the dry beach. Little information is present on the importance of wind-driven flow in the inlet domain, but with a predominant landward wind direction wind is likely to enhance tidal flow and sediment import into the basin. Inside the basin we can expect wind to be important for mixing and estuarine circulations, and in shallow areas wind is effective in generating large currents and tidal flat degeneration. The eastward migration of the tidal divides in the Wadden Sea might for a major part be related to the prevailing wind direction (Fitzgerald *et al.*, 1984; Van Veen *et al.*, 2005).

The wave climate near Texel Inlet is dominated by wind-generated waves in the North Sea basin. Contributions of swell are minor. Most frequently wave directions (~90%) lie between southwest and north. Wave-climate measurements, representative for Texel Inlet, are conducted at the nearby Eierlandse Gat wave buoy located at a water depth of 26 m (Paris co-ordinates X: 106.514, Y: 587.985 km). Analysis of long-term time series (1979-2001) reveals a mean significant wave height of 1.3 m from the west, with a corresponding significant wave period of 5 seconds. The wave period increases with the wave height. The highest waves occur from north-westerly directions due to the larger fetch. During storms wind-generated significant wave heights can reach heights over 6 m. Wave

periods ($T_{1/3}$) vary between 4 to 5 seconds for low wave conditions, and over 10 seconds for the highest waves. Figure 5-5 summarizes the main characteristics of the wave field.

Waves are an important factor for sand transport on the ebb-tidal delta. The gross ebb-tidal delta volume might be related to tides or tidal prism (e.g. Hayes, 1975; Oertel, 1975), but waves redistribute the sediments and contribute to the sediment bypassing mechanism (FitzGerald, 1988). Waves contribute directly to the sediment transports due to radiation stresses generated by wave breaking of obliquely incident waves that generate currents, and due to wave asymmetry. Indirectly waves enhance bed-shear stresses and stir-up sediment, allowing more sediment into suspension to be transported by the tidal and wind-driven flow.

To obtain an estimate of the dominant components of the wave climate for sediment transport, we have sorted the Eierlandse Gat observations over the period 1979 - 2001 (Fig. 5-5). A sub-division in six wave height classes and four direction classes between 180° and 360° is made. Wave directions between 0° and 180° are generated by offshore directed wind and of negligible height near the Texel Inlet. For each class a representative morphological wave height (H_{mor}) is determined using,

$$H_{mor} = \left(\frac{1}{n} \sum_{i=1}^{i=n} H_{m0}(i)^k \right)^{\frac{1}{k}} \tag{5.1}$$

where, n represents the total number of observations [-], H_{m0} is the significant wave height [m] and k is the power relation between transport and wave height [-], a value of 2.5 is used. The total *M*orphological *I*mpact (*MI*) for each class is obtained by multiplying with the probability of occurrence.

Waves from the direction classes between southwest (225°) and north (360°) contribute near-equal to the morphological impact. Due to the non-linear relation between waves and sediment transport, especially the larger wave heights are important. Only 20% of the observations exceed the 2 m wave height, but these waves account for 70% of the morphological impact. At the Eierlandse Gat wave buoy the southward component of the morphological impact exceeds the northward component, which results in a net southward directed wave-driven transport (similar to the observations of Sha, 1989a). Note that the littoral drift along the North-Holland coastline is northward, directed towards the inlet (Van Rijn, 1997).

Although measurements of the wave-climate are absent in the direct vicinity of Texel Worldwide studies of inlet systems have shown the effectiveness of ebb-tidal deltas in modifying the nearshore wave climate and reducing the wave energy on the adjacent coastlines (e.g. Oertel, 1972; Hine, 1975; FitzGerald, 1988; Van Rijn, 1997). The shallow ebb-tidal delta shoals provide a natural breakwater for the adjacent shorelines. Refraction on the large shoal areas, wave breaking on the shoals (especially during the high wave-energy events with large morphodynamic impact) and wave blocking by the supratidal shoal areas can largely modify and distort the nearshore wave climate. At Texel Inlet it is expected that the larger refraction and wave sheltering of the waves from the north results in a net northward directed transport along the North-Holland coastline,

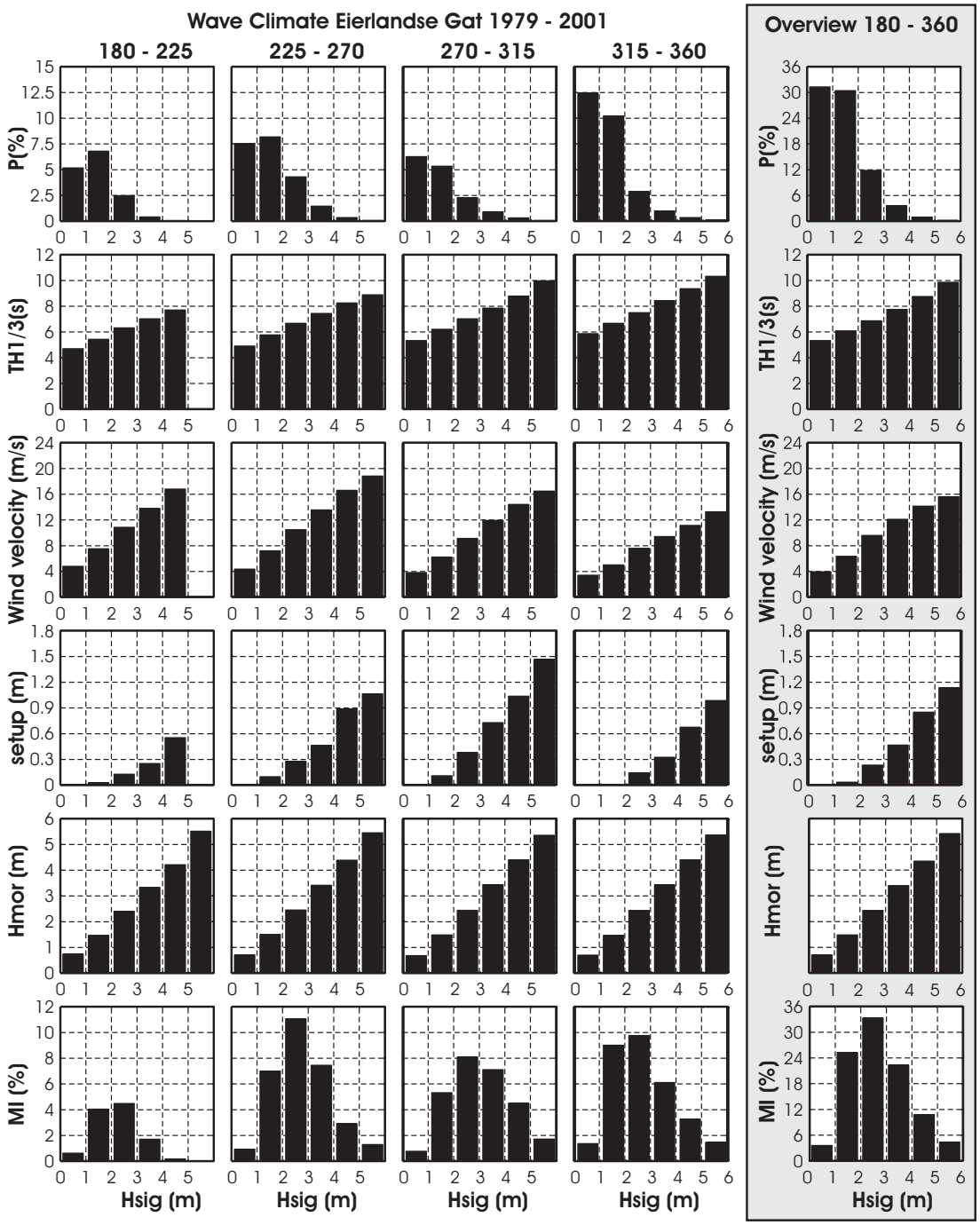

Figure 5-5: Characteristics of the wave climate of station Eierlandse Gat (1979-2001). From top to bottom: probability of occurrence (%), significant wave period (s), wind velocity (m/s), set-up (m), morphological wave height (m) and morphological impact (%); see text for explanation.

and vice versa, the larger reduction of southern waves results in a southward directed transport along the Texel coastline. Thus, on either side of the inlet wave-driven transports are directed towards the inlet.

The sheltering effect of the ebb-tidal delta effectively limits the wave-heights in the basin. The locally generated waves in the basin will therefore only have a limited effect in the relative deep western part of the basin near Den Helder.

5.3 Hydrodynamics of Texel Inlet

5.3.1 Flow in Marsdiep

Tidal discharge measurements in Texel Inlet have been conducted regularly since 1939 (De Reus and Lieshout, 1982; Blok and Mol, 2001); see Table 5-1. Discharge measurements were traditionally based on 13-hour observations over a single tidal cycle that were converted to mean conditions using the ratio between measured and mean tidal range. As the residual discharges are small compared to the total discharge through the channels relatively large fluctuations in the residual discharge magnitudes of consecutive measurements occur. Based on this data estimates of the tide-averaged discharges in Marsdiep range between 0 and -200 m^3/tide (export). These fluctuations partly relate to the crude upscaling of the single-tide observations to mean tidal conditions, the possible influence of meteorological forcing (such as wind driven flow or set-up effects), and the accuracy of the observations that is not exactly known. In addition the large variability in position of channels and shoals on the ebb-tidal delta up to 1975 must have played a role in determining the discharges in the individual channels of the ebb-tidal delta.

Table 5-1: Water volumes of ebb and flood discharges (x10^6 m^3) converted to representative mean tide conditions (from Rijkswaterstaat, various sources see text).

		Molengat	***Westgat***	***Schulpengat***	***Nieuwe Schulpengat***	***Breewijd*** *	***Marsdiep***
1938	flood	-	-	-	-	-	944
	ebb	-	-	-	-	-	1081
1939	flood	227	406	228	-	*228*	-
	ebb	175	465	271	-	*271*	-
1951	flood	187	409	290	-	*290*	-
	ebb	122	581	297	-	*297*	-
1958	flood	179	302	443	-	*443*	-
	ebb	132	393	485	-	*485*	-
1966	flood	-	-	-	-	-	1052
	ebb	-	-	-	-	-	1101
1974	flood	156	145	394	376	*770*	896
	ebb	145	159	468	385	*853*	1092
1975	flood	188	110	323	363	*686*	953
	ebb	130	153	424	413	*837*	1045
1981	flood	179	406		378	*784*	910
	ebb	152	503		380	*883*	1049
1997	flood	176	869			*869*	904
	ebb	101	925			*925*	948
2001	flood	143	-			*879*	1010
	ebb	95	-			*1090*	1115

* Prior to 1971 the Schulpengat is a single channel, since 1971 a two-channel system consisting of the Schulpengat and Nieuwe Schulpengat was formed. The upper domain, where Schulpengat and Nieuwe Schulpengat merge is called Breewijd.

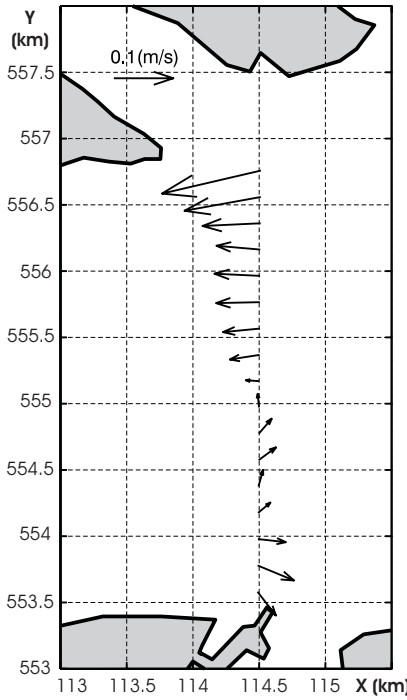

Amplitude of Volume transport (m^3/s)			
Tidal Component	1998-2000	1999	2000
o1	5139	4113	4310
k1	3915	4732	3962
mu2	9367	9218	8784
n2	10580	10490	10239
nu2	4076	3181	4587
m2	68564	68908	67278
lab2	3528	3518	3429
l2	7205	7380	6849
s2	17837	16661	17687
k2	3503	3973	4489
m4	7410	7121	7672
1mn6	3592	3492	3491
m6	6596	6614	6403
sms6	6534	6641	6463
net flow	-2587	-2029	-2589

Overview of tidal components most important for the volume transport in Marsdiep. Based on NIOZ ferry observations (source: Ridderinkhof 2002).

Figure 5-6: Overview of tide-averaged velocity distribution in Marsdiep. Based on harmonically analysed NIOZ-ferry data for the year 1999 (Buisman 2001, Personal Communication).

It is only through analysis of the recent NIOZ-ferry measurements (Ridderinkhof *et al.*, 2002) that a reliable quantitative indication of the residual flow through the Marsdiep inlet gorge could be obtained. In 1998 the Royal Netherlands Institute of Sea Research (NIOZ) started a long-term high-frequent measuring campaign of e.g salinity, surface temperature and flow through the inlet gorge. Flow is measured by a 1.5 MHz Acoustic Doppler Current Profiler (ADCP) attached to the hull of the ferry from Den Helder to Texel island. ADCPs use sound waves to measure current speed using the Doppler effect. A sound wave is transmitted at fixed frequency and returns as backscatter from reflection of small particles in the water. Under the assumption that these small particles travel with the horizontal water velocity, the Doppler shift change of frequency can be used to calculate velocity magnitudes and direction.

During day-time the ferry (*ms* Schulpengat) sails the 4.5 km wide Marsdiep every 30 minutes. The raw data are transmitted to NIOZ and processed. Preliminary results of the flow observations have been made available by NIOZ for analysis (also see Bonekamp *et al.*, 2002; Ridderinkhof *et al.*, 2002). The flow data have been used to calculate time-series of depth-averaged flow at eighteen equidistantly distributed aggregation points. Harmonic analysis has been applied to these time-series to derive tidal mean flow conditions and amplitudes and phases of the main tidal flow constituents. The residual flow through the inlet of about 115×10^6 m^3/tide is seaward directed due to the internal dominance of flood flow along the North-Holland coastline and larger ebb flow along the Texel coastline (Fig. 5-6). An important characteristic of the Texel basin is that it does not form a closed system but the basin connects to the neighbouring Vlie basin allowing an exchange between the two systems. The residual flow mainly results from throughflow from the Vlie to Texel Inlet, due to the higher amplitude of the vertical tide in the Vlie basin (Ridderinkhof, 1988).

5.3.2 Flow in the main ebb-tidal delta channels

To obtain an estimate of the flow patterns in the main channels of the ebb-tidal delta (Marsdiep, Molengat, Breewijd and Nieuwe Schulpengat) three 13-hour ADCP campaigns were conducted between 2002 and 2004 by Rijkswaterstaat (Blok and Mol, 2001; Rab, 2004a,b). During each campaign multiple transects were run obliquely on the channel axis and continuously over a tidal cycle resulting in 10 three-dimensional flow field distributions of the main ebb-tidal delta channels and inlet gorge. Although these datasets do not provide long-term time-series they allow for an estimate of the discharge and velocity distributions in the individual channels. Table 5-2 and Figure 5-7 give an overview of the transect locations.

The raw data were thoroughly analyzed by Rijkswaterstaat to remove systematic effects and data outliers (see Reports of Blok and Mol, 2001; Rab, 2004a,b). The vertical coordinates for each bin were referenced to mean water level. Velocity data in the near surface layer (the blank-after-transmit area) were extrapolated assuming a constant velocity. Data in the near-bottom layer were exponentially interpolated between zero at the bed and the upper cell value. Data in each bin was treated as a time series, and a harmonic analysis was performed to obtain an estimate of the main tidal current amplitudes and residual velocities.

To obtain synoptic time-series for each bin harmonic analysis is applied to the measurements. Note that the short time period of observations allows to resolve the dominant semidiurnal M_2 tide only that therefore represents all semidiurnal tides. The addition of the quarter-diurnal amplitude(M_4) and sixth-diurnal (M_6) overtides enables to represent the measurements accurately. The mean, M_2, M_4 and M_6 are resolved in major and minor axis of the tidal flow ellipses. In the confined channels of Marsdiep, Breewijd and Molengat the major and minor direction are considered representative for the along-channel and the across-channel component of the velocity respectively.

Figure 5-7 presents an overview of the measured transect-averaged flood, ebb and residual discharges respectively. Flood enters the inlet mainly from Nieuwe Westgat and Schulpengat (~50 %), and Nieuwe Schulpengat (~40 %). Discharges through Molengat are minor (~10 %). Vice versa, during ebb the majority of the flow is directed from Marsdiep towards the southern part of the ebb-tidal delta (~90 %). Tide-averaged the outflow of Molengat to Marsdiep is flood dominated, whereas in northward direction no pronounced flow dominance is observed. Hence, lateral inflow over the Noorderlijke Uitlopers of Noorderhaaks must occur.

Table 5-2: Overview transect locations ADCP survey's (2001-2004)

Transect	*Date*	*Location*			
		X_0	Y_0	X_1	Y_1
Campaign 1					
Marsdiep (1)	15-2-2001 (06:18-20:33)	112.904	553.299	111.911	556.108
Breewijd (2)	15-2-2001 (06:20-20:58)	109.845	551.178	107.443	553.277
Molengat (3)	15-2-2001 (06:28-21:08)	109.825	555.730	109.092	551.000
Campaign 2					
Molengat (4)	17-9-2004 (07:30-22:00)	110.649	556.374	109.176	553.695
Molengat (5)	20-9-2004 (06:36-21:03)	110.011	555.887	108.700	554.771
Molengat (6)	18-9-2004 (06:07-20:52)	109.580	559.645	108.064	559.668
Molengat (7)	16-9-2003 (04:33-20:46)	109.873	562.264	108.393	562.611
Campaign 3					
Breewijd (8)	30-9-2004 (04:00-18:15)	107.133	553.542	109.960	551.085
Nieuwe SG (9)	1-10-2004 (04:13-18:02)	109.792	547.979	107539	548.049
Nieuwe SG (10)	27-10-2004 18:17 / 28-10-2004 15:55	109.530	544.638	106.633	546.654

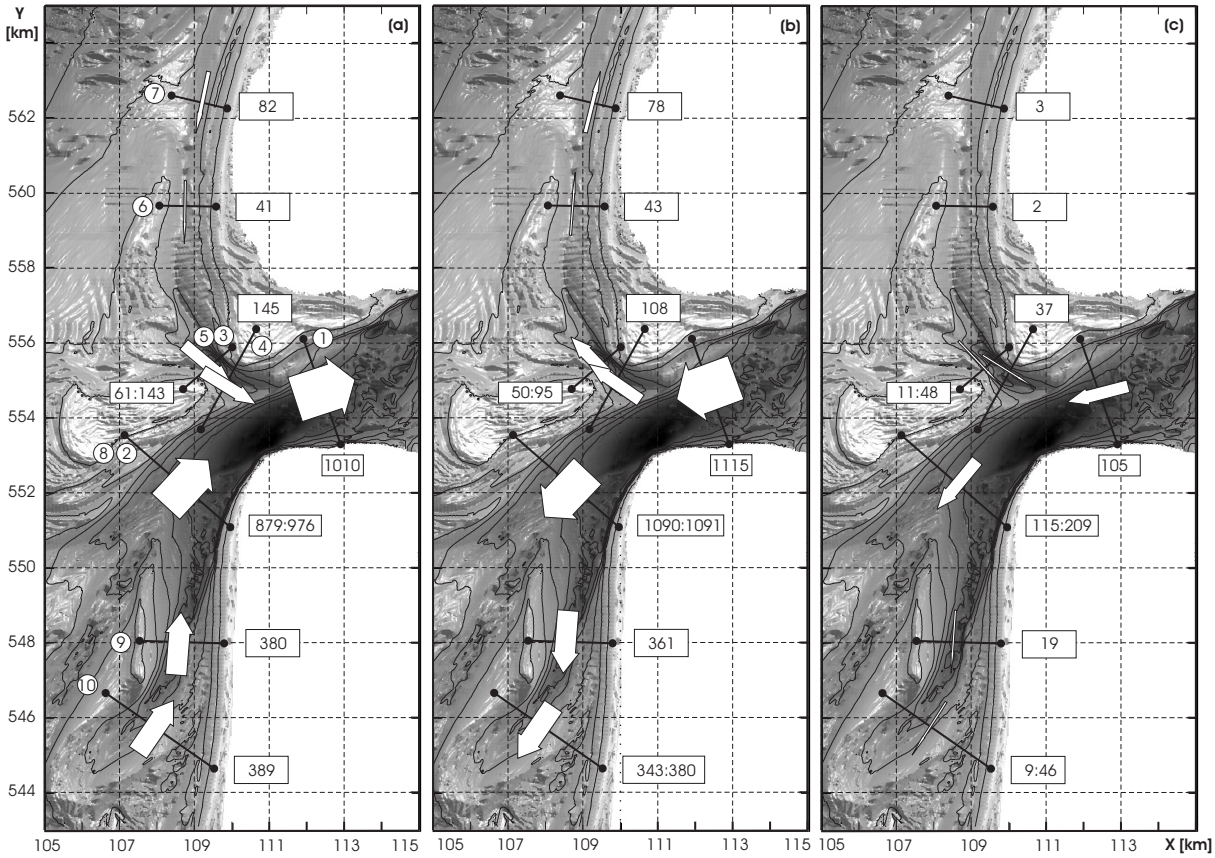

Figure 5-7: Overview ADCP discharge measurements (2001-2004). Left to right: (a) flood, (b) ebb and (c) residual discharges in 10^6 m^3. In Molengat and Breewijd several measurements are taken here the maximum and minimum values are shown as [minimum : maximum].

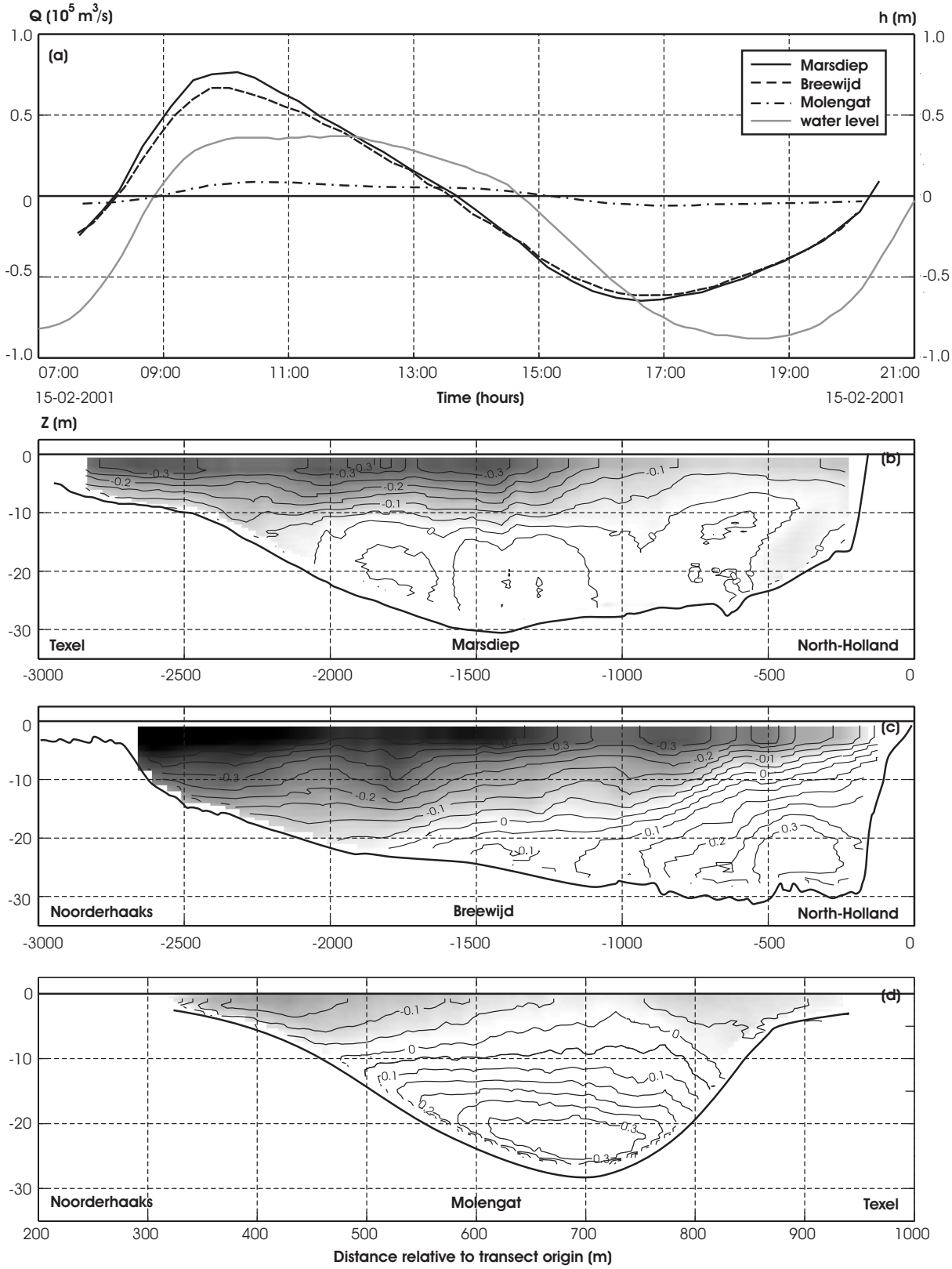

Figure 5-8: ADCP flow measurements campaign 1, (a) overview of the transect-averaged discharges in Marsdiep [transect 1], Breewijd [transect 2] and Molengat [transect 3]. (b-d) Along-channel tide-averaged velocities for Marsdiep, Breewijd and Molengat respectively. Positive values denote flood-dominant velocities, negative values (in gray) ebb-dominant velocities. Notice the difference in x-scaling between the plots.

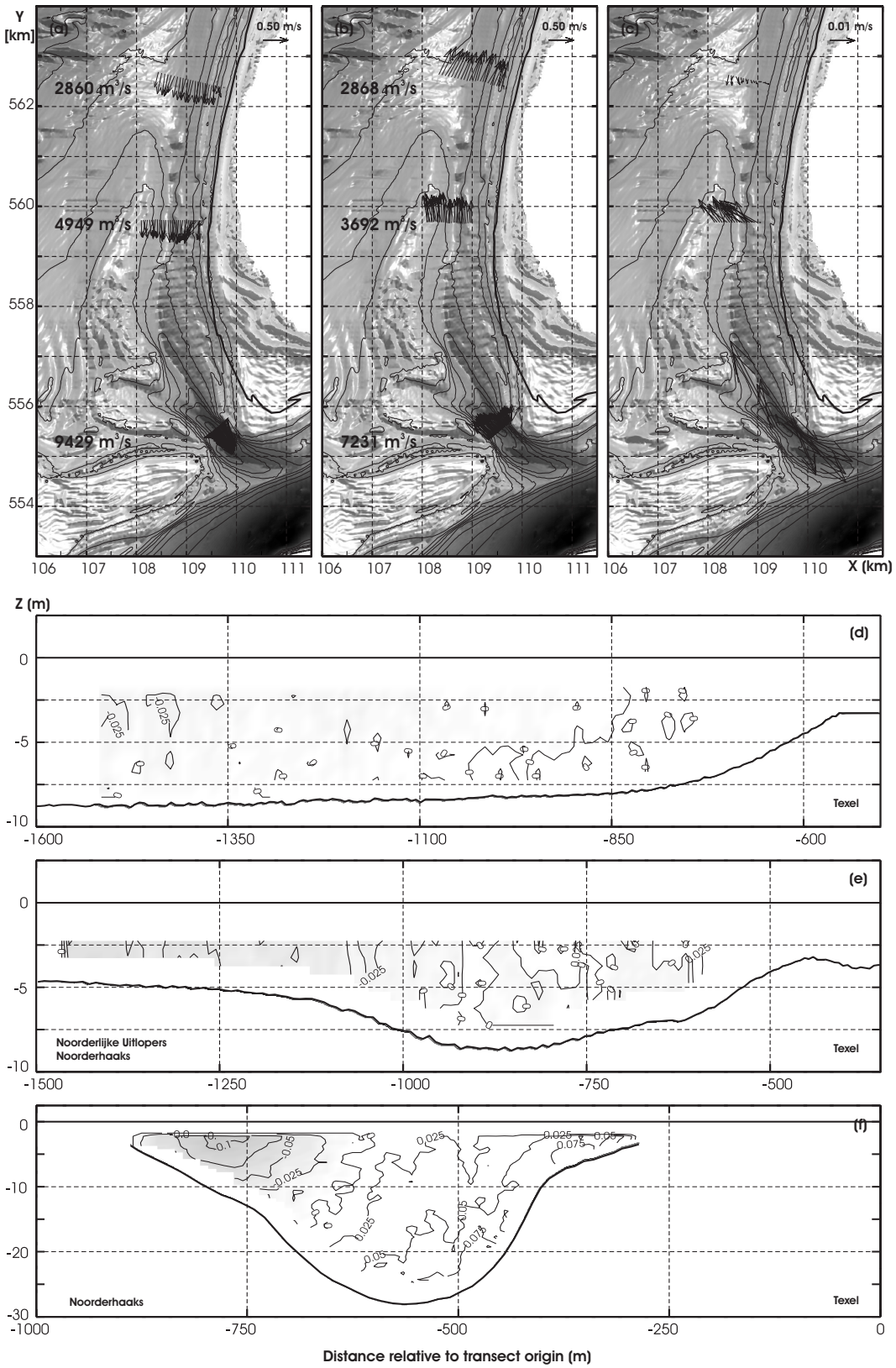

Figure 5-9: Overview ADCP measurements campaign 2 transects 5, 6 and 7. (a) Maximum flood discharges and depth-averaged velocity vectors, (b) maximum ebb discharges and depth-averaged velocity vectors, and (c) depth-averaged residual velocities. (d-f) Along-channel residual velocities in transects 5 (d), 6 (e) and 7(f) respectively. Positive values denote flood dominant velocities, negative values ebb-dominant velocities (notice the difference in x and z scaling).

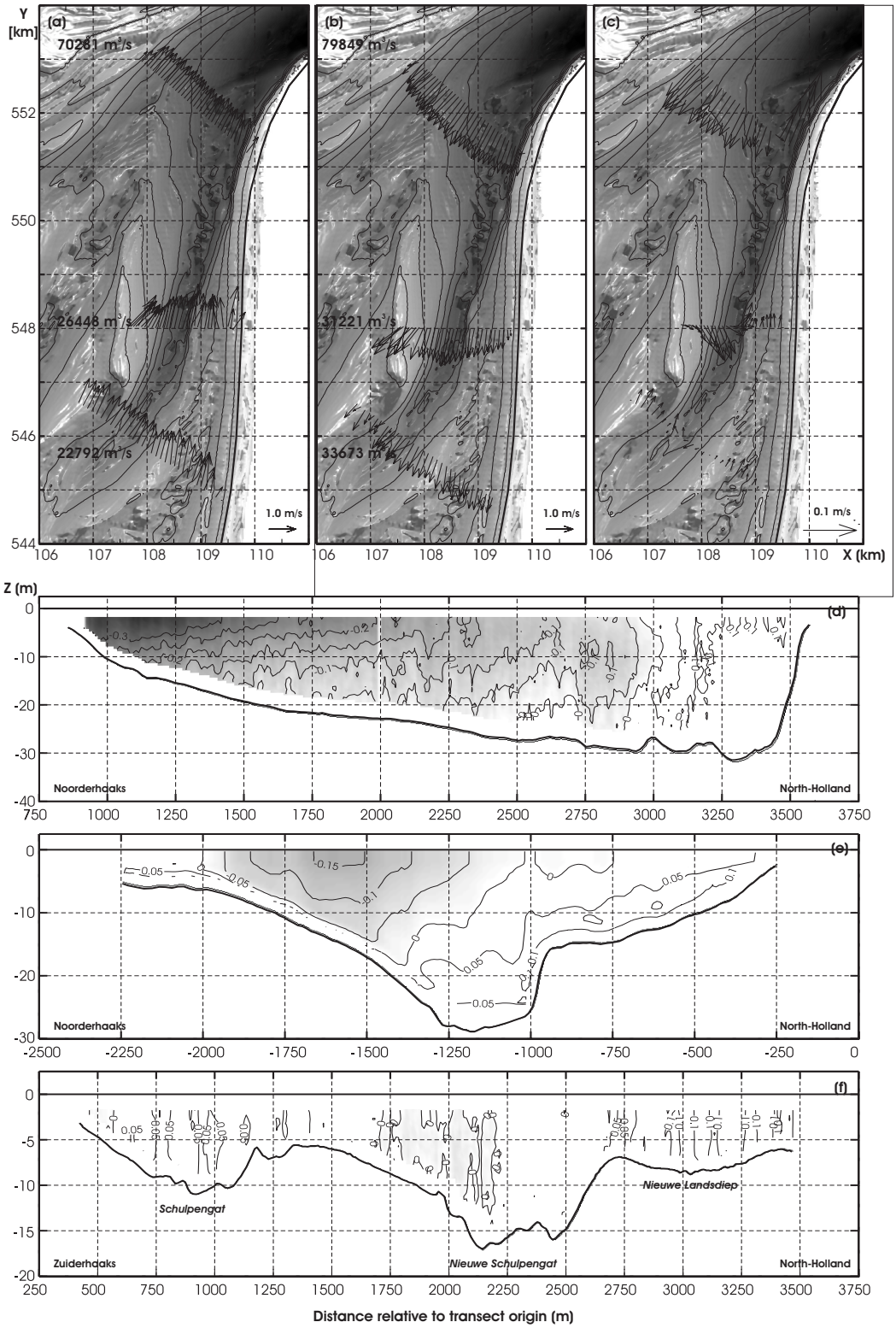

Figure 5-10: ADCP campaign 3 overview of transects 8, 9 and 10. (a) Maximum flood discharges and depth-averaged velocities, (b) maximum ebb discharges and depth-averaged velocities, and (c) depth-averaged residual velocities. (d-f) Along-channel residual velocities in transects 8 (d), 9 (e) and 10 (f) respectively. Positive values denote flood dominant velocities, negative values ebb-dominant velocities (notice the difference in x and z scaling).

Campaign 1: Marsdiep, Breewijd and Molengat[(1)]

In the spring of 2001 velocities were measured simultaneously in the Marsdiep inlet gorge [1], and the connecting Breewijd [2] and Molengat [3] channels on the ebb-tidal delta (Blok and Mol, 2001); for transect locations see Fig. 5-7. Measurements in Marsdiep and Breewijd were executed with a 1200 kHz system of the Broadband type. Molengat was measured at a 600 kHz frequency.

The tide- and transect-averaged discharges (Fig. 5-8a) show a residual flow through the inlet of 127 million (M)m^3/tide that is seaward directed. Discharges in Molengat are minor (~10%) compared to the discharges in Marsdiep and Breewijd. The phase difference between the horizontal and vertical tide illustrates the mixed standing-progressive characteristic of the tide.

During the period of ADCP observations wind and waves were absent but fresh-water discharge in the basin was major. Yearly-averaged, the total fresh-water discharge is in the order of 500 m^3/s, while preceding the measurements discharges exceeded 900 m^3/s. The resulting residual velocity distributions in the channels show characteristics typical for density driven circulations (Hansen and Rattray, 1965) wherein salinity differences between ebb flow of lower salinity and flood flow of higher salinity results in the upper layers of the water column being dominated by a (large) ebb residual, while the lower layers are flood dominant. In Marsdiep (Fig. 5-8b) and Molengat (Fig 5-8d) a more-or-less vertical segregation occurs, while Breewijd is dominated by a diagonal shear.

In Breewijd longitudinal residual flood flow in excess of 0.3 m/s in the direction of the Wadden Sea is observed along the North-Holland coastline in the deeper part of Breewijd. Along the Noorderhaaks equally strong residual ebb velocities are directed onto the ebb-tidal delta (Fig. 5-8c). This tilted residual flow pattern might (partly) be related to the transects depth variation, and acceleration of flow at the western tip of Helderse Zeewering.

The effect of density differences on the residual flow (and sediment transports) in Marsdiep and Breewijd has been subject to a more detailed study; Elias and De Ronde (2006) presented in Chapter 7 of this thesis. Using a Delft3D model application it is shown that density-driven flow patterns and magnitudes have potential large impact on the residual sand transport in the inlet gorge and proximal ebb-tidal delta channels. Largest sediment transports of non-cohesive sediment (d_{50} of 250 μm) were modelled at the location of maximum vertical salinity gradients and residual flow velocities. In the basin, where longitudinal salinity gradients prevail, the density-driven sand transports were minor.

Campaign 2: Molengat

To obtain insight in the interaction of Molengat and adjacent Texel coastline, ADCP velocity measurements were collected in four separate transects during the autumn of 2003 (Fig. 5-7 and Fig. 5-9); only transects 5, 6 and 7 are analysed in more detail. During the

[1] in the following section [..] indicates the transect number as shown in Figure 5-7

measurements wind and waves were minor therefore the measurements can be considered fairly representative for tidal conditions.

The maximum flood outflow into Marsdiep equals ~ 9400 m^3/s (Fig. 5-9a). The significant increase in discharge magnitude between successive transects indicates that a large lateral inflow over the Noorderlijke Uitlopers of Noorderhaaks spit must occur. Maximum ebb discharges of ~ 7200 m^3/s are smaller than the maximum flood discharges (Fig. 5-9b). In northward direction the ebb-flood difference and residual flow velocities minimize (Fig. 5-9).

Similarly to campaign 1 harmonic analysis was performed on the observations (using the M_2, M_4 and M_6 tidal components) to obtain an estimate of the residual flow velocities. Figure 5-9c summarizes the transect averaged residual flow velocities, while Figure 5-9d,e and f present the residual flow distributions in detail for each of the transects. The residual velocities in Molengat are small. The flow distribution shows a tendency of an ebb dominant and seaward residual flow along the margin of the Noorderlijke Uitlopers of Noorderhaaks, and a flood dominant flow along the Texel coast. However, especially in transects 6 and 7 velocities are minor and these values may be in the range of the accuracy of the measurements and analysis method.

The outflow to Marsdiep is governed by larger ebb dominant velocities along the Noorderhaaks and smaller flood dominant flow in the middle of the channel and along the Texel coastline. Residual velocities are small compared to the larger velocities observed in the 2001 campaign (Fig. 5-8d). This dissimilarity is an indication of the pronounced effects of density differences even for flow in this channel.

Campaign 3: Breewijd and Nieuwe Schulpengat

The discharges and flow distributions in the southern half of the ebb-tidal delta were investigated using three successive ADCP campaigns in Breewijd and Nieuwe Schulpengat collected during the autumn of 2004 (Rab, 2004a).

The ebb and flood discharge magnitudes show that the majority of the ebb and flood flow is transported through the seaward Schulpengat and Nieuwe Westgat channel (Fig. 5-10a,b), and a smaller part through Nieuwe Schulpengat.

The velocity distribution of Breewijd (transect 8, Fig. 5-10e) is governed by flood dominant velocities along the North-Holland coast and ebb-dominant velocities near Noorderhaaks. The residual flood velocity magnitudes are small compared to the residual ebb velocities. The pronounced diagonal shear, observed in the 2001 campaign, is not observed (hence, this relation is related to density stratification). The distinct separation of flood and ebb flow is plausibly related to the phase lag between the horizontal and vertical tide, and the strong curvature of the coast around the tip of Helderse Zeewering. As a result of this phase lag ebb-flow still dominates the central part of the channel as flood starts. Seeking the path of least hydraulic resistance flood therefore enters along the channel margins (the Holland coast). Contraction of flood flow around the tip of Helderse Zeewering accelerates the velocities into the inlet. While on the other hand the ebb flow originating from the Texelstroom is directed seaward from Texelstroom, along the

Texel coastline and Noorderhaaks due to inertia of flow. Consequently, contraction and acceleration of ebb flow at the tip of Helderse Zeewering is not distinctively observed.

The middle transect shows a clear dominance of ebb flow along the Bollen van Kijkduin shoal. The landward part of the channel is dominated by the flood residual velocities that are smaller in magnitude. Note the steep inner channel slope that is plausibly related to the presence of erosion-resistant layers. This embankment is considered to form a separation between Nieuwe Schulpengat and Nieuwe Lands Diep. The most southern transect indicates a flood residual flow in the nearshore Nieuwe Lands Diep channel and on the Bollen van Kijkduin shoal. In Nieuwe Schulpengat no clear dominance is observed.

5.4 Morphodynamics of Texel Inlet

5.4.1 Introduction

Direct measurements of sediment transports in Texel Inlet are not available. Some estimates on sediment transport rates have been obtained by applying a sediment transport formula to flow observations. Most relevant is the pioneering study of Sha (1989a) coupling the Engelund and Hansen (1967) transport formulation and measured flow over two tidal cycles in twenty tidal stations placed in the upper part of the main ebb-tidal delta channels. Although no estimates on transect-averaged rates are given, Sha concludes to a flood-dominant transport in the inlet and Molengat, whereas Schulpengat and Nieuwe Schulpengat are concluded to be ebb-dominant. However, it was also indicated that due to the short-term flow time-series a large inaccuracy and uncertainty in the results exists.

A second analysis was presented by Steijn (1997) proposing a conceptual transport model based on the analysis of velocity measurements in combination with the van Rijn (1986) transport formula, and observed morphodynamic changes. Steijn concludes to a net influx of sediment due to wave-generated transports along the North-Holland coast of 0.5 Mm^3/year. Approximately 1 Mm^3/year bypasses the inlet system along the western margin of the ebb-tidal delta due stirring of sediment by waves and transport by large tidal flow velocities due to contraction of flow around the delta front. Nieuwe Schulpengat and Schulpengat are ebb-dominant (0.25 Mm^3/year), while along the southern margin of Noorderhaaks sediment transport in the order of 0.5 Mm^3/year is directed towards the inlet. Along the northern margin and over the Noorderhaaks transports are estimated to be in the order of 1.75 Mm^3/year. Molengat is flood dominant with a residual transport rate of 0.75 Mm^3/year. The residual sediment influx towards the Wadden Sea was initially estimated to range in the order of 3 Mm^3/year, but in an updated version of the model the sediment influx in Marsdiep was reduced to zero (Steijn and Jeuken, 2000).

With the ongoing measurements and advances in measuring techniques (re)analysis of longer time-series of bedforms and sedimentation and erosion patterns can provide more insight in the sediment transport patterns and rates.

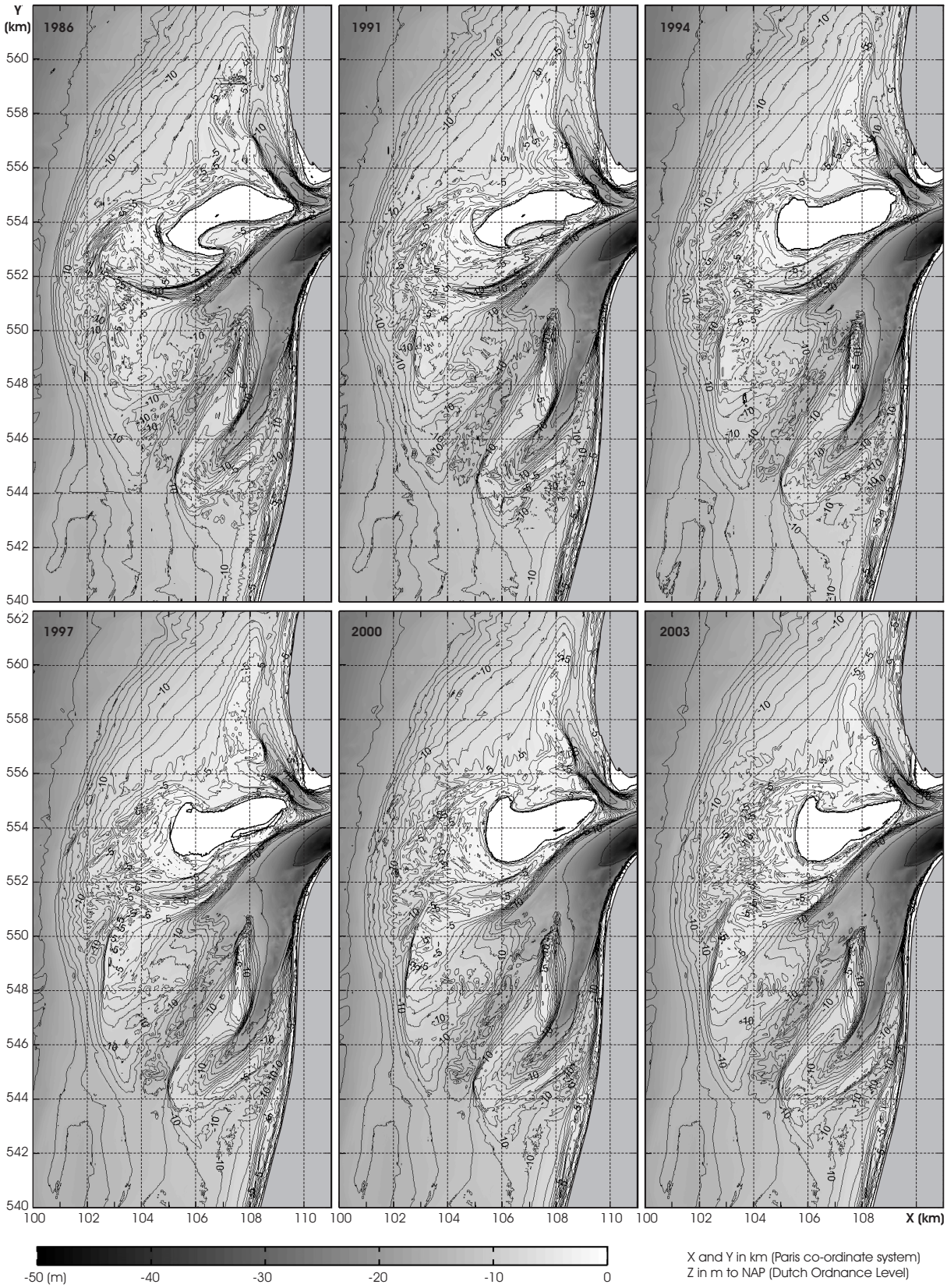

Figure 5-11: Impressions of the ebb-tidal delta bathymetries measured over the period 1986 - 2003. Where relevant complete maps have been compiled by filling in missing data with the nearest measurements available.

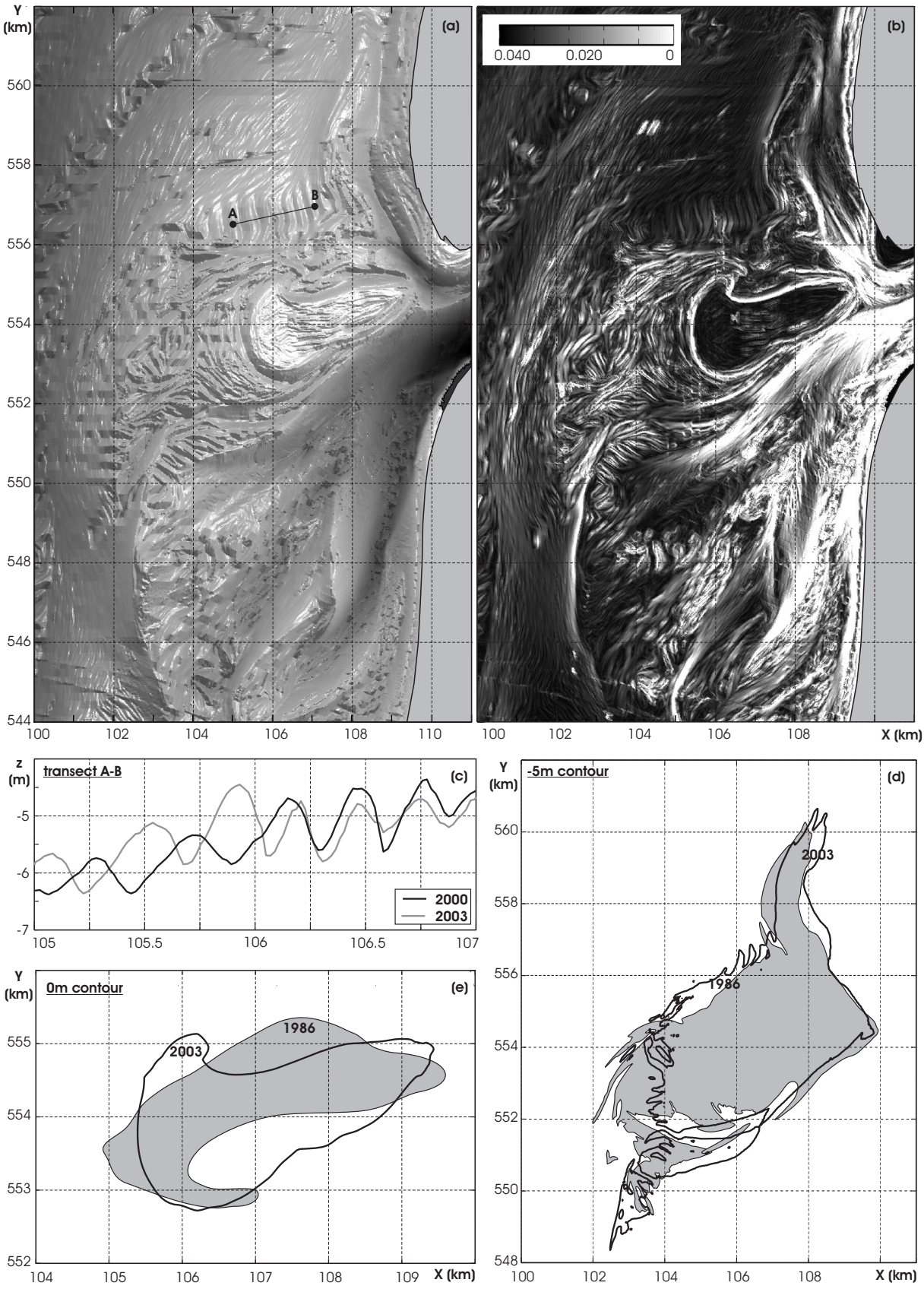

Figure 5-12: 3D representation of major bedforms, bathymetric features and slopes (a and b) based on the 2003 *Vaklodingen*, (c) cross-section A-B illustrates the presence of saw-tooth bars, (d and e) displacement of Noorderhaaks illustrated by the 5 m and 0 m depth contour.

5.4.2 Main features and characteristics of the ebb-tidal delta

Echo-sounding based bathymetric surveys of the ebb-tidal delta have been performed every three years since 1987; digitized measurements are available since 1925, although less frequently measured. Datasets, checked for errors, are made available by Rijkswaterstaat (RIKZ); see de Kruif (2001) for an overview of data till 2001. Recently Elias *et al.* (2003b) and Elias and Van der Spek (2006) have used these maps to analyze the long-term changes (decades to centuries) in ebb-tidal delta behaviour. However, the distribution, evolution, shape and size of typical ebb-tidal delta elements, such as ebb and flood channels, channel margin linear bars, terminal lobe and swash-bars, and the analyses of smaller-scale bedform patterns (see Fig. 5-12a,b) can also provide useful insights in the partitioning of flow and sediment transports on the ebb-tidal delta, see e.g. Hayes (1975), Hine (1975), Hubbart *et al.* (1979), Boothroyd (1985), FitzGerald (1996) and Kana *et al.* (1999). Such knowledge is essential to validate and calibrate processes-based models to study short-term responses on scales of tides and years to decades.

Estimates of transport rates on the Texel ebb-tidal delta are obtained by quantitative analysis of sedimentation-erosion patterns over the period 1986-2003. We focus on the recent morphological developments as since 1986 high-resolution (20x20m) maps are available (see overview in Fig. 5-11). Moreover, during this period the basic configuration of channels and shoals remained remarkably stable (despite significant erosion rates). Prior to 1986 alterations were dominated by the southward extension of the main channels Schulpengat and Nieuwe Schulpengat, and the observed large changes might not be representative for the present morphological developments (Elias *et al.*, 2003b).

Partitioning of tide-generated flow, dominating in channels, and wave-driven flow prevailing over the shallow platforms is characteristic for ebb-tidal deltas (Hine, 1975). The asymmetrical shape of the ebb-tidal delta, the larger scale bedforms and bathymetric features, and the updrift-oriented main-ebb channels point to the presence of such partitioning in the Texel ebb-tidal delta. A distinction can be made in a wave-dominated northern and a tide-dominated southern sub-domain, divided by the supra-tidal Noorderhaaks shoal (Elias *et al.*, 2003b). Largest changes in geometric shape are observed in this supra-tidal area as Noorderhaaks reformed from a concave spit with apex pointed southward to a more northward dipping configuration (Fig. 5-12e). Meanwhile the shoal area slightly increased from about 4 to 5 km^2.

The northern sub-domain consists of the sub-tidal and supra-tidal Noorderhaaks swash-platforms. The spit formation of Noorderlijke Uitlopers of Noorderhaaks, the large number of (landward migrating) saw-tooth bars along the northern margin of the supra-tidal Noorderhaaks (Fig. 5-12a,c) and the northward spit formation at the western tip of this shoal (Fig. 5-12d) indicate that the morphologic developments are dictated by landward and northward directed transports. Landward migration of Molengat is the main actor in the structural erosion of the adjacent Texel coastline (Cleveringa, 2001). This channel migration is related to the lateral (shoreward) movement of Noorderlijke Uitlopers of Noorderhaaks under the influence of wave-driven transports. It is expected that eventually the shoal will attach to the Texel coastline. The possible merger of Noorderlijke Uitlopers of Noorderhaaks with the coastline is an important aspect for coastal management as this could (temporarily) solve the coastal erosion problems.

Initially, after construction of the Zuiderzee, Noorderhaaks migrated eastward thereby decreasing the cross-sectional area of Molengat (Elias *et al.*, 2003b). Consequently, channel velocities and depth increased until stability in the proximal part of the channel was reached. A balance formed between lateral sediment supply by Noorderhaaks, minimal cross-sectional area and maximum channel velocities. In this stable state the along-channel velocities are capable of flushing the lateral sediment supply into the basin during flood and northward during ebb where it contributes to the spit formation of the Noorderlijke Uitlopers of Noorderhaaks. As Noorderlijke Uitlopers of Noorderhaaks stretches northward the flushing of sediment by Molengat is less efficient allowing the shoal to migrate shoreward; see the landward curvature of the distal part of Noorderlijke Uitlopers of Noorderhaaks (Fig. 5-11). The shoreward migration constrains the flow in Molengat and it is expected that flow will eventually seek the path of least resistance forming a new spill-over channel by breaching the spit. The original channel then looses its functionality allowing the abandoned spit to merge with the Texel coastline. Such spit breaching and channel relocation are common phenomena in ebb-tidal delta systems related to the decreasing efficiency of tidal channels with increasing length (Hine, 1975; FitzGerald, 1988).

In the southern sub-domain the main tidal channels prevail. The Bollen van Kijkduin and Franse Bankje shoals facing and flanking the Nieuwe Schulpengat are an indication of the ebb-dominant character of the distal part. Despite the deep channel, hence large velocities and sediment transport capacity, the Bollen van Kijkduin and Franse Bankje remained remarkably stable in shape and position since 1986.

The presence of the large Nieuwe Schulpengat and Nieuwe Lands Diep tidal channels adjacent to the coastline induce a structural loss of sediment from the adjacent beaches (Elias and Cleveringa, 2003). Stone revetments that attach to the Helderse Zeewering were constructed to counteract this erosion and stabilize the coastline position of the upper part of the Holland coast (north of km. 550). In southward direction numerous groins were constructed, and since 1986 beach and dune nourishments maintain the sediment volume of the beaches. Overall, the nourishments have been successful as only a small portion of the coast, stretching between km. 545-547, is still subject to an ongoing retreat related to the small clockwise rotation of the distal part of Nieuwe Schulpengat. This rotation and slight onshore movement displaces the Franse Bankje shoal landward thereby decreasing the width and increasing the depth of Nieuwe Lands Diep. The larger velocities closer to the coastline increase the loss of sediment from the beaches.

The western (seaward) margins of Noorderhaaks and Zuiderhaaks exhibit a contrasting behaviour. The margin of Noorderhaaks is mildly sloped, covered by multiple bar systems (Fig. 5-12a,b) and exhibits a landward retreat. On the broad sub-tidal swash-platforms along the western and northern margins of Noorderhaaks the northward spit developments, the ripples and smaller scale bedforms, and the large number of saw-tooth bars separated by runnels along the northern side of the supra-tidal Noorderhaaks shoal all testify to the wave dominant character of this area (Fig. 5-12 a,b). Although, the major closure-induced channel relocation appeared in a time span of approximately 40 years (Elias *et al.*, 2003b) the reworking of the abandoned ebb-tidal delta deposits still continues. Plausibly this redistribution of this sediment is the dominating process governing the present ebb-tidal delta evolution.

In contrast to the landward retreat of Noorderhaaks, the seaward margin of Zuiderhaaks strongly developed over the last years into a remarkable straight and steep southward-directed slope. The southward outbuilding of Zuiderhaaks is an indication of ebb-dominant transport through Nieuwe Westgat and (the seaward side of) Schulpengat. The absence of an ebb-shield facing Schulpengat is plausibly due the interaction of flood and ebb flow resulting in a net seaward diversion of the sediment transports thereby contributing to the outbuilding of Zuiderhaaks. The slopes plot in Figure 5-12b illustrates the presence of a spill-over lobe (ebb-shield) with landward dipping bedforms facing the Nieuwe Westgat channel. So far Schulpengat and Nieuwe Schulpengat were considered to be the main channels on the ebb-tidal delta, but the seaward outbuilding and ebb-shield formation of Nieuwe Westgat point to the possible importance of this channel for the (future) ebb-tidal delta developments.

5.4.3 Sedimentation-erosion patterns (1986 - 2003)

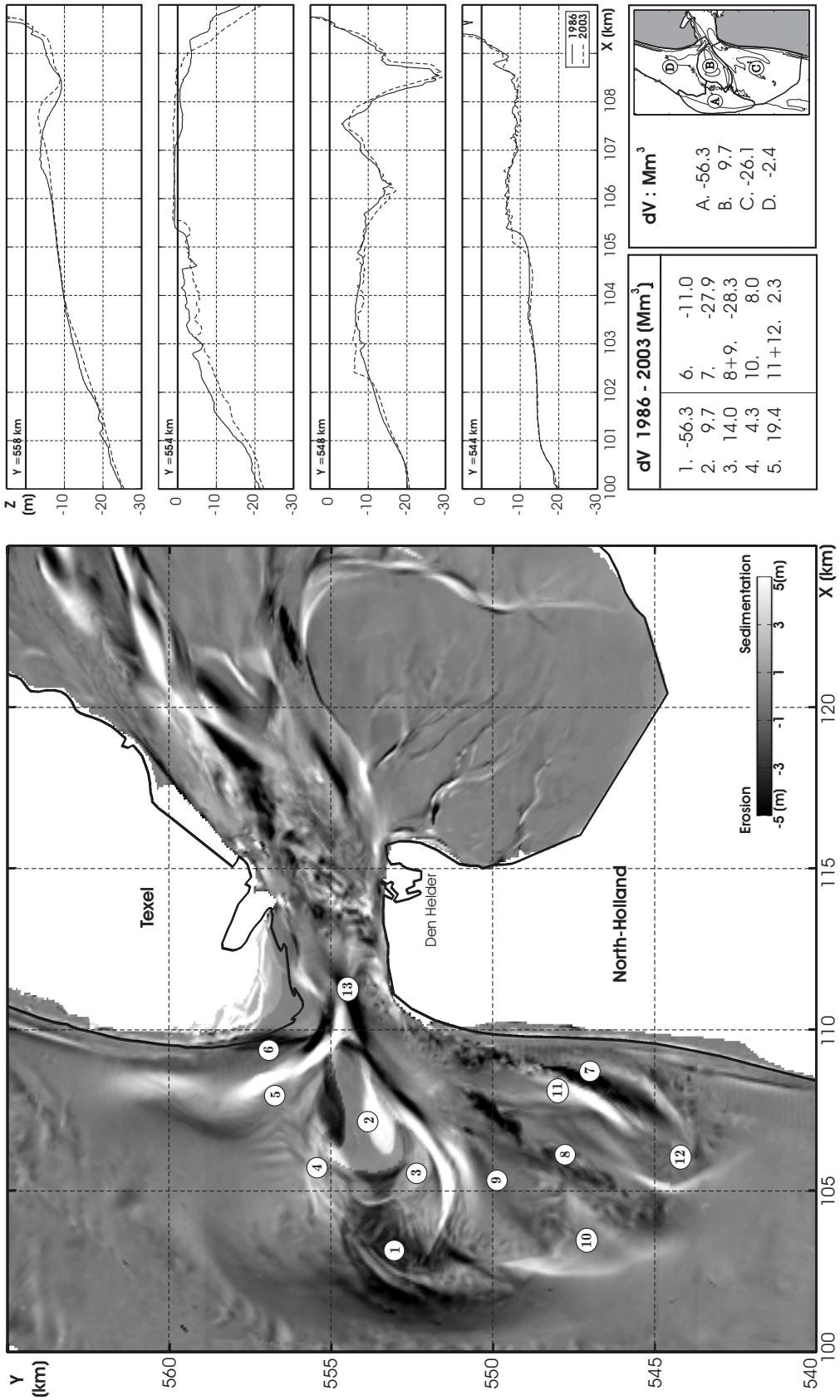

Figure 5-13: Sedimentation-erosion patterns 1986 - 2003 (see text for explanation).

The sedimentation–erosion pattern presented in Figure 5-13 (subdivided in areas [1] to [12]), derived by subtraction of the 1986 bathymetry from the 2003 bathymetry, summarizes the recent morphological changes. The interaction of tidal, wind and wave-driven flow with the compound ebb-tidal delta bathymetry produces a complex pattern of mutually linked sedimentation-erosion areas. Largest erosion (-56 Mm^3 [1]) is observed on the seaward margin of Noorderhaaks due to a re-distribution of sediment in landward direction. The interaction of waves and tides is expected to play an important role. Depth-induced wave breaking on the mildly sloping ebb-tidal delta front and refraction of waves creates compound patterns of crossing wave-crests. Concentrated wave breaking zones rise suspended sediment concentrations that can subsequently be transported by the wave and tidal currents (Oertel, 1972). Tidal currents on the ebb-tidal delta margin are larger then on the open-sea due to contraction of flow around the ebb-tidal delta front.

Tides, onshore directed wind-driven flow, wave-asymmetry and wave-breaking contribute to the landward transports resulting in e.g. accretion of the intra- and supra-tidal part of Noorderhaaks (10 Mm^3 [2]), accumulation of sand in the former Westgat (14 Mm^3 [3]), and spit formation at the north-western margin of Noorderhaaks (4 Mm^3 [4]). In addition a vast amount of sediment is accumulated in the Noorderlijke Uitlopers of the Noorderhaaks spit (19 Mm^3 [5]). Landward migration of the spit and the Molengat channel induces significant erosion along the Texel coastline; since 1986 over 11 Mm^3 [6] was eroded from the near-shore area.

South of Noorderhaaks the morphodynamic developments are tide-dominated due to the presence of the tidal channels Nieuwe Westgat, Schulpengat, Nieuwe Schulpengat and Nieuwe Lands Diep. After closure the evolution of the ebb-tidal delta and coastline were governed by the increasing size and southward extension of the channels (see Chapter 3, Figure 3-7). The channels developed up to about 1986 until a maximum southward extension was reached. The maps of 1986 to 2003 (Fig. 5-11) show limited change in distribution of the channels, but considerable erosion; the total sediment accumulation on the shoals of ~10 Mm^3 [10,11,12] is small compared to the large erosion of the main channels (~ 56 Mm^3 [7,8,9]). The main developments are: (1) an increasing depth of the channels Nieuwe Schulpengat (-28 Mm^3 [7]), Schulpengat and Nieuwe Westgat (-28 Mm^3 [8,9]), (2) a seaward and southward outbuilding of Zuiderhaaks (8 Mm^3 [10]) and Franse Bankje, (2 Mm^3 [11,12]). The alternating patterns of sedimentation and erosion in the distal part of Nieuwe Schulpengat, Bollen van Kijkduin and Franse Bankje relate to a small anti-cyclonic rotation and migration of the channel. The Franse Bankje facing Nieuwe Schulpengat forms part of this channels ebb-shield, and is an indication of the ebb-dominant character of the distal part of the channel.

In total during the period 1986-2003 over 75 Mm^3 of sediment (mainly sand) is eroded from the ebb-tidal delta front and adjacent coastlines[2]. This amount increases towards 95 Mm^3 if the foreshore of the adjacent coastal sections is also taken into account. The corresponding sedimentation rate of the basin (Appendix A) shows that these sediments are imported into the basin. This implies that sand transport rates through Marsdiep, during this period, are at least 5 to 6 Mm^3/year.

[2] These transport rates are considerably larger then previous estimates. Therefore in Appendix A the sediment budget of the Western Wadden Sea is reanalysed.

5.4.4 Detailed bedform analysis

Introduction

Various studies show the direct link between bedform morphology (viz. size and orientation of ripples), and tidal dominance and flow magnitude (e.g. Boothroyd and Hubbard, 1975; Hine, 1975; Boothroyd, 1985; Ashely, 1990; Lobo *et al.*, 2000). Assuming that the bedforms are created by and in equilibrium with present-day hydrodynamic conditions, the bedform distribution, arrangement and morphology provides information about bottom currents (Boothroyd, 1985).

During the period 2002 - 2003 a series of multi-beam surveys was conducted at various locations in the ebb-tidal delta (Nieuwe Schulpengat 11 km^2, Molengat 3 km^2, and multiple 2 km^2 surveys on Noorderhaaks). Measurements were conducted using a Reson Seabat 8125 multibeam echo sounder coupled with a DGPS-Long Range Kinematic positioning system. Multibeam surveying is based on the return time of many acoustic signals transmitted simultaneously. The Reson Seabat sends 240 beams at a rate of 14 pulses per second. The angle between the beams is 0.5°, which means that a horizontal path of roughly three times the water-depth can be measured accurately. Collected data are filtered for discrepancies and corrected for errors due to pitch, roll and heave of the measuring ship during the post-processing procedure. All measurements were referenced to Dutch Ordenance System. Analysis by Rijkswaterstaat shows an 95% accuracy interval of 15 cm. More information on the measurements is presented in Rab (2003).

An impression of the dominant transport vectors on the Texel ebb-tidal delta is obtained from bedform analysis of this multi-beam data. Only slipface orientations of the large-scale bedforms, classified as sandwaves and large megaripples or dunes (Boothroyd, 1985; Ashely, 1990) having wave lengths over 50 m and wave heights over 0.5 m, have been determined from bathymetric cross-sections of the bedforms taken perpendicular to the crest. These large bedforms have long response times, only undergoing minor changes in size and shape when imposed to high-frequency processes such as waves and spring/neap cycles. For that reason, they provide indications of the long-term (averaged over periods of several days to months) dominant transport directions. In Marsdiep and Texelstroom additional observations along the Helsdeur and single-beam transect data are used.

Nieuwe Schulpengat and Nieuwe Lands Diep

In the autumn of 2002 high-resolution multi-beam surveys were performed in the Nieuwe Schulpengat and Nieuwe Landsdiep channels (Rab, 2003). After thorough analysis of the recorded data, removing systematic effects and data outliers, a high-resolution map of approximately 11 km^2 of seafloor bathymetry was obtained (Fig. 5-14). Nieuwe Schulpengat extends in southward direction, diminishing in depth and curving seaward. The shallow Nieuwe Lands Diep is located landward of Nieuwe Schulpengat along the North-Holland coastline. A prominent feature is the steep inner channel slope of Nieuwe Schulpengat roughly located at the -15m contour, which may result from the presence of erosion resistant Eemian clay deposits (Van der Spek and Van Heteren, 2004).

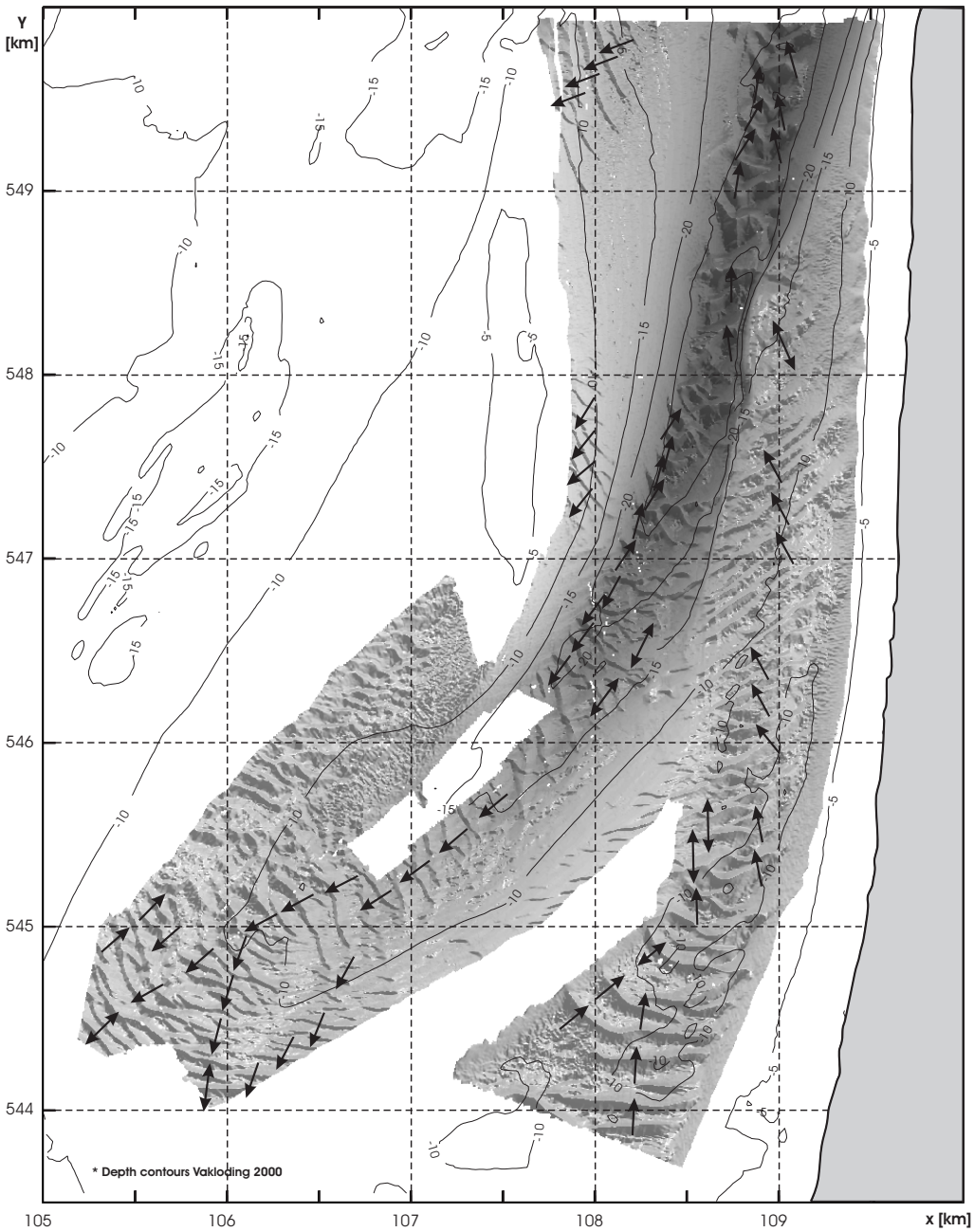

Figure 5-14: Multi-beam based bathymetric map of the Nieuwe Schulpengat area. Arrows indicate dominant slipface orientations of the major bedforms.

The bed of the Nieuwe Schulpengat channels is covered with large to very large compound dunes or sand waves. The largest sand waves up to 4.25 m in height, having wavelengths over 200 m are observed in the deeper parts of Nieuwe Schulpengat (below -20m) where the highest tidal velocities occur. Three-dimensional (e.g. cuspate crestlines) dominate the northern part of the channel plausibly these are related to the large flow velocities that accelerate at the tip of Helderse Zeewering. Up to a certain treshold, the size of the bedform increases with the current velocity. In addition, the existence of coarser sediments in the deeper part of the channel and the channel depth itself allow for the formation of these bedforms. Slip-face asymmetries point toward a predominantly flood-orientated transport (i.e. to the north).

In southward direction, as tidal flow velocities diminish and the depth of Nieuwe Schulpengat decreases, the dominant sand waves are smaller in height (maximum of 2 m) and length (up to 100 m), and have a more two-dimensional setting with relatively straight crestlines. Similar sand waves are also observed in the shallow region along the coastline and in Nieuwe Lands Diep, where the dominant slip-face orientations suggest a net northward sand transport.

In the distal part of Nieuwe Schulpengat, where the channel converges with the spillover lobe, sand waves are smaller in height, ranging between 0.5 and 2.0 m having wave lengths between 50 to 110 m. In contrast to the nearshore area, the slip-face orientations of the dominant sand waves indicate that transports are ebb-dominant.

Molengat

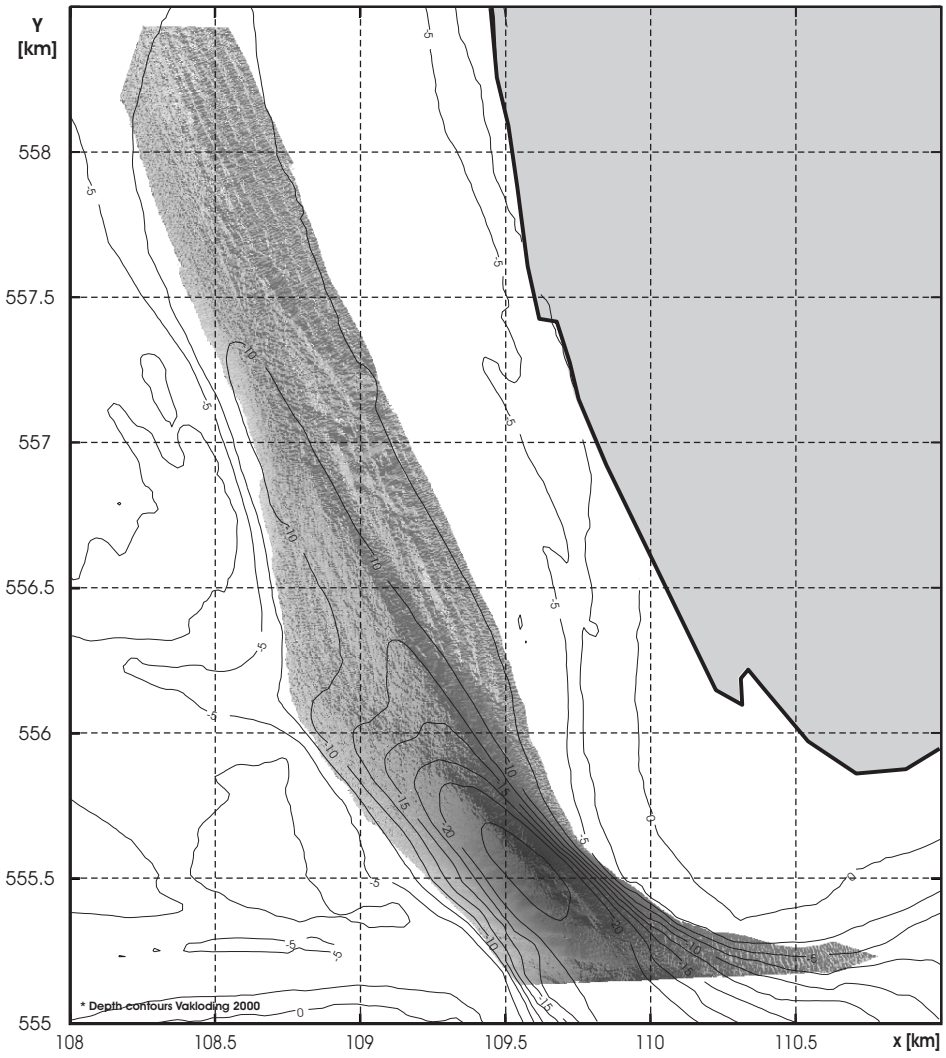

Figure 5-15: Multi-beam based bathymetric map of Molengat.

Multi-beam data obtained in the southern part of Molengat does not show pronounced bed structures (Fig. 5-15); the lateral lines are related to measuring inaccuracies rather then realistic bathymetric features. Most interesting is the distinct difference in the steeper landward than seaward channel slope. Whether this dissimilarity is related to presence of erosion resistant layers on the landward slope is unclear. Core data analysis by Van der Spek and Van Heteren (2004) does not reveal clear evidence of erosion resistant layers in the channel slopes. Only in the deepest part of the channel a thin layer of Holocene clay deposits forms a smooth bed whereon ripples remain undeveloped.

Based on MEDUSA (Multi-Element Detector system for Underwater Sediment Analysis) surveys Koomans (2004) concludes to the presence of an erosion resistant layer plausibly stabilizing the landward channel slope. In this southern part of the channel grain size diameters are large varying between 300 and 350 μmm.

Noorderhaaks

Multiple multi-beam surveys were conducted at the south-eastern embankment of Noorderhaaks to obtain an estimate of the temporal variability in bed structures. Figure 5-16a,b shows the results of 2 km^2 of seafloor bathymetry obtained from measuring campaigns during the months August and October of 2002. The area is dominated by a range of smaller scale bedforms ranging in height between 0 and 0.25 m. Several larger bedforms of nearly 1m in height occur below the 10m depth contour. A cross-shore transect taken over these bedforms (Fig. 5-16c) reveals an ebb-dominant asymmetry and seaward propagation at a rate of 0.70 to 0.85 m/day.

Analysis of the smaller scale bedforms focuses on five successive measurements taken throughout a spring-neap modulation (27-08, 02-09, 09-09, 12-09 and 16-09-2002). These measurements were performed to assess the variability in bedform characteristics and migration rates during different stages of the spring-neap tidal modulation. All measurements show similar characteristics in bedforms of which Figure 5-16d presents a representative depiction.

Bedform migration rates for three 30x30 m squares (see square A, B and C, bottom panel of Fig. 5-16) were followed through the measurements using a '*moving-window-approach*'. This method uses the displacement needed for an optimal correlation in standard deviations between the defined area at timepoint (i) and timepoint (i+1) where i= 1:4 (in total 5 surveys were taken see Fig 5-16e). Correlation values between 0.98 and 0.99 were obtained between the successive measurements. The displacement needed to obtain an optimal correlation is a measure of the bedform migration rate and direction. Figure 5-16d shows the displacement of area A, B and C respectively wherein migration rates vary between 7 and 16 m/day. The largest migration rates were observed during spring tide. Interesting is that the smaller bedforms migrate eastward (towards the basin), opposite to the migration direction of the larger bedforms (illustrated in Fig. 5-16c).

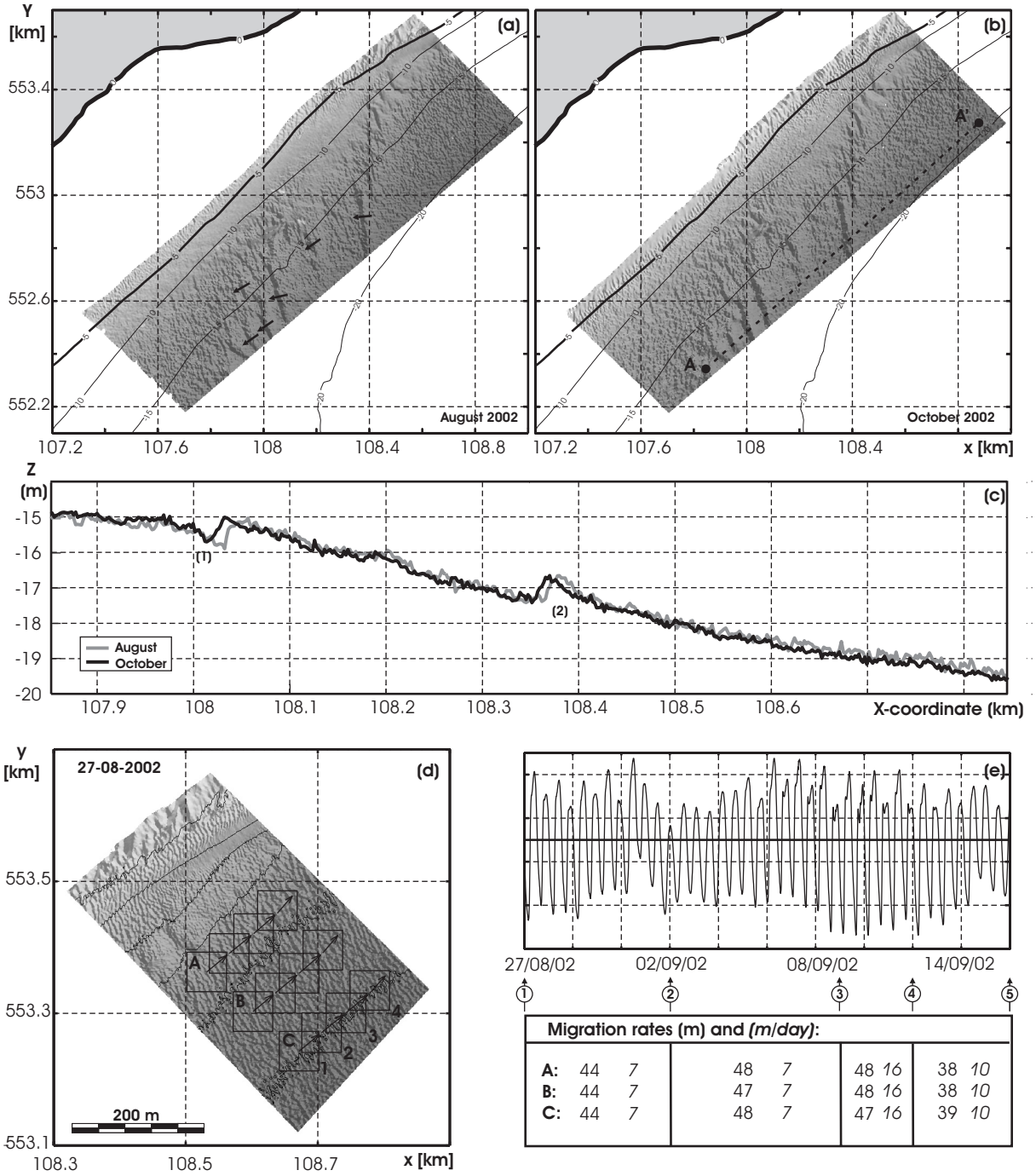

Figure 5-16: Overview multibeam measurements of the southeast margin of Noorderhaaks. Top panels: batymetric maps for the survey of (a) August, (b) October and (c) details of transect A-A'. Bottom panels: results for 5 successive measurements during a spring-neap cycle, see subplot (e) for time-points. (d) Representative overview of measured bedforms and migration directions for squares A,B,C (see text for explanation), (e) measured tidal water levels in station Den Helder and the observed bedform migration rates in the Table.

Marsdiep and Texelstroom

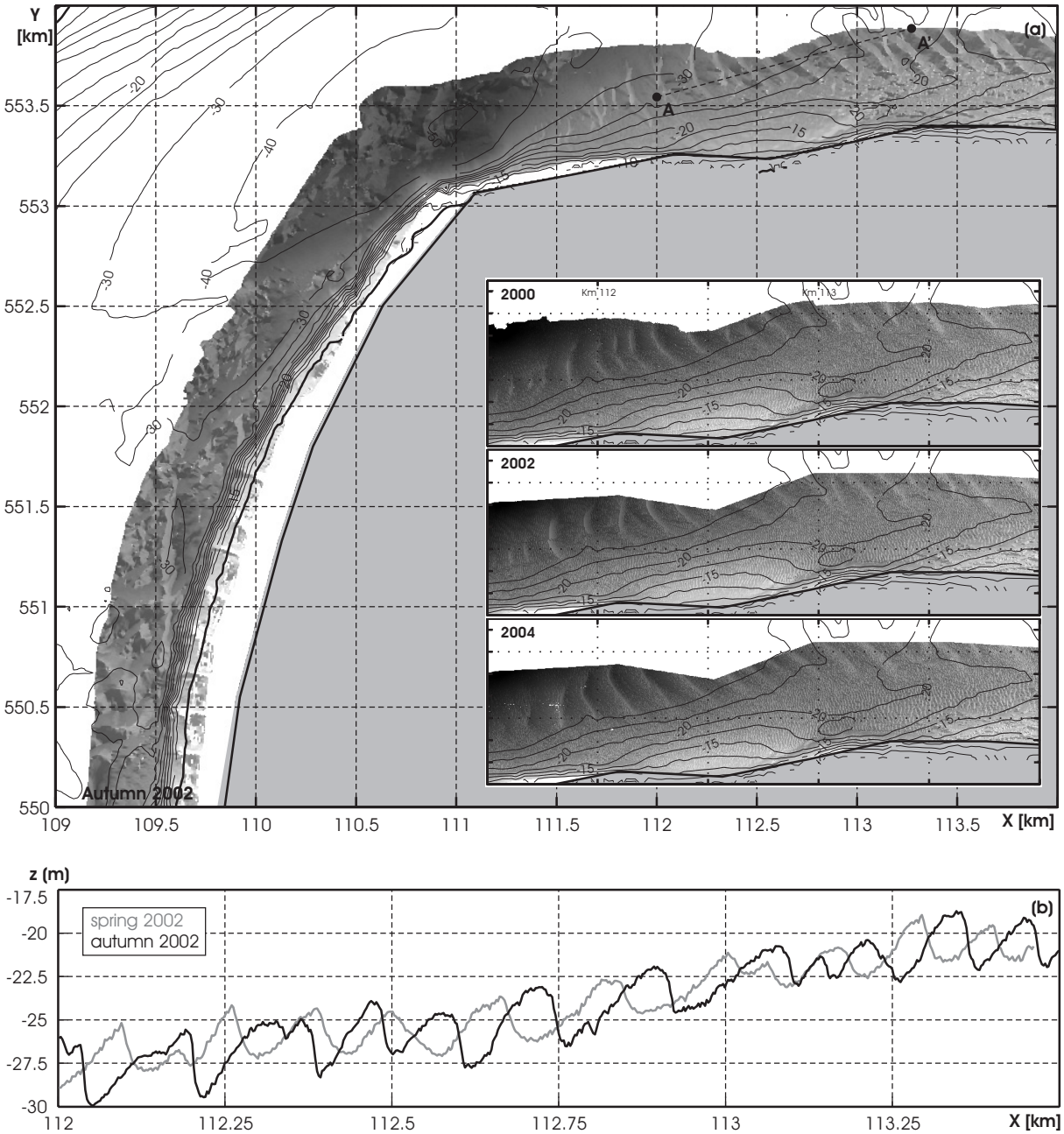

Figure 5-17: Multi-beam data of the Helderse Zeewering. (a) Bedforms in a stretch along the Helderse Zeewering collected in the autumn 2002 for maintenance of the seawall; inserts show details of multi-beam data collected in the spring of 2000, 2002 and 2004. The bottom panel (b) shows a cross-section over bedforms in transect A-A' for the spring and autumn of 2002.

Additional multi-beam data are available in a 500 m wide stretch along the Helderse Zeewering, that were collected yearly for maintenance purposes during the autumn and spring since 1999 (Hoogheemraadschap Hollands Zuiderkwartier, Personal Communication). Figure 5-17 illustrates the main features of selected maps. Along the North-Holland coast (north-south direction) and in the deep scour hole Helsdeur no clear bedforms are observed that can be used to estimate sediment transport directions. The ab-

sence of such bedforms might be attributed to the presence of erosion-resistant layers and large flow velocities due to acceleration of flow around the tip of Helderse Zeewering.

Table 5-3: Bedform characteristics for the Helderse Zeewering transect over the period 1999-2004. For each year the spring (upper line: S) and autumn observations (lower line: A) are plotted

	Wave height			***Height Class (m)***			***Asymmetry***		***Wave length (m)***		
	min	*mean*	*max*	*0-2*	*2-3*	*> 3*	*ebb*	*flood*	*min*	*mean*	*max*
1999S	1.70	3.0	4.5	1	3	3	96	47	55	70	80
A	-	-	-	-	-	-	-	-	-	-	-
2000S	1.30	2.9	4.35	2	5	3	89	39	45	65	87
A	1.75	4.30	3.95	1	5	3	102	41	98	144	193
2001S	1.40	2.6	4.0	2	4	5	87	39	33	61	91
A	1.90	3.00	4.30	1	3	6	88	36	64	129	183
2002S	1.95	2.70	3.4	1	6	2	91	61	52	73	108
A	1.40	3.30	3.95	1	4	6	88	35	52	178	122
2003S	0.90	2.40	3.4	3	4	4	89	41	37	66	88
A	1.00	2.90	4.45	2	3	6	91	38	78	133	179
2004S	2.30	3.0	4.0	0	5	3	102	41	53	72	89
A	1.40	3.20	4.45	2	1	7	96	40	82	134	190

Distinct bedforms in the form of mega-ribbles or sandwaves (dunes) having maximum wave heights of nearly 4.50 m and lengths over 190 m occur in east-west direction along Helderse Zeewering, east of the scour pit Helsdeur. In Table 5-3 the main characteristics of the bedform field are summarized (based on the analysis of transect A-A'). Similar bedforms occur in the various measurements showing an eastward migration (towards the basin). During spring the bedform heights vary between 0.9 and 4.5 m, with an average of 2.6 m. The average length is 90 m. The bedforms are distinctively flood dominant having mean slipface ratios of 2 (slip-face ratio's for individual sand waves are defined as length of the flood ramp/length of the ebb-ramp). The 2-3 m height class prevails.

During autumn most of the bedforms are over 3 m in height with a maximum of 4.5m, however due to the larger variation in smaller and higher bedforms the mean bedform height reduces to 2.6 m. A slip face ratio of 2.5 indicates an even more flood dominant character of the bedform field. A distinct difference occurs in the considerable larger wavelength of 145 m.

Using the *'moving-window approach'* propagation velocities were determined for selected transects. The eastward propagation velocities range between 40 and 60 m/year. Similar velocities are observed in the NIOZ-ferry data[3], wherein bedforms in three transects were followed over a two-year period. The bedforms in the most eastern transect along the North-Holland coast propagate eastward with a mean velocity of 42 m/year. Transects in the central part of Marsdiep show north-eastward propagating bedforms (towards Texelstroom) with average velocities of around 40 m/year (values vary between 3 and 70 m/year).

[3] Based on figures presented on www.NIOZ.nl. The detailed analysis of the NIOZ ferry data might provide valuable insights in bedform orientation and migration in the near-future.

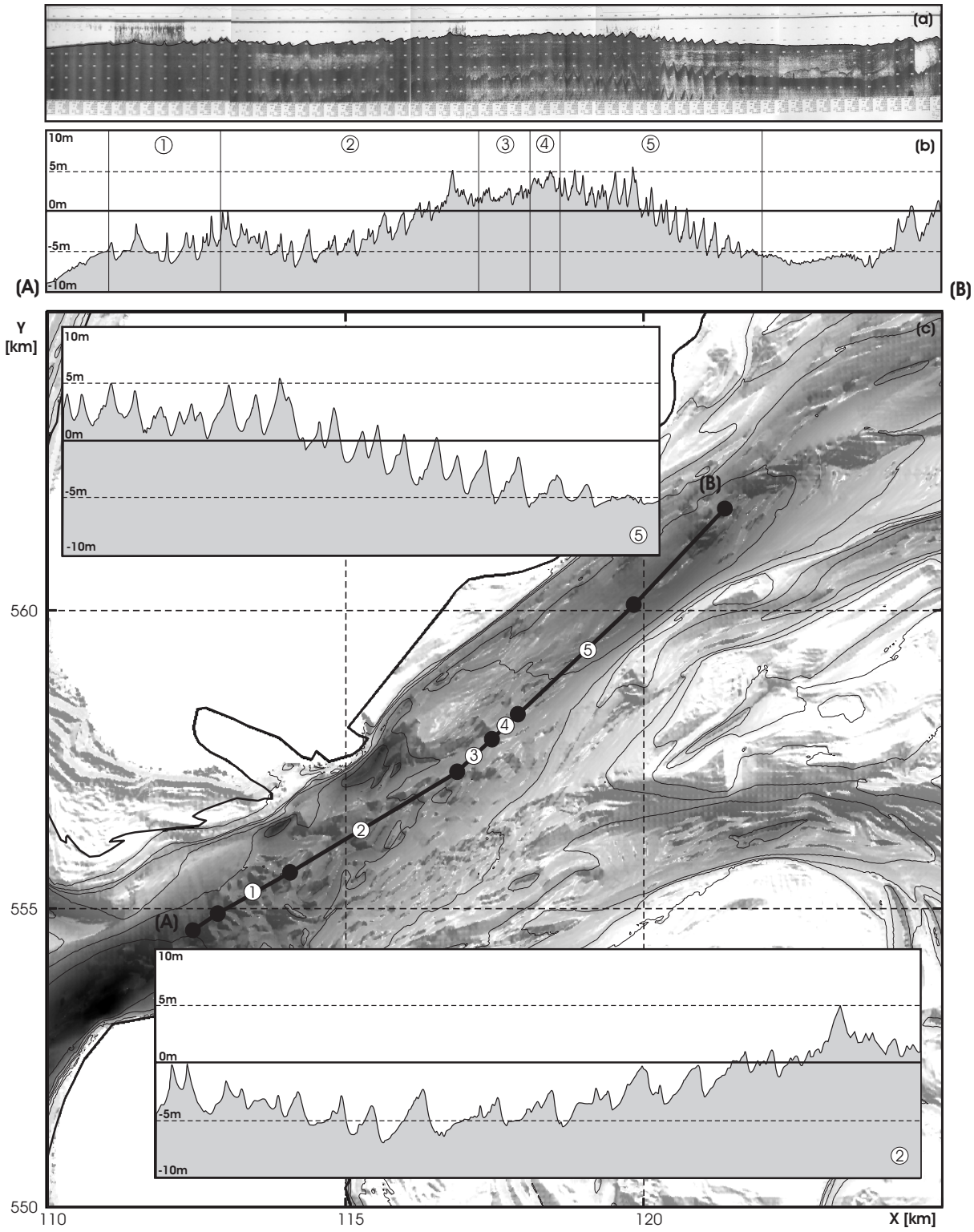

Figure 5-18: Single beam survey of bedforms in Marsdiep and Texelstroom: (a) recorded data profile A-B see (c) for location, (b) digitized and rescaled (in the vertical) profile of the surface, (c) overview of measured transects, inserts show details of flood-oriented bedforms in sections of Marsdiep (2) and Texelstroom (5).

A single-beam high-resolution profile, made available by TNO-NITG for analysis (TNO-NITG, Personal Communication), confirms the presence of eastward-oriented dunes in Marsdiep (Figure 5-18). Travelling from Helsdeur to Texelstroom we subsequently observe: no ripples near Helsdeur, reasonable symmetric bedforms in area 1, large flood-oriented bedforms in area 2, no clearly defined bedforms in area 3, symmetric bedforms in area 4, and large flood-oriented bedforms in area 5.

Summarizing: the sand-wave orientations point to a net flood dominated transport along the North-Holland coastline: from Nieuwe Landsdiep, into Nieuwe Schulpengat and Breedwijd, towards Marsdiep and into the basin. Nieuwe Schulpengat can be divided in an ebb dominant seaward part (along the inner slope of Bollen van Kijkduin) and in the channel south of Bollen van Kijkduin (below km. 547). Flood-dominant transports govern the transports in the landward and northern part of the channel. Despite an ebb-dominant flow there are indications that flood-dominant transports prevail in the proximal part of Texelstroom.

5.5 Summary Observations

Schematic depictions of the flow and sediment transport patterns on the ebb-tidal delta based on the analysis of recent measurements on flow, bedforms, sedimentary structures and sedimentation-erosion patterns are presented in Fig. 5-19 (a,b). The overall patterns correspond reasonably well with the conceptual transport model of Sha (1989a). The main differences are observed in the ebb-dominant transport in major parts of the Molengat and Schulpengat channel, and the large sediment transport rate towards the basin.

The NIOZ ferry observations show a seaward-directed residual flow through the inlet of about 115×10^6 m^3/tide resulting from flood-dominant flow along the North-Holland coastline and a larger ebb-dominant component along the coastline of Texel. The majority of the flow is directed onto the southern part of the ebb-tidal delta into Nieuwe Schulpengat, Schulpengat and Nieuwe Westgat. Velocities in Nieuwe Schulpengat are ebb-dominant along the Bollen van Kijkduin and flood-dominant along the North-Holland coast. Discharges through Molengat are minor (~10 %) compared to the large discharge in Marsdiep. The proximal part of the channel, the outflow of Molengat to Marsdiep, is flood dominated, whereas in northward direction no pronounced flow dominance is observed.

Despite a relative stability in the shape and form of the main channel and shoal areas on the ebb-tidal delta over the period 1986-2003 there are large morphological changes. Analysis of the sedimentation-erosion patterns shows that sediment redistribution, and local interaction between channels and shoals dictate the present morphological developments.

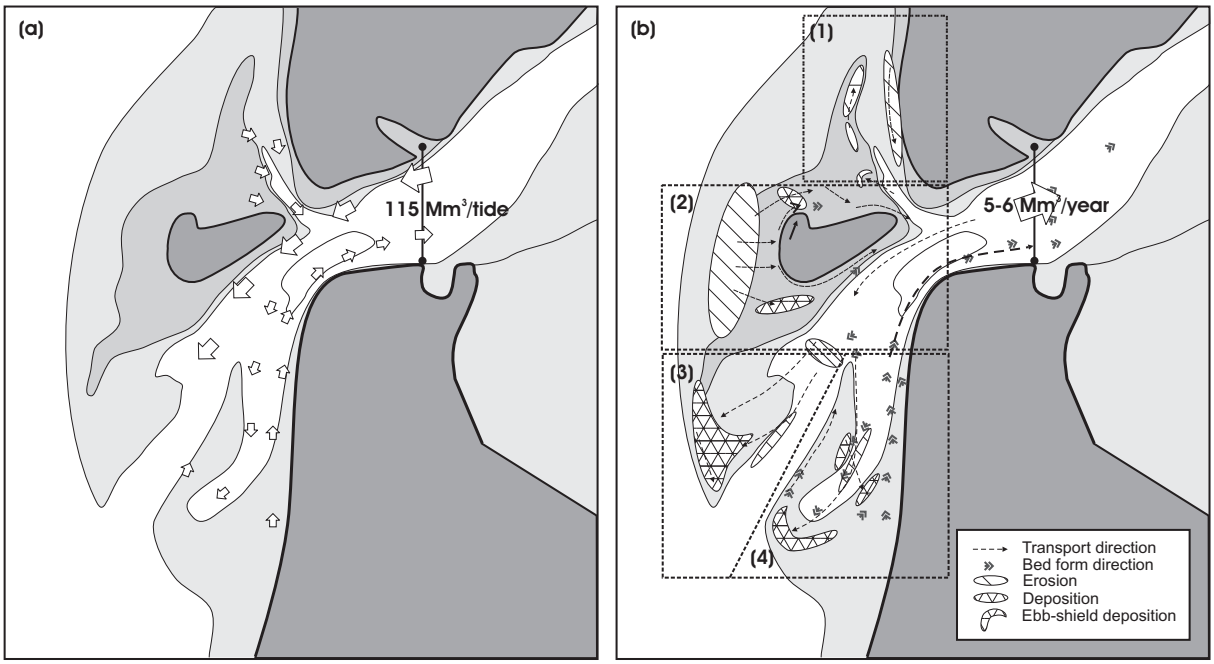

Figure 5-19: Summary of (a) flow patterns, (b) morphologic development and estimated transport paths based on the analysis of field data over the period 1986-2003.

In the north (Fig. 5-19b, area 1) the landward migration of the Noorderlijke Uitlopers of Noorderhaaks and the corresponding displacement of Molengat induce severe erosion of the Texel coastline. The central part of the ebb-tidal delta (Fig. 5-19b, area 2) is dominated by landward displacement of sediments; erosion of the western margin of Noorderhaaks and deposition north and south of the supra-tidal part of Noorderhaaks. The channels Schulpengat and Nieuwe Schulpengat enlarge in depth. In the south we distinguish two areas, separated by Schulpengat, with dissimilar morphological behaviour (Fig. 5-19b, area 3 and 4). Zuiderhaaks (area 3) forms the spill-over lobe of the Nieuwe Lands Diep and Schulpengat channel showing a trend of sedimentation and southward growth. The Nieuwe Schulpengat area (area 4) is governed by the local interaction of the channel with the adjacent shoals. The Bollen van Kijkduin shoal migrates southward, inducing a small southward displacement and clock-wise rotation of Nieuwe Schulpengat and landward migration of the adjacent Franse Bankje shoal. Slip-face asymmetries of the dominant bedforms indicate that large flood dominant transports along the North-Holland coast into Marsdiep and towards Texelstroom prevail.

The total sedimentation of the ebb-tidal delta is small compared to the erosion volume. As also the adjacent coastlines lose sediment a net sediment transport towards the basin must exist. The sand influx over the period 1986-2003 is estimated to range between 5 to 6 Mm^3/year. In the basin corresponding rates of sedimentation are observed.

5.6 Discussion and Conclusions

Insight in the present-day behaviour of the Texel inlet system is obtained by focussing the analysis on recent measurements (1986-2003) that were obtained accurately, after stabilization of the channels on the ebb-tidal delta. The recent Acoustic Doppler Current Profiler measurements allow for the quantification of the flow in the inlet channel, and main ebb-tidal delta channels. A residual ebb-dominant flow of about 115 Mm^3/tide prevails, due to residual ebb-flow along the Texel coastline and a smaller contribution of residual flood-flow along the North-Holland. This segregation in ebb- and flood-dominated flow domains prevails in the main channels. Flood dominates along the North-Holland and Texel coastline, while ebb-residuals dominate along the landward margins of Noorderlijke Uitlopers of Noorderhaaks, Noorderhaaks and Bollen van Kijkduin.

Analysis of high-resolution multi-beam data provides indications of the dominant sand transport patterns. Major flood-orientated bedforms are observed in Nieuwe Lands Diep, the proximal part of Nieuwe Schulpengat (Breewijd) and along the Helderse Zeewering towards Texelstroom. Analysis of the sedimentation-erosion patterns of ebb-tidal delta and basin show that the present-day morphological developments (on ebb-tidal delta scale) are governed by sediment redistribution; sediment is eroded from the ebb-tidal delta (including adjacent shorelines) and deposited in the basin. The sediment influx is estimated to range between 5 to 6 Mm^3/year. Due to the presence of large tidal channels along the adjacent coastlines only small volumes of sand are expected to bypass the system.

The central part of the ebb-tidal delta is dominated by landward displacement of sediments due to erosion of the western margin of Noorderhaaks and deposition north and south of the supra-tidal part of Noorderhaaks. In the southern part of the ebb-tidal delta morphological developments are governed by (1) a southward outbuilding of Zuiderhaaks, and (2) local interaction of Bollen van Kijkduin, Nieuwe Schulpengat and Franse Bankje that results in a small clock-wise rotation of the distal part of Nieuwe Schulpengat and adjacent shoals. In the northern part, northward outbuilding and landward migration of the Noorderlijke Uitlopers of Noorderhaaks and the corresponding displacement of Molengat induces severe erosion of the Texel coastline.

The sediment re-deposition from the ebb-tidal delta into the basin is interpreted as a second-stage response to the effects of closure of the Zuiderzee. The majority of the Noorderhaaks deposits originate from the pre-closure ebb-tidal delta configuration wherein the main-ebb channel (Westgat) was westward orientated. Noorderhaaks was formed as an ebb shield balancing seaward supply of sediment by the ebb-tidal currents and landward wave-driven transports (Elias *et al.*, 2003b). The closure of the Zuiderzee distorted this balance as the changed tidal characteristics of the basin forced an asymmetrical ebb-tidal delta development with updrift directed main channels. This initial (first-stage) response lasted approximately 40 years, and the scouring of the large tidal channels eroded over 200 Mm^3 from the ebb-tidal delta. Due to the large tidal prism and corresponding large tidal transports involved, the channels regained an equilibrium state in a faster rate than the shoal areas (e.g. the abandoned ebb-shield Noorderhaaks). The present ebb-tidal delta development is dictated by the ongoing adjustment of these shoal areas.

Appendix A : SEDIMENT BUDGET OF THE WESTERN WADDEN SEA

The sediment import into the Wadden-Sea forms one of the major sources of sand loss in the Dutch coastal sand balance (Stive and Eysink, 1989; Mulder, 2000). Partly, sediment import is related to relative sea-level rise (Louters and Gerritsen, 1994), and partly import relates to infilling of closed of channels after the damming of the Zuiderzee in 1933 (Elias *et al.*, 2003b; Elias *et al.*, 2006). Previous studies agreed on the net sediment influx into the basin since the Zuiderzee damming, but estimates of the present import rates and predictions on future evolution vary. Based on sand-budget studies of the Texel basin by e.g. Sha (1990), Van Marion (1999), Louters and Gerritsen (1994), Ligtenberg (1998), Steijn and Jeuken (2000) and Elias *et al.* (2003b) point to a net import of sediment in the order of 0 to 3 Mm^3/year. An underlying assumption in these previous sediment budget studies was that the individual inlets can be defined as 'more or less' unconnected sub-systems separated by tidal divides. The location of these tidal divides corresponds roughly with the *Vaklodingen* areas, therefore analysis of the individual inlet systems was primarily based on the corresponding *Vaklodingen* datasets (see e.g. Chapter 3, Fig. 3-6 for the sediment volume change of Texel basin). The Texel *Vaklodingen* showed a large sediment import following the Closure of the Zuiderzee, while at present the sediment volume changes fluctuate around zero. Based on this decrease in sediment influx, it was concluded that the basin had completed much of the adaptation to the closure.

In principal basin and ebb-delta form a coherent morphological system (Oost, 1995; De Vriend and Ribberink, 1996) and the volume change of ebb delta and basin are related; if the ebb-tidal delta erodes (see Chapter 5.4.3) a corresponding rate of sedimentation in the basin is expected. Comparing the sediment volume change of Texel basin and ebb-tidal delta in detail (Fig. 5-20 for the period 1965 to present) we can observe a clear imbalance between ebb-tidal delta and basin changes; the ebb-tidal delta looses nearly 100 Mm^3 of sediments, while the basin volume remains near constant. A similar but opposite discrepancy is observed in the Vlie inlet system.

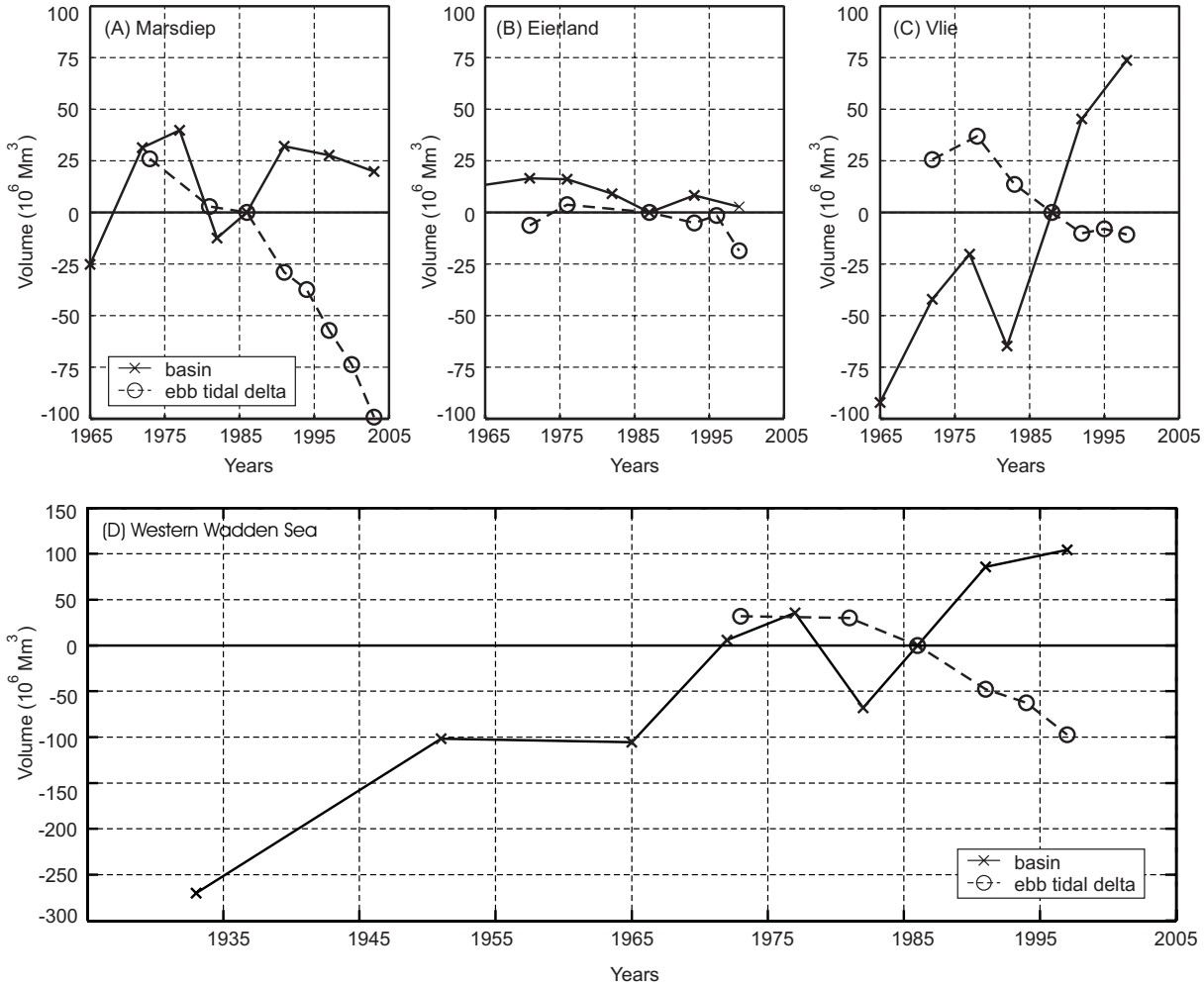

Figure 5-20 upper plots (from left to right): Sediment volume changes relative to the 1985/1986 value of the Marsdiep, Eierlandse Gat and Vlie ebb-tidal deltas and basin over the period 1965 to present. Volumes and balance areas are based on Rijkswaterstaat *Vaklodingen* data see Figure 5-21 for area definition. Data made available by RIKZ (Walburg 2006, Personal Communication). Lower plot: cumulative changes of the western Wadden Sea (basin changes expanded with estimates of the 1925, 1950 and 1965 volumes).

The main characteristics of the ebb delta changes are: (a) a major loss of sediment from the Marsdiep ebb delta of nearly 100 Mm^3 between 1985 and 2003, (b) small possibly increasing erosion of Eierlandse gat (25 Mm^3), (c) initially erosion but at present a near stable Vlie ebb-tidal delta volume. In total the three ebb-tidal deltas loose 95 Mm^3 of sediment over the period 1986-1997. During this period a near-equal amount of sediment (105 Mm^3) is deposited in the basin. This is mainly due to the large sedimentation in the Vlie basin (75 Mm^3). In the Marsdiep basin periods of erosion and sedimentation alternate, but since 1991 a small erosion trend prevails (~10 Mm^3). The near corresponding rates of sedimentation in the basin and erosion of the ebb-tidal deltas and coasts indicate the exchange of sediment between the basins of Marsdiep and Vlie.

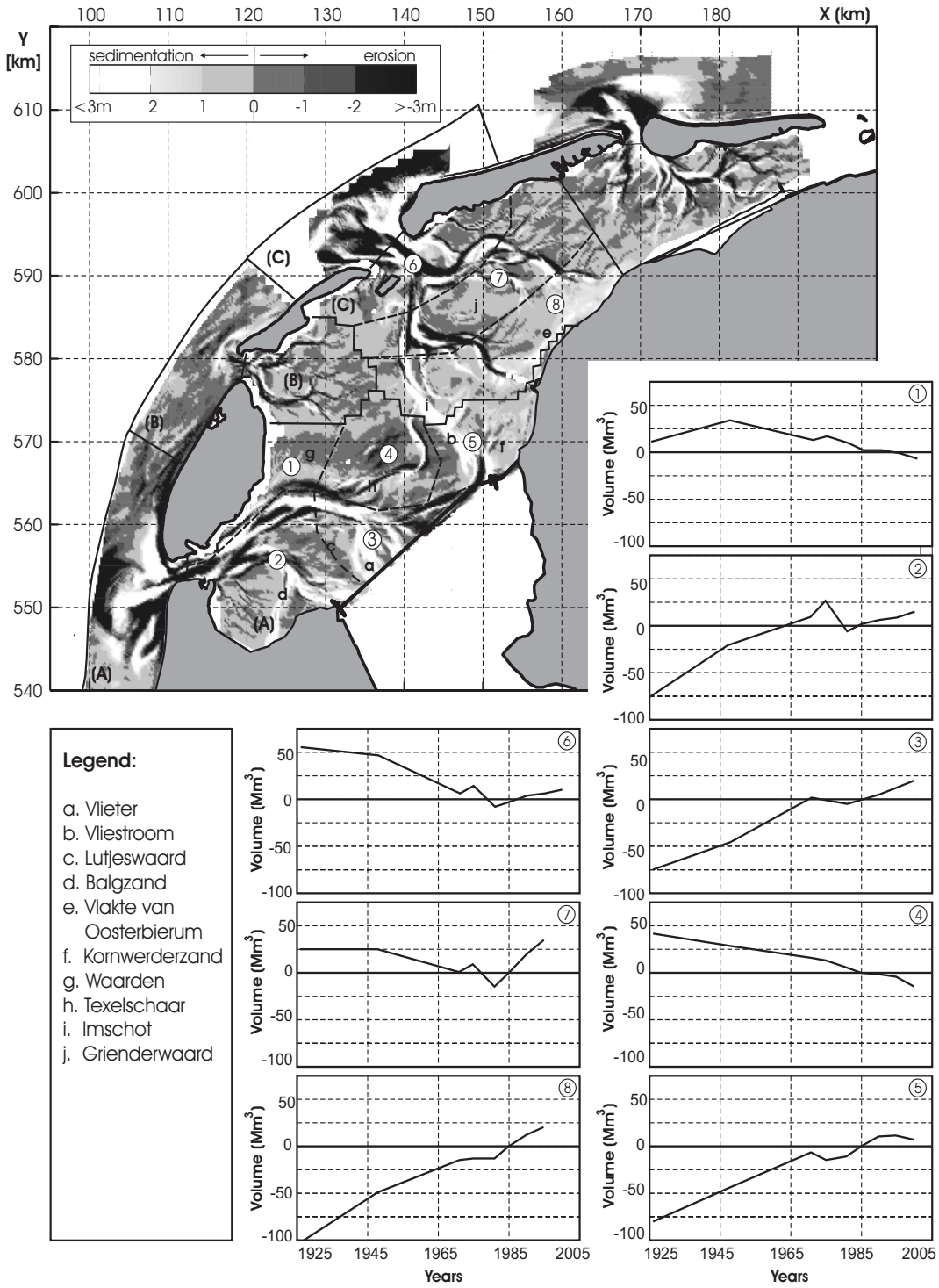

Fig. 5-21 upper plot: Sedimentation-erosion patterns over the period 1925 - 1995, and detailed sediment budgets for selected polygons (1-8) in the Texel and Vlie basins over the period 1925 - 2005. Volumes have been determined using the UCIT Toolbox [(1)] and *Vaklodingen* datasets and are relative to the 1985 volume.

[1] UCIT is a Marine and Coastal Analysis Toolbox, under development at WL| Delft Hydraulics since 2004 (initiated by Van Koningsveld *et al.* 2004). Note that the data between 1985 and 2005 have been linearly interpolated to 5 year intervals to create complete maps.

Looking over the period 1927 - 1997 in total nearly 400 Mm^3 of sediment was deposited in the basin (Fig. 5-20d). Assuming that the basin also imports sediment to keep in pace to the increase in accommodation due to relative sea-level rise, then approximately half of the sedimentation was already needed to compensate for the present sea-level rise of 20 cm/century. This implies that (1) only half of the deposits is related to regaining equilibrium after closure of the Zuiderzee, and (2) sediment import rates are still considerably larger then needed to compensate for sea-level rise, hence the effects of the damming have not damped out.

An important conclusion from the individual sand balances is that we cannot describe the individual inlets separately as the major erosion occurs at the Marsdiep ebb-tidal delta and the main sedimentation in the Vlie basin. The complete sand-balance of the western Wadden Sea must be considered as a whole. The main characteristics are:

- a strong sediment import since damming of the Zuiderzee of ~ 6 Mm^3/year;
- relative large fluctuations between 1950 and 1986 possibly related to 18.5 year tidal modulations, or an indication of the measuring accuracy;
- the recent sediment import (1986 to present) ranges between 9 to 10 Mm^3/year. Most of the sediments, 5-6 Mm^3/year, are supplied by Texel inlet.

The large changes in sediment volumes of ebb-tidal deltas and basin are clearly reflected by the changes in Wadden Sea bathymetry and summarized by the smaller scale sand balances of Figure 5-21. Extensive sedimentation areas are observed in the terminal parts of channels (see, e.g. the Vlieter [a], Vliestroom [b]) where tidal currents reduced to almost zero and the loss of discharge caused the channels to accrete rapidly (Fig. 5-21 time-series [2,3,5]). Sedimentation was also observed on the major shoal areas such as Lutjeswaard [c], Balgzand [d] and Vlakte van Oosterbierum [e], and the spill-over lobe (Kornwerderzand [g]) facing Doove Balg, this sedimentation area extends eastward along the Frisian coast [time-series 5,8]. An opposite response is present in the area between Waarden [f] and Kornwerderzand [g] where erosion prevails [time-series 1,4]. This erosion is for a major part related to the scouring of the channel Texelschaar [h] and continues up to present.

Vlie inlet is dominated by large sedimentation along the margins of the basin [time-series 8]. A major part of this sedimentation is related to the infilling of the former access channels to the Zuiderzee (at the location of Imschot [i]). Significant sedimentation is also observed along the Frisian coastline where the shoal areas between Grienderwaard [j] and the Vlakte van Oosterbierum [e] accreted [time-series 8]. The notably smaller erosion values of the Vlie ebb-tidal delta and the proximal part of the basin near the inlet [time-series 6] render it likely that much of the sediments are supplied by the Marsdiep basin. The Texelschaar [h] scouring must have contributed significantly to the infilling near Imschot [i], while in addition the net eastward directed wind and wave driven currents transport sediments from e.g. the Texel basin and Doove Balg spill-over lobe eastward.

Chapter 6
Sand transport patterns in Texel Inlet; Part 2, Quasi Real-time Model Data Analysis

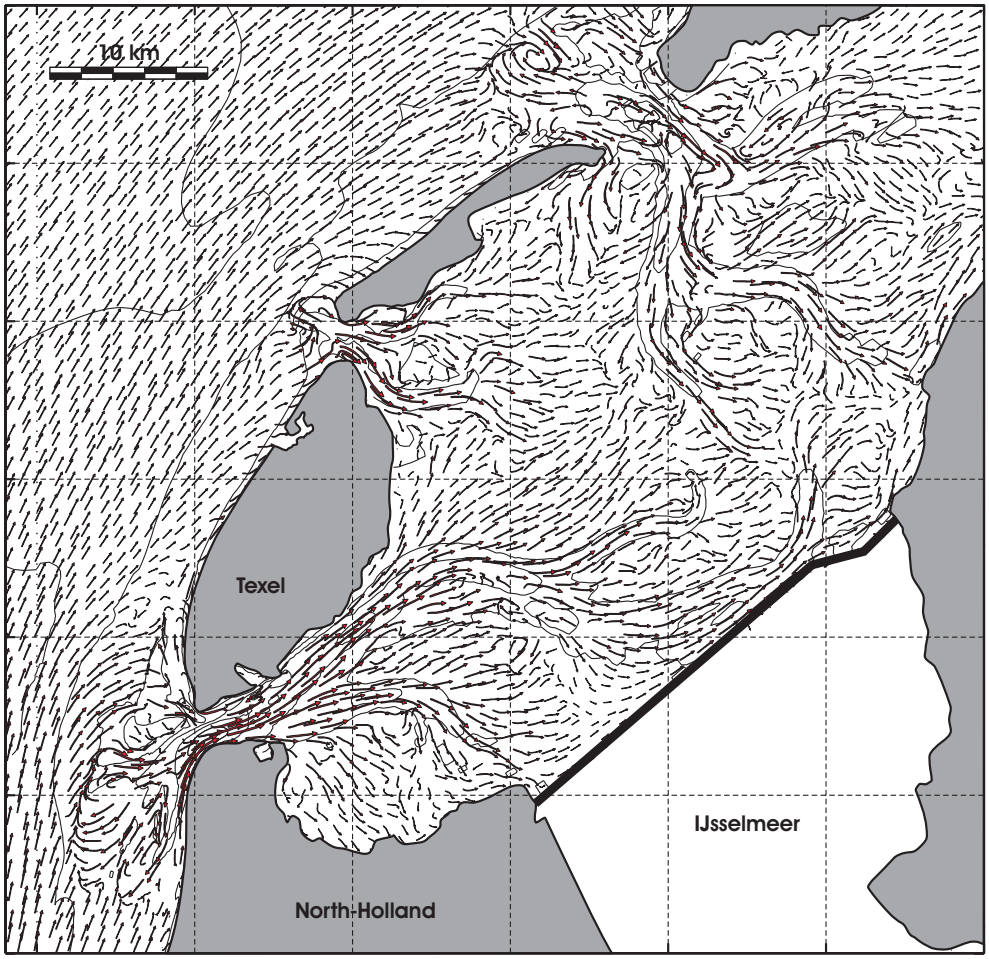

Impression of modeled tidally-driven residual sediment transport patterns

6.1 Introduction

Field data providing detailed descriptions of water, flow and sediment-transport variations on the intra-tidal and intra-event scales with the necessary spatial and temporal detail over the inlet domain are scarce, if not absent. Even at Texel Inlet, that is probably one of the longest and most frequently monitored inlet's worldwide with the availability of high-quality observational datasets of water levels, wind, waves, currents and discharges, bathymetry, bedforms and sediments (see Chapter 5), there is still only limited spatial and temporal data coverage. The conceptual descriptions of morphological behavior and transport patterns presented in Chapter 5 are therefore for a major part founded on expert judgment based interpretations of the available data, moreover conclusions on inherent behavior and the underlying dominant processes are absent.

Process-based models using physical laws describing the water motion, sediment transport and bottom change by a series of mathematical formulations have long been applied in the modeling of short-term coastal processes. Recent studies by e.g. Wang *et al.* (1995), Cayocca (2001), Van Leeuwen (2002), Hibma (2004) and Van Maren (2004) have shown that nowadays such models can be successfully applied even in the complex environments of tidal inlet systems. Nevertheless, the morphodynamic modeling of inlet associated ebb-tidal deltas has not received much attention (NWO-ALW, 1999); to our knowledge, so far no convincing validation studies on the spatially detailed description of water, flow and sediment transport variations on the (intra-)tidal and event scales for ebb-tidal deltas exist.

In this Chapter we use the state-of-the-art Delft3D Online Morphology model to obtain synoptic, more-or-less realistic, data of high spatial and temporal resolution over the inlet domain. The model results enable the validation of the observation based conceptual ideas on flow and transports, and make identification of the dominant processes and mechanisms in the instrumented and un-instrumented areas of the system possible. By assimilation of the obtained insights of Chapters 5 and 6 we derive a schematic representation of the dominant transports patterns for the present state of Texel Inlet.

6.2 Method and Model

6.2.1 Method

Delft3D Online morphology is used to obtain insight in the physics behind the observed morphodynamic changes of Texel inlet, and to identify the relevance of the governing processes and mechanisms. The Delft3D Online Morphology model calculates morphologic changes simultaneously with the flow calculations. One of the major assets of this type of model is the capability to increase the spatial and temporal resolution of point-oriented field observations. Observations are used to force the model 'as realistically as possible' (quasi real-time by measured time-series of wind, waves and tides) and the model results provide synoptic more-or-less realistic data of high spatial and temporal resolution over the entire inlet domain. Analysis of this data can provide valuable information on governing flow and sediment transport patterns in the instrumented and the un-instrumented areas. Additionally, such model approach allows for identification of the dominant processes, systematically checking mechanisms by varying the forcing conditions (see Table 6-1).

Table 6-1: Overview model simulations and forcing processes (see text for explanation)

	Process			
Simulation	***Tides***	***Set-up***	***Wind***	***Waves***
A. Quasi real-time	yes	yes	yes	yes
B. No wave forcing	yes	yes	yes	no
C. Water level forcing	yes	yes	no	no
D. Tidal forcing	yes	no	no	no
Process definition	D	C-D	B-C	A-B

The quasi real-time reference simulation **(A)** includes all forcing processes. In addition to this reference simulation three model experiments were defined (Table 6-1). Each experiment was run over a 10-month period in 1-month intervals (1-12-1998 / 1-10-1999) resulting in a total of 40 simulations. To obtain a manageable set of result files for each individual simulation maps of month-averaged flow and transport vectors were determined and transport rates integrated over a number of predefined cross-sections calculated (89 in total). The total sediment transport vectors per experiment were derived by weighted summation of the monthly results and scaled to million (M)m^3/year.

The tidal experiment **(*D*)** uses the amplitudes and phases of the main tidal components (water levels) on the open-sea boundaries. The forcing conditions were derived through harmonic analysis of the quasi real-time boundary time-series. Importantly, the M_0 (mean water-level) component was excluded (set to zero) from the forcing series, therefore in the tidal experiment only the locally generated M_0 components are accounted for. This modification of the M_0 allows evaluating the importance of set-up by comparison of the differences in results of the tidally forced and water-level-forced simulation (**C versus D**). Set-up forcing represents the contribution of the (spatial variations in) large-scale

wind-driven setup of the southern North-Sea (major) and the M_0 variation imposed by the open-sea tide (minor).

An estimate of the contribution of the locally generated wind-driven flow is obtained by analysis of the differences between the experiments using water level forcing versus no wave forcing (**B versus C**). In addition comparison of the no-wave and quasi real-time experiment (**B versus A**) provides insight in the importance of wave and wave-tide interaction for flow and transport.

The ultimate goal is to realistically model the medium to long-term morphological changes (years to decades). As yet keeping computational effort feasible limits us to depth-averaged simulations over a 10-month period, wherein morphological change is still limited compared to the scale of the ebb delta[1]. We nevertheless feel that this approach is a first important step in obtaining understanding of local phenomena and dominant processes on smaller scales, which is essential to understand the short-term and long-term functioning of the ebb delta in the coastal system.

6.2.2 Basics of Delft3D Online Morphology

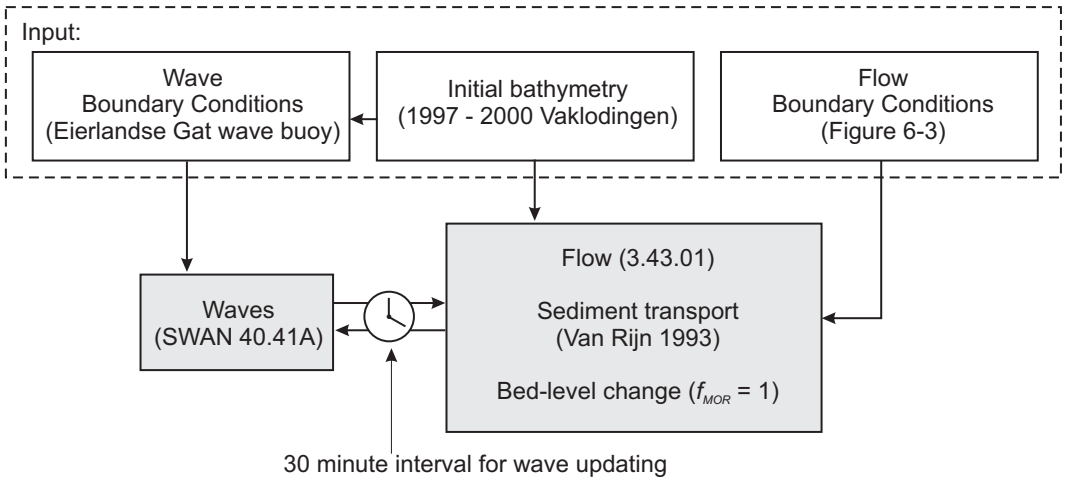

Figure 6-1: Schematic representation of Delft3D Online Morphology as applied in this study.

The Delft3D Online Morphology system has been used to obtain estimates of the water motion and sediment transports in the inlet domain (Lesser *et al.*, 2004, see Chapter 4 of this thesis for a short introduction). The main components are the coupled Delft3D-Wave and the Delft3D-Flow module (Fig. 6-1), and a steering module (MORSYS) describing the sequence of alternating calls between waves and flow[2]. Delft3D-Flow (version 3.43.01) forms the core of the model system simulating water motion due to tidal

[1] With the advances in modelling system and the rapidly increasing computer capacity the computational horizon is rapidly expanding making quasi real-time simulations over medium term scales (years to decades) possible.

[2] In more recent versions of Delft3D (starting from version 3.25) the MORSYS steering module is no longer needed as wave coupling is internally controlled by the flow module.

and meteorological forcing by solving the well-known unsteady shallow-water equations (Stelling, 1984). The Alternating Direction Implicit method is used to solve the vertical and horizontal momentum and continuity equations (Stelling, 1984; Leendertse, 1987) on a staggered grid.

Wave effects, such as enhanced bed shear stresses and wave forcing due to breaking, are integrated in the flow simulation by running the 3rd generation SWAN wave processor (Version 40.41A). The SWAN-model is based on discrete spectral action balance equations, computing the evolution of random, short-crested waves (Holthuijsen *et al.*, 1993; Booij *et al.*, 1999; Ris, 1999). Physical processes included are: generation of waves by wind, dissipation due to whitecapping, bottom friction and depth induced breaking, and, non-linear quadruplet and triad wave-wave interactions. Wave propagation, growth and decay is solved periodically on subsets of the flow grid. The results of the wave simulation, such as wave height, peak spectral period, and mass fluxes are stored on the computational flow grid and included in the flow calculations through additional driving terms near surface and bed, enhanced bed shear stress, mass flux and increased turbulence (see e.g. Walstra *et al.*, 2000).

The Online Morphology add-on supplements the flow model results with sediment transport computations (Lesser *et al.*, 2004). In this study the default Van Rijn (1993) transport formulation is used (for non-cohesive sediment only). Herein, the total sediment transport is obtained from the sum of the bed load and suspended load transports. Bed load transports represent the particle movements in the wave boundary layer due to currents and waves. Suspended load transports are the transports above the bed layer due to e.g. transport of sediment by high-frequency oscillating flow (cross-shore orbital motion and advective transports by the time-averaged current velocities including wave effects such as wave motion induced reduction of current velocities near the bed, and enhancement of near-bed concentrations due to wave stirring). Before bed-level updating sediment transport rates are corrected for bed-slope effects. Overview of the implementation of the Van Rijn transport formulations (Van Rijn, 1993) in Delft3D are presented by Lesser *et al.* (2004) and Walstra and Van Rijn (2003), and summarized in Chapter 4 Appendix A.

6.2.3 Texel Outer Delta (*TOD*) model application

The *TOD*-model application contains the inlets of Texel, Eierlandse Gat and Vlie, the adjacent coastlines and barrier islands. The Eierlandse Gat and Vlie inlet are included in the model domain to enable the simulation of the important internal residual volume transport between Vlie and Texel Inlet. The well-structured, orthogonal curvilinear grid has 38871 points, with a maximum resolution of 80x120 m at the location of Texel Inlet (see Fig. 6-2 for flow and wave grids). The North-Holland coastline, the landward coastline in the back-barrier basin, and the island coastlines form closed boundaries (free-slip conditions). The northern basin periphery is chosen on the Terschelling tidal watershed and set as a zero-velocity Neumann boundary (see Roelvink and Walstra, 2004 for details). Open-sea boundaries are located "far away" outside the sphere of Texel inlet's influence and prescribed as water-level elevations.

Forcing conditions

Realistic (quasi real-time) simulations are forced by water level time-series that contain tidal and non-tidal contributions. In general the tidal contribution is most important, but due to the funnel shape of the North Sea, wind-driven set-up can significantly influence the mean water levels during storm events (Chapter 5 Fig. 5-4b). The size of the model allows for the generation of the local wind-driven flow, but is too small to generate the larger-scale wind driven set-up. To obtain 'as realistically as possible' estimates of the flow and sediment transport patterns in the inlet and on the ebb-tidal delta both the tidal and non-tidal forcing must be represented correctly. The forcing conditions have been derived from a large-scale model that was calibrated on the measured water levels of the tidal gauges along the Dutch coast through Kalman filtering. This water level data was made available by Rijkswaterstaat (personal communication) for a 10-month period (01-12-1998 / 01-10-1999). This period includes seasonal variations in storm events and is fairly representative for the year-averaged conditions.

Quasi real-time simulations are forced additionally by wind and waves. The uniform wind stresses on the free surface are based on hourly data of a wind climate, derived from measurements of station De Kooy near Den Helder (Fig. 6-3b and c). Wind stress magnitudes are computed by,

$$\left|\overrightarrow{\tau_s}\right| = \rho_a C_d U_{10}^2 \tag{6.1}$$

wherein ρ_a is the density of air (kg/m^3), U_{10} the wind speed 10m above the free surface (m/s) and C_d the wind drag coefficient. Wind speed depended wind drag coefficients have been defined accordingly,

$$C_d = C_d^A + \left(C_d^B - C_d^A\right)\frac{U_{10} - U_{10}^A}{U_{10}^B - U_{10}^A} \tag{6.2}$$

with $U_{10}^A = 0$ [m/s], $U_{10}^B = 100$ [m/s], $C_d^A = 0.00063$ [-] and $C_d^B = 0.00723$ (coefficients based on Roelvink *et al.*, 2001).

The transformations of waves on the delta front and shoals are simulated using the SWAN wave model. Waves are forced by spatially constant, but time-varying series of wave heights, periods and directions (see Fig. 6-3d and e for time-series of wave heights and direction). By updating the wave field every 30 minutes an accurate representation of the wave forcing through the tidal cycle is obtained. These time-series are based on the measurements of the Eierlandse Gat wave buoy and prescribed on the open-sea boundaries using a Jonswap shape of the wave spectrum with a peak enhancement factor of 3.3. At the lateral boundaries the specification of uniform wave heights introduces some errors in the nearshore area due to water depth restrictions. By using a large-scale grid these disturbances are located well outside the domain of interest and do not affect the local model results at Texel inlet. Wave propagation, growth and decay due to generation of waves by wind, the dissipation due to whitecapping, bottom friction (Jonswap coefficient of 0.067 m^{2}s^{-3}), depth induced breaking (Battjes and Jansen breaker criterion of 0.73), and non-linear quadruplet and triad wave-wave interactions (Lumped Triad Approximation with a = 0.1 and b = 2.2) are solved half-hourly on two nested wave grids

(see Fig. 6-2 bottom plots). The nested wave grid is of similar resolution as the flow grid to obtain an accurate representation of the wave-breaking process in the nearshore and on the ebb-tidal delta.

Table 6-2: Wave-climate characteristics (percentage of occurrence) of the Eierlandse Gat station over the period 1979-2001 versus *observations over the period (1-12-1998 - 1-10-1999).*

H_{sig}	***Direction class (deg)***												
(m)	***15***	***45***	***75***	***105***	***135***	***165***	***195***	***225***	***255***	***285***	***315***	***345***	***Total***
0.5	5.5	2.7	1.5	1.1	1.3	1.4	2.6	5.7	4.4	3.8	5.6	9.3	44.9
	7.0	*4.8*	*0.8*	*0.4*	*0.3*	*0.1*	*1.3*	*6.2*	*5.0*	*5.5*	*4.9*	*6.1*	*38.4*
1.5	3.0	1.6	1.0	0.5	0.5	0.7	2.6	8.1	4.2	3.3	4.8	7.4	37.7
	3.2	*1.9*	*0.6*	*0.1*	*0.2*	*0.3*	*1.1*	*10.4*	*5.0*	*4.1*	*6.0*	*7.5*	*36.0*
2.5	0.4	0.2	0.1	0	0	0	0.6	4.5	2.0	1.5	1.7	1.9	12.9
	0.4	*0.1*	*0.1*	*0*	*0*	*0*	*0.2*	*3.9*	*1.8*	*1.4*	*2.0*	*1.7*	*11.3*
3.5	0	0	0	0	0	0	0	0.1	0.2	0.2	0.2	0.2	0.9
	0.1	*0*	*0*	*0*	*0*	*0*	*0*	*1.0*	*0.5*	*0.7*	*1.0*	*0.4*	*4.3*
4.5	0	0	0	0	0	0	0	0	0	0	0	0.1	0.1
	0	*0*	*0*	*0*	*0*	*0*	*0*	*0.1*	*0.1*	*0.3*	*0.8*	*0.1*	*1.6*
5.5	0	0	0	0	0	0	0	0	0	0	0	0	0
	0	*0*	*0*	*0*	*0*	*0*	*0*	*0*	*0*	*0.1*	*0.2*	*0*	*0.3*
Total	8.9	4.5	2.6	1.6	1.8	2.1	5.8	18.4	10.8	8.8	12.3	18.9	97
	10.7	*6.8*	*1.5*	*0.5*	*0.5*	*0.4*	*2.6*	*21.6*	*12.4*	*12.1*	*14.9*	*15.8*	*100*
	21.5						24.2		19.6		31.2		
	20.4						*24.2*		*24.5*		*30.7*		
	(Offshore directed)						(ZW)		(W)		(NW)		

Table 6-2 summarizes the main characteristics of the 10-month wave climate in relation to the long-term (1979-2001) observations. For calm and mean conditions ($H_{sig} < 3.5$m) the selected wave-climate is reasonably representative for the long-term conditions. The occurrence of storm conditions ($H_{sig} > 3.5$m) is overestimated for all directions. Due to their significant morphological impact this might lead to somewhat overestimated sediment transports on the ebb-tidal delta compared to the long-term average.

No wave measurements were available in the inlet domain for validation of the wave model. The SWAN wave model has been extensively verified worldwide (see e.g. Ris, 1999; Roelvink et al., 2001a, b; Lin et al., 2002; Rogers, 2003) and in the Dutch coastal area e.g. the Haringvliet, the Petten sea defences, the Friesche Zeegat and recently the Flyland studies. These studies have proven the SWAN model's capability of reproducing wave-heights and period distributions satisfactorily, even in the complex areas such as inlet systems.

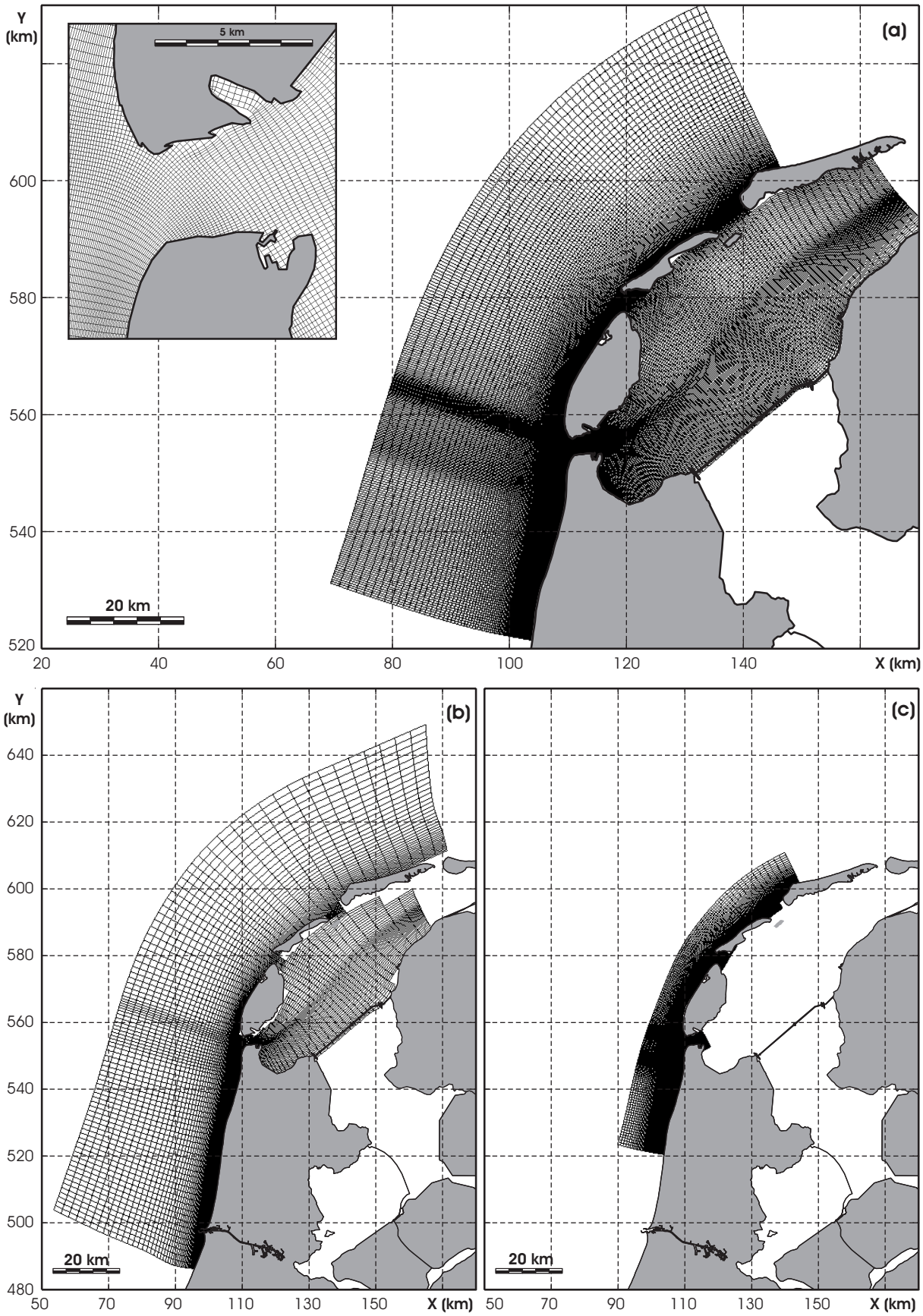

Figure 6-2: Delft3D model grids for (a) flow (the insert shows details of the grid resolution at the Texel inlet gorge), (b) large-scale wave grid and (c) detailed wave grid.

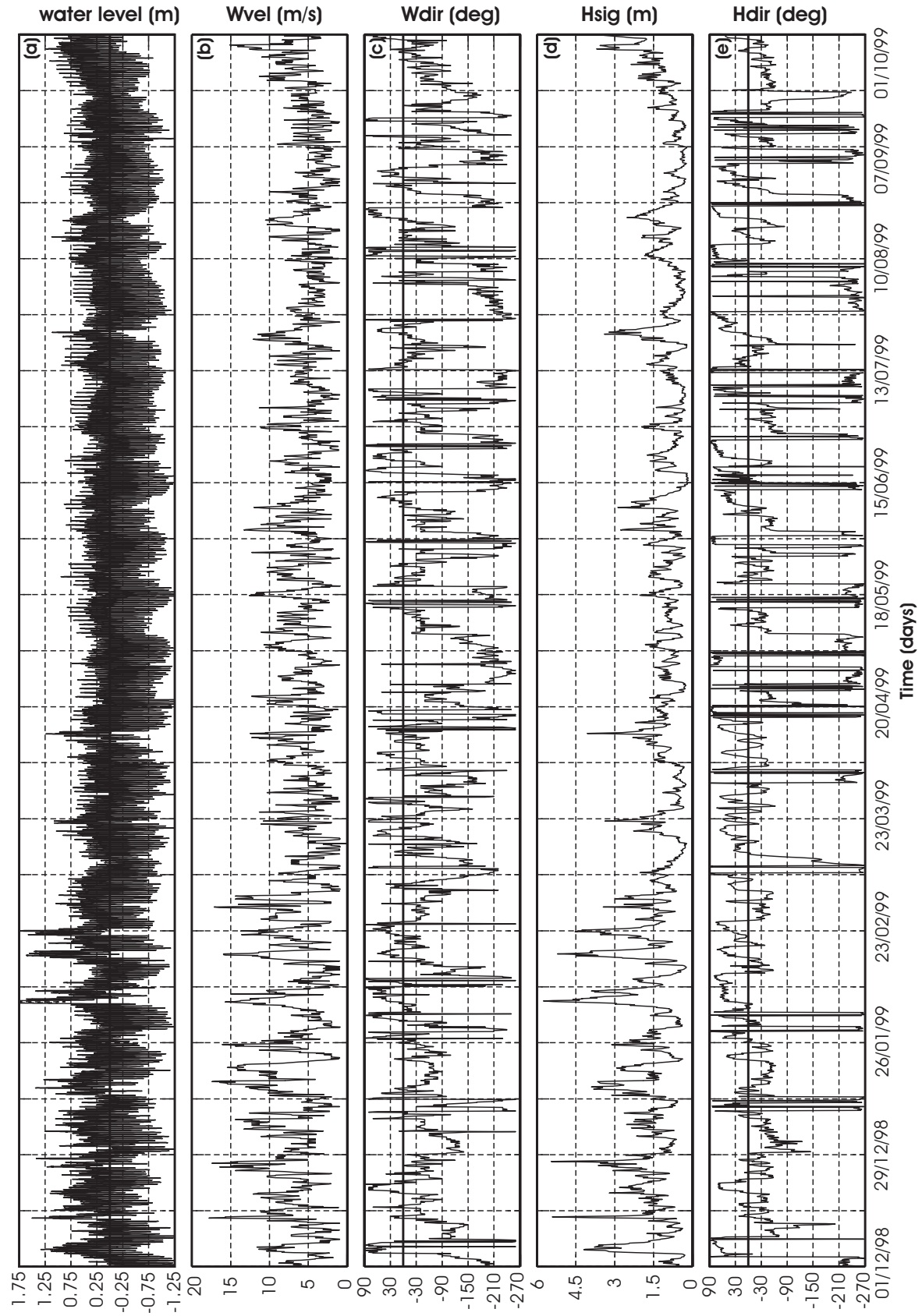

Figure 6-3: Forcing time-series measured over the period 01-12-1998/01-10-999 for: (a) water levels Den Helder tidal station, (b and c) wind velocities and directions station De Kooy Den Helder, (d and e) significant wave heights and directions station Eierlandse Gat.

Bed schematization

The bed morphology of the nearshore, inlets and basin is based on the 1997 bathymetric measurements (De Kruif, 2001). In the inlet gorge and near-field bed-levels are updated using 2001, 2002 and 2003 observations to obtain a bottom schematization as accurate as possible. Depths in the deeper region are based on Dutch Continental Shelf data supplied by TNO-NITG (Frantsen, 2001). Depending on the resolution of available observations, depth measurements were triangularly interpolated or grid-cell averaged to the curvilinear grid. The initial bathymetry was smoothened to reduce the small-scale disturbances (~ 0-0.1m) in the bathymetry. In this manner unrealistically high sediment transports due to the 'noise' in the bathymetry are prevented.

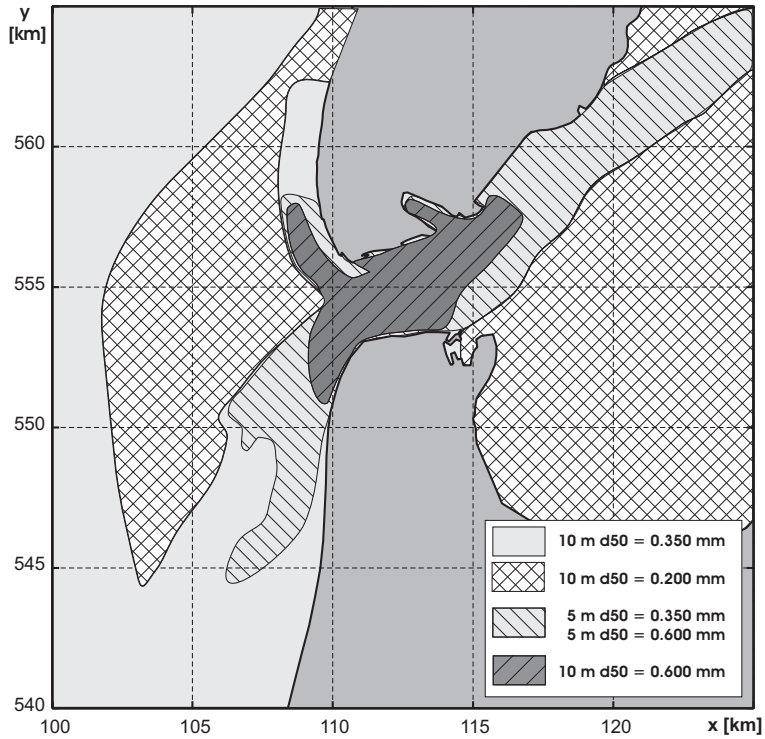

Figure 6-4: Initial sediment distribution of Texel Inlet.

An important aspect concerns the presence of erosion-resistant layers and spatially varying grain diameters over the ebb-tidal delta domain (see section 5.2.2 Fig. 5-2). In general smaller grain diameters are observed on the shoal areas and larger grain sizes in the channels. To account for this variability a 10 m thick sediment layer was applied with multiple sediment fractions[3] (Fig. 6-4). The ebb delta shoals Noorderhaaks and Zuiderhaaks, and the basin (with the exception of the main channels) are prescribed by a d_{50} of

[3] In this respect the *TOD*-model schematization differs from the model used in Chapter 4 that was based on a single grain diameter of 250 μm. Although multiple fractions are used these are still uniformly distributed in the sediment layer. The latest versions of Delft3D allow for the detailed vertical specification of bed characteristics in the form of multiple layers, layer thickness and distribution of the sediment fractions per layer. This interesting development might enable the (schematized) modelling over longer time spans (centuries) taking into account e.g. Holocene and Pleistocene deposits.

200 μm. In the main channels, below the 10 m depth contour, d_{50} sediment diameters are prescribed by 350 or 600 μm. The inlet channel Marsdiep is set to 600 μm to account for the additional presence of non-erodible layers, and to prevent excessive erosion of the channel floor. Outside the ebb-tidal delta domain, grain diameter of the adjacent coastal sections was set to the higher-than-measured value of 350 μm. Coarser sediments are more difficult to displace reducing the morphological changes outside the area of interest where grid resolution is coarse. No sediment influx was specified at the open-sea boundaries, but equilibrium sediment concentrations were assumed to exist (solved automatically by the model).

Based on experience from previous modeling studies the bottom roughness is here prescribed by a constant Chézy coefficient of 61 $m^{1/2}/s$ (derived from the hydrodynamic calibration of tidal velocities). Note that from a hydrodynamic viewpoint similar results (water levels, velocities) can be obtained by using Chézy or Manning. However, for morphodynamics Chézy was preferred over the Manning coefficient as for depth-averaged flow the shear-stress at the bed is given by a quadratic friction law of the form:

$$\vec{\tau}_b = \frac{\rho_0 g \vec{U} \left|\vec{U}\right|}{C_{2D}^2} \tag{6.3}$$

where $\left|\vec{U}\right|$ is the depth-averaged velocity magnitude (m/s) and C_{2D} the 2D Chézy coefficient which can be a constant coefficient or can be derived from the Manning's formulation:

$$C_{2D} = \frac{\sqrt[6]{H}}{n} \tag{6.4}$$

where H is the total water depth (m) and n is the manning coefficient ($m^{1/3}/s$). Assuming a typical channel cross-section with a deep channel and shallow flanks, and a cross-sectional averaged equal bed shear stress for both the Manning as the Chézy formulation, then in case of Manning the shear stress in the channel is smaller and on the shoal larger then the Chézy formulation. Experience from previous model studies has shown that this can lead to exaggerated scour of the channels.

In total a 10-month period was simulated in monthly intervals; each month the simulation was started from the initial bathymetry to enable comparison between rough and calm conditions. The time step for the flow computations is 60 seconds to fulfill the maximum courant number criterion of 15. Settings of 1.0 m^2/s and 1.0 m^2/s for the uniform horizontal eddy viscosity and eddy diffusivity coefficients have been applied respectively. Default settings for the calculation of sediment transports and morphological change are used (Van Rijn 1993 transport option). Sediment transport computations are initiated after a 1440 minutes spin-up time. A morphological scale factor of 1 is applied (no morphological acceleration, see Lesser *et al.*, 2004). Computations start from a uniform water level. A two-day spin-up prior to the actual computations is sufficient to dissipate the errors induced by the discrepancy between boundary conditions and initial state. Table 6-3 summarizes the main parameter settings.

Table 6-3: Summary of the main model parameter settings

Module	*Parameter*	*Value*	*Description*
Flow	Δt	60	flow time step (s)
	ρ	1023	water density (kg/m^2)
	K	1	horizontal eddy viscosity (m^2/s)
	N	1	horizontal eddy diffusitivity(m^2/s)
	C	61	Chézy coefficient (m$^{1/2}$/s)
	Dryflc	0.1	threshold depth (m)
	Rouwav	FR84	stress formulation due to wave forces (-)
	Cstbnd	true	boundary condition (-)
	Bndneu	true	Neumann boundary condition (-)
Wave	spectrum	JONSWAP	shape of wave spectrum (-)
	gamma1	3.3	peak enhancement factor JOHNSWAP spectrum (-)
	setup	false	wave-related water level setup (-)
	forcing	wave energy dissipation rate	computation of wave forces (-)
	generation mode	3-rd	generation mode for physics (-)
	breaking	B&J model	depth-induced breaking model (-)
	alfa1	1	coefficient for wave energy dissipation in the B&J model (-)
	gamma2	0.73	breaker parameter in the B&J model (-)
	triads (LTA)	true	non-linear triad wave-wave interactions (-)
	alfa2	0.1	coefficient for LTA (-)
	beta	2.2	coefficient for LTA (-)
	bottom friction	JONSWAP	bottom friction formulation (-)
	coeff	0.067	coefficient for bottom friction (-)
	diffraction	false	(-)
	wind growth	true	formulation for exponential wave growth (-)
	white capping	true	formulation for white capping (-)
	quadruplets	true	quadruplet wave-wave interactions (-)
	ref	true	refraction is activated for waves propagation in spectral space
	freq	true	frequency shift is activated for wave propagation in spectral space (-)
Transport	MORFAC	1	morphological scale factor (-)
	THRESH	0.2	threshold sediment thickness (m)
	EQMBC	true	equilibrium sediment concentration profile at open boundary
	DENSIN	true	include effect of sediment on water density (-)
	AKSFAC	1	Van Rijn's reference height factor
	RWAVE	2	estimated ripple height factor (-)
	ROUSE	false	set equilibrium sediment concentrations to Rouse profiles (-)
	ALFABS	1	longitudinal bed gradient factor for bed load transport (-)
	ALFABN	15	transverse bed gradient factor for bed load transport (-)
	SUS	1	current-related reference concentration factor(-)
	BED	1	current-related transport vector magnitude factor (-)
	SUSW	0.5	wave-related suspended sediment transport factor (-)
	BEDW	0.5	wave-related bed-load sediment transport factor (-)
	SEDTHR	0.5	threshold depth for sediment computations (m)
	FWFAC	0.1	tuning parameter for wave streaming (-)
	RHOSOL	2650	density sediment (kg/m^2)
	RHODRY	1600	dry bed density (kg/m^2)
	d50	200 / 350 / 600	median grain diameter sand (μm)

6.2.4 Model Limitations

Depth-averaged flow

Computational time restrictions do not allow for the full three-dimensional simulation of the elaborate model domain over sufficiently long periods. It was assumed that on ebb-tidal delta scale the large-scale horizontal circulation patterns dominate the morphological developments, and 3D effects are only of minor importance to these circulations. Local model results are therefore less accurate in areas where 3D currents are important, e.g. shallow shoal areas or swash platforms where wave-induced mass flux and undertow are dominant transport mechanisms. Furthermore, sediment import (or export) due to density-stratification induced secondary circulations is not accounted for. The importance of density stratification (during a tidal cycle) is investigated in Elias and De Ronde (2006); Chapter 7 of this thesis. It is shown that density stratification has a pronounced effect on the flow and sediment transports in the inlet gorge and proximal ebb-channels during periods of extreme fresh-water discharge.

Nevertheless, by focusing the analysis of the model results on transect-integrated transports and relative differences between varying simulations rather then focusing on 'grain diameter level' valuable insights in the present ebb-tidal delta behavior and the underlying processes and mechanisms for the observed development can be obtained.

Bathymetric schematization

One of the main problems in quasi real-time simulations is how to deal with the initial mismatch between the bathymetric schematization and the boundary forcing. Part of this discrepancy is 'natural'; by definition equilibrium between morphodynamics and hydrodynamics fails to exist due to the phase-lag in morphological and hydrodynamic adaptation times to the dynamic forcing conditions. Part of this mismatch is artificial, related to the imposed initial bathymetric model schematization; the model is forced by detailed sets of forcing conditions for a specific time frame (1-12-1998/1-10-1999), whereas the ebb-tidal delta bathymetry is based on 1997 to 2003 observations. Therefore the modeled sediment transports will partly be related to the 'natural' discrepancy of dynamic flow and lagging bed updating, and partly to the 'forced' discrepancy resulting from the bathymetric schematization. A third factor is the initial removal (hence larger sediment transport rates) of irregularities from the bed by the model.

In long-term morphodynamic simulations part of these discrepancies would be resolved in the calibration phase, and the model would be calibrated until the model results and measurements provide an acceptable match in sedimentation-erosion patterns or sediment transport rates. The short-term quasi real-time simulations do not allow such extensive validation and calibration. It is therefore difficult to separate the 'natural' and 'forced' sediment transports. Starting from well-constructed an initially smoothed bed,, and allowing a significant spin-up interval before morphological updating minimized errors.

Ideally modeled sediment transports would be validated against field measurements, but such measurements are not (yet) present for Texel Inlet. The ongoing NIOZ-ferry measurements might provide an impression of the transport of suspended matter through Marsdiep in the near future; such datasets would provide an indispensable tool for model validation.

For now the morphological behavior of the model is therefore evaluated qualitative rather then quantitatively, focusing on the representation of the gross characteristics of observed sediment transport and morphological change as presented in Chapter 5.

6.2.5 Model calibration and validation

Model calibration and validation are closely related important aspects of the numerical modeling process. In this study model calibration focuses on the correct representation of the (tidal) water levels and flow in the Marsdiep inlet. The focus is on tides as these are considered to be the main forcing mechanism (Bonekamp *et al.*, 2002; Elias *et al.*, 2005) and detailed observations are present. Due to the absence of wave measurements at the Texel ebb-tidal delta no validation on waves could be performed. The calibrated model results are evaluated on the representation of the main characteristics of the observed inlet behavior (bathymetric changes) as described in Chapter 5.

Water levels

The simulated water levels for the tidal stations Texel Noordzee, Den Helder, Harlingen and Vlie Haven were harmonically analyzed in the same manner as the water-level observations. Comparing Table 6-4a and b shows a good general correspondence between the simulated and measured water level amplitudes and phases of the main tidal constituents. The tidal constituents have been selected on the importance for flow through the inlet (Ridderinkhof *et al.*, 2002).

In addition to the tidal constituents, to evaluate the correct reproduction of the non-tidal contributions to the water levels, modeled time series of the mean water levels for the Den Helder and Texel Noordzee tidal stations were compared to the observations. A good correspondence, Mean Absolute Error (MAE) below 0.02 m in Den Helder and 0.04 m at Texel Noordzee, was obtained. The MAE is defined as:

$$MAE = \left\langle \left| \frac{1}{N}\sum_{N=1}^{N} |y_n| - \frac{1}{N}\sum_{N=1}^{N} |x_n| \right| \right\rangle \tag{6.5}$$

where X and Y are the observed and predicted values of $n = 1..N$ values (Sutherland *et al.*, 2004).

Table 6-4a: Observed Amplitudes (A) and phases (φ) of water levels stations Texel Noordzee, Den Helder, Harlingen and Vlie Haven (period: 01-01-1999 / 01-10-1999).

	Stations							
	Texel Noordzee)		***Den Helder***		***Harlingen***		***Vlie Haven***	
Components	***A (m)***	***φ (°)***	***A (m)***	***φ (°)***	***A (m)***	***φ (°)***	***A (m)***	***φ (°)***
M2	0.79	-6	0.67	-8	0.85	80	0.82	40
O1	0.09	-5	0.09	1	0.09	35	0.08	14
K1	0.07	-1	0.06	9	0.07	41	0.06	16
2N2	0.01	112	0.01	92	0.02	-174	0.02	147
mu2	0.08	-124	0.08	-120	0.12	-37	0.09	-73
N2	0.13	-92	0.10	-95	0.14	-4	0.13	-46
nu2	0.04	172	0.04	170	0.06	-109	0.05	-137
L2	0.06	-112	0.06	-113	0.08	-24	0.07	-61
S2	0.22	-103	0.18	-101	0.21	-8	0.21	-56
K2	0.05	74	0.04	77	0.04	168	0.05	122
M4	0.10	-159	0.11	-178	0.12	58	0.04	-82
MS4	0.06	107	0.07	87	0.06	-25	0.03	-177
2MN6	0.05	14	0.03	16	0.02	107	0.03	81
M6	0.09	109	0.06	110	0.04	-16	0.05	176
2MS6	0.08	7	0.06	5	0.04	-111	0.05	75

Table 6-4b: Modeled Amplitudes (A) and phases (φ) of water levels stations Texel Noordzee, Den Helder, Harlingen and Vlie Haven (period: 01-01-1999 / 01-10-1999).

	Stations							
	Texel Noordzee)		***Den Helder***		***Harlingen***		***Vlie Haven***	
Components	***A (m)***	***φ (°)***	***A (m)***	***φ (°)***	***A (m)***	***φ (°)***	***A (m)***	***φ (°)***
M2	0.79	-6	0.70	-6	0.74	88	0.80	39
O1	0.09	-5	0.09	2	0.08	43	0.08	18
K1	0.07	-1	0.07	9	0.06	50	0.06	22
2N2	0.02	110	0.02	100	0.02	-172	0.02	150
mu2	0.08	-123	0.08	-117	0.10	-19	0.08	-69
N2	0.13	-92	0.11	-92	0.11	3	0.13	-47
nu2	0.04	171	0.04	172	0.05	-97	0.05	-140
L2	0.06	-112	0.06	-110	0.07	-11	0.07	-61
S2	0.22	-103	0.18	-100	0.18	0	0.20	-56
K2	0.05	74	0.04	77	0.03	163	0.05	120
M4	0.10	-160	0.11	179	0.10	95	0.07	-91
MS4	0.06	107	0.06	83	0.06	12	0.04	176
2MN6	0.05	8	0.01	26	0.01	-144	0.04	61
M6	0.09	104	0.02	153	0.01	-61	0.09	151
2MS6	0.08	2	0.01	51	0.01	-169	0.08	51

Tidal flow

On the ebb-tidal delta long-term time-series of flow suitable for model validation are absent. The validation therefore focuses on the inlet gorge, where preliminary results of the ongoing NIOZ-ferry observations have been made available by NIOZ for analysis (also see Bonekamp *et al.*, 2002; Ridderinkhof *et al.*, 2002). Flow data for the year 1999 have been used to calculate the amplitudes and phases of the main tidal constituents of depth-averaged flow at eighteen equidistantly distributed aggregation points in Marsdiep. For each aggregation point the model results were harmonically analyzed in a similar manner as the observations.

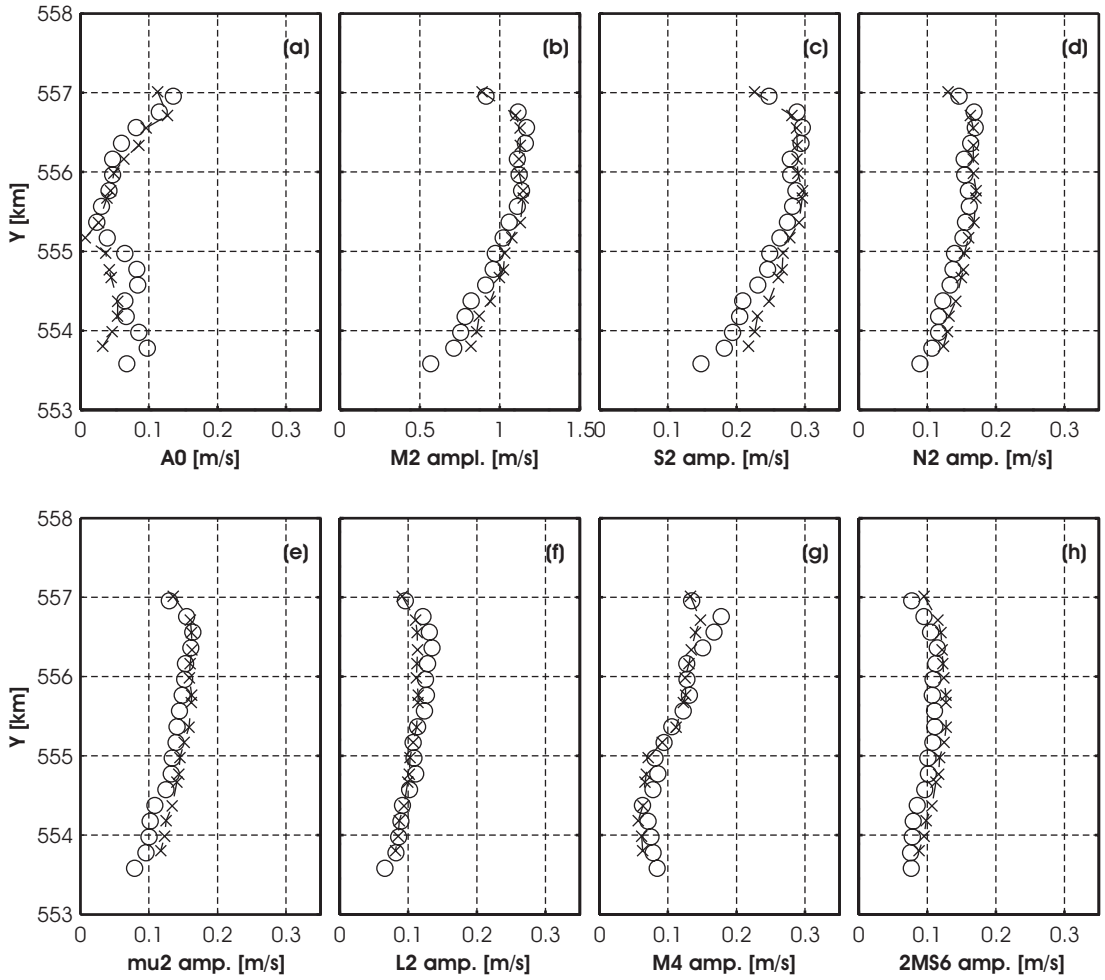

Figure 6-5: Comparison of observed (dots) and modeled (x) velocity amplitudes of the main constituents in Marsdiep: (a) A_0, (b) M_2, (c) S_2, (d) N_2, (e) mu_2, (f) L_2, (g) M_4, (h) $2MS_6$.

Table 6-5: Modeled and observed amplitudes of volume transport for the 7 main constituents

Tidal Component	**Modeled (m^3/s)**	**NIOZ-ferry observations (m^3/s)**		
		1998 - 2000	**1999**	**2000**
M2	67557	68564	68908	67278
S2	18089	17837	16661	17687
N2	10350	10580	10490	10239
mu2	9673	9367	9218	8784
L2	7297	7205	7380	6849
M4	6623	7410	7121	7672
2MS6	7523	6534	6641	6463

Figure 6-5 and Table 6-5 show the in general good correspondence between modeled and observed amplitudes of the seven main contributors to the flow and discharge in the Marsdiep channel (see Ridderinkhof *et. al.* 2002 for details on the NIOZ-ferry measurements).

In the inlet gorge, where the cross-sectional area is minimal, residual velocities are strong being in the order of 0.2 m/s whereas the maximum instantaneous flow velocities are in the order of 2.0 m/s (Fig. 6-12). Comparison of Figure 6-12 and Chapter 5 Figure 5-6 shows that the qualitative features of the simulated flow in the inlet gorge represent the observations reasonably well. The internal dominance of larger ebb flow along the North-Holland coastline and a smaller flood flow along the Texel coastline and landward margin of Noorderhaaks is adequately reproduced, although the modeled residual discharge of 95 Mm^3/tide underestimates the observed long-term value of 115 Mm^3/tide by 20 %. Notice that the residual discharge is minor compared to the gross water motion in the inlet. In correspondence with the Rijkswaterstaat flow measurements (Blok and Mol, 2001) the major part of the simulated flow is directed from Marsdiep to Breewijd with only a minor contribution of flow through Molengat. In Molengat the observed segregation in ebb-dominant velocities along the Noorderlijke Uitlopers of Noorderhaaks and flood-dominant velocities along the Texel coast is reproduced. From Breewijd the major component of flow (~ 75%) is directed via Schulpengat and Nieuwe Westgat onto the Zuiderhaaks. Nieuwe Schulpengat transports a minor part (~ 25%) of the total residual flow (see the model results section 6.3.2 for detailed descriptions of the flow patterns).

Sediment transports and bathymetric change

Lack of suitable field data on sediment transport rates does not allow for a quantitative analysis of the modeled sediment transports (Fig. 6-6). The ongoing NIOZ-ferry measurements might provide an impression of the transport of suspended matter through Marsdiep in the near future; such datasets would provide an indispensable tool for model validation. For now the morphological behavior of the model is evaluated qualitatively by comparison of the year-averaged sediment transport rates in selected transects with the estimated transport paths and directions as presented in the conceptual descriptions of Chapter 5.

Based on the analysis of observations (Chapter 5.4) the main characteristics of the morphological behavior of the ebb-tidal delta can be summarized as:

- A net sediment import into the basin ranging between 5 to 6 Mm^3/year.
- A net influx of sediment along the North-Holland coast into Marsdiep towards Texelstroom.
- Local interaction between Bollen van Kijkduin, Nieuwe Schulpengat and Franse Bankje determining the erosion-sedimentation in this part of the ebb-tidal delta and coast. The distal part of Nieuwe Schulpengat is ebb-dominant.
- Erosion of Schulpengat and southwestward outbuilding of Zuiderhaaks
- Sedimentation along the northern and southern margin of the supra-tidal Noorderhaaks shoal.
- Landward and northward migration of Noorderlijke Uitlopers of Noorderhaaks (and Molengat).
- Flood dominant transports in Molengat along the Texel coast into Marsdiep, and ebb-dominant transport along the landward margin of Noorderlijke Uitlopers of Noorderhaaks.

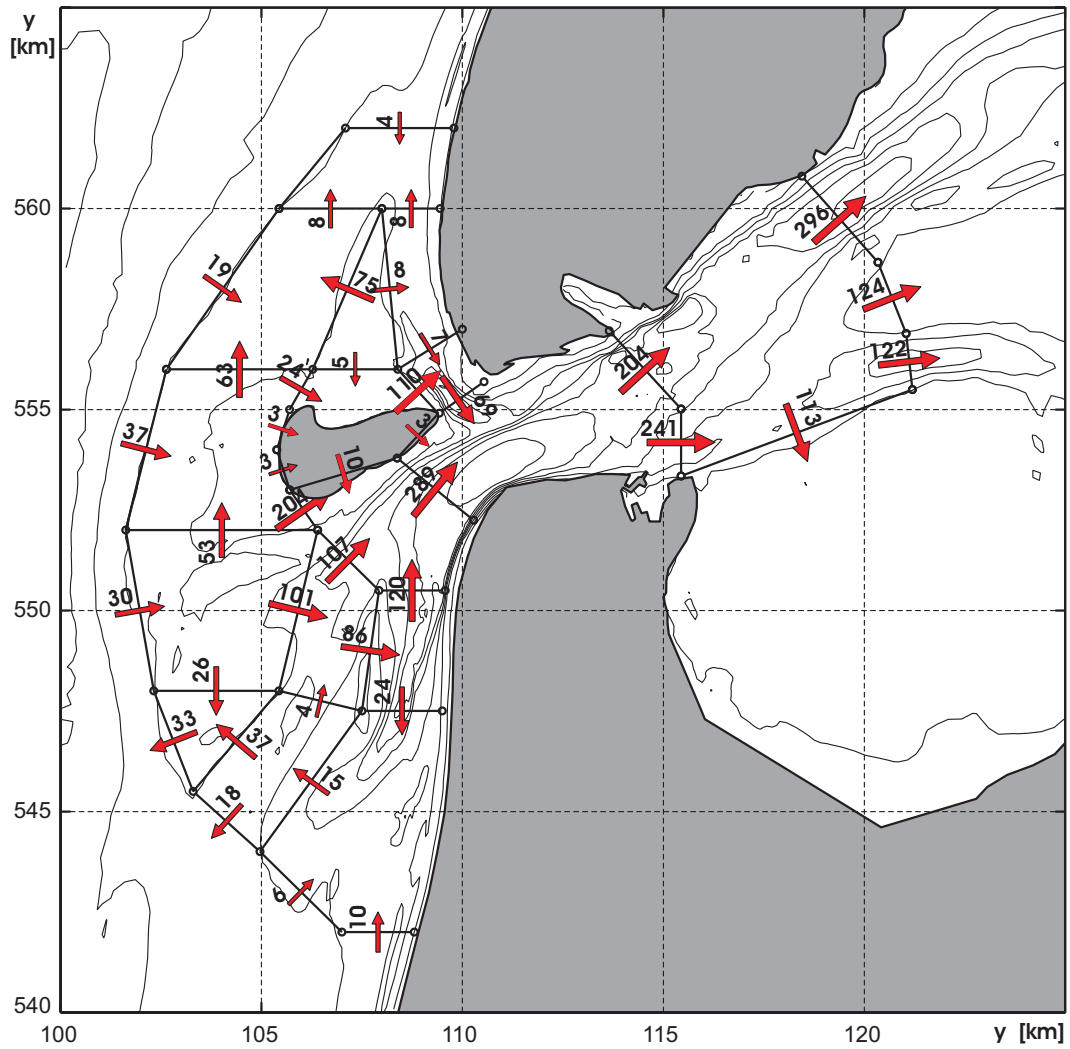

Figure 6-6: Residual sediment transport vectors (in 0.01 Mm^3/year) through a number of selected transects.

The residual transport rates and volume changes plotted in Figure 6-6 and 6-7 summarize the main trends in morphological model behavior. Residual transport vectors are determined in 89 representative cross-sections by weighted summation of the monthly results (for clarity in Figure 6-6 the number of plotted cross-sections was reduced, in the detailed model results section 6.3.3. all vectors are shown).

In general the ebb-tidal delta development shows similar characteristics to the observations (Fig. 6-7). Erosion prevails in the distal part of the ebb-channels, and on the western margin of Noorderhaaks, although the modeled erosion is concentrated more on the upper part of the swash-platform. The sedimentation on the northward side of Noorderhaaks and the southern part of Zuiderhaaks indicates that the ebb-tidal delta is pushed shoreward and extends in alongshore direction.

The main tidal channels (Schulpengat and Nieuwe Schulpengat) increase in depth. Alternating patterns of sedimentation and erosion at the Bollen van Kijkduin and Franse Bankje are observed which point to the southward outbuilding of Bollen van Kijkduin and the interaction with Nieuwe Schulpengat and Franse Bankje.

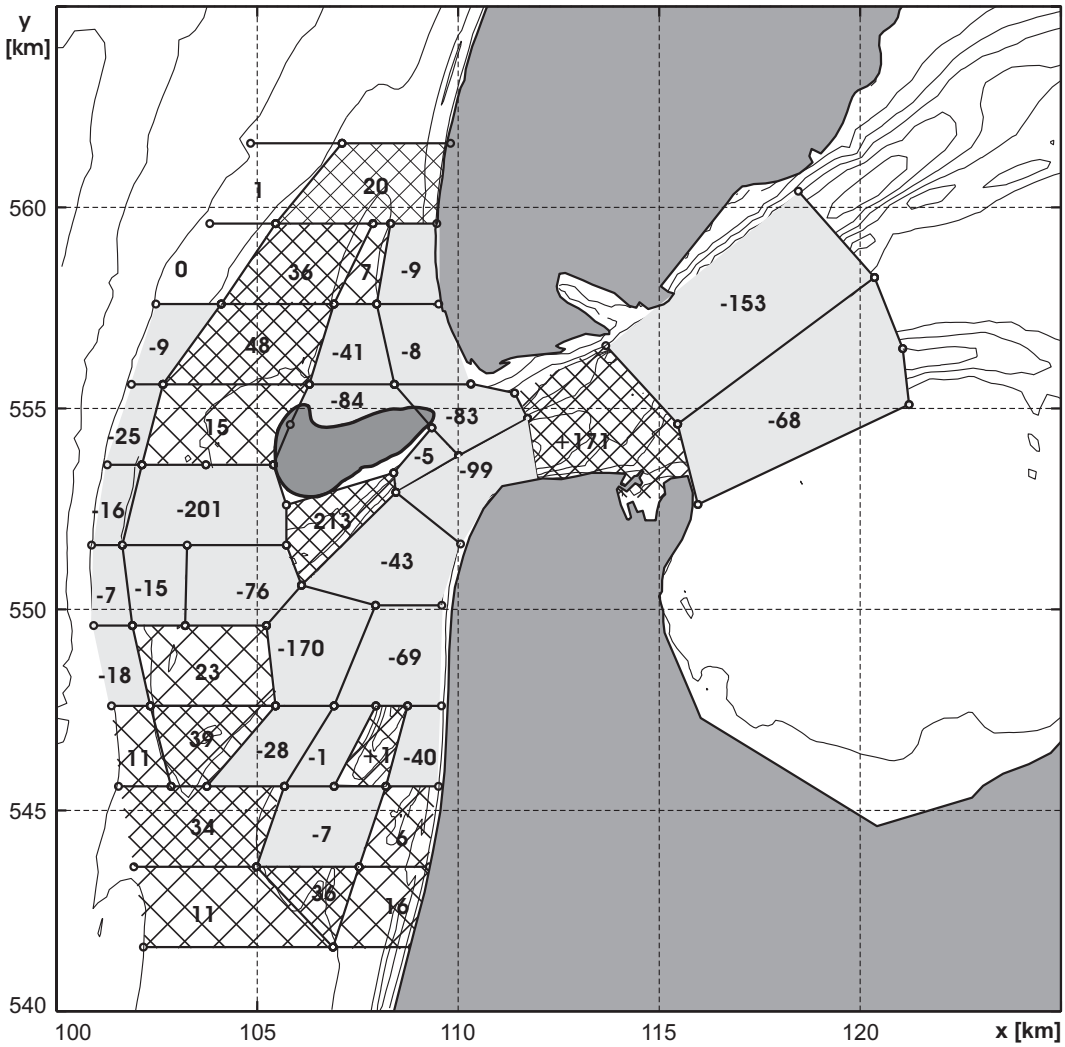

Figure 6-7: Residual sediment volume change (in 0.01 Mm^3/year) based on the in and out flux of sediment for selected cells (- is erosion and + sedimentation).

Differences are observed in the Molengat - Noorderlijke Uitlopers of Noorderhaaks area. The observed northward spit growth is modeled, however the landward displacement of the distal part of Noorderlijke Uitlopers and Molengat is not reproduced.

Comparing the sediment budgets of the gross features, then we observe that the modeled erosion of the western margin of 58 Mm^3 corresponds reasonably well to the observations (56 Mm^3, see domain A in Fig. 5-13). The 20 Mm^3 accretions on and around Noorderhaaks (domain B) exceed the 10 Mm^3 observation, while erosion of the southern part of the ebb-tidal delta is over predicted (30 Mm^3 compared to 26 Mm^3). This discrepancy mainly arises through overestimated sedimentation on Zuiderhaaks and Franse Bankje. In the Molengat system (domain C) the modeled erosion (-5.0 Mm^3) exceeds the measured value of -2.4 Mm^3. Despite overestimated transports on the ebb-tidal delta, the sediment import into Marsdiep of 4.5 Mm^3/year is somewhat smaller then the observed value of 5-6 Mm^3/year. This discrepancy might be related to neglecting salinity-stratification, or due to the short-term forcing conditions wherein northwestern storm events were over-represented.

In respect to the gross characteristics of the ebb-delta behavior it is concluded that the modeled patterns correspond reasonably well to the observations. Sediment redistribution of the western margin landward, erosion of the proximal main channels and sediment import into the basin is reproduced. Main differences are present in the more landward location (above the 10 m depth contour) of the erosion area on the western margin of Noorderhaaks, and the interaction of the Molengat and Noorderlijke Uitlopers of Noorderhaaks where the landward displacement is not reproduced. Plausibly these discrepancies arise from the 2DH assumption, wherein typical wave-induced phenomena such as Stokes drift and mass flux are not (fully) represented, therefore the developments in the wave-dominated areas are less accurately reproduced. Due to the absence of wave-data on the ebb-tidal delta no specific validation and calibration could be performed, this aspect needs further investigation in future studies.

Due to this rather limited validation on modeled sediment transports rates the results are used qualitatively rather then quantitatively. Observations provide quantitative transport rates and magnitudes while the model results provide qualitative descriptions of the relative importance of the underlying processes and transport paths. Integration of the model results and observations is presented in the synthesis and discussion (section 6.4).

6.3 Model Results and Discussion

6.3.1 Introduction

Four different experiments each consisting of 10 individual simulations have resulted in over 200 gigabytes of available model data. To obtain a manageable set of result files for each individual simulation month-averaged transport magnitudes and vectors were determined in predefined cross-sections. In addition, weighted averaging of the monthly results is used to estimate the year-averaged flow and transport maps. The month- and year-averaged values form the basis of the model results section. In order to correctly interpret the averaged results where relevant snap-shots or time-series of the transport or flow fields are presented in detail.

The first part of this Chapter presents modeled tidal flow patterns in order to understand the tidal rectification by interaction of the alongshore, northward propagating open-sea tidal wave with the cross-shore inlet currents and compound ebb-tidal delta bathymetry. Interaction of tides with ebb-tidal structures and currents is known to result in compound flow patterns with local circulation cells and complex morphodynamic behavior. In the next section we focus on the morphodynamics by analysis of sediment transport patterns, month- and year-averaged transport magnitudes and governing mechanisms. First, patterns are discussed on ebb-tidal delta scale, and secondly local sediment transport patterns and underlying mechanisms are presented in more detail for (1) Molengat and Noorderlijke Uitlopers of Noorderhaaks, (2) Noorderhaaks and (3) Nieuwe Schulpengat and Schulpengat.

Where relevant interpretations of the model results are given in association with the descriptions.

6.3.2 Flow patterns and residual flow

Tidal flow patterns on the ebb-tidal delta are particularly complex due to interaction of the alongshore propagating open-sea tide, the complex ebb-tidal delta bathymetry and the across inlet currents. A representative tide, wherein the tidal range approximately equals mean conditions, was selected to obtain insight in the tidal distortion by the ebb-tidal delta (Fig. 6-8). Notice the phase difference between the horizontal and vertical tide in the time-series that illustrates the mixed standing-progressive tide in Marsdiep. Time-velocity asymmetry between the horizontal and vertical type is a typical phenomenon in inlet systems and (partly) explains the existence of separate ebb- and flood-dominated channels.

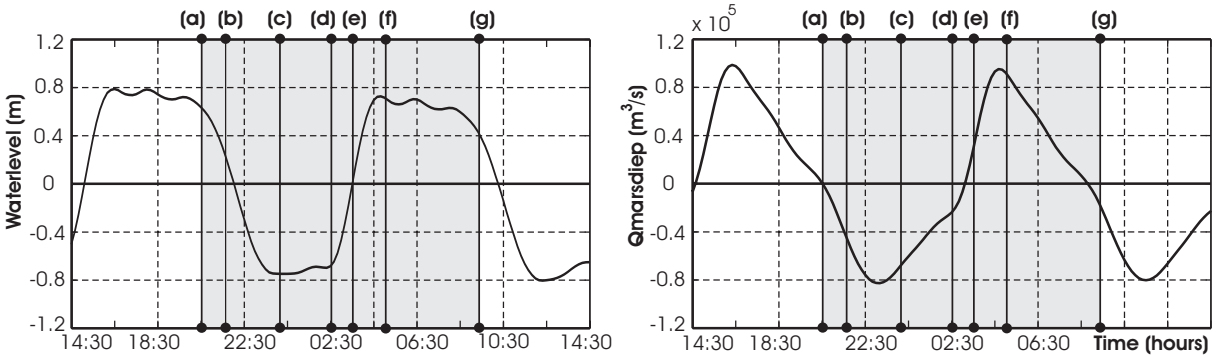

Figure 6-8: Selected representative tide (left water level and right discharges) for analysis of the mean tidal flow patterns (17-01-199 20:30/09:00), (a) to (g) indicate the time-points of the instantaneous snap-shots of flow shown in the subplots of Figures 6-9 and 6-10.

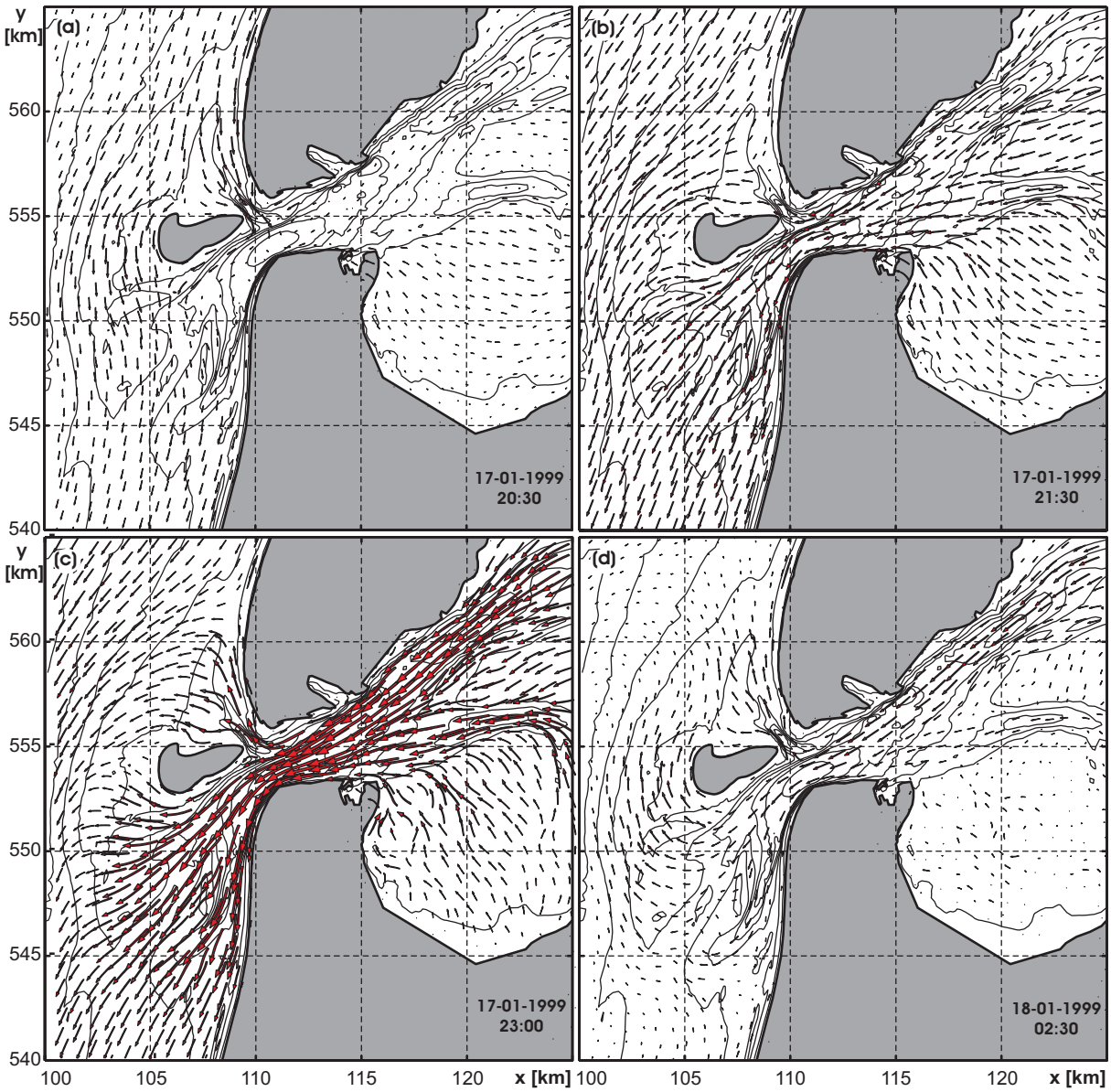

Figure 6-9: Tidal flow patterns during 4 stages of a selected tide; (a) 17-01-199 20:30, (b) 21:30, (c) 23:00, and (d) 18-01-1999 02:30.

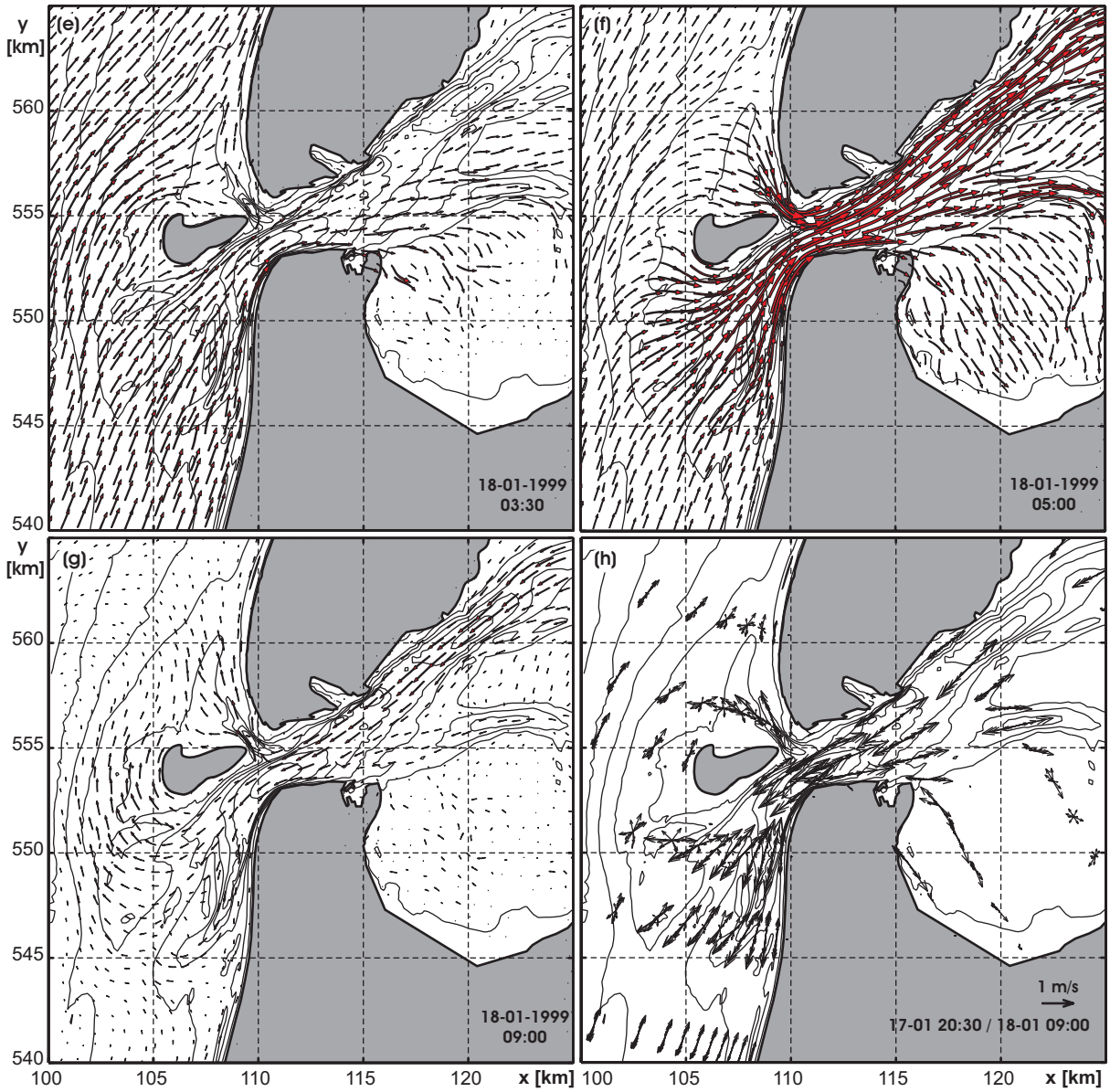

Figure 6-10: Tidal flow patterns during 3 stages of a selected tide; (e) 18-01-199 03:30, (f) 05:00, (g) 09:00, and (h) tidal roses over the period 17-01 20:30/18-01-1999 02:30 provide an indication of velocity magnitudes and eccentricity of the tide.

Figures 6-9 and 6-10 illustrate the flow patterns for the selected stages (a) to (g). A phase lag occurs between flow reversal in the basin and on the open-sea (Fig. 6-9a, 17-01 20:30). Already considerable southward flow velocities occur in the open-sea, on the ebb-tidal delta margin and in Molengat while velocities in Marsdiep are minimal. Initially, flood flow through Molengat is directed seawards along the southern margin of Noorderhaaks and onto the ebb-tidal delta. As a result a phase-lag exists between initiation of ebb in Marsdiep and in Molengat (Fig. 6-9b, 17-01 21:30).

During ebb, the majority of the flow is directed from Texelstroom into Marsdiep (Fig. 6-9bcd, 17-01 21:30-02:30). In the narrow constriction of the inlet gorge flow accelerates and maximum peak ebb velocities of 1.8m/s occur locally. The southwest directed ebb-jet is mainly directed into Breewijd (approximately 90% of the ebb discharge) and drives the

velocity field on the ebb-tidal delta. Ebb velocities in the main channels exceed 1 m/s and extend up to 10 km updrift (with respect to the direction of tidal wave propagation) of the inlet gorge. Along the North-Holland coast, in the narrow Nieuwe Schulpengat channel velocities accelerate due to contraction of flow and velocity magnitudes of 1.5 m/s are observed. Ebb velocities in Molengat are directed northward along the Noorderlijke Uitlopers of Noorderhaaks spit, curve seaward over the spit and are redirected southward around Noorderhaaks through interaction with the open-sea tide. Sheltered by the supra-tidal Noorderhaaks a low-velocity zone develops on the seaward margin of the ebb delta.

Flood enters the inlet from the south. ADCP observations (Blok and Mol, 2001) show that an approximate 0.5 to 1-hour phase lag in transition from flood to ebb flow between inlet and on the open sea occurs, and it takes approximately 1-hour between the beginning of the ebb-tide and complete current reversal in Marsdiep. When open-sea velocities are minimal, in the inlet gorge still relatively large seaward flow (up to 0.8 m/s) prevails, which curves westward and northward along the southern and western margins of Noorderhaaks (Fig. 6-9d, 18-01 02:30).

At peak flood (Fig. 6-10f, 18-01 05:00) flow is directed from South to North outside the ebb-tidal delta perimeter with velocities ranging between 0.5 and 0.7 m/s (depending on depth). Interaction of the tidal flow and ebb-tidal delta bathymetry results in accelerated and diverted flow velocities towards the inlet. Plausibly, the presence of the supra-tidal Noorderhaaks forming a sort of funnel-shape explains the flow acceleration on the ebb-tidal delta due to the decreasing cross-sectional channel area.

Acceleration of flow due to convergence of flow streamlines around the western tip of Helderse Zeewering locally increases the velocities to nearly 2.0 m/s. In Molengat flood flow is directed to the south and into Marsdiep, opposite to the open-sea tide. Similar to the southern part of the ebb-tidal delta flow accelerates due to the constricted area between Noorderhaaks and Texel coastline. From Marsdiep flow is directed into the main channels Texelstroom and Malzwin, and onto the flats. Segregation of flow in the basin and bottom friction reduces the flow velocities in Malzwin and on the flats effectively. In the deep nearly straight upper-part of Texelstroom velocities remain considerable and maximum velocities of nearly 1.5 m/s occur over a considerable distance.

The current roses of Figure 6-10h summarize the flow over the tidal cycle. The current roses are constructed by plotting the instantaneous velocity vectors in 60-minute intervals over the tidal cycle for a selected number of locations. Similarly to tidal ellipses, current roses visualize the eccentricity of the tidal flow, having the advantage that the individual contributions of the instantaneous velocity vectors to the residual field are still visible. The channels are dominated by large uni-directional flow velocities, while flow on the shoals, on both the downdrift as updrift side, is bi-directional due to interaction with the shallows shoal areas (also see Van Leeuwen *et al.* 2003). On the shallow Noorderhaaks shoals the currents have an anti-cyclonic rotational character. Sha (1989a) suggests that these circular tidal currents, downdrift of the inlet, result from the interaction between the shore-parallel tidal currents and the inlet currents. As a result there is a preferential sediment deposition on the downdrift side of the inlet and channel formation on the updrift side.

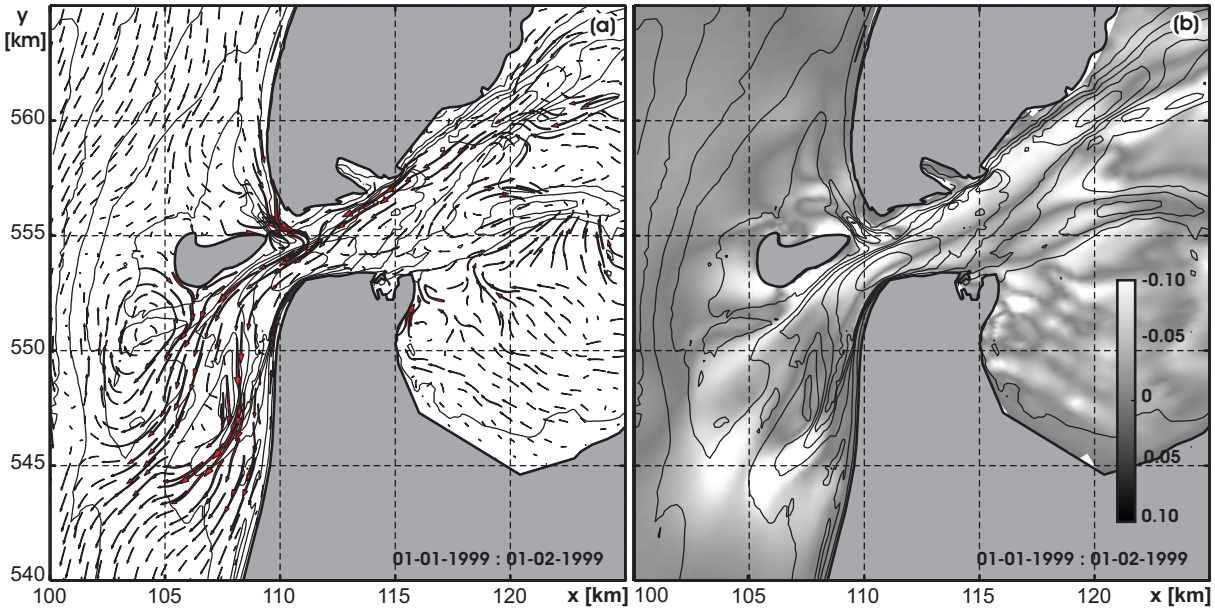

Figure 6-11: (a) Curved vector representation of the residual tidal flow patterns and (b) residual velocity magnitudes (m/s) based on a 1-month tidal simulation of January 1999 (negative values indicate ebb-dominance and positive values flood dominance).

The instantaneous flow velocities provide detailed overviews of the tidal flow patterns on the ebb-tidal delta. However, for long-term morphologic development not the gross water motions are important, but the residual flows and tidal asymmetries. The residual flow field (Figure 6-11) is obtained from averaging the (Eulerian) velocities over a 1-month period (01-01-1999/01-02-1999). As in this tidal simulation no M_0 component is specified in the open-sea boundary conditions, and no additional forcing mechanisms (such as wind or density differences) are included, the residual flow is locally generated. Ridderinkhof (1988a; 1988b) showed that the tidally driven residual current velocity field in the basin is dominated by isolated residual eddies, which are an order of magnitude larger than the residual velocities associated with the throughflow from Vlie to Texel Inlet. This throughflow results from the larger tidal amplitude in Vlie inlet. The residual eddies result from the pronounced variations in channel geometry and bottom bathymetry that increase the importance of the advective terms (Ridderinkhof, 1988a). On the ebb-tidal delta tidal residual eddies (headland eddies) are generated due to vorticity generation by the interaction of the tide with the sloping bottom near the coasts (Zimmerman, 1981). The classical transport patterns of counter rotating residual eddies with a central ebb-dominated main channel and marginal flood channels along the adjacent coastlines (e.g. Zimmerman, 1981; Oertel, 1988; Ridderinkhof, 1988a) are not clearly observed. This discrepancy is due to the presence of (the supra-tidal) Noorderhaaks shoal in front of Marsdiep that prohibits such eddies to form. Noorderhaaks is believed to play an important role in the present flow (and transport) patterns on the ebb-tidal delta as the shoal constrains the ebb and flood flow, and contributes to the southward deflection of the ebb flow thereby effectively separating the ebb-tidal delta in a northern and southern subdomain (Elias *et al.*, 2003b).

In the inlet gorge, where the cross-sectional area is minimal, residual velocities are strong being in the order of 0.2 m/s whereas the maximum instantaneous flow velocities are in

the order of 2.0 m/s (Fig. 6-11). Comparison of Figure 6-11 and Figure 5-6 show similar qualitative features of the simulated and observed flow in the inlet gorge. The internal dominance of larger ebb flows along the North-Holland coastline and smaller flood flow along the Texel coastline and landward margin of Noorderhaaks is adequately reproduced.

In correspondence with the Rijkswaterstaat flow measurements (Blok and Mol, 2001; see Chapter 5 section 5.3.2) the major part of the simulated flow is directed from Texelstroom, into Marsdiep and towards Breewijd with only a minor contribution of flow through Molengat (from hereafter the channels Breewijd, Marsdiep and proximal Texelstroom are defined as main inlet circulation). Flow through Schulpengat and Nieuwe Breewijd is directed onto Zuiderhaaks. Interaction of the southward ebb flow with the alongshore-northward flood flow diverts the ebb flow seaward and northward. On Zuiderhaaks (facing Nieuwe Westgat) a large tidal circulation cell develops; the clockwise rotation results from northward residual flow on the margin of the ebb-tidal delta that interacts with the southwestward ebb current. The combined contributions of the northward diversion of the ebb-flow and contraction of tidal flow around the ebb-tidal delta perimeter, results in relative large residual velocities on the western margin of the ebb delta. Downdrift of Noorderhaaks flow decelerates, and on the shoal area Noorderlijke Uitlopers of the Noorderhaaks and in the proximal part of Molengat the residual flow is directed towards the inlet (flood dominant). Flood dominant velocities are also observed along the adjacent coastlines of Texel and North-Holland.

6.3.3 Sediment transport patterns and magnitudes

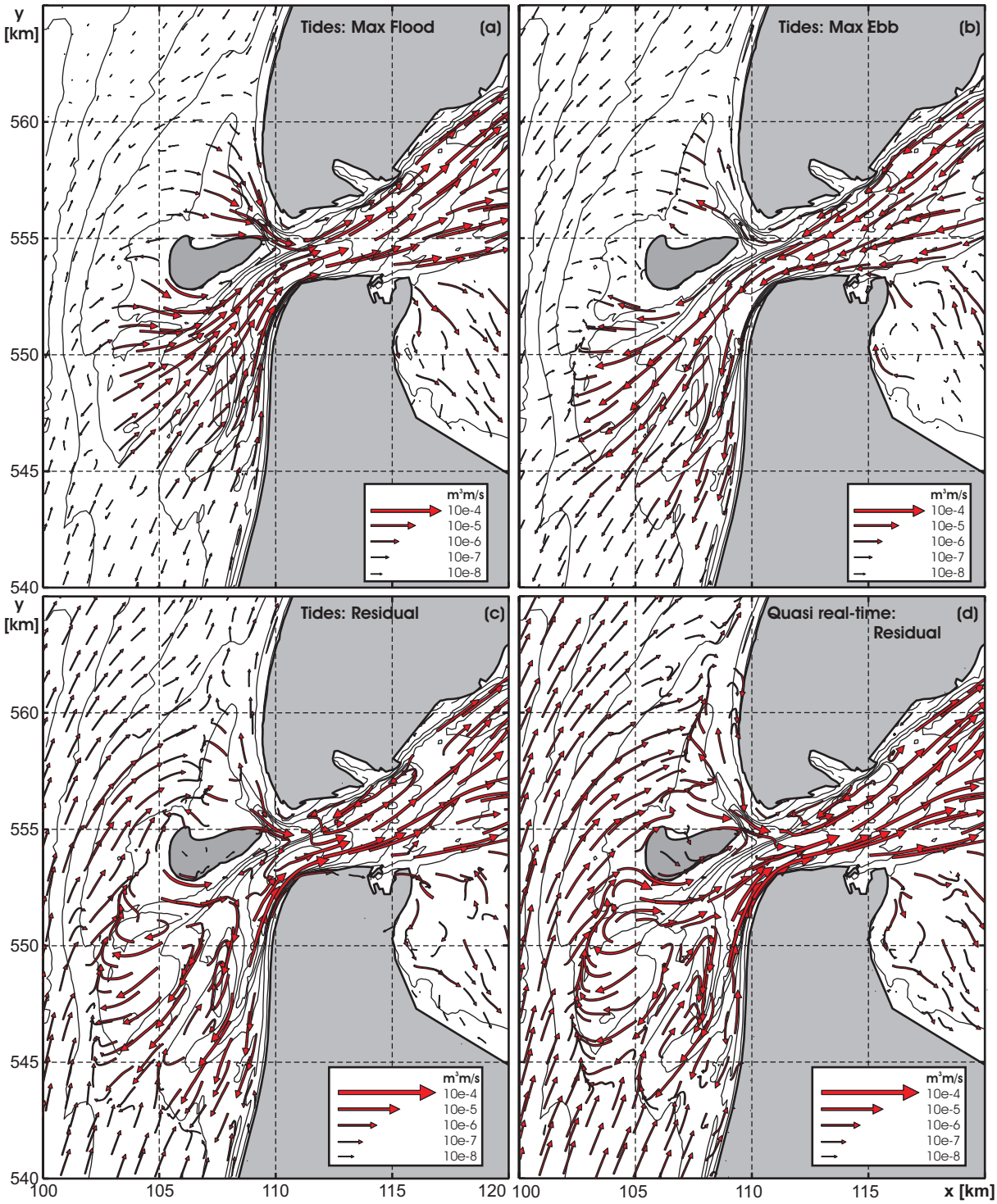

Figure 6-12 top: Tidal sediment transport patterns for (a) maximum flood (17-2-1999 23:00), (b) maximum ebb (17-2-1999 4:50). Bottom: tide-averaged sediment transport patterns for (c) tidal forcing [D] and (d) quasi real-time forcing [A].

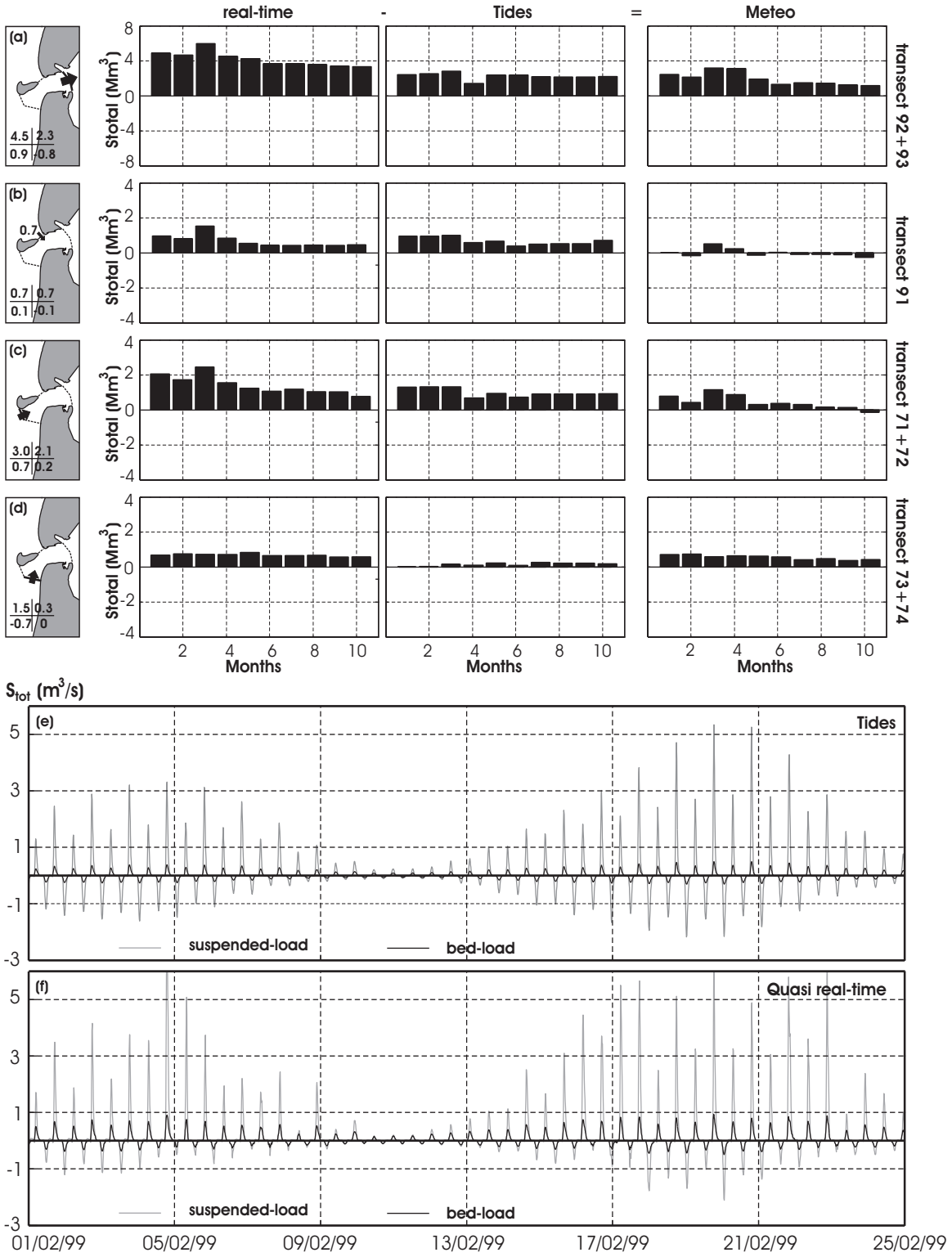

Figure 6-13: Transect-integrated and month-averaged transports for Marsdiep (a), Molengat, (b) Nieuwe Westgat (c), and Nieuwe Schulpengat and Schulpengat (d). Year-averaged values are presented as numbers in the inserts of (a-d), top values: Quasi real-time (l) and tidal (r) experiments, bottom values represent the contributions of waves (l) and wind (r). The bottom two panels illustrate time-series of instantaneous sediment transports integrated over the Marsdiep cross-section for the (e) tidal and (f) quasi real-time simulation.

Figures 6-12 and 6-13 provide impressions of the modeled sediment transport patterns on ebb-delta scale, transport magnitudes and the importance of the processes wind, waves, tides and setup. Outside the ebb-tidal delta domain (roughly bounded by the 15 m depth contour) instantaneous and residual sediment transport rates are small compared to the large transports in the inlet channels.

The qualitative correspondence in residual transport patterns between tidal and quasi real-time forcing in the southern part of the ebb-tidal delta (Fig. 6-12c and d respectively) illustrates that the interaction of the inlet currents with the compound ebb-tidal delta bathymetry forms the principal mechanism for sediment transports. Due to the non-linearity between flow and transport the major contribution to the residual transport pattern occurs around maximum ebb and flood[(4)]. During ebb the majority of the transports is flushed seaward onto the southern part of the ebb-tidal delta (Fig. 6-12b). Sediment transports through Nieuwe Schulpengat contribute to the accumulation of sand in the Bollen van Kijkduin and Franse Bankje shoals. Transports through Schulpengat and Nieuwe Westgat induce the outbuilding of Zuiderhaaks. Ebb-tidal transports on the western margin of the ebb-tidal delta are minor due to the sheltering effect of Noorderhaaks. Flood transports enter the ebb-tidal delta from the south increasing substantially towards the inlet gorge (Fig. 6-12a) due to acceleration of the flow velocities. Near Helsdeur transports are further increased due to contraction of flow around the sharp curvature of Helderse Zeewering. As a result in the proximal part of the ebb-tidal delta the flood flow and transports exceed the ebb flow and transports resulting in a net import of sediment (see Fig 6-13a). Addition of non-tidal processes, mainly set-up in the inlet gorge, enhances the sediment import rates (Fig. 6-13a).

Despite relative small residual velocities (compared to the channels) the tidal transports on the western margin of Noorderhaaks show a distinct northward and landward direction. Waves augment these transports. The large shoal complex forms a wide 'surf-zone' area as the location of wave-breaking varies over this domain depending on the wave-height/water depth ratio; large waves lose their energy well ofshore on the ebb-tidal delta front, while smaller waves can propagate relatively undisturbed towards the major shoal areas. Similair to normal surfzone processes such as observed along the uninterrupted Holland coast, loss of momentum and dissipation of wave energy due to wave-breaking become dominant contributors to the sediment transport (Stive *et al.*, 1990; Van Rijn, 1997). Analysis of the wave energy distributions (not plotted) shows that the majority of the wave energy decay occurs on the shallow shoal areas of Noorderhaaks and Zuiderhaaks where depth-limited wave breaking is the main process. As most of the wave energy is dissipated on the ebb-tidal delta, wave penetration of open-sea waves into the basin is limited. Maximum predicted wave heights in Texel inlet are generally below 1 m in Texelstroom and smaller on the flat areas. The non-tidal mechanisms enhance the landward and northward transport of sediment on the Noorderlijke Uitlopers of Noorderhaaks (Fig. 6-12d). Most of the sediments supplied to the northern part of the ebb-tidal delta are transported back into the main inlet circulation along the northern margins of the supra-tidal part of Noorderhaaks, through the Molengat channel, and into

[4] Maximum ebb and flood are here related to the maximum transport rates in Marsdiep.

Marsdiep. As a result of this circuitous route only little sand actually bypasses the inlet onto the downdrift Texel coastline and foreshore. The sediment bypassing mechanism at Texel inlet is probably more of an episodic phenomenon; sand accumulates in the downdrift Noorderlijke Uitlopers of the Noorderhaaks spit that eventually will breach and attach to the downdrift shoreline (see FitzGerald, 1982; FitzGerald, 1988 for spit breaching mechanisms).

Analysis of monthly-averaged transport rates in Marsdiep indicates that sediment import into the basin is a more-or-less continuous process wherein both tidal and non-tidal contributions play an important role (Fig. 6-13a). The non-tidal part consists of near equal but opposite directed wind- and wave-driven contributions, and a larger input by set-up. Most of the sediments are supplied through the southern part of the ebb-tidal delta. Tide and wave-driven transports along the southern margin of the supra-tidal Noorderhaaks (Fig. 6-13c), and setup-driven contributions through Nieuwe Schulpengat (Fig. 6-13d) form the major part. A minor part is supplied by the tide-driven sediment transports through Molengat (Fig. 6-13b).

Time-series of instantaneous transports in Marsdiep (plotted for the month of February 1999) show a clear spring-neap modulation (Fig. 6-13e); sediment transports peak during spring tide while reducing to almost zero during neap tide. Sediment import is governed by the suspended load component due to the larger flood than ebb currents, whereas the bed-loads are minor. Storm events drastically increase the instantaneous sediment import of sand (Fig. 6-13f), but as these occur mainly during a short period the month-averaged contribution remains fairly limited; during the rougher winter months sediment import is 1.1 to 1.4 times the magnitude of the calm summer transports.

For cohesive material an opposite response might occur as studies in the Lister Dyb tidal inlet (Danish Wadden Sea) have shown. The annual sediment accumulation in the Lister Dyb basin results from a small continues sediment import every tidal period under fair weather conditions (Lumborg and Pejrup, 2005). Sediment import is disrupted by major export events (of short duration). These export events are related to longer periods of windy weather. The related wave activity is especially important for the erosion processes at the intertidal flats where the bed shear stresses increase and sediment is mobilized that can then be exported during ebb. Partly, this difference in response between Texel inlet and Lyster Dyb relates to the cohesive versus non-cohesive sediment application. But, also the basin bathymetry might play an important role. Near the inlet the basin is deep and wave-sheltered. The main shoals are located to south of the main channel Texelstroom. Wind and waves are mostly from the western quadrant and will enhance the eastward flood dominant transport and counteract the ebb transports. Augmented eastward transport contributing to increasing tidal asymmetry driven transports (see Chapter 4) might explain the large sedimentation in the back part of the basin along the Frisian coast.

6.3.4 Detailed analysis of sediment transport patterns and magnitudes

The 'Molengat system'

The northern part of the ebb-tidal delta, *'Molengat system'*, consists of two main morphological elements. The shallow spit Noorderlijke Uitlopers of Noorderhaaks, where waves and wave-tide interaction play an important role, and the Molengat channel wherein tidal dominance increases towards Marsdiep (Fig. 6-14). The spit developed strongly after closure of the Zuiderzee extending in northward direction and curving landward. After an initial rapid growth and extension, the spit has retained its stability during the last decades despite the anticipated breaching and merging with the Texel coast (Sha, 1989b; Cleveringa, 2001, also see Chapter 5 [Fig. 5-11 and 5-12]). Conjugate with its northward extension, the spit migrated landward inducing a similar landward displacement of Molengat. The migration of Molengat is one of the main actors in the structural sand losses from this part of the Texel coastline.

Sediments are supplied to the spit due to landward transports from the western margin of the ebb-delta. In addition, the ebb-chute and ebb-shield formation on the spit (located at Y-coordinate = 556.5 km) indicates that sediments are also supplied by the ebb-tidal currents through Molengat; illustrated in the model results of Fig. 6-14a. The ebb chute more or less forms a separation between the southern and northern part of the spit whereon transports are opposite directed. South of the ebb-chute sediment transports are eastward directed towards Molengat and into the main inlet circulation [18,19,22,23][5]. North of the ebb-chute transports contribute to the outbuilding of the spit [12,5]. Plausibly, the relatively strong ebb-dominant (northward) velocities through Molengat along the landward margin of the spit retard the landward wave-driven transports and landward spit migration by transporting the sediments northward [11]. The observed stability of Noorderlijke Uitlopers of Noorderhaaks indicates that a fair balance between landward and seaward transports must exist. In this respect an interesting feature in the model results are the counteracting transports on the distal part of the spit. During storm events wave-generated transports dominate over the tidal transports and a strong landward transport prevails (see transect [9] months 1-3). During calm conditions waves contribute to the northward and seaward extension of the spit (see transect [9], months 4-8). In the model the seaward transport rates are probably overestimated.

Sediment bypassing, or sand transfer from the ebb-tidal delta shoals onto the Texel shoreline is limited. Approximately 0.01 Mm^3/year is estimated to be transported northward [4,5] but this is merely due to growth of the spit. Along the coastline sediment transports are primarily directed towards the inlet. Increasing transport rates towards Marsdiep indicate an eroding area [11,18,22]. Partly, these flood-dominant transport results from wave-sheltering and refraction by the ebb-tidal delta. Noorderhaaks prohibits waves from the southern quadrant to reach the Texel coastline, and as a result waves

[5] [ ] indicates transect number in the corresponding Figure. For selected transects details of the year-averaged rates and contributions of the various processes are presented in the supplement Figure (positive values denote flood dominant transports (towards the inlet), and negative values ebb-dominance).

from the north dominate and the wave energy flux is directed southward. In addition to the ebb-dominant supply of sediment through Molengat, a landward sediment transport, around the tip of the supra-tidal Noorderhaaks, contributes to the redistribution of sediment from the western margin of Noorderhaaks onto the Noorderlijke Uitlopers of the Noorderhaaks spit. This sediment supply is largely wave-driven; especially during high wave-energy events a significant landward supply of sediment arises [16,24].

'the Noorderhaaks system'

The central part of the ebb-tidal delta is governed by landward-directed sediment redistribution (Fig. 6-15). Sediments are transported from the western fringe of the ebb-tidal delta, that consequently erodes, along the northern and southern margin of the supra-tidal Noorderhaaks area back into the main inlet circulation [24, 39,40].

The deformation of the northwestern tip of the supra-tidal Noorderhaaks into a small spit development is primarily wave-driven [24]. Behind this spit, in the lee side of Noorderhaaks, a wave- and tide-sheltered area develops favorable for sedimentation. Towards Marsdiep sediment is picked up again primarily by tides and smaller contributions of set-up and waves [23], and in the observations a small tidal channel has developed at this location (Chapter 5 Fig. 5-11). Tides are the main transport mechanisms for sediment exchange between Molengat and Marsdiep [22]. During calm conditions this transport is in the order of 0.5 Mm^3/year, but this increases to over 1.5 Mm^3 during storm events.

Despite the absence of main channels one of the main actors in the large erosion of the ebb-tidal delta margin are tides and wave-tide interaction in particular. A large tidal circulation cell develops facing Nieuwe Westgat (see Fig. 6-16 for details) that initiates a landward-directed flow and transport along the Noorderhaaks margin [41,42,27,28] and a southward transport towards Zuiderhaaks. Landward sediment transports are greatly augmented by wave associated suspension of sediment [39]. Partly, sediment settles just south of Noorderhaaks, contributing to the infilling of the former Westgat channel. The remainder is supplied to the inlet circulation where it is transported southward onto the Zuiderhaaks during ebb and northward into the basin during flood. The relative large role of tides continuously redistributing sediment from the western margin landward is a plausible explanation for the observed large sediment loss in this area.

The small southward sediment transports on top of the supra-tidal Noorderhaaks result from major storm events were the associated set-up levels submerge the normally supra-tidal Noorderhaaks.

'the Schulpengat system'

After closure of the Zuiderzee the southern part of the ebb-tidal delta was governed by the scouring of the main tidal channels. Initially Schulpengat developed as a single channel but since about 1956 a two-channel system was formed on the ebb-tidal delta (Schulpengat and Nieuwe Schulpengat [see Fig. 5-1]). The southward growth of Nieuwe Schulpengat was one of the main actors in the large sand losses from the Holland coast. Largest changes occurred in a period of 40 years after closure, but the channel reached a

maximum extension in the nineties. Due to the presence of large tidal channels tides and set-up are dominant processes.

The sediment transport patterns of Figure 6-16a illustrate the presence of two main circulation patterns, separated by Schulpengat. The landward *'Nieuwe Schulpengat circulation'* determines the nearshore transport patterns. Ebb-directed tidal transports distribute sediments along the landward margin of the Bollen van Kijkduin, through Nieuwe Schulpengat, onto Franse Bankje. While on the seaward side of Franse Bankje and Bollen van Kijkduin transports are directed northward. On Bollen van Kijkduin a net southeastward component prevails. This southeastward component might explain the small migration of the shoal during the last decades; Van Veen (2005) already explained the formation (maintenance) of shoals through recirculation of sediment by evasive ebb and flood transports [67,68]. The small southward migration of Bollen van Kijkduin induces similar migration and clockwise rotation of the distal part of Nieuwe Schulpengat, which explains the ongoing larger erosion of the adjacent section of the North-Holland coast. Along the coast transports are flood dominant. The increasing transport rates along the North Holland coast contribute to the sand losses.

The *'Zuiderhaaks circulation*' governs the sediment transports seaward of Schulpengat. Schulpengat forms a separation between the two circulation cells with the landward part of the channel being flood-dominant and the seaward part ebb-dominant. The sediment transport vectors illustrate that the seaward (and southward) outbuilding of Zuiderhaaks results from ebb-dominant contributions through the Nieuwe Westgat and Schulpengat channels [53,59,23]. Waves play a role in this outbuilding [59]. Waves transport sediments along the seaward margin of Noorderhaaks into the inlet circulation (Fig, 6-16a). During flood these sediments are transported towards the basin, but during ebb these sediments are transported through Nieuwe Westgat and Schulpengat back onto the Zuiderhaaks shoal. Despite landward-directed transport due to wave breaking on the shoal, the indirect contribution of wave-tide interaction governs the development (see the wave driven contributions in transect [47] and [59]).

Along the Zuiderhaaks margin a northward transport prevails towards Noorderhaaks.

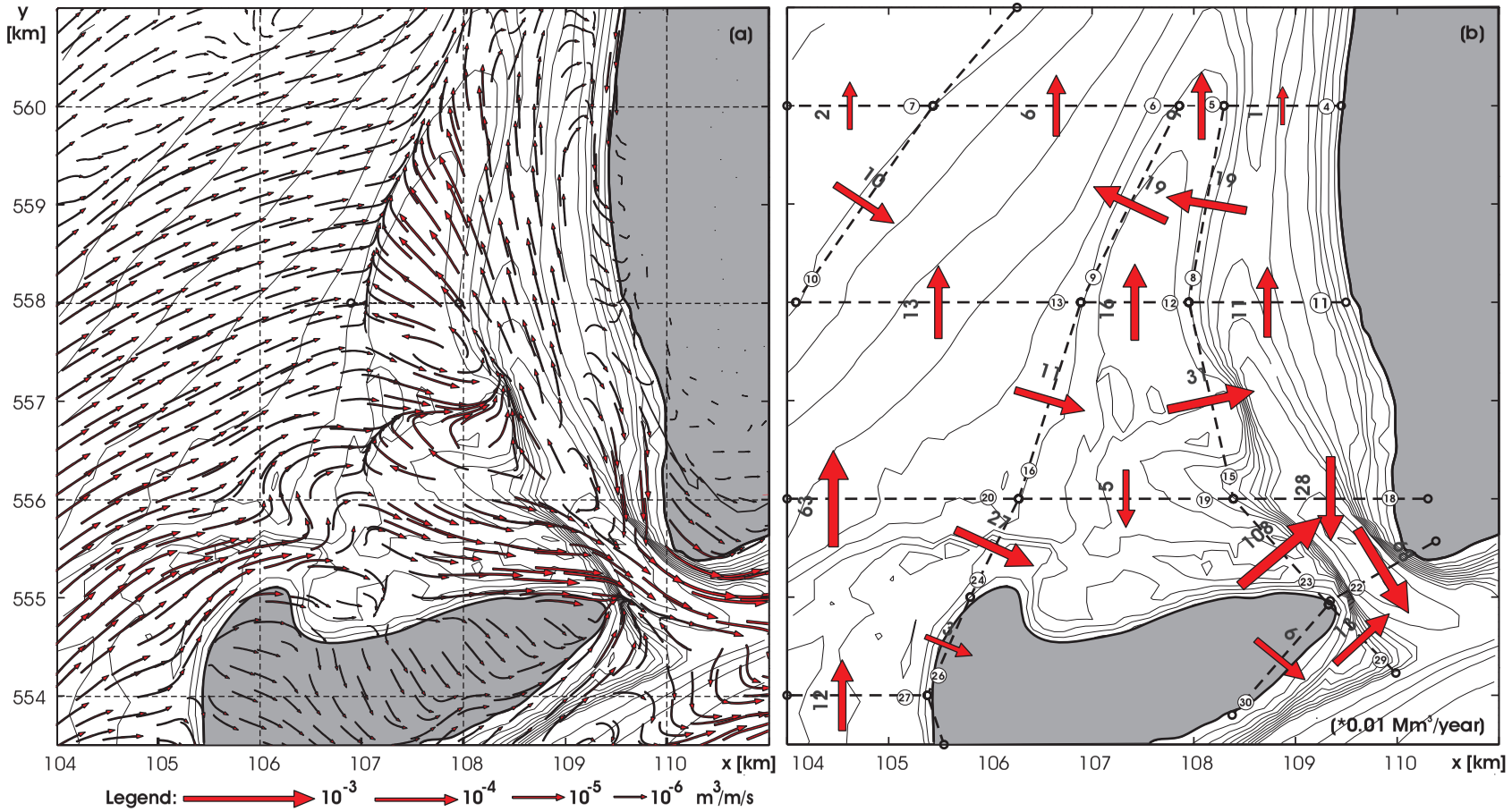

Figure 6-14: Model results for the '*Molengat system*'. Left page: (a) Curved vector representation of the sediment transport patterns. (b) year-averaged transport magnitudes integrated over selected transects. Right page: details of the monthly mean transports through selected transects and contributions of the separate processes.

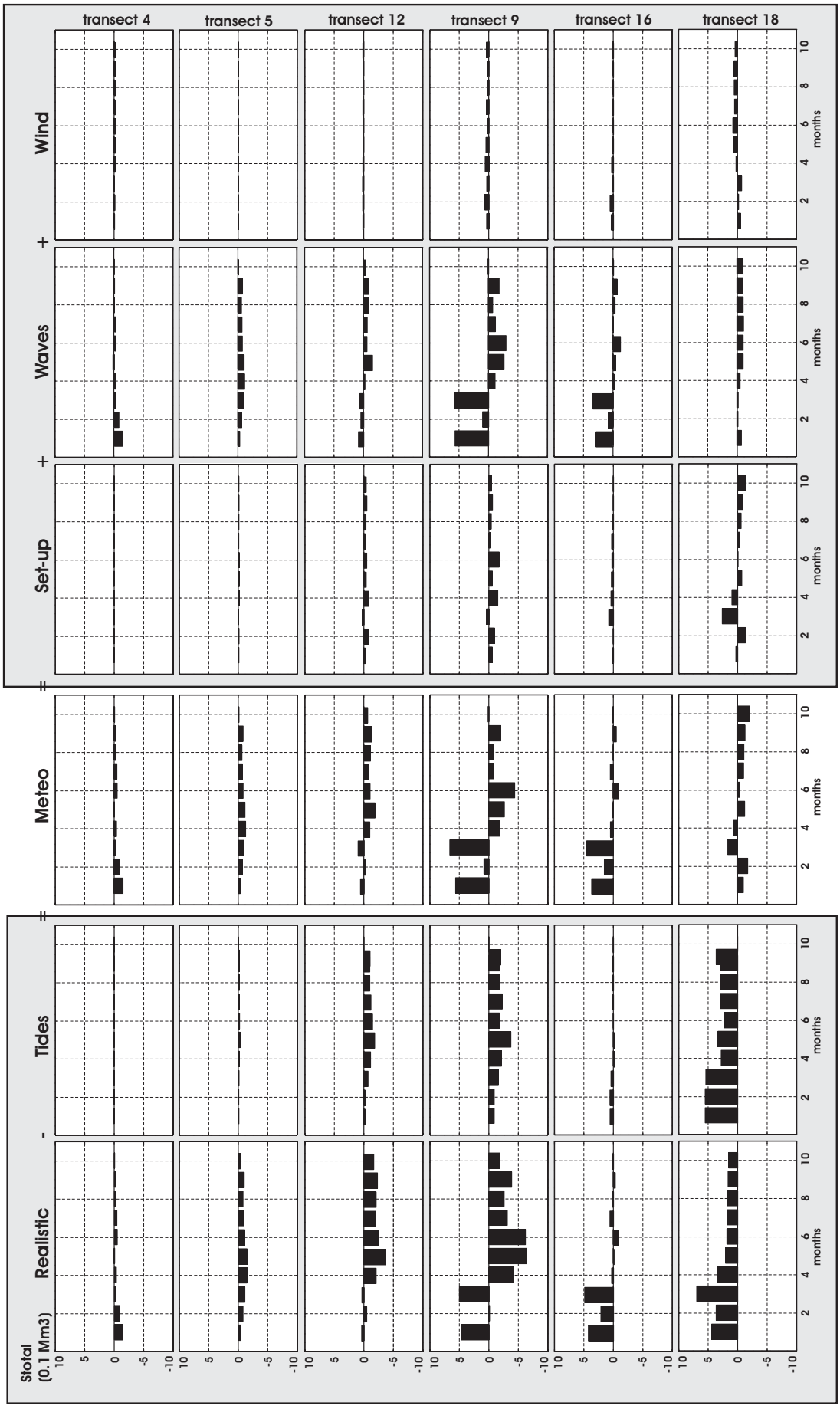
transect 4
transect 5
transect 12
transect 9
transect 16
transect 18
Wind
Waves
Set-up
Meteo
Tides
Realistic
Stotal
(0.1 Mm3)
months

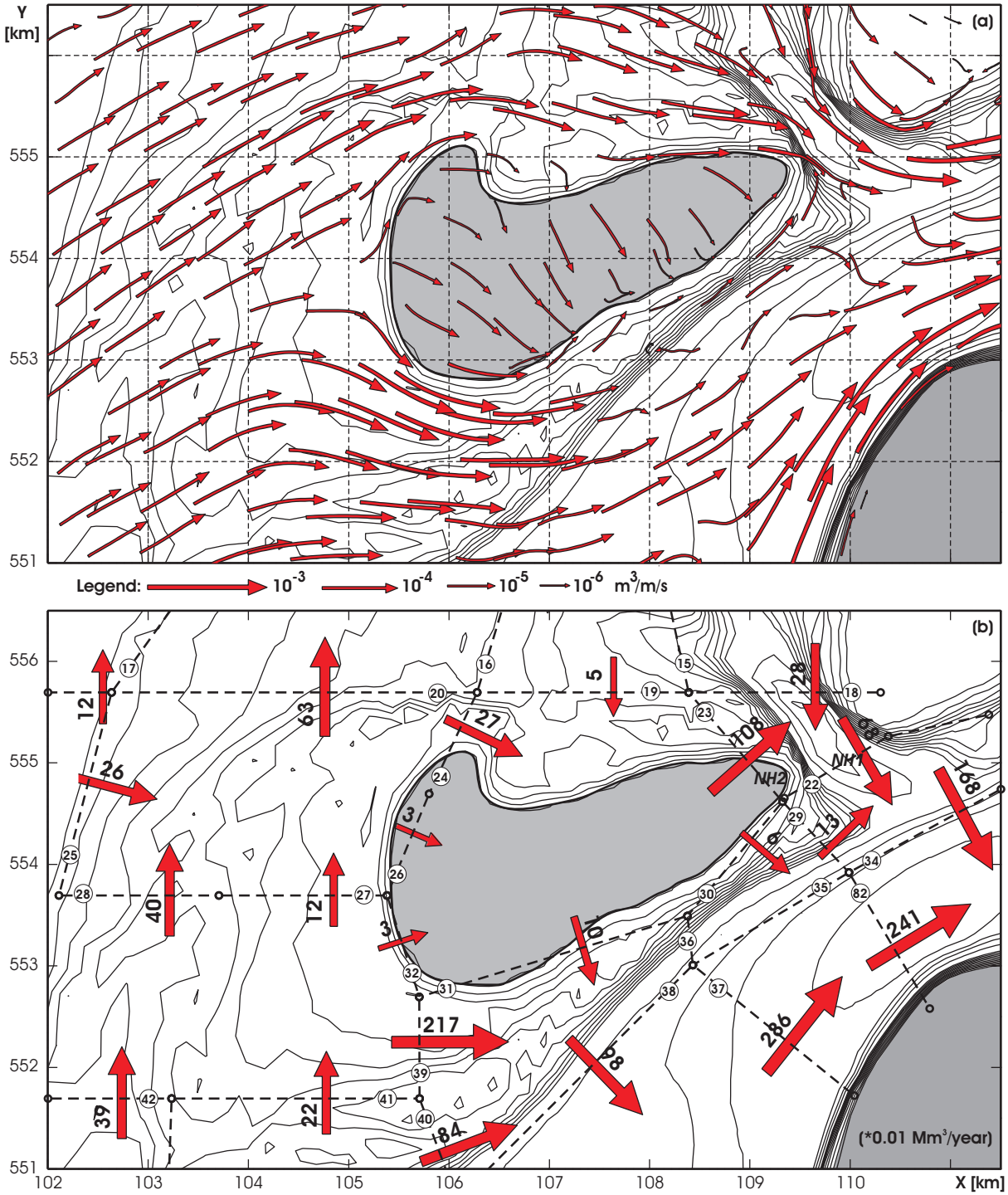

Figure 6-15: Model results for the '*Noorderhaaks system*'. Left page: (a) Curved vector representation of the sediment transport patterns. (b) year-averaged transport magnitudes integrated over selected transects. Right page: details of the monthly mean transports through selected transects and contributions of the separate processes.

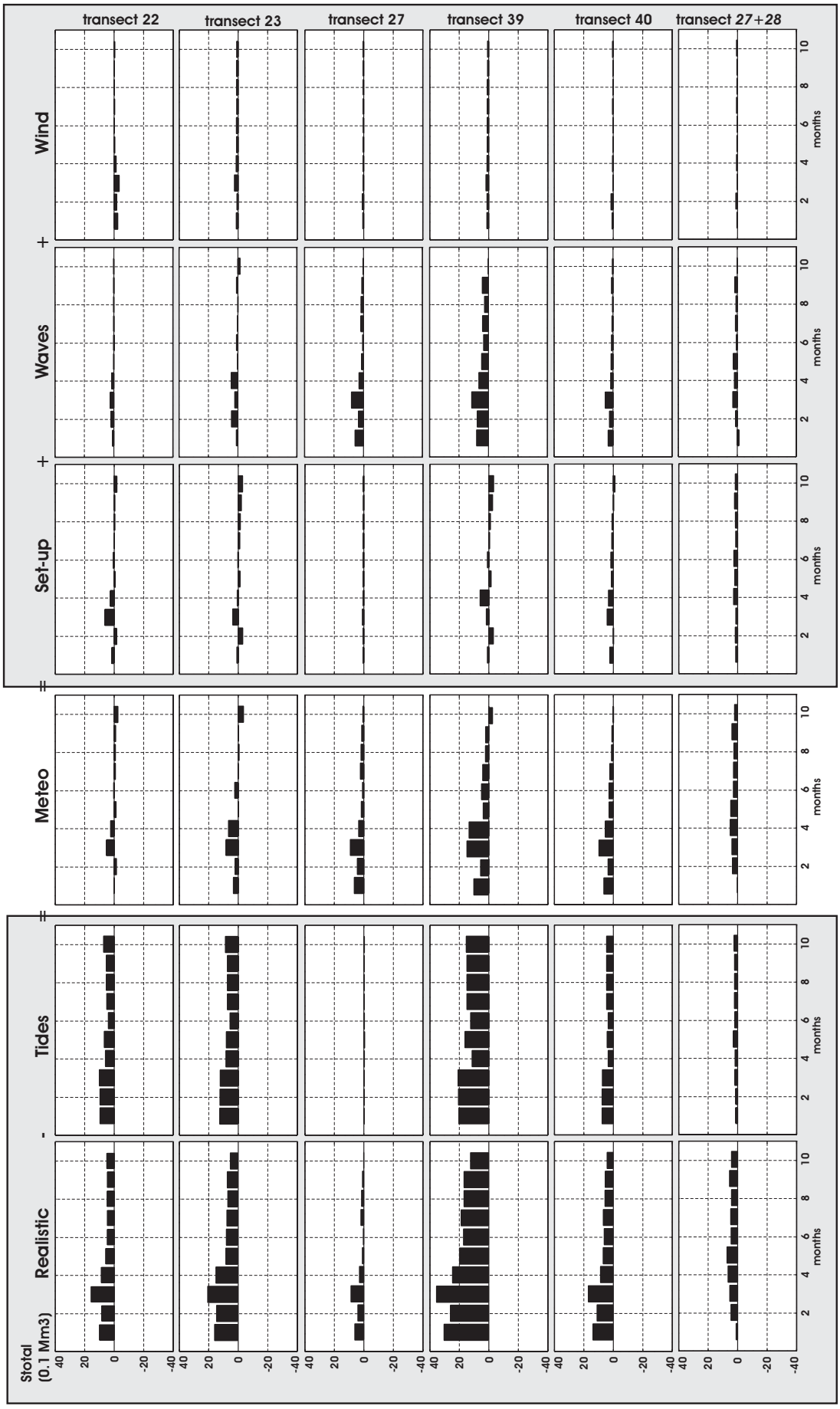
transect 22
transect 23
transect 27
transect 39
transect 40
transect 27+28
Wind
Waves
Set-up
Meteo
Tides
Realistic
Stotal (0.1 Mm3)
months

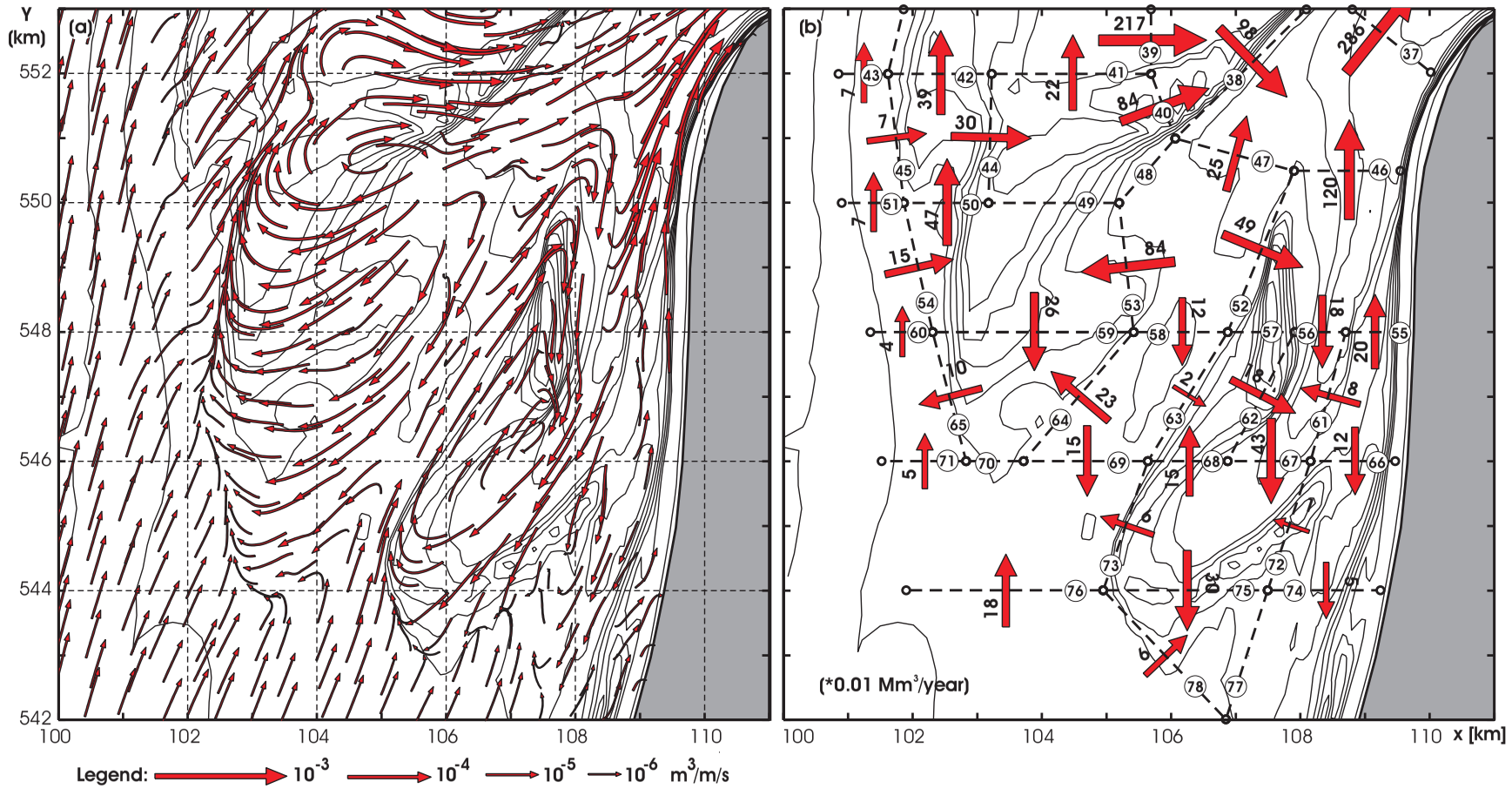

Figure 6-16 (left page): Model results for the '*Schulpengat system*'. Left page: (a) Curved vector representation of the sediment transport patterns. (b) year-averaged transport magnitudes integrated over selected transects. Right page: details of the monthly mean transports through selected transects and contributions of the separate processes.

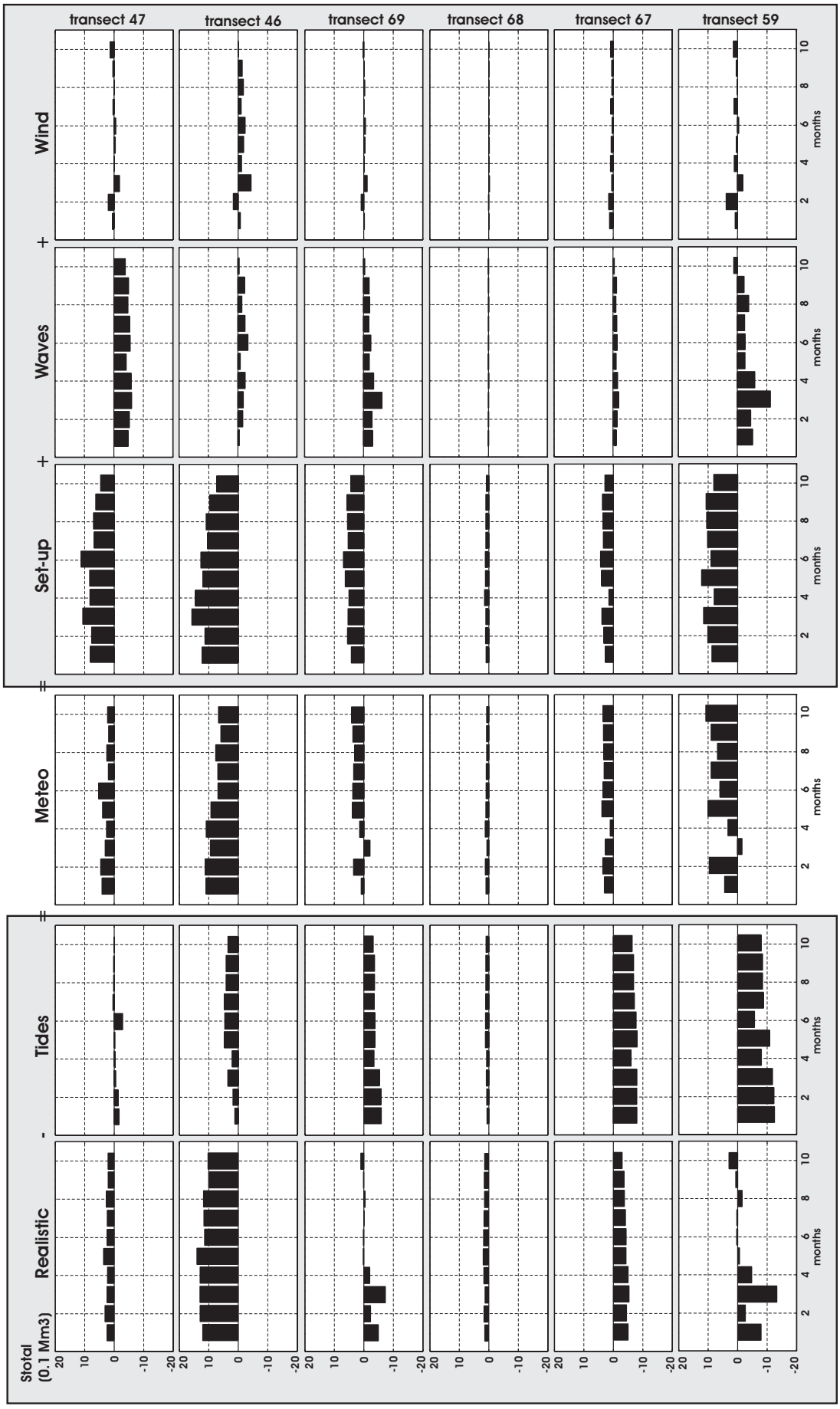
transect 47
transect 46
transect 69
transect 68
transect 67
transect 59
Wind
Waves
Set-up
Meteo
Tides
Realistic
Stotal
(0.1 Mm3)
months

6.4 Synthesis and Discussion

Model results provide additional evidence for the schematic sand transport patterns presented in Chapter 5 and summarized in Fig 5-19. Both observational data and model results demonstrate that the present morphological developments on the ebb-tidal delta are dictated by sediment redistribution on the ebb-tidal delta and by sediment exchange between ebb-tidal delta and basin; sediment is eroded from the ebb-tidal delta (including adjacent shorelines) and deposited in the basin. Largest erosion prevails on the western margin of Noorderhaaks were tides and waves are important for the landward displacement of sediments. Locally, sedimentation and erosion patterns are governed by channel-shoal interactions (e,g. the interaction of Molengat-Noorderlijke Uitlopers of Noorderhaaks (Fig. 6-17a [1]) and Nieuwe Schulpengat-Bollen van Kijkduin (Fig. 6-17a [4]).

One of the main features of the present day sediment dynamics of Texel inlet is the large sediment import into the basin (estimated to range between 5 - 6 Mm^3/year over the period 1986-2003). Similar to Chapter 4, three basic requirements need to be fulfilled to explain the sediment influx:

(1) ***Sediment demand;*** Reanalysis of the basin volume changes (Chapter 5 Appendix A) shows that the western Wadden Sea still demands sediment to compensate for the distorted balance between channel and shoal areas that arose from Closure of the Zuiderzee, but also sediments are demanded to compensate for relative effects of sea-level rise.

(2) ***Sediment availability;*** Noorderhaaks can be considered as an abundant source of sediment originating from the pre-closure situation where it was formed as a balance between sediment supply by the ebb-tidal currents through Nieuwe Westgat and landward displacement driven by waves. After closure, with the main channels switching westward, Noorderhaaks forms an abundant source of sediment, located conveniently in front of the inlet, that is redistributed landwards.

(3) ***Sediment transport capacity;*** Sediment transport capacity is present in the form of the large tidal prisms and associated tidal currents in the inlet gorge and proximal part of the ebb delta channels (this was defined as main inlet circulation). The presence of the supra-tidal Noorderhaaks and Helderse Zeewering, and segregation in ebb- and flood dominated zones are believed to play a crucial role in the flood-dominant transport capacity of the main inlet circulation. This latter statement is conceptually explained below.

Inlet dynamics and Main Inlet Circulation

At an ideal inlet (see e.g. Oertel, 1988 for an explanation) a (free) jet outflow forms on the seaward side of the inlet during the ebbing tide, and material eroded from the inlet gorge is deposited at the bed below the far field of the jet were flow segregates and velocities drop beyond the sediment fall velocity (Fig. 6-18 [a1]). During flood the return flow towards the inlet is uniformly distributed in a convergent flow towards the inlet [a2], and since the velocity field is distributed over a broad arc the flood velocities that correspond to the near-field of the ebb-jet are lower than during ebb. The residual velocity field [a3] is therefore ebb-dominant in the axial part of the near-field and flood-dominant

in the lateral parts. Such velocity fields cannot develop at Texel inlet due to the presence of the large Noorderhaaks shoal area facing the inlet gorge. The ebb-jet is primarily southwestward directed due to the orientation of Texelstroom and deflection by Noorderhaaks [b1]. Sheltering by the supra tidal Noorderhaaks results in low-velocity areas westward and northward of this shoal. Flood enters the ebb-tidal delta from the south and flow velocities increase substantially towards the inlet gorge [b2] as a funnel shape forms between Noorderhaaks and the North-Holland coast, wherein velocities accelerate due to decreasing cross-sectional area. Flood dominance is further enhanced by time-velocity asymmetry of the tidal currents (Postma 1961, 1967); maximum flow velocities occur do not occur at midtide but near ebb or flood. As flood starts still relative large ebb velocities dominate the central channel resulting in flood (initially) concentrating along the North-Holland coastline. As a result flood velocities particularly increase due to contraction of flow streamlines around the sharp curvature of Helderse Zeewering.

The associated transport fields show a distinct horizontal segregation of ebb- and flood-dominant parts; see the dominance plot of Figure 6-18 [b3] based on modeled maximum ebb and flood tidal transport rates only. Flood-dominant transports prevail along the North-Holland coastline and on the shallow platforms of Noorderhaaks, whereas ebb-dominance is observed in the distal parts of the channels and along the Texel coastline. Sediment supply along the Noorderhaaks enhances the observed segregation. The large circulation cell located on Noorderhaaks (enhanced by wave driven currents and wave stirring) is capable of supplying sediments from the ebb-tidal delta front into the main inlet circulation. During ebb these sediments are transported towards Zuiderhaaks enlarging the ebb dominance, while during flood these are transported into the basin that acts as a sediment trap.

Sediment transport patterns

Large velocities in the proximal part of the ebb delta channels (defined as main inlet circulation (Fig. 6-17a *MIC*) are capable of transporting vast amounts of sediments into the basin during flood (tides and setup are the main processes). Sediments are supplied by northward littoral drift along the North-Holland coastline and southward transports along the Texel coastline that are captured by the tidal channels Molengat and Nieuwe Schulpengat (Fig. 6-17a [a and f]), erosion of the western margin of the ebb-tidal delta [c], and scouring of the main channels. In the basin sediments partly settle and partly sediments are redistributed back onto the ebb-tidal delta where a subdivision in three ebb-dominant areas can be made: the Molengat system [b], the Zuiderhaaks system [d], and the Nieuwe Schulpengat system [e]. Smaller scale circulation cells dominate the local behavior of these individual subsystems.

A minor part of the ebb sediments is transported through Molengat onto the Noorderlijke Uitlopers of the Noorderhaaks shoal where it contributes to the northward extension of the shoal (Fig. 6-17b [circulation cell 1]). The stability of the Noorderlijke Uitlopers of Noorderhaaks relates to the seaward sediment transport during calm conditions, and landward transports during storm conditions. With ongoing northward extension the tidal contribution decreases and the spit curves seaward. The balance between storm and calm conditions entails that eventually during a (series of) major storm events the spit is

expected to breach and merge with the Texel coastline. The structural erosion of this coastline points to the loss of sediment due to wave-dominated transports along the Texel coastline towards the inlet. Therefore, even merged deposits will largely be transported back into the inlet system by the wave driven transports and sediment bypassing onto the downdrift coastline is minimal.

The major part of the ebb transports is directed through Nieuwe Schulpengat, Schulpengat and Nieuwe Westgat onto the southern part of the ebb-tidal delta. Ebb-tidal transports through Nieuwe Schulpengat distribute sediments onto Franse Bankje (Fig. 6-17b [circulation cell 4]). Despite large velocities and transport rates the Nieuwe Schulpengat and adjacent shoal areas of Bollen van Kijkduin and Franse Bankje have remained stable in position which indicates that much of the sediment is transported back into the main inlet circulation. Partly, transport occurs from Franse Bankje landward (due to wave-breaking induced transports) into Nieuwe Landsdiep, and along the North-Holland coast towards the inlet. Partly, flood (tidal) transports in Schulpengat redistribute sediments along the seaward margins of Bollen van Kijkduin. Recirculation of sediment by evasive ebb and flood transports possibly explains the maintenance of Bollen van Kijkduin.

Separated by Schulpengat the Zuiderhaaks forms a second sub-system (Fig. 6-17b [circulation cell 3]). The Schulpengat and Nieuwe Westgat channels supply sediments that contribute to the southward extension of the shoal. Only small net changes occur due to the redistribution of sediments along the seaward margin of Zuiderhaaks in northward direction onto Noorderhaaks. The large circulation cell located in front of Nieuwe Westgat redistributes sediments back from the western margin of Noorderhaaks into the main inlet circulation. The presence of this large circulation cell results in a continuous influx of sediment from the western margin of the Noorderhaaks explaining the large sediment losses in this area. Waves further enhance the erosion rates. Once sediments are captured in the inlet circulation the majority is deposited in the basin.

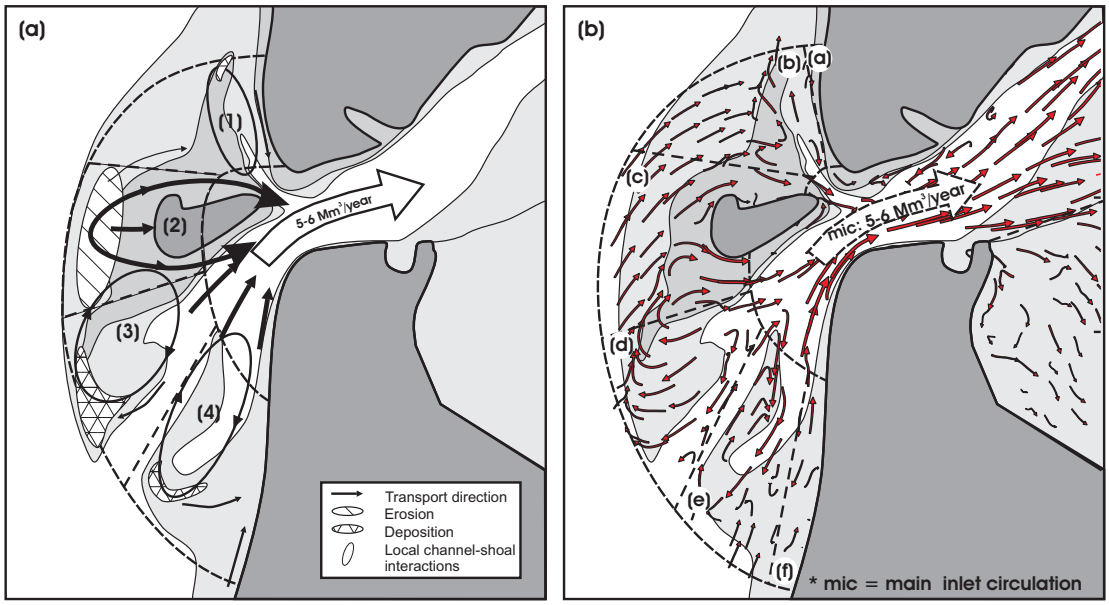

Figure 6-17: Conceptual description of sand transport patterns on Texel ebb-tidal delta (vectors indicate residual transport directions from model results).

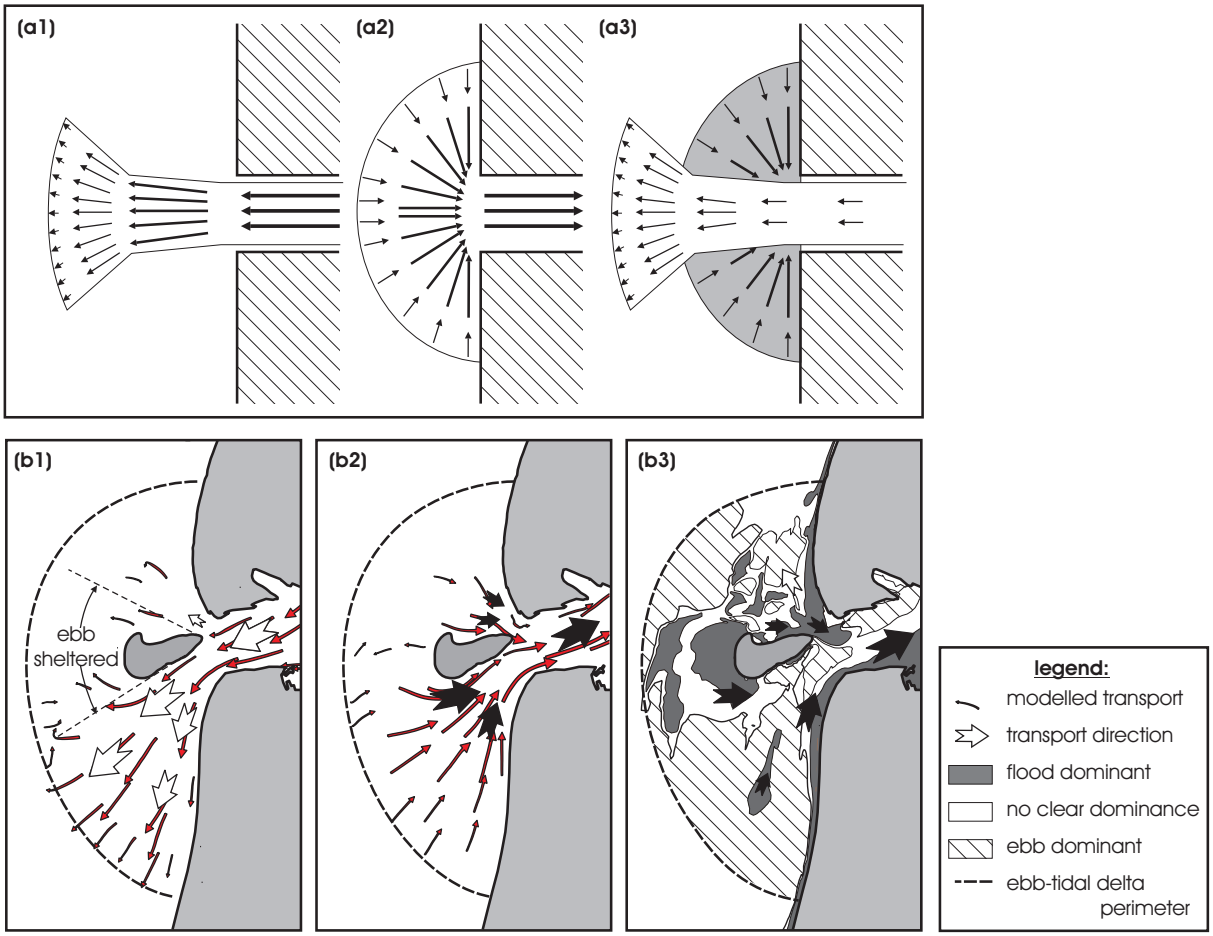

Figure 6-18 top: (a1-a3) Free-jet description following Oertel (1975) for ebb, flood and residual flow respectively in schematized inlets. Bottom (b1-b3): modeled ebb transports, flood transports, and dominance of residual transport patterns in Texel inlet.

6.5 Conclusions

Delft3D Online Morphology calculates morphologic changes simultaneously with the flow calculations. One of the major assets of this type of model is the capability to increase the spatial and temporal resolution of point-oriented field observations. Observations are used to force the model 'as realistically as possible' (quasi real-time by measured time-series of wind, waves and tides) and the model results provide synoptic more or less realistic data of high spatial and temporal resolution over the entire inlet domain.

Quasi real-time simulations were made to determine flow and sediment transports in Texel inlet (focusing on the ebb-tidal delta). Validation of the model results with the observations showed that the model is able to simulate the dominant features in the flow and transport patterns even in the complex ebb-tidal delta domain. Analysis of the model data provides valuable information on governing flow and sediment transport patterns in the instrumented and the un-instrumented areas, and allows for identification of the dominant processes by systematically checking mechanisms.

Model results provide additional evidence for the schematic sand transport patterns presented in Chapter 5. Both observational data and model results show that the present morphological developments on the ebb-tidal delta are dictated by sediment redistribution on the ebb-tidal delta and sediment exchange between ebb-tidal delta and basin; sediment is eroded from the ebb-tidal delta (including adjacent shorelines) and deposited in the basin. Sediment import into the basin (mainly due to tides and setup) is estimated to range between 5 - 6 Mm^3/year. Three basic requirements are identified to explain the sediment influx: (1) *Sediment demand;* Reanalysis of the basin volume changes shows that the western Wadden Sea still demands sediment to compensate for the effects of Closure of the Zuiderzee and relative sea-level rise. (2) *Sediment availability;* Noorderhaaks can be considered as an abundant source of sediment originating from the pre-closure situation conveniently located in front of the inlet, feeding the main inlet circulation with sediments. (3) *Sediment transport capacity;* Sediment transport capacity is present in the form of the large tidal prisms and associated tidal currents in the inlet gorge and proximal part of the ebb delta channels (main inlet circulation). The presence of the supratidal Noorderhaaks and Helderse Zeewering, and segregation in ebb- and flood velocities dominated zones form a crucial role in the flood-dominant transport capacity of the main inlet circulation.

Much insight in the processes and mechanisms governing the ebb-tidal delta of Texel inlet was obtained by the analysis of the 10-month period. As a next step the obtained insights in processes and mechanisms must be translated to representative forcing conditions in order to make long-term model simulations predictions of future evolution.

Chapter 7
Density-Stratification related sand transport in a mixed-energy tide-dominated (METD) inlet system

Satellite image of Kornwerderzand (www.earth.google.com)

Abstract:

Analysis of velocity fields in the inlet gorge and main ebb-delta channel of Texel Inlet during a period of high fresh-water discharge in the basin revealed a typical density-driven flow distribution of ebb-dominant flow in the top layers and flood-dominant flow in the near-bed regions. A 3D model application of the Delft3d Online Morphology system was capable of reproducing the dominant features of the residual flow patterns accurately when fresh-water discharge in the basin was included. Analysis of the model results illustrates that vertical density differences are largest in the inlet gorge at the location of the measurements. Density differences between bed and surface layer are essential to tilt the tidal residual flow patterns from a situation of horizontal shear to a more lateral shear in the inlet channel and diagonal shear in the main ebb-delta channel. As a result ebb and flood velocities are more distinctively separated; flood flow concentrates in the near-bed regions along the coast due to larger salinities and ebb flow of smaller density prevails in the upper layers along the main ebb-delta shoal. Using the Van Rijn (1993) transport formulation it is shown that the altered residual flow distribution and flow magnitudes have a potentially large impact on the residual sand transport in the inlet gorge and proximal ebb-delta channels.

7.1 INTRODUCTION

In the north of the Netherlands the Texel tidal inlet forms the first and largest inlet of the Dutch Wadden Sea. During the last century the inlet has undergone large morphological changes after damming of a major part of its back-barrier basin in 1932 (Elias *et al.*, 2003b; Elias and van der Spek, 2006, [chapters 2 and 3]). The resulting sediment import is regarded as one of the main causes for the significant sand losses of the adjacent coastlines of Texel and North-Holland (e.g. Van Rijn, 1997; Stive *et al.*, 1998; Mulder, 2000). So far studies addressed the importance of tides, wind and waves (Bonekamp *et al.*, 2002; Elias *et al.*, 2005; Elias *et al.*, 2006, [see Chapters 4 and 6]). Little is known about the importance of density-stratification for sediment import into the basin.

Prior to damming (small) rivers discharged water into the back part of the Zuiderzee basin, approximately 120 km south of the inlet. After closure, there is no direct river runoff into the remaining active part of the basin; rivers now discharge in the endyked fresh-water lake IJsselmeer. Episodically, after periods of rainfall when water levels in IJsselmeer are high, fresh-water is discharged into the Texel basin through two discharge sluices, that are located only 25-35 km south of the inlet. Observations by Zimmerman (1976) indicate that the bulk of the fresh-water discharged through the discharge sluices leaves the Wadden Sea via Texel inlet.

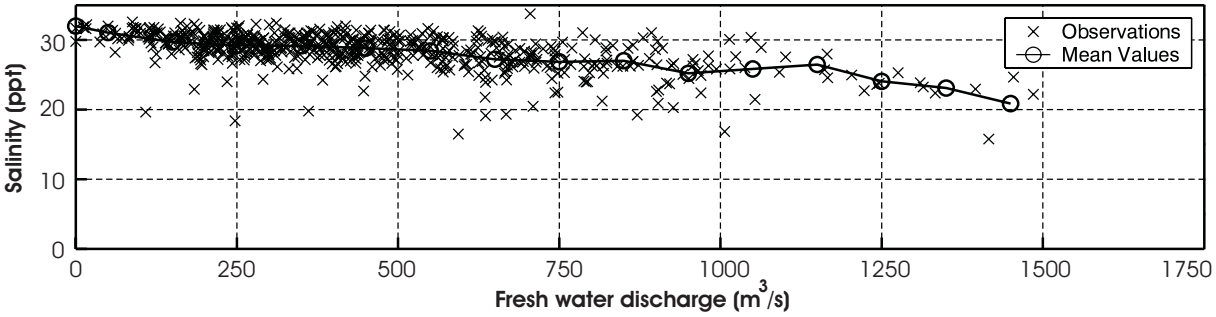

Figure 7-1: Relation between fresh-water discharges into the basin and surface salinity values in Marsdiep over the period 1977-1990; salinities measured monthly near Den Helder at -2 m MSL from 1977-1990 and since 1990 at -1 m MSL. The solid line indicates mean values per 50 m^3/s class.

Yearly-averaged, the total fresh-water discharge is in the order of 500 m^3/s. However, significant seasonal variations occur; during dry periods (e.g. summer) discharges can reduce to zero, while increasing to 1500 m^3/s after periods with high rainfall. A relation between increasing fresh-water discharge in the basin, and decreasing surface salinities in the inlet throat Marsdiep is observed (see Fig. 7-1).

The interaction of tidally-induced and density-driven flow is known to play an important role in the residual flow and sediment transport patterns of fine sediments in estuaries (e.g. Postma, 1967; Fischer, 1972; Postma, 1981; Dyer, 1986; Uncles, 2002). However, the effect of salinity variations for the sediment exchange of sand (e.g. non-cohesive sediment of medium grain size) between basin and ebb-tidal delta is an unstudied field of research.

The present paper focuses on the importance of stratification for the residual flow and transport of sand in the Texel inlet system. High-resolution flow data obtained from simultaneously executed 13-hour Acoustic Doppler Current Profiler (ADCP) observations in the inlet gorge and main ebb-delta channel, during a period of major fresh-water discharge in the basin (over 900 m^3/s), are studied. The location of the ADCP transects are indicated by *MD* (Marsdiep), *BW* (Breewijd) and *MG* (Molengat) in Figure 7-2. The high fresh-water discharge magnitudes and relative low values of observed surface salinity, 24 ppt. (22-01-2001) and 26 ppt. (19-02-2001), suggest that stratification could be important during the period of ADCP observations. The detailed ADCP velocity measurements are used to validate a three-dimensional model application based on the process-based Delft3d Online Morphology system. The availability of high-resolution flow observations provides a unique test-case to evaluate the Delft3D model performance in reproducing the complex three-dimensional inlet flow patterns. Comparison of model results obtained from a '*tidal*' model simulation (tidal forcing only), and a '*realistic*' model simulation (forcing by tides and measured fresh-water discharges) allows to estimate the importance of stratification on the larger scale residual flow and sand transport patterns in the inlet.

7.2 Regional Setting

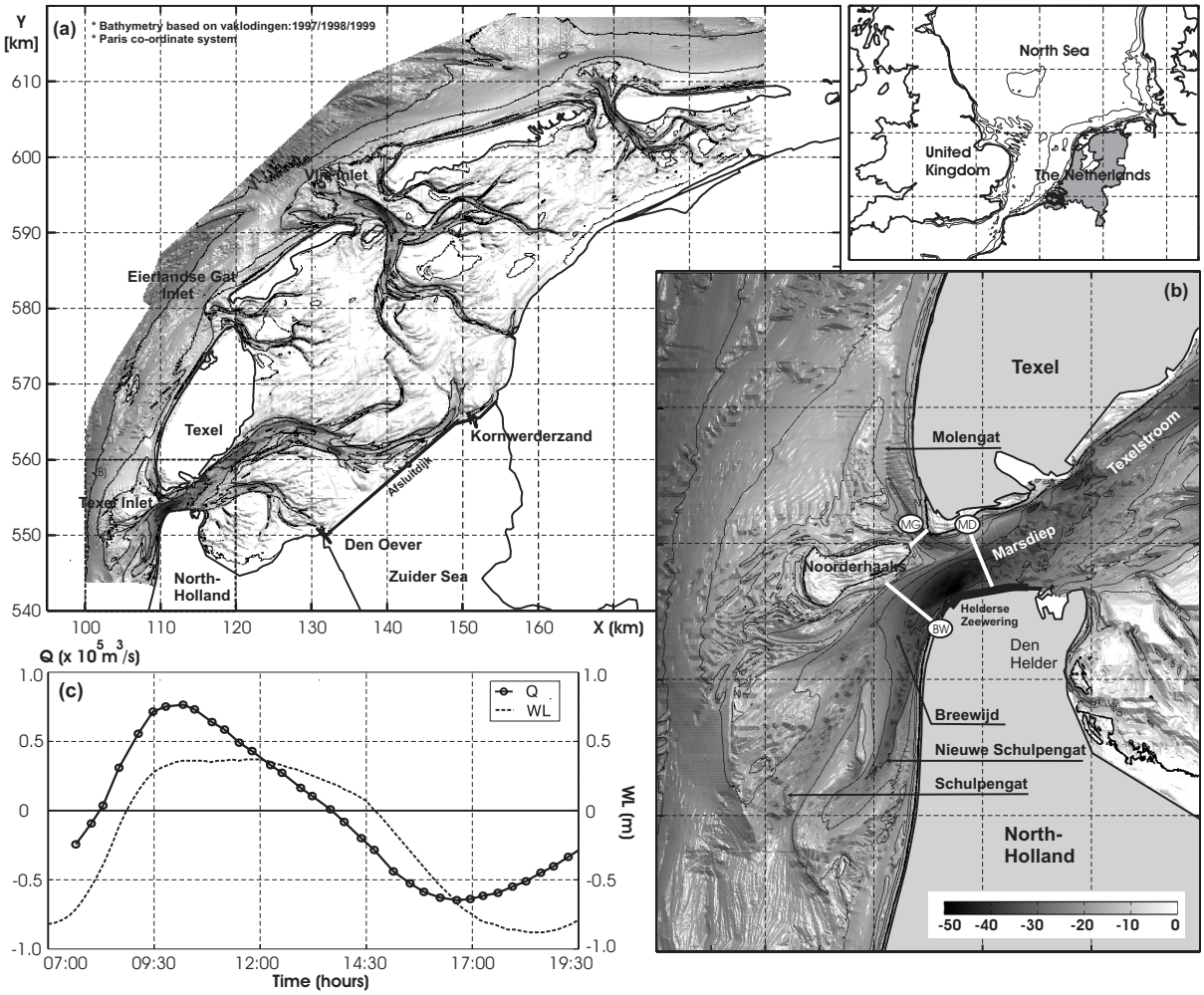

Figure 7-2: Location map of (a) the Western part of the Dutch Wadden sea and (b) Texel Inlet in detail, (c) impression of the measured water level and discharge in the Marsdiep (*MD*) transect.

Fig. 7-2 shows an impression of the present-day geometry and bathymetry of the western part of the Wadden Sea. The basin reformed after completion of the closure dam Afsluitdijk in 1933 that separated the Zuiderzee from the inlet. The discharge sluices Den Oever and Kornwerderzand are located at the western and eastern end of the dam respectively. Episodically fresh water from IJsselmeer (the former Zuiderzee) is discharged through these sluices into the basin.

Marsdiep forms the inlet throat (see insert Fig. 7-2b) connecting the main channel in the basin, Texelstroom, and the main channels, Schulpengat and Nieuwe Schulpengat, on the ebb-tidal delta (the upper part where the Schulpengat channels merge is called Breewijd). An important geometrical element is the Helderse Zeewering; a seawall that protects the southern embankment of Marsdiep against erosion. At the tip of Helderse Zeewering a large, over 53 meters deep, scour hole (Helsdeur) has formed in the course of time.

During and prior to the period of ADCP observations, spring of 2001: 15-02-2001 06:00 / 15-02-2001 21:00, wind and waves were absent but fresh-water discharge in the basin was major. Therefore the semi-diurnal tidal movement, possibly in combination with density-driven contributions, are the main driving forces behind the horizontal water flow through the inlet. Figure 7-2 (insert c) shows the measured water levels (location tidal station Den Helder) and discharge through the Marsdiep transect during the observations.

7.3 Method, Data, and Model

The residual circulation in estuaries and tidal lagoons is particularly complex as the flow can result from the combined forcing of tides, density gradients, wind- and wave-stresses interacting with a compound bathymetry and Coriolis. Numerous studies on estuarine circulations were performed and analytical solutions identifying the contributions of individual mechanisms were obtained; see e.g. Hansen and Rattray (1965) for density-driven flow, Friedrichs and Aubrey (1988), Speer and Aubrey (1985), Speer *et al.* (1991) and Parker (1991) for tidal flow. The relative importance of the density- and tidally-induced component was identified by e.g. Li and Valle-Levinson (1998). Parker (1991), Uncles (2002) and Van de Kreeke and Zimmerman (1990) provide detailed overviews of relevant studies.

In this study we do not aim to resolve the individual contributions of the various mechanisms analytically. Insight in the importance of density differences for the residual flow and sediment transport is obtained through field-data analysis in combination with process-based modelling. Three simultaneously executed 13-hour ADCP observations in the inlet throat and main ebb-delta channels were performed, and the resulting three-dimensional velocity fields are harmonically analyzed. The analysed data is used to validate and calibrate a three-dimensional process-based model, based on the state-of-the-art Delfd3D Online Morphology model system (Lesser *et al.*, 2004). Comparison of the model results for a hypothetical simulation driven by tides only, and a 'realistically-forced' simulation, including forcing by tides and fresh-water discharge in the basin, enables to estimate the stratification induced distortion of the (tidal) residual flow and sediment transport field in the inlet gorge of Texel Inlet.

7.3.1 ADCP observations

Nowadays, three-dimensional observations of velocity fields can be made accurately using broadband ADCP's (Vennell, 1994; Brubaker, 1999; Old, 2001; Li *et al.*, 2004). In the spring of 2001 three vessel-based ADCP surveys were performed to collect velocity data in the main channels of the Texel tidal inlet simultaneously (see Blok and Mol, 2001 for details). Measurements in Marsdiep and Breewijd were executed with a 1200kHz system of the Broadband type, while Molengat was measured at a 600 kHz frequency. The ADCP transects were run obliquely on the channel axis and continuously over a tidal cycle (15-02-2001 06:00 / 15-02-2001 21:00). Depending on the channel and tidal elevation

the transect lengths varied; Marsdiep and Breewijd 2300-2800 m, and Molengat 580-950 m. In total 44 tracks were obtained in Marsdiep, 51 in Breewijd and 80 in Molengat. The raw data were thoroughly analyzed, to remove systematic effects and data outliers. The ADCP was configured to obtain data in 1 m vertical bins, and 10 m horizontal bins. The vertical coordinates for each bin were referenced to mean water level. Velocity data in the near surface layer (the blank-after-transmit area) were extrapolated assuming a constant velocity. Data in the near-bottom layer were exponentially interpolated between zero at the bed and the upper cell. Data collected in each bin was treated as a time series. Table 7-1 summarizes the tide-averaged discharges for each transect.

Table 7-1: Locations and measured discharges of the ADCP transects

Transect	***Location***		***Discharge*** ***(10^6 m^3/tide)***		
	(X_0,Y_0)	(X_1,Y_1)	Ebb	Flood	Residual
Marsdiep	112.904 , 553.299	111.911 , 556.108	-992	865	-127 (ebb)
Breewijd	109.845 , 551.178	107.443 , 553.277	-970	753	-217 (ebb)
Molengat	109.825 , 555.730	109.092 , 551.000	-85	122	37 (flood)

Tide-averaged, the residual flow through the inlet of 127 million (M) m^3/tide is seaward directed. The majority of flow is directed from Marsdiep to Breewijd, and only a minor contribution through the Molengat channel. The larger ebb surplus in Breewijd compared to Marsdiep indicates a direct exchange of flow between Molengat and Breewijd channel. However, this exchange cannot explain the large increase in residual discharge from Marsdiep to Breewijd of 90 Mm^3/tide. In this paper we focus on the dominant channels Marsdiep and Breewijd.

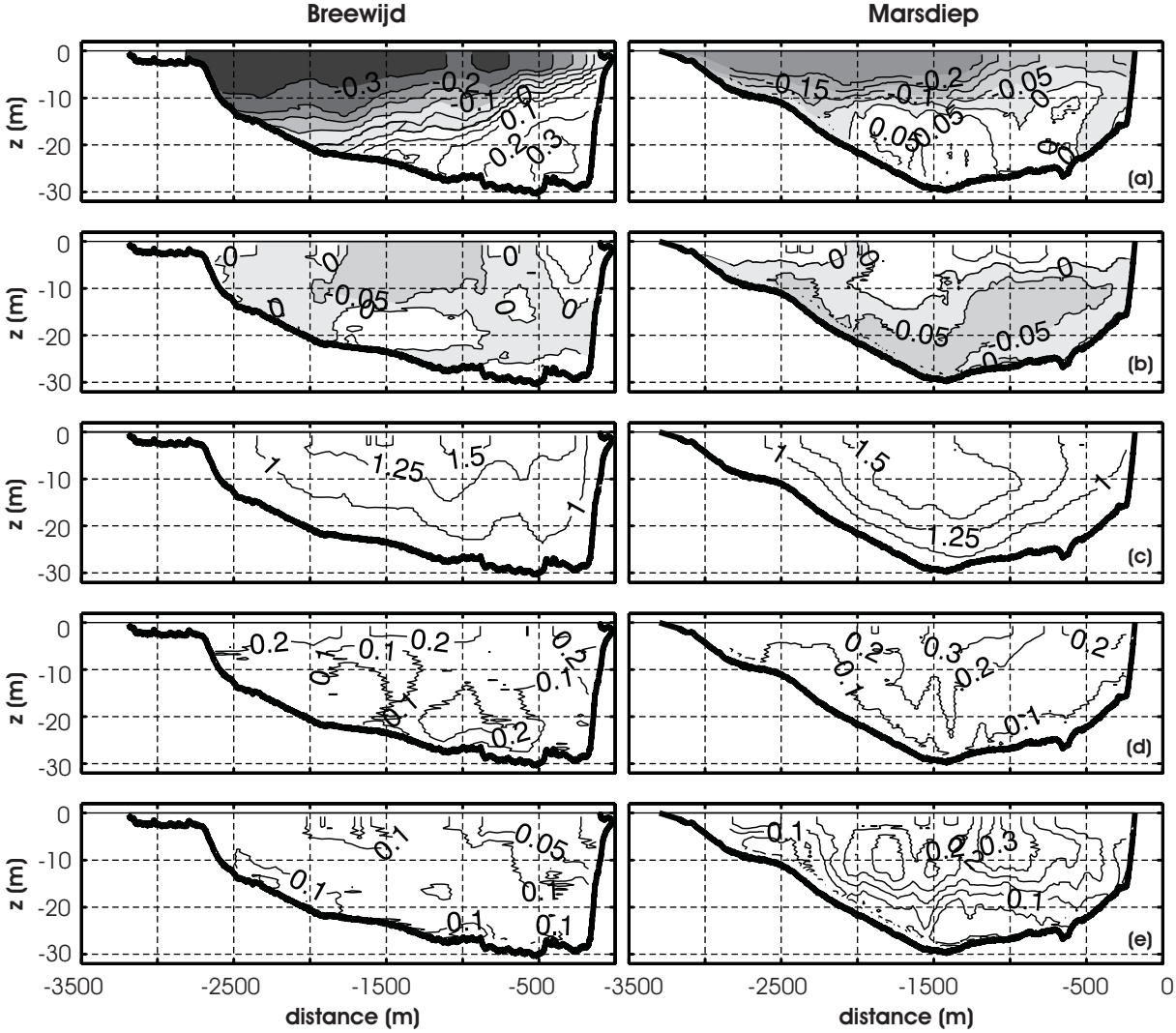

Figure 7-3: Harmonically analysed flow in Breewijd (left) and Marsdiep (right). From top to bottom (a) residual flow in along-channel (major) and (b) across-channel (minor) direction (gray is ebb-dominant, white is flood dominant), velocity amplitudes of the (c) M_2, (d) M_4, and (e) M_6 in major direction. Distance is along the transect relative to origin (see Table 7-1).

To obtain an estimate of the main tidal current amplitudes and residual velocities a harmonic analysis was performed on the ADCP flow data. Note that the short time period of observations allows to resolve the dominant semidiurnal tide only; we are unable to distinguish between the different semidiurnal tides (e.g. S_2, N_2 and M_2). The M_2 tide therefore represents all semidiurnal tides. Additionally, Nyquist-frequency restrictions allow to resolve the quarter-diurnal amplitude (M_4) and sixth-diurnal (M_6) overtides only. M_4 being the double frequency of the M_2 tide and generated by nonlinear terms of advection, continuity and bottom friction, while M_6 results from friction (Aubrey and Speer, 1985; Parker, 1991). The M_2, M_4 and M_6 constituents are resolved in major and minor axis of the tidal ellipses. In the confined deep channels of Marsdiep and Breewijd the major and minor direction are representative for the along-channel and the across-channel component of the velocity respectively. The measured vertical and horizontal

tides are well represented when distortion of the fundamental M_2 component with its non-linear higher harmonics (M_4 and M_6) is included (not shown).

Analysis of the ADCP flow observations reveals complex residual flow patterns in the measured transects. Relative large longitudinal residual flow velocities (Fig. 7-3a) and significant smaller transverse velocities (Fig. 7-3b) are observed in Marsdiep (right panels) and Breewijd (left panels). The longitudinal velocity distribution of Marsdiep is typical for density driven circulations; salinity differences between ebb flow of lower salinity and flood flow of higher salinity results in the upper layers of Marsdiep being dominated by a large ebb residual and a flood dominance in the lower part of the transect.

The residual flow field of Marsdiep is dominated by this transversally uniform vertical structure a more diagonal structure is observed in Breewijd. Longitudinal residual flood flow in excess of 0.3 m/s in the direction of the Wadden Sea is observed along the North-Holland coastline in the deeper part of Breewijd. Along the Noorderhaaks equally strong residual ebb velocities are directed onto the ebb-tidal delta (Fig. 7-3a left). This tilted residual flow pattern might (partly) be related to the depth variation of the transect. Since the horizontal pressure gradient is proportional to depth below water level, the tendency of the heavier seawater to replace the lighter freshwater is stronger in the deeper part of the channel then along the Noorderhaaks shoal. Therefore landward flow dominated the deeper channel, and to retain mass conservation, the seaward flow is concentrated along Noorderhaaks (Valle-Levinson and Lwiza, 1995).

The velocity amplitudes of the semidiurnal component in Marsdiep exceed the amplitudes in Breewijd (Fig. 7-3c left and right) due to constriction of streamlines in the narrow inlet gorge and the resulting Bernoulli-type acceleration of flow. Maximum velocities are observed in the central part of the channels, decreasing due to friction towards the channel embankments and bed. The associated amplitude growth from Breewijd to Marsdiep is not limited to the M_2 but also the overtide amplitudes of the M_4 and especially the M_6 increase (Fig. 7-3d and e respectively). In Breewijd the overtides are reasonably uniformly distributed over the cross-sections with M_4 variations between 0.1 to 0.2 m/s; the M_6 is smaller, 0.05 - 0.1 m/s. In Marsdiep the M_4 and M_6 amplitudes are larger and of near-equal magnitude (0.1-0.3 m/s). Strongest overtides are observed in the top and central part of the transect.

The internal generation of overtides is commonly related to non-linearity's in advection, continuity and bottom friction (Speer *et al.*, 1991). The large increase in overtides between Breewijd and Marsdiep may also have been caused by increased friction due to the transition from the wider ebb-delta channel Breewijd to the narrow inlet gorge, transferring energy from the M_2 to the M_4 and M_6 (Blanton, 2002).

7.3.2 Delft3D Model

Main characteristics

The Delft3D online morphology system is a state-of-the-art model capable to simulate water motion and sediment transports (Lesser *et al.*, 2004). Delft3D-FLOW forms the centre of the model system simulating flow, in this case, due to tidal and density-driven forcing (as meteorological contributions are absent) by solving the well-known unsteady shallow-water equations (Stelling, 1984). The Alternating Direction Implicit method is used to solve the vertical and horizontal momentum and continuity equations (Stelling, 1984; Leendertse, 1987) on a staggered grid.

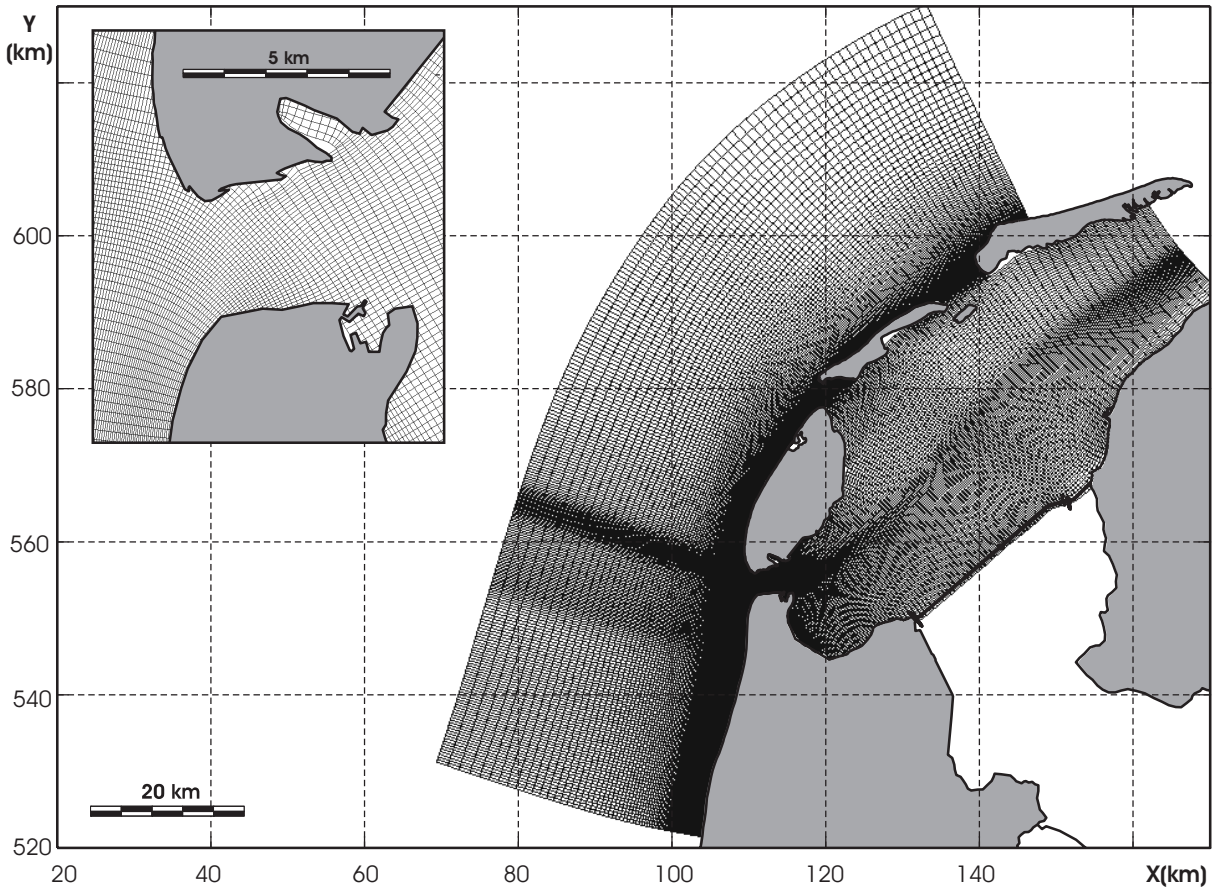

Figure 7-4**:** Delft3D model grid, insert shows Texel inlet in more detail.

Simulations have been made using an application that contains the Texel Inlet and adjacent coastlines; the so-called Texel Outer Delta (*TOD*) model (more details are presented in Elias *et al.*, 2005; Elias *et al.*, 2006, [Chapter 4 and 6 of this thesis]). The Eierlandse Gat and Vlie inlet are included in the model domain to enable the simulation of the important internal residual volume transport between Vlie and Texel Inlet. The well-structured, orthogonal curvilinear grid has 38311 points, with a maximum resolution of 80x120 m at the location of Texel Inlet (Fig. 7-4). The grid has been updated with 10 σ-layers spaced irregularly in the vertical; relative layer thicknesses from bottom to surface layer are 2, 4, 6, 10, 18, 24, 20, 10, 4 and 2% of the vertical respectively.

The time step for the flow computations is 15 seconds. Default settings of 1.0 m^2/s and 1.0 m^2/s for respectively the uniform horizontal eddy viscosity and eddy diffusivity coefficients have been applied. The k-ε turbulence closure model was used. The geographic latitude was specified to include the Coriolis force.

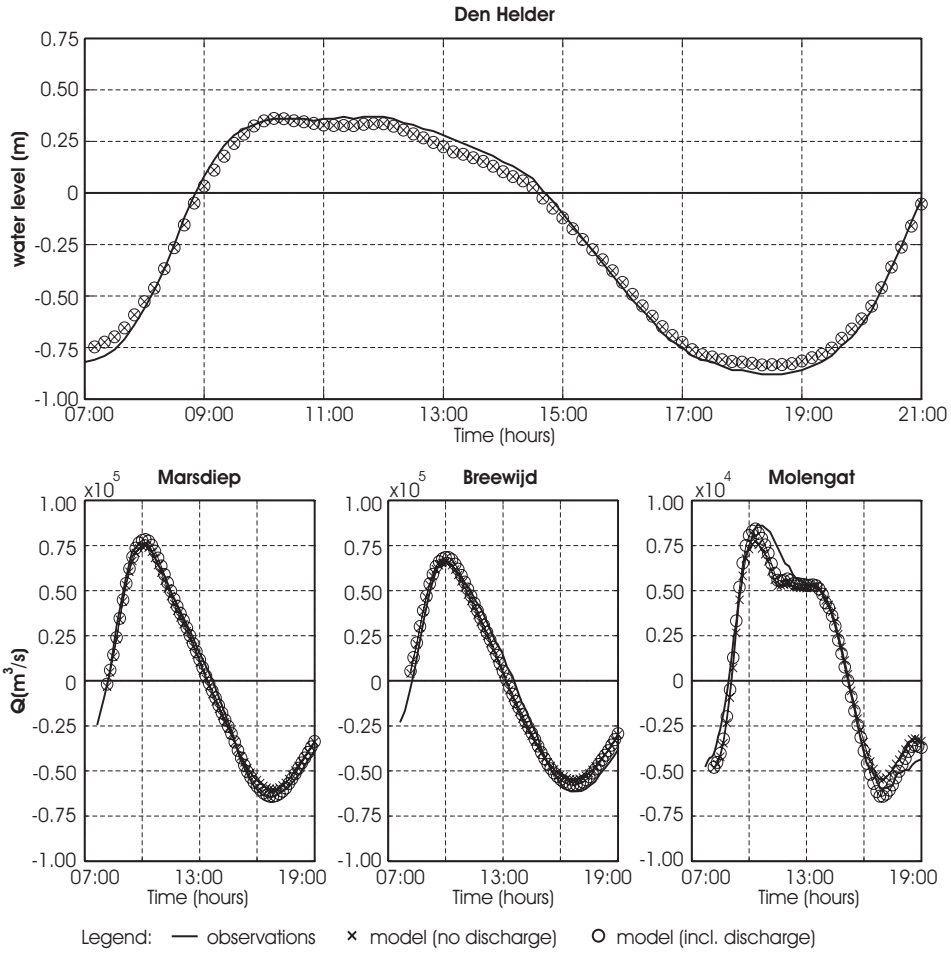

Figure 7-5 top: Validation of model results for measured water levels in Den Helder tidal station . Bottom (from left to right) discharges in the main transects of Marsdiep, Breewijd and Molengat. Crosses represent results for the homogenous simulation and circles represent the stratified results (note the difference in discharge scaling of Molengat).

The North-Holland coastline, the landward coastline in the basin, and the island coastlines form closed boundaries (free-slip conditions). The northern basin periphery is chosen on the Terschelling tidal divide and prescribed as a zero-velocity boundary. Open-sea boundaries are located 'far away' outside the sphere of influence of Texel Inlet and prescribed as time-varying water level elevations. The forcing conditions (water levels) have been derived from nesting the *TOD*-model in the larger-scale PROMISE model that describes the tidal movement of the southern North Sea with a realistic tidal height forcing at the northern boundary and in the English Channel (Gerritsen *et al.*, 2001).

The simulated water levels for the Den Helder tidal station were compared with the observed water levels. Small corrections (< 0.05 m) on the open-sea boundary conditions have been made until a good correspondence is observed between observations and model

results (Fig. 7-5, top). Bottom roughness is used as tuning parameter to calibrate the flow. Cross-sectional averaged discharges have been computed for the channels Marsdiep, Breewijd and Molengat and compared to the observations, see Fig. 7-5 (bottom panels). For this case-study a Manning coefficient of 0.029 $m^{1/3}/s$ presents best results.

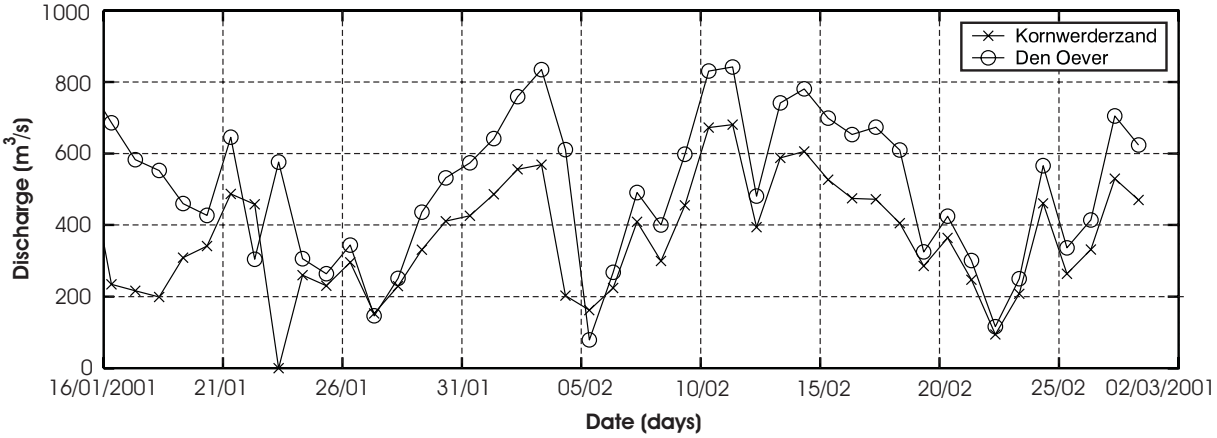

Figure 7-6: Measured fresh-water discharges through discharge sluices in Den Oever en Kornwerderzand (16-01 / 02-03-2001).

Simulations were made inclusive (*'realistic simulation'*) and exclusive (*'tidal simulation'*) of fresh-water discharge in the basin. Fresh-water discharges are prescribed by hourly observations of fresh-water discharges (see Fig. 7-6) at the location of the Kornwerderzand and Den Oever discharge sluices. In addition to these discharges in the basin, the salinity in Texel Inlet is also influenced by the fresh water from the river Rhine that propagates northward along the Holland coast. During the observations a relative constant salinity of 32 ppt. was observed and prescribed on the open-sea boundaries.

Estimates of sediment transport rates are obtained by including the Online Morphology add-on to the flow simulation. Delft3D Online Morphology (release 5.25.02.r.1) computes sediment transport within the flow simulation. Both suspended-load and bed-load sediment transport of non-cohesive sediment are computed each computational time-step and bed levels are updated. The underlying transport formulations of Van Rijn (1993) are used. The transport formulations consist of separate formulae for bed and suspended load, taking into account the critical shear stress for initiation of motion and adjustment for bed-slope effects. See Lesser *et al.* (2004) and Walstra and Van Rijn (2003) for detailed model descriptions.

Default settings for the calculation of sediment transports and morphological change are used. No morphological acceleration is applied; a similar time step for the hydrodynamic and morphodynamic calculations. Effects of sediment concentrations on the density are included. Bottom sediment characteristics for the morphological computation include: the use of a single fraction of non-cohesive sand ($d_{50} = 250\ \mu$m), no hindered settling, a sediment density of 2650 kg/m^3, a dry bed density of 1600 kg/m^3 and an initial sediment mass at the bed of 16000 kg/m^2.

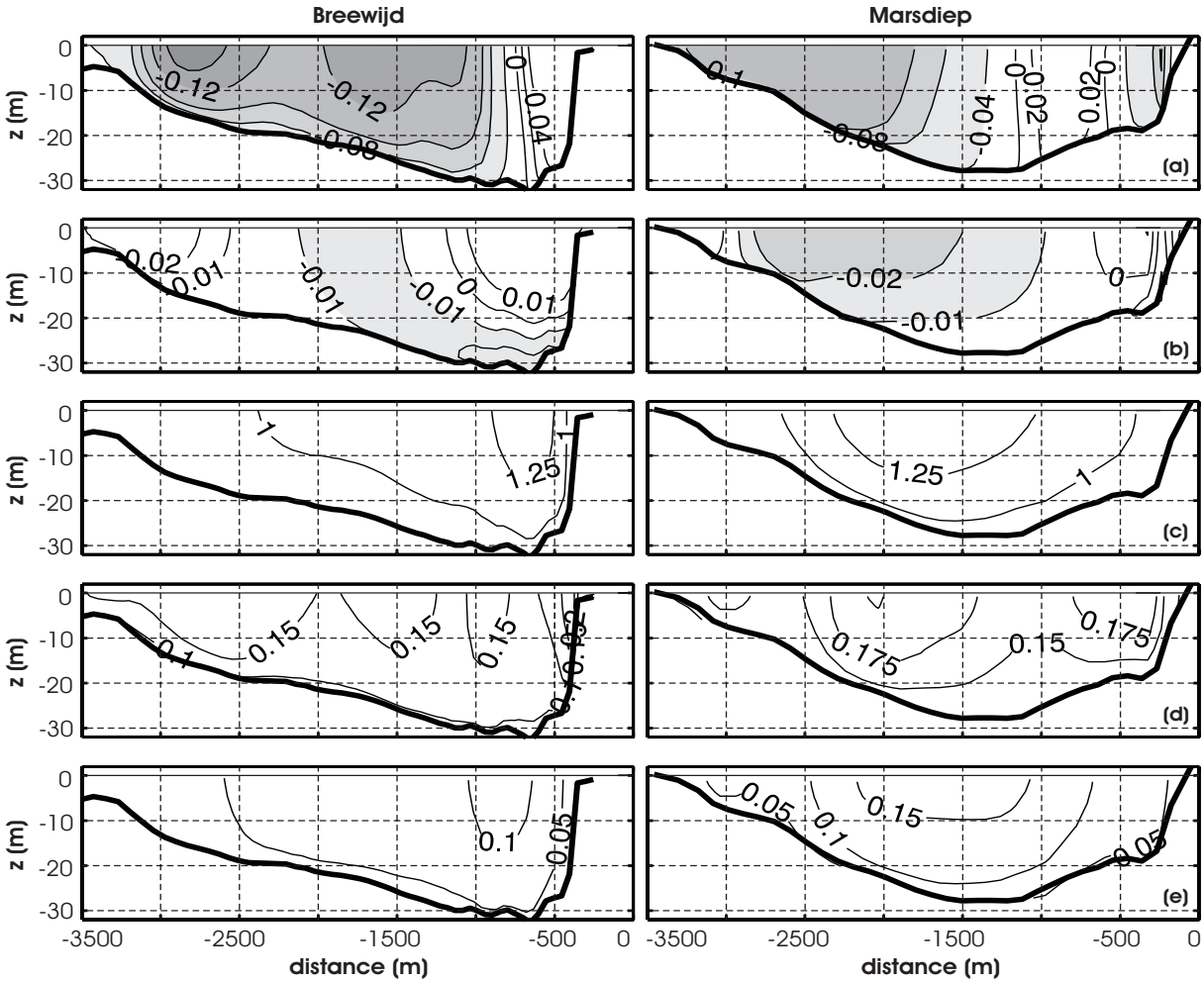

Figure 7-7: Harmonically analyzed '*tidal*' flow results (no fresh-water discharge) for Breewijd (left) and Marsdiep (right). From top to bottom: (a) Residual flow in major and (b) minor direction (gray is ebb-dominant and white flood dominant), velocity amplitudes of (c) M_2, (d) M_4 and (e) M_6.

Prior to the actual computations a number of sensitivity and validation runs were executed. The end results of each of these runs were used as start-up for the next simulations to dissipate the induced errors due to the discrepancy between boundary conditions and initial state. In the final computations a spin-up time of over a year was effectively reached ensuring a well-established back-ground estuarine circulation pattern.

Residual flow in Marsdiep and Breewijd

Validation of the flow velocities focuses on the Marsdiep and Breewijd transect. The simulated flow model results for both transects were harmonically analyzed in a same manner as the ADCP observations, for the *'tidal'* and the *'realistic'* simulation. Fig. 7-7 and 7-8 present the results.

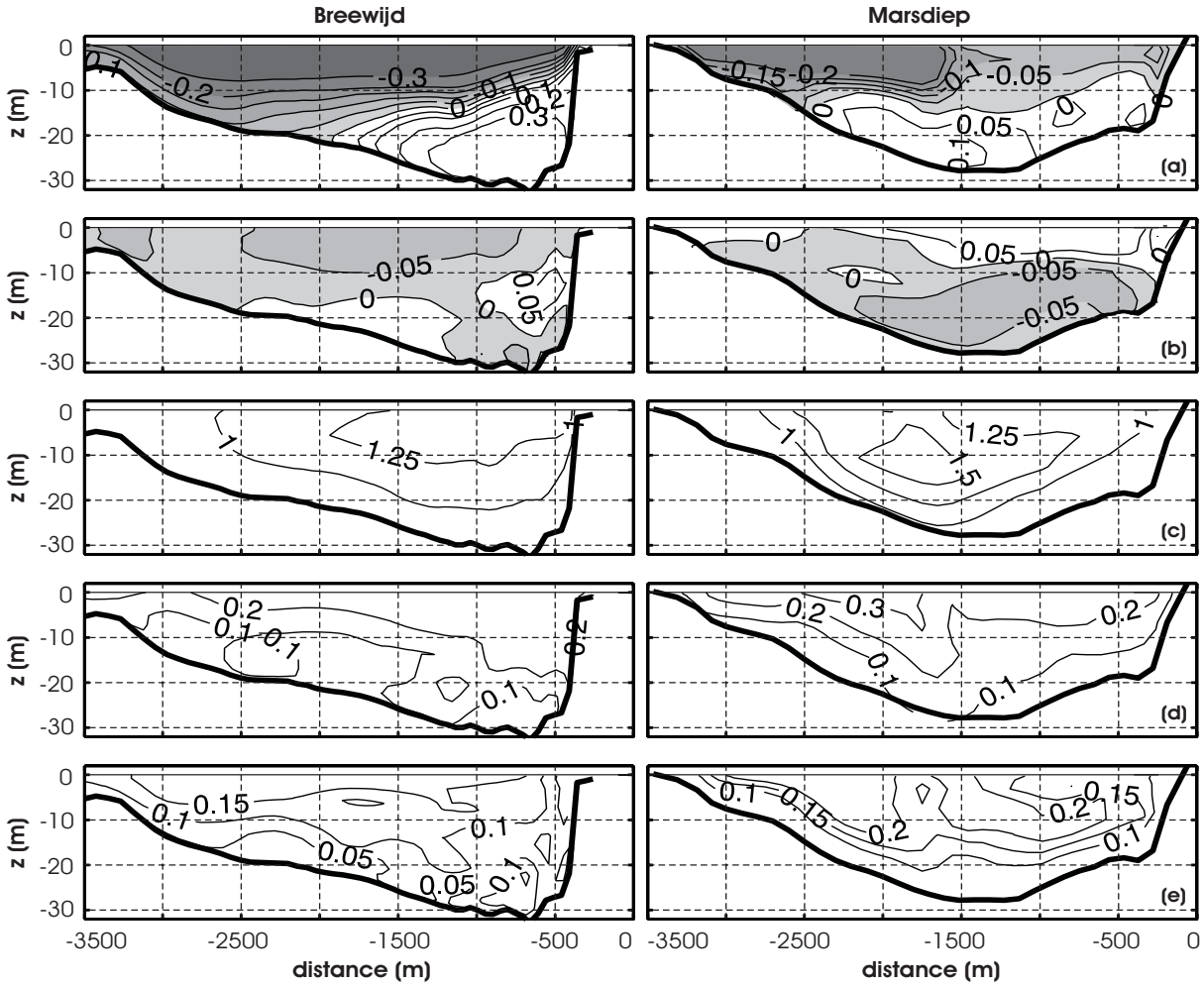

Figure 7-8: Harmonically analyzed *'realistic'* flow results (including fresh-water discharge) for Breewijd (left) and Marsdiep (right). From top to bottom: (a) Residual flow in major and (b) minor direction (gray is ebb-dominant and white flood dominant), velocity amplitudes of (c) M_2, (d) M_4 and (e) M_6.

The main features of the residual flow field are both qualitatively as quantitatively reasonably well reproduced if freshwater discharges in the basin are included (compare Fig. 7-8 and Fig. 7-3). Due to density differences the structure of the tidal residual flow changes significantly; the flow patterns alter from a situation of horizontal shear (Fig. 7-7) to predominant vertical shear in Marsdiep and diagonal shear in Breewijd (Fig. 7-8). The lateral and vertical segregation in ebb- and flood-dominant parts of both the Marsdiep and Breewijd are adequately reproduced although residual flow magnitudes are somewhat over predicted. Modelled tidal amplitudes of the semi-diurnal, quarter-diurnal and sixth-diurnal are comparable in pattern and magnitude to the observations. Noteworthy is the observed and modelled transfer of energy from the M_2 to the M_4 and M_6 between Breewijd and Marsdiep. The lesser detail in the model results is due to the relative coarse 10-layer schematization in the vertical.

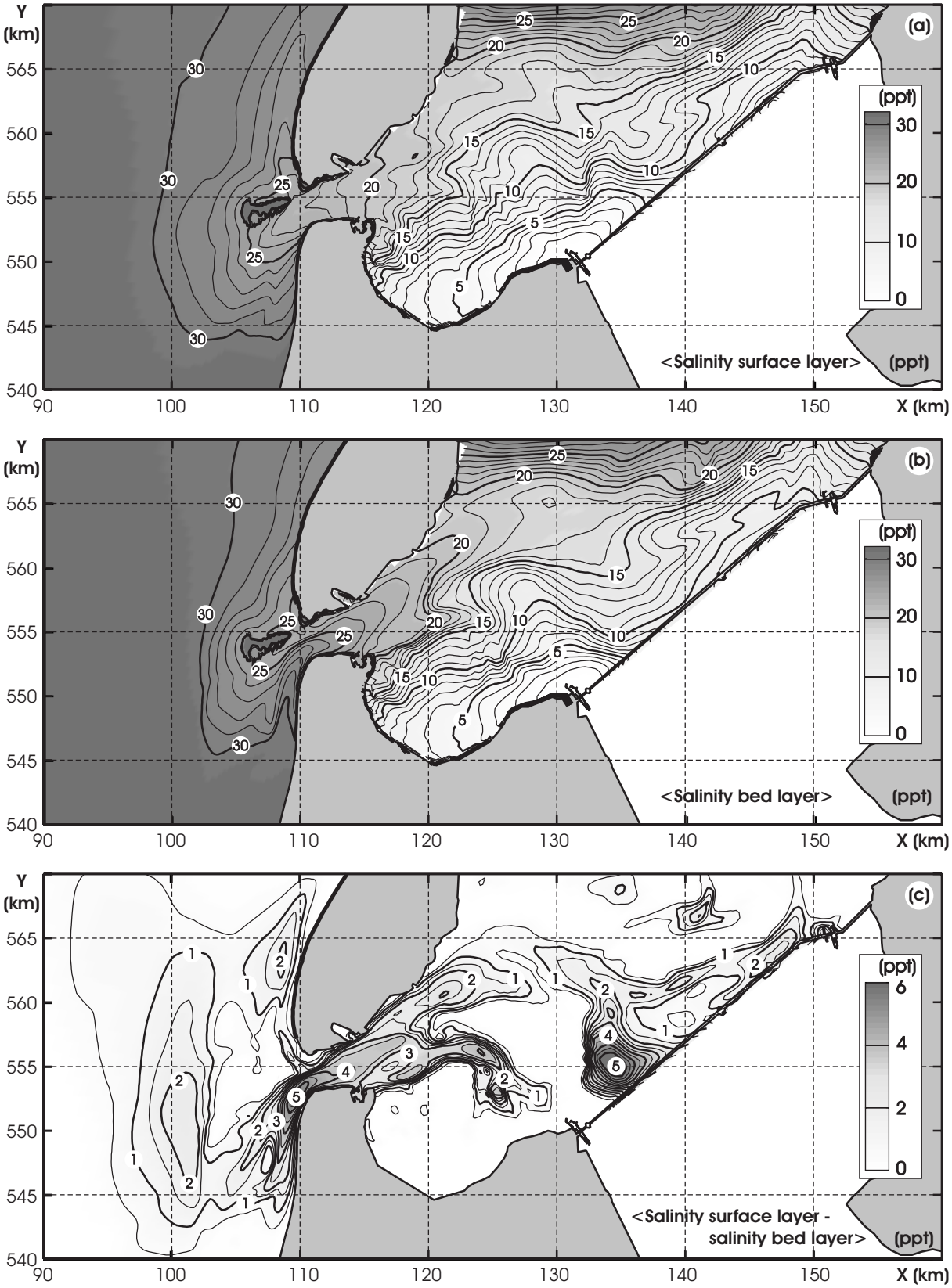

Figure 7-9: Modelled tide-averaged salinity values for (a) the surface layer, (b) the bed layer and (c) salinity difference between surface and bed layer.

Stratification

Unfortunately, salinity observations are not present for the period of interest therefore validation material is absent. As part of a continuous measurement campaign a point measurement of surface salinity in Marsdiep was obtained by Rijkswaterstaat on 22-01-2001 (24 ppt.) and on 19-02-2001 (26 ppt.). These values are in the range of the model predictions (Fig. 7-9). The longitudinal distribution of the salinities in the basin has similar characteristics as the distributions presented by Postma (1954) and Zimmerman (1976). Their studies showed that on the relative shallow shoal areas turbulence generated by friction between tidal water motion and bed is capable of completely mixing the water column and vertically conditions are relative homogeneous (see Fig. 7-9a). Towards the inlet gorge salinity magnitudes increase towards 20 to 25 ppt. in Marsdiep. On the ebb-tidal delta in southward direction salinity in the surface layer increases towards the open sea magnitude of 32 ppt. The southward extension of fresh-water influence is limited to the ebb-delta domain. In northward direction the fresh-water influence extends along the coastline.

The longitudinal salinity gradients are largest in the basin (Fig. 7-9c). Such gradients are known to drive residual flow and sediment transport of fine marine sediments (Dronkers, 1984; Dyer, 1986). These gradients drive a shear flow circulation with low density water flowing offshore at the surface and higher density water moving shoreward at the bottom (Simpson *et al.* 1990). In the inlet gorge vertical salinity gradients are maximal (see Fig. 7-9c) due to saline water in the near-bed region. This distinct, salt-wedge like feature, results from the density difference between open sea and basin water, and from the preferential flow paths during ebb and flood. Ebb flow from the basin mainly originates from Texelstroom. Due to inertia of flow the major part of the flow is directed from Texelstroom along the Texel coast and along the landward side of Noorderhaaks onto the ebb-tidal delta. Flood enters the inlet from the south along the North-Holland coastline, where it accelerates around the tip of Helderse Zeewering due to convergence of flow streamlines. Due to the higher salinity flood flow concentrates in the near-bed region along the coast during flood (Fig. 7-9b), while fresh-water outflow dominates the surface layers (Fig. 7-9a) along the Noorderhaaks shoal.

7.4 Model Results

7.4.1 Effects of stratification on sediment transport

A first estimate on the importance of density differences for sediment transport of non-cohesive sediment (sand) of medium grain size ($d_{50} = 250\ \mu$m) is obtained by plotting the difference between the residual transport magnitude of the *'tidal'* (1) and *'realistic'* experiment (2), computed accordingly,

$$dS = \sqrt{\left(\langle s_{x1}\rangle - \langle s_{x2}\rangle\right)^2 + \left(\langle s_{y1}\rangle - \langle s_{y2}\rangle\right)^2} \tag{7.1}$$

where $<s_x>$ and $<s_y>$ are the tide-averaged flow and sediment transport values in x and y direction respectively (see Fig. 7-10). Main differences are observed in Texelstroom, Marsdiep and the proximal ebb-delta channels where the vertical salinity variation and flow velocities most pronounced (Fig. 7-9). In the basin where the longitudinal differences prevail a small influence on the velocities can be observed (not shown) these might be important for fine-grained (cohesive) sediments, but did not result in significant sand transports. Further analysis therefore focuses on the inlet throat were transport differences are largest.

7.4.2 Residual flow and sediment transport

The residual flow field (for bed velocities Fig. 7-12a) is obtained from averaging the flow vector fields over the tidal period (in 10 minute intervals). The distortion of the alongshore-propagating tidal wave due to interaction with the complex bed bathymetry of the ebb-tidal delta and the inlet currents creates a complex residual circulation. The inlet gorge and ebb-tidal delta are dominated by the ebb residual. Ebb-tidal currents through Texelstroom accelerate in the narrow constriction of the inlet gorge and the outflow dominates the updrift part of the ebb-tidal delta. Maximum tidal residual velocities are in the order of 0.15 m/s, whereas maximum flow velocities are in the order of 1.5 m/s. Strongest residual currents are observed in the inlet gorge where the cross-sectional area is minimal. In correspondence to long-term ferry observations (Ridderinkhof *et al.*, 2002) an internal dominance of ebb flow along the North-Holland coastline and flood flow along the Texel coastline is reproduced. Ebb tidal flow is directed primary from Marsdiep into Breewijd, and into the Schulpengat, Nieuwe Breewijd and Nieuwe Schulpengat channels.

Fresh-water discharge into the basin increases the residual flow velocities considerably (Fig. 7-12b). In the realistic simulation residual flow velocities of 0.3 m/s are observed locally, and especially the near-bed velocities in Helsdeur are distinctively flood dominated. Analysis of the Breewijd transect (Fig. 7-8) shows that density differences tilt the gravitational flow from a situation of horizontal shear to a more lateral shear in Marsdiep and diagonal shear in Breewijd. As a result ebb and flood are more distinctively separated; flood flow concentrates in the lower regions along the North-Holland coast due

to larger salinities, and ebb flow in the upper layers along Noorderhaaks (Fig. 7-9). Especially for sand transport these augmented (residual) near-bed flood velocities induce a large sediment transport in Breewijd towards Marsdiep (compare Fig. 7-12b and d).

More insight into the influence of density differences on sediment transport and flow is obtained by analysis of the instantaneous velocities. Three representative points have been selected in Marsdiep and Breewijd (see Fig 7-12a for location of *P1*, *P2* and *P3*).

As a result of the phase lag between horizontal and vertical tide (see Fig. 7-2) and inertia of flow, ebb velocities dominate along the Texel coastline and Noorderhaaks as flood flow enters the inlet along the North-Holland coastline. An approximate 1/2 hour phase difference between initiation of flood along the North-Holland coastline and along the Noorderhaaks (compare *P2* and *P3*) exists. Flood flow accelerates around the tip of Helderse Zeewering, due to contraction, and locally surface velocities over 1.5 m/s are observed. An approximate 1-hour phase lag develops between the initiation of ebb along Noorderhaaks and initiation of ebb along the North-Holland coast (compare *P2* and *P3*). Contraction and acceleration of ebb flow at the tip of Helderse Zeewering is not observed; due to inertia of flow ebb is directed seaward from Texelstroom along the Texel coastline and Nooderhaaks. Largest residual transports are observed in the landward part of Breewijd (*P3*) where the asymmetry between maximum flood (1.6 m/s) and ebb velocities (1.1 m/s) is largest.

As a result of density-driven flow the residual (Fig. 7-12) and momentaneous flow velocities change considerably (compare Fig. 7-11, left and right panels). In Marsdiep (*P1*) a phase-lag develops between the initiation of ebb (or flood) between surface and bed layers. Near the bed the flood period increases, while in the surface layers the ebb velocities are augmented. The larger near-bed ebb-flood asymmetry augments sediment import. A contrasting behaviour is observed between the seaward (*P2*) and landward part (*P3*) of Breewijd. Similar to Marsdiep a phase-lag develops between the ebb-flood initiation in surface and bed layers. Along Noorderhaaks the large increase in ebb-velocities increases the ebb-dominant transport towards the ebb-tidal delta. This increase is small compared to the augmented flood transports along the North-Holland coastline. Here the large flood velocities increase the transports, but the major increase in residual transports results from the near-zero ebb transports. During ebb a near-zero velocity zone develops in the lee-side of Helderse Zeewering where sediment settles. The asymmetry between near-zero ebb transports and augmented flood transports explains the large flood-dominant residual transport vectors of Figure 7-12d.

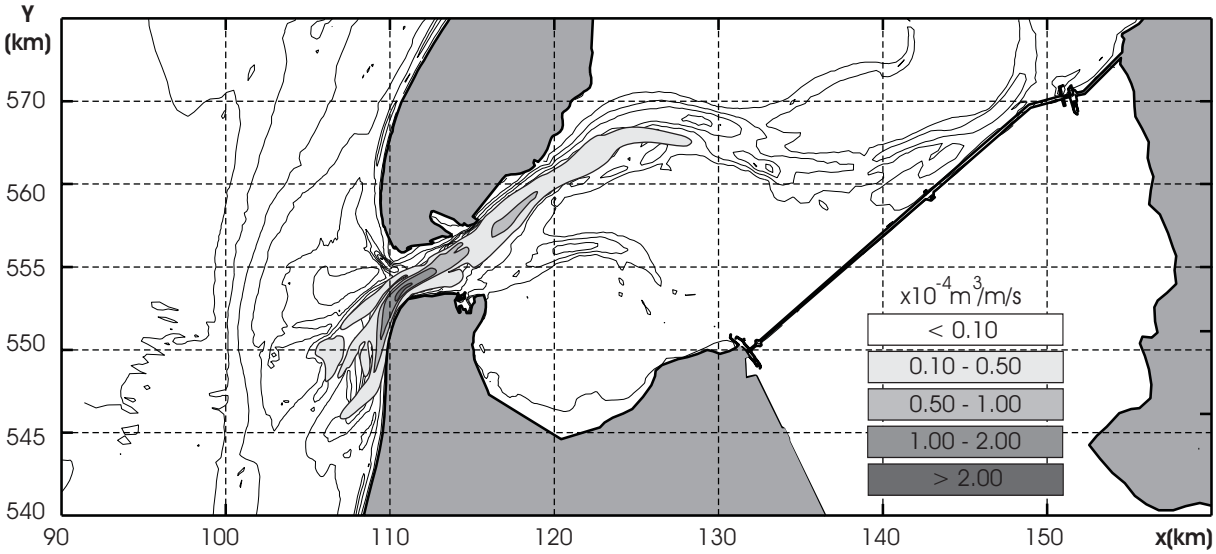

Figure 7-10: Differences in tide-averaged sediment transport magnitudes, $<dS>$ between the *'tidal'* and *'realistic'* experiment.

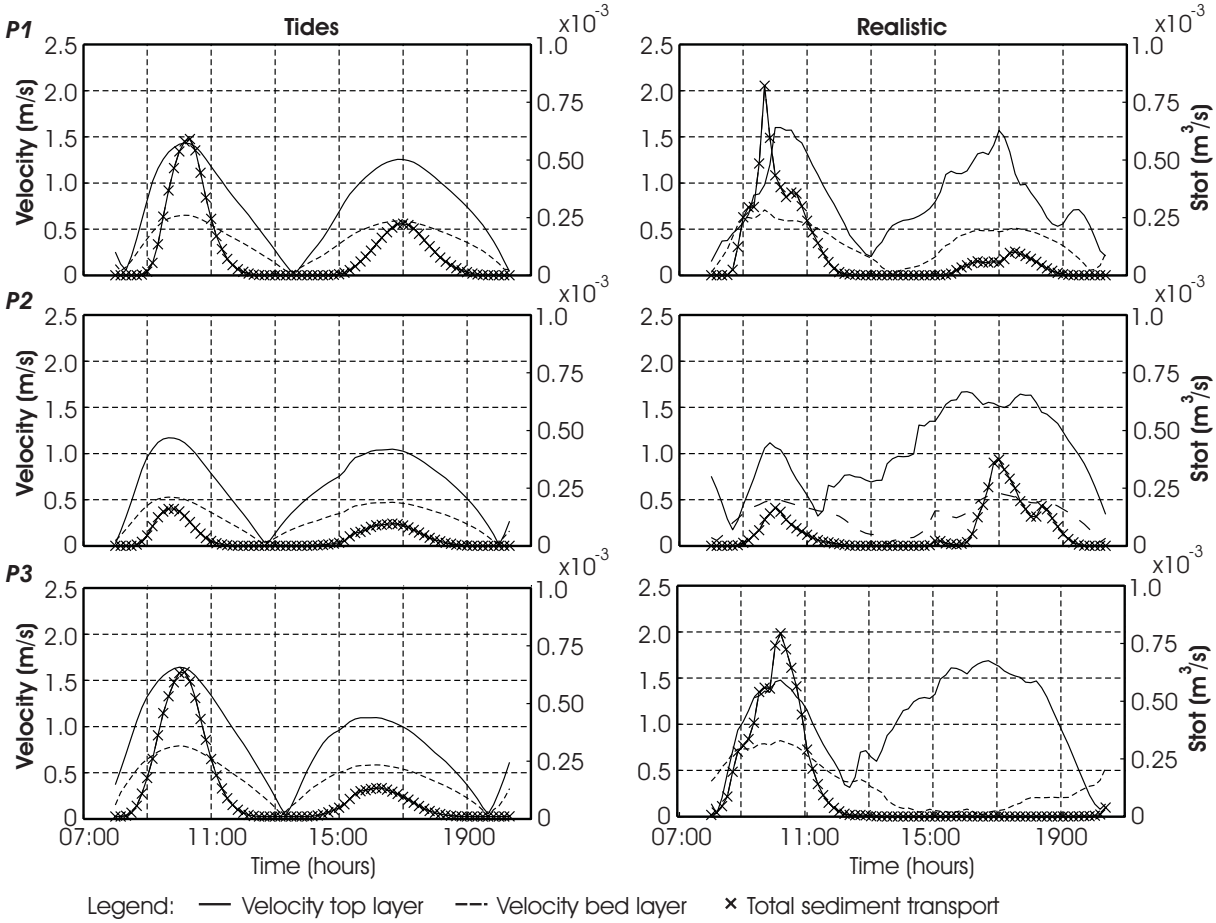

Fig 7-11: Time series for flow in the bed and surface layer, and total sediment transports in points *P1*, *P2* and *P3* (top to bottom) for the *'tidal'* (left) and *'realistic'* experiment (right).

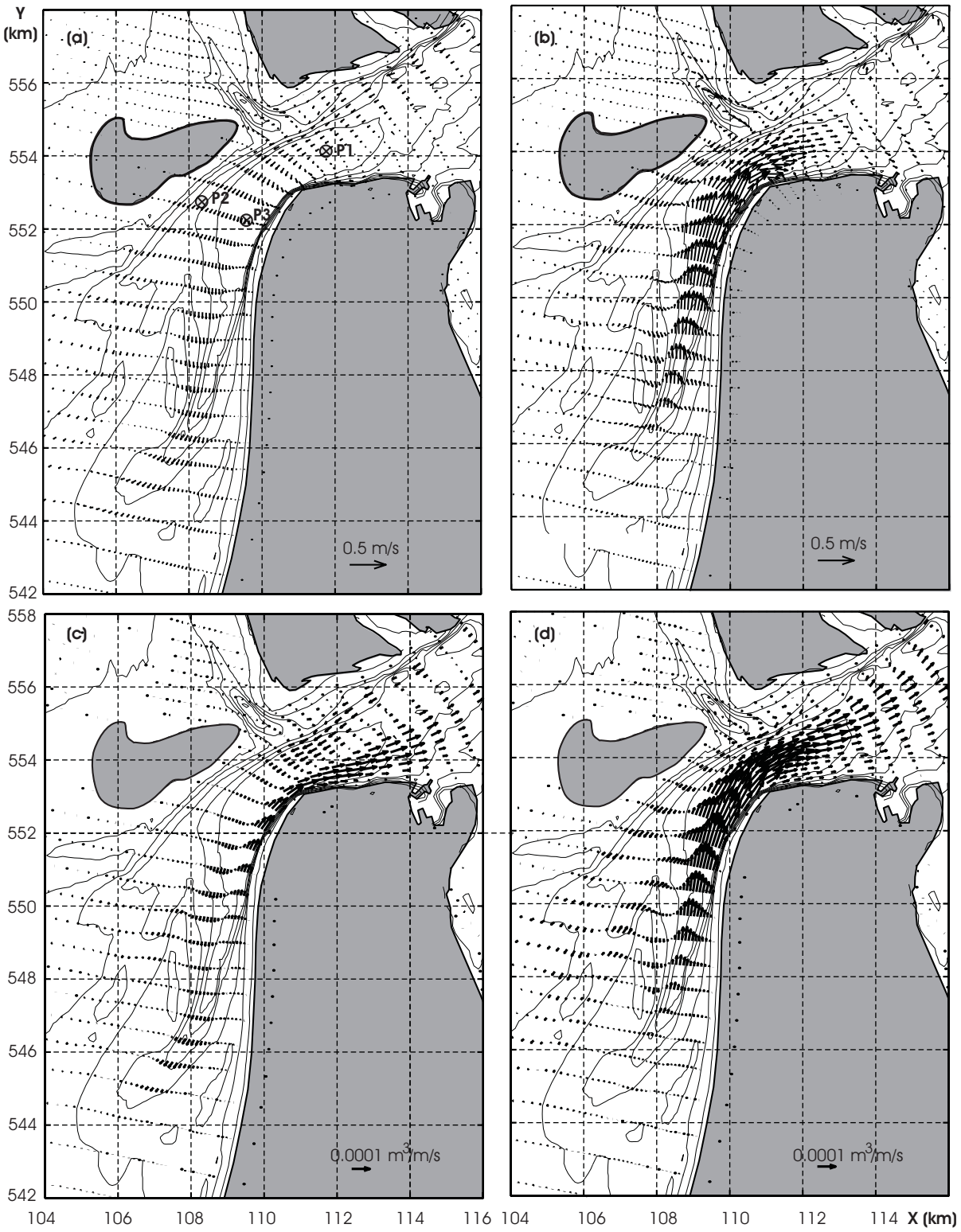

Figure 7-12: Residual bed velocities (top) and residual total transports for the *'tidal'* (left) and *'realistic'* experiment (right).

7.5 Discussion

The main mechanisms for generating tidal residual velocities in the Western Wadden Sea were discussed in detail by Ridderinkhof (1988a; 1988b). Ridderinkhof used a numerical model of the western part of the Dutch Wadden Sea, estimated the different terms in the tidal momentum equations and showed that the tidally driven residual current velocity field in the basin is dominated by isolated residual eddies, which are an order of magnitude larger than the residual velocities associated with the throughflow from Vlie to Texel Inlet. Near the inlets the eddies result from variations in channel geometry and bed structures. Among others Geyer and Signell (1990), Geyer (1993) indicate the local nonlinear transfer of tidal energy around headlands, while Zimmerman (1981) showed the formation of counter rotating eddies due to vorticity production by frictional torque. In Texel Inlet especially the strong curvature of Helderse Zeewering has a pronounced influence on the residual flow patterns as is illustrated by the significant differences between patterns and magnitudes of the residual flow and amplitudes between the closely located Breewijd and Marsdiep transects (compare Fig. 7-7 and 7-8, left and right).

During periods of high freshwater discharge density differences are important for the residual flow patterns in the inlet gorge and main ebb-delta channels. Density differences are essential to create a tilt of the tidal flow from a situation of horizontal shear (Fig. 7-7) to a more lateral shear in Marsdiep and diagonal shear in Breewijd (Fig. 7-8). Ebb and flood flow are more distinctively separated; flood flow concentrates in the lower layers of the water column along the North-Holland coast due to larger salinities, and ebb flow of smaller density prevails in the upper layers along Noorderhaaks. As a result, augmented residual ebb-flow along the Texel coastline and Noorderhaaks, and residual flood flow along the North-Holland coastline occur, differences in flow magnitudes of 0.2 m/s are observed, that can drive considerable residual sediment transport into Marsdiep and Breewijd; see Fig. 7-10 and Fig. 7-12.

The strength of the density-driven flow usually relates to the salinity gradient. Studies by e.g Dronkers (1984), Dyer (1986) and van de Kreeke and Zimmerman (1990) showed the importance of longitudinal salinity gradients for driving residual flow and sediment transport of fine marine sediments. In the basin where the longitudinal gradients are largest sand transports are small. In the inlet gorge and proximal ebb channels of Texel Inlet longitudinal salinity gradients are relative small compared to the gradients in the basin, but vertical salinity gradients maximize. Along the North-Holland coast a large vertical salinity difference exists between bed and surface layer (tilting the tidal flow and increasing residual velocities). This salinity difference is related to two different processes: firstly, a lateral variation in depth, since the horizontal pressure gradient is proportional to the depth below water level, the tendency of the heavier seawater to replace the lighter freshwater is stronger in the deeper part of the channel then in the shallow part along Noorderhaaks (Hamrick, 1979; Wong, 1994). Secondly, the phase difference between the horizontal and vertical tide. Due to inertia of flow relative large ebb-velocities dominate in Marsdiep, concentrated along Noorderhaaks. Flood of higher salinity therefore enters along the North-Holland coastline in the near-bed region. Contraction of flow at the tip of Helderse Zeewering increases the velocities considerably (see Fig. 7-11 *P3*). During ebb in the lee-side of Helderse Zeewering a low velocity zone develops as fresher

basin water flows over the denser open-sea water forming an efficient sediment trap. Augmented transports during flood and reduced transports during ebb explain the large residual influx of sediment towards the basin.

An estimate of the importance of the density differences for residual sediment transport of non-cohesive sediment with a d_{50} of 250 μm was obtained using the sediment transport formulations of Van Rijn (1993). Note that the modelled sediment transports are not a realistic depiction of the transport rates in Texel Inlet. A single grain diameter of d_{50} of 250 μm used in the model is representative for the mean grain size of the entire ebb-tidal delta, but in reality grain diameters vary significantly from 150 μm on the ebb-delta shoals to over 450 μm in the deeper channels (Sha, 1990). Especially the larger grain diameters in Marsdiep and Breewijd (and the presence of erosion resistant layers) could limit the sediment transport rates considerably. Nevertheless, relatively, the comparison of the tidal and realistic simulation illustrates that density differences can cause significant sediment transport of medium grain-sized sand.

The results presented in this study show that stratification is important for the residual flow distribution in the inlet gorge and ebb-tidal delta. Moreover, the altered flow distributions have potential large impact on the residual sediment transports. However, the analyzed period does not provide a representative depiction of the long-term (e.g. year-averaged) conditions; the results represent a situation wherein stratification in Texel Inlet was at its peak. The measured monthly-mean discharges exceeded 900 m^3/s and during the period of observations wind and waves were absent, therefore mixing on the ebb-tidal delta was minimal. Such conditions are only observed sporadically; 95 % of the observations during the period 1977 - 1990 show smaller discharge values (see Fig. 7-1). Additional model simulations and/or analysis of the ongoing NIOZ-ferry measurements (Ridderinkhof *et al.*, 2002) might present more insight in the long-term effects of stratification on the sediment exchange between ebb-tidal delta and basin.

7.6 Conclusion

During a period of high fresh-water discharge in the basin thirteen-hour measurements of the vertical flow field in the inlet gorge (Marsdiep) and main ebb-delta channel (Breewijd) of Texel Inlet were obtained simultaneously using ship-mounted broadband Acoustic Doppler Current Profilers. Harmonic analysis of this data revealed complex residual flow patterns. Main features of the residual flow field in Marsdiep and Breewijd are the dominance of longitudinal residual flow velocities over the transverse velocities, and a typical density-driven distribution of ebb-dominant flow in the top layers along Noorderhaaks and flood-dominant flow in the near-bed regions along the coastline.

The Delft3D model is capable of representing the main characteristics of the vertical flow patterns if fresh-water discharge in the basin is included. Model results show that density differences are essential to tilt the tidal flow from a situation of horizontal shear to a more lateral shear in Marsdiep and diagonal shear in Breewijd. As a result ebb and flood are more distinctively separated; flood flow concentrates in the lower regions along the

North-Holland coast due to larger salinities, and ebb flow of smaller density prevails in the upper layers along Noorderhaaks. The altered residual flow patterns and magnitudes have potential large impact on the residual sand transport in the inlet gorge and proximal ebb-delta channels. Maximum sediment transports of non-cohesive sediment (d_{50} of 250 μm) were modelled at the location of the largest vertical salinity gradients and residual flow velocities. In the basin, where longitudinal salinity gradients prevailed, the density-driven sand transports were minor.

7.7 Acknowledgements

The work herein was carried out as co-operation between RIKZ (Dutch National Institute for Coastal and Marine Management) and Delft University of Technology. Funding was provided by the Dr. Ir. Cornelis Lely Foundation and the Delft Cluster Project: Coasts 03.01.03. Data were made available by the Directorate-General of Public Works and Water Management. The Delft3D model was made available by WL | Delft Hydraulics. Tidal analysis tools were provided by dr. J.G. Bonekamp. The authors thank ir. M. Buisman, dr. J. Cleveringa, Prof. J. van de Kreeke, Prof. J.A. Roelvink and Prof. M.J.F. Stive for their constructive comments and contributions to the manuscript.

Chapter 8
Conclusions and Recommendations

The objective of this study is to increase the fundamental understanding of the behaviour, evolution and physical processes underlying the dynamics of tidal inlets. Texel Inlet is used as a study site because of the abundant data as well as its crucial role in the sand-exchange between the Holland coast and the Wadden Sea.

The morphodynamics of Texel Inlet are studied over a wide range of temporal scales, ranging from long-term descriptions of historic inlet evolution, 1550 A.D. to present, to detailed analyses of hydrodynamics and morphodynamics on the tidal and seasonal process scale. A range of methodologies, varying from morphological interpretation of maps to understand long-term morphological developments and behaviour, to numerical process-based modelling and detailed analysis of field measurements to obtain fundamental knowledge of inlet processes was applied.

This sub-chapter summarizes the conclusion sections of the separate Chapters that make this thesis by addressing the research questions formulated in Chapter 1 (section 1.3.2). An additional section (8.2) is included that specifically focuses on the important translation of the obtained scientific research results towards practical coastal maintenance aspects of Texel Inlet and the adjacent coastlines. The final section (8.3) provides recommendations on aspects needing further investigation.

8.1 Conclusions

8.1.1 Determine the characteristics of the 'natural' ebb-tidal delta evolution, and determine the (cumulative) effects of human intervention

Over 400 years of regular bathymetric surveys of Texel Inlet and its ebb-tidal delta form a globally unique morphodynamic dataset. During the inlet's recorded history substantial changes in ebb-tidal delta evolution have occurred under the influence of the cumulative effects of human intervention. Analysis of the ebb-tidal delta evolution shows different stages, each characterized by specific orientations of the main channels and shoals. Prior to construction of extensive coastal defence works on the southern shore of the inlet in 1750 A.D. (predecessors of Helderse Zeewering) the ebb-tidal delta showed a downdrift

asymmetry, while the inlet gorge migrated southward. Periodic shoal breaching and downdrift channel relocation were the dominant mechanisms for sediment bypassing (major shoal bypassing). This period is most representative for the 'natural' behaviour.

After construction of the coastal defence works, a stable ebb-tidal delta with a westward stretching main ebb-channel developed over a period of c. 60 years. Sediment bypassing took place as minor shoal bypassing; the main channel remained in position and smaller parts of the swash platform (periodically) migrated landward over the ebb-tidal delta (e.g. the formation, migration and attachment of *Onrust*). Damming of the Zuiderzee, completed in 1932 A.D., separated the major part of the back-barrier basin and distorted this stable state; a two-stage adaptation of the ebb-tidal delta is observed. The initial (first-stage) response of the ebb-tidal delta lasted approximately 40 years. In this period the changed tidal characteristics of the basin and increased tidal prisms through the inlet forced an asymmetrical ebb-tidal delta development with updrift (southward) directed main channels. Over 200 million m^3 of sand was eroded from the ebb-tidal delta and coastlines (due to scouring of channels) and deposited in the basin.

The *back-barrier steering mechanism* is revealed to trigger the observed morphological developments on the ebb-tidal delta. After closure, the imbalance between the location of the largest residual tidal flow and the presence of tidal channels on the ebb-tidal delta and the balance in the upper part of the basin provides a larger sediment availability during flood than during ebb. This spatially uneven sediment availability plausibly explains why sediment is imported into the basin despite the residual export of flow. Due to the large tidal prism and corresponding significant tidal transports involved, the channels regained an equilibrium state in a faster rate than the shoal areas (e.g. the abandoned ebb-shield Noorderhaaks). The present (second-stage) ebb-tidal delta development is dictated by the ongoing morphological adjustment of these shoal areas. Sand is eroded from the western margin of the ebb-delta and deposited landward under influence of tidal circulation cells, and landward wind- and wave-driven flow. The sediment availability due to landward migration and scouring of the ebb-delta in combination with the transport potential of the large tidal channels explains the ongoing sediment influx, that is estimated to range between 5 and 6 Mm^3/year into the basin.

The well-monitored large-scale changes on the ebb-tidal delta, which were initiated by the construction of the coastal defence works and closure of the Zuiderzee, show that incorporation of inlet modifications and back-barrier processes is vital for a correct description of the ebb-tidal delta dynamics and processes of Texel Inlet.

8.1.2 Determine the present inlet behaviour, the governing processes and dominant physical mechanisms responsible for flow and sediment fluxes.

- What are the characteristics of the water motion and which mechanisms are most dominant?
- What are the characteristics of the sediment transports and which mechanisms are most dominant?
- How does the current field contribute to a net, tidally-averaged, transport of sediments in the tidal inlet; what is the contribution of tidal asymmetries, estuarine circulation, residual currents and waves?

Tidal flow patterns on the ebb-tidal delta are particularly complex due to interaction of the alongshore propagating open-sea tide, the compound ebb-delta bathymetry and the across inlet currents. In the inlet gorge, where the cross-sectional area is minimal, residual velocities are strong being in the order of 0.2 m/s whereas the maximum instantaneous flow velocities are in the order of 2.0 m/s. The seaward-directed residual flow through the inlet of about 115×10^6 m^3/tide results from flood-dominant flow along the North Holland coastline and a larger ebb-dominant component along the coastline of Texel.

The presences of the Noorderhaaks shoal area facing the inlet gorge is of prime importance for the velocity fields. The ebb-jet is primarily directed southwestward (into Nieuwe Schulpengat, Schulpengat and Nieuwe Westgat) due to the orientation of Texelstroom (inertia of flow) and Noorderhaaks deflection. Sheltering by the supra-tidal part of Noorderhaaks results in low-velocity areas westward and northward of this shoal. Flood enters the ebb-delta from the south and flow velocities increase substantially towards the inlet gorge as a funnel shape forms between Noorderhaaks and the North Holland coast wherein velocities accelerate due to decreasing cross-sectional area. Flood dominance along the North Holland coast is further enhanced by time-velocity asymmetry of the tidal currents; maximum flow velocities do not occur at midtide but near maximum ebb or flood. As flood starts relatively large ebb velocities dominate the central part of the channel resulting in flood flow (initially) concentrating along the North Holland coastline. As a result flood velocities particularly increase due to contraction of flow streamlines around the sharp curvature of Helderse Zeewering.

Velocity observations and morphological model simulations during a period of major fresh-water discharge in the basin revealed that density stratification might also play an important role. Vertical density differences between bed and surface layer are largest in the inlet gorge and proximal ebb-tidal delta channels, and tilt the tidal residual flow patterns from a situation of horizontal shear to a more lateral shear in Marsdiep and diagonal shear in Breewijd. As a result ebb and flood velocities are more distinctively separated; flood flow concentrates in the near-bed regions along the coast due to larger salinities and ebb flow of smaller density prevails in the upper layers along the main ebb-delta shoal. The altered residual flow distribution and flow magnitudes have a potentially

large impact on the residual sand transport (import) in the inlet gorge and proximal ebb-delta channels.

Residual velocities in Nieuwe Schulpengat are ebb-dominant along the Bollen van Kijkduin and flood-dominant along the North Holland coast. Discharges through Molengat are minor (~10 %) compared to the large discharge through Marsdiep. On Zuiderhaaks (facing Nieuwe Westgat) a large tidal circulation cell developes; the clockwise rotation results from northward residual flow on the margin of the ebb-delta that interacts with the southwestward ebb current. The combined contributions of the northward diversion of the ebb-flow and contraction of tidal flow around the ebb-delta perimeter results in relatively large residual velocities on the western margin of the ebb delta. Downdrift of Noorderhaaks flow de-accelerates. On the shoal area Noorderlijke Uitlopers of the Noorderhaaks and in the proximal part of Molengat the residual flow is directed towards the inlet (flood dominant). In the northward direction, no pronounced flow dominance is observed in the channel.

Large morphological changes have occurred over the period 1986-2003 despite a relative stability in the shape and form of the main channels. Analysis of the sedimentation-erosion patterns shows that sediment redistribution on the ebb-delta, sediment exchange between ebb-delta and basin, and the local interaction between channels and shoals dictate the present morphological developments. One of the main characteristics of the present day sediment dynamics of Texel inlet is the substantial sediment import into the basin that is estimated to range between 5 to 6 Mm^3/year. This large import is due to:

(1) ***Sediment demand:*** Reanalysis of the basin volume changes shows that the western part of the Wadden Sea still needs sediment to compensate for the loss of inter-tidal area due to Closure of the Zuiderzee. In addition sediments are needed to compensate for the effects of relative sea-level rise.

(2) ***Sediment availability:*** Noorderhaaks can be considered as a relic originating from the pre-closure situation were it was formed as a balance between seaward sediment supply by the ebb-tidal currents through Nieuwe Westgat and landward displacement by wave-driven transports. After closure, with the main channels switching westward, Noorderhaaks forms an abundant source of sediment, located conveniently in front of the inlet, that is redistributed landwards by tides and waves.

(3) ***Sediment transport capacity:*** Sediment transport capacity is present in the form of the large tidal prisms and associated tidal currents in the inlet gorge and proximal part of the ebb-delta channels. The large tidal circulation cell located on Zuiderhaaks and the southwestern part of Noorderhaaks facing Nieuwe Westgat is capable of supplying sediments from the ebb-delta front to the main inlet circulation (wave-driven currents and wave-stirring augment these transports). During ebb, sediments are transported towards Zuiderhaaks enlarging the ebb-dominance, while during flood sediments are transported into the basin which acts as a sediment trap.

Sediment import could not be explained by locally applying the Groen (1967) transport relation to the modeled tidal flow fields as the ebb-residual sediment export dominates over the flood-dominant tidal-asymmetry-driven import. Nevertheless, tidal asymmetries

play an important role in the sediment influx into the Wadden Sea as was shown by running the Delft3D Online Morphology model (using tidal forcing). The sediment influx is dominated by the large flood-dominant transports along the North Holland coastline that exceed the minor ebb transports along the Texel coastline. One of the main factors for the discrepancy between *local* and *complex* model results is the dominance of the suspended-load component over the bed-load. The sediment transport is therefore not only determined by the velocities, but also by the temporal (and spatial) variability of the concentrations. During flood sediment concentrations are higher then during ebb.

The continuous large sediment import into the basin since closure partly results from the sediment demand of the basin in order to adapt to the effects of closure, and additionally sediment is needed to keep in pace with the increase in accommodation due to relative sea-level rise. The availability of sediments on the ebb-tidal delta and transport capacity due to the large tidal velocities are equally important. By running the Delft3D Online Morphology model during various stages of the morphological adaptation process insight in the changing importance of the forcing conditions was obtained. Initially, following the Closure, sediment import into the basin was primarily related to the scouring of large tidal channels along the Texel and North Holland coastlines. This initial response lasted approximately 40 years, until the adaptation of the channels reduced the 'scour-related' transports. Nevertheless a continuous large sediment import remains which is described as a second-stage response. As the tidal channels developed in a southward direction, the main shoal areas were pushed landward, increasing in height and alongshore extension; the western ebb-delta margin might be considered being an abundant source of sediment resulting from the pre-closure channel configuration. Sand is transported landward mainly by tides and waves from the western margin of the ebb-delta front enlarging the landward intra- and supra-tidal shoal area of Noorderhaaks, and the northward and southward extension of the Noorderlijke Uitlopers of Noorderhaaks and Zuiderhaaks respectively. On these shallow shoal areas tidal, wave and wave-breaking related transports increase, while the presence of large tidal channels along the landward sides forms efficient pathways for along-channel sediment transport towards the basin during flood (tides and setup are the main processes). The basin acts as a sediment trap due to its large sediment demand.

In conclusion, tides and set-up are the main driving forces for the sediment transport in the inlet gorge and into the basin. On the ebb-tidal delta, the importance of the individual forcing mechanisms varies spatially as well as temporally. In the large channels on the southern part, tides and setup are the driving forces, while on the shallow shoal areas waves play an increasing role. During rougher 'storm' conditions, wave-driven transports contribute directly to the landward sediment transport. During calm conditions, waves stir-up sediment that are transported by the tidal currents and contribute to seaward expansion of the ebb-tidal delta. A clear example is Noorderlijke Uitlopers of Noorderhaaks that is pushed landward during the severe winter months and shows a southward outbuilding in the calm summer period.

8.1.3 Determine the potential of state-of-the-art process-based models in inlet research; e.g. how can process-based models be used in inlet research?

The availability of high-quality observational datasets of water levels, wind, waves, currents and discharges, bathymetry, bedforms and sediments make Texel Inlet probably the longest and one of the most frequently monitored inlet's worldwide. Even with all this data present there is still only limited spatial and temporal data coverage over the inlet domain. Quasi real-time (high-resolution) model simulations are indispensable assets to obtain such coverage. Observations are used to force the model 'as realistically as possible' (quasi real-time by measured time-series of wind, waves and tides) and as sediment transports and flow are resolved simultaneously the model results provide synoptic more or less realistic 'field-data' of high spatial and temporal resolution over the entire domain. In this manner spatial variations in velocities and concentrations are fully resolved in the instrumented and un-instrumented areas of the domain.

Inlet research can greatly benefit from the integrated analysis of field data and high-resolution model data as was shown by the Texel Inlet case study using the stat of the art process-based model *Delft3D Online Morphology*. Quasi real-time simulations using measured time-series of water levels, wind and waves were made over a 10-month period. Validation of the model results with observations showed that the model is able to simulate the dominant features in the flow and transport patterns even in the complexity of the ebb-tidal delta domain. In other words, quasi real-time model simulations can provide a valuable tool in identifying the qualitative transport patterns, especially for inlet systems that are measured at lower resolution and frequency as Texel inlet. Additionally, by varying the forcing conditions the model data allows to perform sensitivity analyses for identification of the dominant processes and mechanisms.

Our ultimate goal of the quasi real-time simulations is to obtain estimates of the long-term transport patterns and magnitudes (years to decades). As of yet, feasible computational effort limits us to the simulation of shorter periods wherein morphologic change is negligible compared to the morphodynamic scale of the inlet. Nevertheless, this approach is still a useful method. By making initial simulations during various stages of the morphological adaptation process, model-data analysis can help to understand changes in inlet dynamics and evolution on longer time scales, as was shown in this study in the analysis of the effects of Closure of the Zuiderzee.

8.2 Coastal maintenance strategies of Texel Inlet

The previous section summarizes the main findings of this thesis. In this additional section we specifically focus on the translation of the obtained insights to improve coastal maintenance strategies of Texel Inlet and its flanking Texel and North Holland coastlines. The translation of scientific research results to coastal maintenance application is considered essential due to the practical relevance of this thesis and the intensive cooperation and support of Rijkswaterstaat RIKZ.

For coastal maintenance the most important conclusions for the present inlet behaviour can be summarized by the following three statements:

1– *Lessons from the past are useful, but do not reflect the present inlet behaviour;*
   - no (major) cyclic ebb-delta behaviour is presently observed.

2– *The basin still demands sediment in order to obtain a dynamic equilibrium state;*
   - Texel and Vlie inlet form a coupled (sand-sharing system), and
   - the effects of closure of the Zuiderzee are far from damped out.

3– *Sediment transport capacity is present due to large shallow shoal areas flanked by large tidal channels;*
   - a continuously large sediment loss occurs from the ebb-tidal delta (including coasts) towards the basin estimated to range between 5 to 6 Mm^3/year.

'Lessons from the past are useful, but do not reflect the present inlet behaviour' is probably the most important conclusion in respect to future coastal maintenance strategies. During the inlets recorded history specific stages in inlet evolution and behaviour can be defined. The (cumulative) effects of large-scale human interventions trigger the different stages; inlet behaviour prior to the intervention is not necessarily representative for the post-construction state due to the changes in forcing.

A clear example of this statement is the previously assumed presence of cyclic ebb-tidal delta behaviour that was often used to describe the present morphodynamic state (see e.g. Sha, 1986; NWO-ALW, 1999). Cyclic morphologic evolution of the main channels and shoals was observed prior to construction of Helderse Zeewering; analysis of bathymetric maps reveals at least two cycles of major channel and shoal formation, migration and merging with the Texel coastline. Such behaviour cannot be observed since the stabilization of the inlet gorge around 1750. With the exception of an approximate 40 year period of southward developing main channels following the closure of the Zuiderzee, the main channels and shoals on the ebb-delta have remained stable in position.

For coastal maintenance, cyclic behaviour is important as periods of sedimentation and erosion alternate. Erosion is observed due to scouring of channels along the coastline and sedimentation occurs by the subsequent merging of the shoal areas. Knowing the presence of cyclic behaviour one would more likely use soft engineering measures, such as sand nourishments, to defend the coastline temporarily during the erosion periods rather than putting in permanent hard structures.

The present ebb-delta behaviour is still largely influenced by closure of the Zuiderzee. The continuous large sediment import into the basin partly results from the sediment demand of the basin in order to adapt to the effects of closure, and partly sediment is needed to keep in pace with the increase in accommodation due to relative sea-level rise. Also the availability of sediments on the ebb-tidal delta and transport capacity due to the large tidal velocities are important. The large erosion rates of the North Holland and Texel coastline were initially related to the scouring of large tidal channels along the coast (e.g. Schulpengat, Nieuwe Schulpengat and Molengat). This initial response lasted approximately 40 years. Nowadays, these channels have reached a maximum extension and remain stable in position. In combination with the stabilization of Texel inlet's basin volume it was concluded that the inlet reached a (near-)equilibrium state (e.g. Steijn, 1997; Van Marion, 1999; Steijn and Jeuken, 2000; Elias *et al.*, 2003). Detailed re-analysis of the basin and ebb-delta changes shows that the effects of closure of the Zuiderzee are far from damped out; a continues large sediment import remains. Sediment budget studies of the Western Wadden Sea (Texel and Vlie inlet combined) and the Texel ebb-delta indicate that the present sediment import into the basin through Marsdiep is at least 5 to 6 Mm^3/year. Comparing the channel-shoal ratio of the western and eastern Wadden Sea indicates that a vast amount of sediment is still needed to obtain such equilibrium. Therefore it is concluded: *'the basin still demands sediment in order to obtain a dynamic equilibrium state'.*

Two important elements contribute to the present sediment transfer from ebb-tidal delta to the basin: (1) the landward sediment supply from the western margin of the Noorderhaaks shoal, and (2) the presence of large tidal channels along the coastlines. Sand is transported landward by tides and waves from the western margin of the ebb-delta front (that might be considered as being an abundant source of sediment resulting from the pre-closure channel configuration). As a result the near-shore intra- and supra-tidal Noorderhaaks area enlarged, the Noorderlijke Uitlopers of Noorderhaaks expanded northward and Zuiderhaaks showed a southward outbuilding. The presence of tidal circulation cells on the extended shallow shoal areas, and the enlarged zones of wave-breaking and wave-breaking related transport augment sediment transports. Large tidal channels along the landward side of the shoal capture these transports and form efficient pathways for along-channel redistribution (into the basin during flood). The basin acts as a sediment trap due to its sediment demand.

Comparing the limited sediment volume available in the ebb-tidal delta deposits with the large quantity of sediment still needed in the basin to regain equilibrium, it is likely that a sediment deficit occurs in the near future (50-100 years). Either the adjacent shorelines will need to deliver the necessary sediments to compensate, or Texel basin fails to regain (and maintain) a dynamic equilibrium. More research is needed to understand this future (long-term) evolution since the North Holland and Texel beaches are our first line of defence against the sea, and the Wadden Sea is an important nature reserve and habitat for numerous species of fish, birds and mammals.

8.3 Recommendations

Long-term morphodynamic modelling

In the introduction section we stated that one of our main goals in this thesis is to investigate if and how process-based models can be used in inlet research. Roelvink's (ALW-NWO 1999, sub-project 2, page 17) statement: *'If you put enough of the essential physics into the model, the most important features of the morphological behaviour will come out, even at longer time scales'* was quoted as a working hypothesis. Nevertheless, in this thesis the long-term trends in inlet behaviour were derived from integrated analysis of field and model data; initial model results were used to test the observational-based hypothesis and conceptual models. This approach was followed to fill in existing gaps in inlet knowledge, necessary for making correct long-term model schematizations. With the obtained knowledge long-term model simulations are within reach, although specific aspects need further investigation in this respect. Some of these aspects are:

(1). the importance of stratification;

Short-term simulations show the potential large impact of density-stratification on sediment import rates. Research is needed to quantify the contributions on the long-term.

(2). the interaction between Texel and Vlie inlet;

Interaction (e.g. sediment exchange) between Vlie and Texel is a so far underestimated but important actor in the sediment transports and sediment demand of the basin. Further research is needed to determine the mechanisms behind this exchange. This entails the detailed modelling of tidal-, wave- and wind-driven flow and transports especially focussed on the basin. An important aspect herein concerns the importance of tidal flow propagation and the contribution of setup. In this respect further coupling with the NIOZ-ferry observations is essential.

(3). the importance of bed stratification and multiple sediment fractions;

An interesting new development within the Delft3D program is the application of '3D' bed schematisations. The bathymetry is no longer a homogeneous sediment layer but the vertical distribution of the sediment distribution can be specified. This feature has been schematically applied in Chapter 6. By using depth-varying bed characteristics (based on e.g. core data) for long-term simulations an imprint of e.g. Holocene - Pleistocene deposits can be added to the simulation. In combination with the use of multiple sediment fractions this might help in obtaining 'realistic' channel configurations even over longer time spans.

(4). making long-term wave, tide, wind and setup schematisations;

Based on the quasi-real time schematisations insight is obtained in the relative importance of wind, waves, tides and setup. The relative importance of these processes varies strongly over the inlet domain. A challenging aspect remains to create correct schematizations of these processes in order to capture the essentials of the long-term characteristics.

Improving fundamental understanding of tidal inlet dynamics

One of the main aspects for limited fundamental understanding of inlet dynamics is the scarcity of field data with sufficient temporal and spatial coverage. This data deficiency was partly resolved in this thesis by quasi real-time model simulations and integrating the analysis of field- and model-data analysis. By applying such an approach to other inlet systems (e.g. the well-monitored Ameland inlet in the Netherlands wherein the effects of human intervention are fairly limited) significant improvements in inlet knowledge can be obtained.

Although, quasi real-time simulations provide detailed patterns of flow and sediment transports (depending on grid resolution) we have still limited our analysis to the gross characteristics of the water motion and sediment transports on the ebb-tidal delta. Collecting field data on flow, sediment fluxes and wave (transformation) on the shallow swash platforms is essential for further validation and calibration of the models if one aims to obtain fundamental understanding of the processes and mechanisms on the smaller scales of e.g. individual channels and shoals.

In addition to continuation of the 'quasi real-time' model approach much insight can also be obtained by a more schematized approach. Schematized in this respect means using the complex process-based model but with simplified inlet geometry (and forcing). A first daunting task in this respect is obtaining a (quasi) equilibrium solution between basin, inlet gorge and ebb-tidal delta. Once such an equilibrium setting develops, this would make an ideal laboratory to test the importance of processes and mechanism, and to test schematization techniques to capture the essential of the dominant processes in order to make long-term morphological simulations.

BIBLIOGRAPHY

ASHELY, G. M. (1990). "Classification of large-scale subaqeuos bedforms: a new look at an old problem. SEPM bedforms and bedding research." *Journal of Sedimentary Petrology*, 60(1), 16-172.

AUBREY, D. G., and SPEER, P. E. (1984). "Updrift migration of tidal inlets" *Journal of Geology*, 92, 531-545.

AUBREY, D. G., and SPEER, P. E. (1985). "A study on non-linear tidal propagation in shallow inlet/estuarine systems: 1. Observations." *Estuarine, Coastal and Shelf Science*, 21, 185-205.

BATTJES, J. A. (1962). *Studie Zeegat van Texel (in Dutch)*, M.Sc. Report. Delft University of Technology, Delft.

BECKERING VICKERS, J. A. (1951). *Nota betreffende het Zeegat van Texel en de aangrenzende oevers (in Dutch)*, Report 51.1. Studiedienst Hoorn, The Hague.

BEETS, D. J., and VAN DER SPEK, A. J. F. (2000). "The Holocene evolution of the barrier and back-barrier basins of Belgium and the Netherlands as a function of late Weichselian morphology, relative sea-level rise and sediment supply" *Netherlands Journal of Geosciences*, 79(1), 3-16.

BERGER, G. W., EISMA, D., and VAN BENNEKOM, A. J. (1987). "210Pb derived sedimentation rate in the Vlieter, a recently filled-in channel in the Wadden Sea." *Netherlands Journal of Sea Research,* 21, 287-294.

BIEGEL, E. J. (1993). *Morphological changes due to sea level rise in tidal basins in the Dutch Wadden Sea versus morphological response model MORRES*, Report IMAU-93.14. Institute for marine and atmospheric research Utrecht, Faculty of Geographical Sciences, Utrecht.

BLANTON, J. O., LIN, G., ELSTON, S.A. (2002). "Tidal current asymmetry in shallow estuaries and tidal creeks" *Continental Shelf Research*, 22, 1731-1743.

BLOK, M., and MOL, J. W. (2001). *Debietmeting zeegat van Texel (in Dutch)*, Report. 01.03, Rijkswaterstaat, Directie Noord-Holland, Informatiedienst Water, IJmuiden.

BONEKAMP, J. G., RIDDERINKHOF, H., ROELVINK, J. A., and LUIJENDIJK, A. (2002). "Comparison modeled and observed water motion and sediment transport in the Texel tidal inlet" *Proc. 25th International Conference on Coastal Engineering*, Cardiff, Wales.

BOOIJ, N., RIS, R. C., and HOLTHUIJSEN, L. H. (1999). "A third-generation wave model for coastal regions, Part I: Model description and validation" *Journal of Geophysical Research*, 104, 7649-7666.

BOON, J.D., and Byrne, R.J. (1981). On basin hypsometry and the morphodynamic response of coastal inlet systems. *Marine Geology,* 40, 27-48.

BOOTHROYD, J. C., and HUBBARD, D. K. (1975). "Genesis of bedforms in meso-tidal estuaries", *Estuarine Research*, L. E. CRONIN, ed., Academic Press, New York, 217-234.

BOOTHROYD, J. C. (1985). "Tidal inlets and tidal deltas" *Coastal Sedimentary Environments*, R.A. Davis, Jr., ed., Springer-Verlag, New York, 445-532.

BRUBAKER, J. M., SIMPSON, J.H.,. (1999). "Flow convergence and stability at a tidal estuarine front: Acoustic Doppler Current Observations", *Journal of Geophysical Research*, 104(8), 18.257-18268.

BRUUN, P., and GERRITSEN, F. (1959). "Natural bypassing of sand at coastal inlets" *Journal of the Waterways and Harbors*, 85, 75-107.

BRUUN, P., and GERRITSEN, F. (1960). *Stability of tidal inlets*, North-Holland Publishing Co.

BRUUN, P. (1962). "Sea-level rise as a cause of shore erosion" *Journal of Waterways Harbors Division*, 88, 117-130.

BUONAIUTO, F. S., and KRAUS, N. C. (2003). "Limiting slopes and depths at ebb-tidal shoals." *Coastal Engineering*, 48, 51-65.

CAYOCCA, F. (2001). "Long-term morphological modeling of a tidal inlet: the Arcachon Basin, France." *Coastal Engineering*, 42, 115-142.

CLEVERINGA, J., and OOST, A. P. (1999). "The fractal geometry of tidal-channel systems in the Dutch Wadden Sea" *Geologie en Mijnbouw*, 78, 21-30.

CLEVERINGA, J. (2001). *Zand voor zuidwest Texel. Technisch advies RIKZ over vier mogelijke ingrepen in het Zeegat van Texel (in Dutch)*, Report RIKZ/OS/2001/031. Rijkswaterstaat RIKZ.

CLEVERINGA, J. (2002). *Projectplan K2005*Waddendeltas. Onderdeel van programma KUST2005 EINDDOEL 2: Morfologische kennisontwikkeling op regionale schaal rond eilandkoppen: 1-25 jaar, 1-50 km.*, Report, Rijkswaterstaat RIKZ, Den Hague.

COELINGH, J. P., VAN WIJK, A. J. M., and HOLTSLAG, A. A. M. (1996). "Analysis of wind speed observations over the North Sea." *Journal of Wind Engineering and Industrial Aerodynamics*, 61, 51-69.

COWELL, P. J., STIVE, M.J.F, NIEDORODA, A. W., DE VRIEND, H. J., SWIFT, D. J. P., KAMINSKY, G. M., and CAPOBIANCO, M. (2003). "The Coastal-Tract (Part 1): A conceptual approach to aggregated modeling of low-order coastal change." *Journal of Coastal Research*, 19(4), 812-827.

DAVIS, R. A., and HAYES, M. O. (1984). "What is a wave-dominated coast?" *Marine Geology*, 60, 313-329.

DE KRUIF, A. C. (2001). *Bodemdieptegegevens van het Nederlandse Kustsyteem. Beschikbare digitale data en een overzicht van aanvullende analoge data (in Dutch)*, Report RIKZ/2001.041. Rijkswaterstaat RIKZ, The Hague.

DE MULDER, E. F. J., GELUK, M. C., RITSEMA, I. L., WESTERHOFF, W. E., and WONG, T. E. (2003). *De ondergrond van Nederland.*, Wolters-Noordhof bv, Groningen/Houten.

DE REUS, J. H., and LIESHOUT, M. F. M. (1982). *Debieten Zeegat van Texel (in Dutch)*, Report WWKZ-82.H205. Rijkswaterstaat RIKZ, The Hague.

DE RONDE, J. G., VAN MARLE, J. G. A., Roskam, A.P., and Andorka Gal, J.H., (1995). *Golfrandvoorwaarden langs de Nederlandse kust op relatief diep water (in Dutch)*, Report RIKZ-95.024. Rijkswaterstaat RIKZ, The Hague.

DE RUIG, J. H. M. (1989). *The sediment balance of the closed Dutch Coast, 1963-1986*, Report GWAO 89.016. Rijkswaterstaat RIKZ, Den Haag.

DE VRIEND, H. (1991). "Mathematical modeling and large-scale coastal behavior, Part 1: physical processes." *Journal of Hydraulic Research*, 29, 727-740.

DE VRIEND, H. J., LOUTERS, T., BERBEN, F. M. L., and STEIJN, R. C. (1989). "Hybrid prediction of intertidal flat evolution in an estuary" *International Conference*

Hydraulic and Environmental Modeling of Coastal, Estuarine and Rivers waters, Bradford, U.K.

De Vriend, H. J. (1996). "Mathematical modeling of meso-tidal barrier islands coasts. Part 1: Empirical and semi-empirical models" Advances in coastal and ocean engineering, P. L. F. Liu, ed., World Scientific Publishing Company, Singapore, 150-197.

De Vriend, H. J., and Ribberink, J. S. (1996). "Mathematical modeling of meso-tidal barrier island coasts. Part II: Process-based simulation models.", *Advances in Coastal and Ocean engineering*, P. L.-F. Liu, ed., World Scientific Publishing Company., Singapore, 150-179.

Dean, R. G. (1988). "Sediment interaction at modified coastal inlets: processes and policies. "Hydrodynamics and Sediment Dynamics of Tidal Inlets", D. Aubrey and L. Weishar, eds., *Lecture Notes on Coastal and Estuarine Studies*, 29, Springer, New York, 412-439.

Doekes, J. (1985). *Invloed van de afsluiting van de Zuider Sea op het getij in de Waddenzee (in Dutch)*, Report GWIO 85.001. Rijkswaterstaat, The Hague.

Dronkers, J. (1984). "Import of fine marine sediment in tidal basins" *Netherlands Journal of Sea Research*, 10, 83-105.

Dronkers, J. (1986). "Tidal asymmetry and estuarine morphology" *Netherlands Journal of Sea Research*, 20, 117-131.

Dronkers, J. (1998). "Morphodynamics of the Dutch Delta", *Proceedings of Physics of Estuaries and Coastal Seas*, Dronkers, J., Scheffers, M. B. A. M., eds., A.A. Balkema Publishers, Rotterdam, 297-304.

Dyer, K. R. (1986). *Coastal and Estuarine sediment dynamics.*, John Wiley & Sons.

Eckart, C. (1958). "Properties of water, Part II. The equation of state of water and sea water at low temperatures and pressures." *American Journal of Science*, 256, 222-240.

Ehlers, J. (1988). *The morphodynamics of the Wadden Sea*, Balkema, Rotterdam.

Eisma, D., and Wolff, W. J. (1980). "The development of the western most part of the Wadden Sea in historical time", *Geomorphology of the Wadden Sea Area*, K. S. Dijkema, H. E. Reineck, and W. J. Wolff, eds., Balkema, Rotterdam, 95-103.

ELIAS, E. P. L., BONEKAMP J.G., and STIVE, M. J. F. (2003a). "Decadal ebb-tidal delta behavior a response to large-scale human intervention" *Proc. 2003 International Conference on Coastal Sediments*, CD-ROM, st. Petersburg, Florida.

ELIAS, E. P. L., and CLEVERINGA, J. (2003). *Morfologische analyse van de ontwikkeling van het Nieuwe Schulpengat en de aangrenzende kust (in Dutch)*, Report RIKZ-2003.040. Rijkswaterstaat RIKZ, The Hague.

ELIAS, E. P. L., STIVE, M. J. F., BONEKAMP, J. G., and CLEVERINGA, J. (2003b). "Tidal inlet dynamics in response to human intervention" *Coastal Engineering Journal*, 45(4), 629-658.

ELIAS, E. P. L., STIVE, M. J. F., and ROELVINK, J. A. (2005). "Impact of back-barrier changes on ebb-tidal delta evolution" *Journal of Coastal Research*, 42(SI), 460-476.

ELIAS, E. P. L., CLEVERINGA, J., BUISMAN, M. C., STIVE, M. J. F., and ROELVINK, J. A. (2006). "Field and model data analysis of sand transport patterns in Texel Tidal inlet (the Netherlands)" *Coastal Engineering*, 53(5-6), 505-529.

ELIAS, E. P. L. AND De Ronde, J.G. (2006). "Density-stratification related sand transport in a tidal inlet system (Texel Inlet, the Netherlands)" *Estuarine, Coastal and Shelf Sciences*, Submitted for review.

ELIAS, E. P. L., and VAN DER SPEK, A. J. F. (2006). "Long-term evolution of Texel Inlet and its ebb-tidal delta (the Netherlands)." *Marine Geology*, 225(1-4), 5-21.

ENGELUND, F., and HANSEN, E. (1967). *A monograph on sediment transport in alluvial streams*, Report, Copenhagen.

ESCOFFIER, F. F. (1940). "The stability of tidal inlets." *Shore and Beach*, 114-115.

EYSINK, W. D. (1979). *Morfologie van de Waddenzee. Gevolgen van zand- en schelpenwinning*, Report R 1336. WL | Delft Hydraulics, Delft.

EYSINK, W. D. (1990). "Morphological response to tidal basins to change" *Proc. 22nd International Conference on Coastal Engineering*, Delft, 1948-1961.

EYSINK, W. D., BIEGEL, E. J., and HOOZEMANS, F. J. M. (1992). *Impact of sea level rise on the morphology of the Wadden Sea in the scope of its ecological function; investigations on empirical morphological relations*, Report ISOS*2, H1300. WL | Delft Hydraulics, The Hague.

EYSINK, W. D. (1993). *Impact of sea level rise on the morphology of the Wadden Sea in the scope of its ecological function. General considerations on hydraulic con-*

ditions, sediment transports, sand balance, bed composition and impact of sea level rise on tidal flats, Report ISOS*2, Project Phase 4. Rijkswaterstaat RIKZ, The Hague.

FISCHER, H. B. (1972). "Mass transport mechanism in partially stratified estuaries" *Journal of Fluid Mechanics*, 53(4), 671-687.

FITZGERALD, D. M. (1982). "Sediment bypassing at mixed energy tidal inlets" *Proc. of 18th International Conference on Coastal Engineering*, Cape Town, 1094-1118.

FITZGERALD, D. M., PENLAND, S., and NUMMEDAL, D. (1984). "Control of barrier island shape by inlet sediment bypassing: East Frisian Islands, West Germany" *Marine Geology*, 60, 355-376.

FITZGERALD, D. M. (1988). "Shoreline erosional-depositional processes associated with tidal inlets" Hydrodynamics and sediment dynamics of tidal inlets, *Lecture Notes on Coastal and Estuarine Studies* 29, AUBREY and D. G. WEISHAR, eds., Springer-Verlag, New York, 186-225.

FITZGERALD, D. M. (1996). "Geomorphic variability and morphologic and sedimentologic controls on tidal inlets." *Journal of Coastal Research*, 23, 47-71.

FITZGERALD, D. M., KRAUS, N. C., and HANDS, E. B. (2000). *Natural mechanisms of sediment bypassing at tidal inlets*, Report ERDC/CHL CHETN-IV-30). US Army Corps of Engineers.

FRANTSEN. (2001). *Bathymetrie van het Nederlandse deel van het Continentaal plat*, Report 01-162-C. TNO-NITG, Utrecht.

FRIEDRICHS, C., and AUBREY, D. G. (1988). "Non-linear tidal distortion in shallow well-mixed estuaries: a synthesis" *Estuarine, Coastal and Shelf Sciences*, 27, 521-545.

GALLAPPATTI, R. (1983). *A depth integrated model for suspended transport*, Communications on Hydraulics, vol. 83-7, Delft University of Technology, Delft, 114p.

GAUDIANO, D. J., and KANA, T. W. (2001). "Shoal bypassing in mixed energy inlets: Geomorphic variables and empirical predictions for nine South Caroline inlets" *Journal of Coastal Research*, 17(2), 280-291.

GERRITSEN, F., and DE JONG, H. (1985). *Stabiliteit van Doorstroomprofielen in het Waddengebied (in Dutch)*, Report WWKZ-84.V016. Rijkswaterstaat, Vlissingen.

GERRITSEN, F. (1990). *Morphological stability of Inlets and channels of the Western Wadden Sea.*, Report GWAO-90.019. Rijkswaterstaat RIKZ, The Hague.

GERRITSEN, H., BOON, J. G., VAN DER KAAIJ, T., and VOS, R. J. (2001). "Integrated modeling of Suspended Matter in the North Sea" *Estuarine, Coastal and Shelf Sciences*, 53(4), 581-594.

GEYER, W. R., and SIGNELL, R. (1990). "Measurements of tidal flow around a headland with a shipboard Acoustic Doppler Current Profiler" *Journal of Geophysical Research*, 95(c3), 3189-3197.

GEYER, W. R. (1993). "Three-dimensional tidal flow around a headland" *Journal of Geophysical Research*, 98, 955-966.

GLAESER, D. J. (1978). "Global distribution of barrier islands in terms of tectonic setting" *Journal of Geology*, 86(3), 283-297.

GLIM, G. W., GRAAFF, N. D., KOOL, G., LIESHOUT, M. F., and BOER, M. D. (1988). *Erosie en sedimentatie in de binnendelta van het Zeegat van Texel 1932-1982 (in Dutch)*, Report ANWX-88.H201. Rijkswaterstaat.

GROEN, P. (1967). "On the residual transport of suspended load matter by an alternating tidal current" *Netherlands Journal of Sea Research*, 3, 564-674.

HALLEWAS, D. P. (1984). "The interaction between man and his physical environment in the county of Holland between circa 1000 and 1300 AD: a dynamic relationship" *Geologie en Mijnbouw*, 62, 299-307.

HANSEN, D. V., and RATTRAY, M. J. (1965). "Gravitational circulation in straits and estuaries" *Journal of Marine Research*, 23, 104-122.

HAYES, M. O. (1975). "Morphology of sand accumulation in estuaries.", *Estuarine Research*, L. E. CRONIN, ed., Academic Press, New York, 3-22.

HAYES, M. O. (1979). "Barrier Island morphology as a function of tidal and wave regime", *Barrier Islands: From the Gulf of St Lawerence to the Gulf of Mexico*, S. P. LEATHERMAN, ed., Academic Press, New York, 1-27.

HIBMA, A., DE VRIEND, H. J., and STIVE, M. J. F. (2003). "Numerical modeling of shoal pattern formation in well-mixed elongated estuaries" *Estuarine, Coastal and Shelf Science*, 57, 981-991.

HIBMA, A. (2004). *Morphodynamic modeling of channel-shoal systems*, Communications on Hydraulic and Geotechnical Engineering, vol. 04-3, Delft University of Technology, Delft, 122p.

HICKS, D. M., and HUME, T. M. (1996). "Morphology and size of ebb-tidal deltas at natural inlets on open-sea and pocket bay coasts, North Island, New Zealand" *Journal of Coastal Research*, 12(1), 47-63.

HINE, A. C. (1975). "Bedform distribution and migration patterns on tidal deltas in the Chatham Harbor Estuary, Cape Cod, Massachusetts", *Estuarine Research*, L. E. CRONIN, ed., Acadamic Press, New York, 235-253.

HOLTHUIJSEN, L. H., BOOIJ, N., and RIS, R. C. (1993). "A spectral wave model for the coastal zone" *2nd Int. Symposium on Ocean Wave Measurement and Analysis*, New Orleans, 630-641.

HOOZEMANS, F. M. J., and VAN VESSEM, P. (1990). *Toestand Kust 1990. Kusttypering en kustligging. Technisch Rapport 2.*, Report. Rijkswaterstaat, Dienst Getijdewateren, Den Haag.

HUBBARD, D. K., BARWIS, J. H., and NUMMENDAL, D. (1979). "The role of waves and tidal currents in the development of tidal inlet sedimentary structures and sand body geometry: examples from the North Carolina, South Carolina and Georgia." *Journal of Sedimentary Petrology*, 49, 1073-1092.

ISRAEL, C. G., and DUNSBERGEN, D. W. (1999). "Cyclic morphological development of the Ameland Inlet, The Netherlands." *Proceedings IAHR Symposium on river, coastal and estuarine morphodynamics*. Department of Environmental Engineering, University of Genoa, 705-714.

JELGERSMA, S. (1961). *Geology and Lithology of the Wadden Sea area*, Report O.105, Haarlem.

JOUSTRA, D. S. (1973). *Geulbeweging in de buitendelta's van de Waddenzee (in Dutch)*, Report W.W.K. 71-14. Rijkswaterstaat RIKZ, The Hague.

KANA, T. W., HAYTER, E. J., and WORK, P. A. (1999). "Meso scale sediment transport at South-Eastern U.S. Tidal Inlets: Conceptual Model Applicable to Mixed Energy Settings" *Journal of Coastal Research*, 15, 303-313.

KLOK, B., and SCHALKERS, K. M. (1980). *De veranderingen in de waddenzee ten gevolge van de afsluiting van de Zuider Sea (in Dutch)*, Report 78.H238. Rijkswaterstaat, The Hague.

KOOMANS, R. (2004). *Sedimenten in het Molengat. Syntheserapport.*, Report 2003-P-042R2. Medusa Explorations BV, Groningen.

KRAGTWIJK, N. G. (2001). *Aggregated scale modeling of tidal inlets of the Wadden Sea; morphological response to the closure of the Zuiderzee*, M.Sc. Thesis, Civil Engineering and Geosciences, Delft University of Technology, Delft.

KRAGTWIJK, N. G., ZITMAN, T. J., STIVE, M. J. F., and WANG, Z. B. (2004). "Morphological response of tidal basins to human interventions" *Coastal Engineering*, 51, 207-221.

LATTEUX, B. (1995). "Techniques for long-term morphological modeling under tidal action." *Marine Geology*, 126, 129-141.

LECONTE, L. J. (1905). "Discussions of "Notes on the improvement of rivers and harbor outlets in the United States", *Transactions of American Soc. of Civil Engineers*, P. A. WATTS, ed., 306-308.

LEENDERTSE, J. J. (1987). *A three-dimensional alternating direction implicit model with iterative Fourth order dissipative non-linear advection terms.*, Report WD-3333-NETH, Rijkswaterstaat.

LENSELINK, G., and KOOPSTRA, R. (1994). "Ontwikkelingen in het Zuiderzeegebied; van Meer Flevo, via de Almere-lagune, tot Zuiderzee.", *In de Bodem van Noord-Holland*, M. RAPPOL and C. M. SOONIUS, eds., Lingua Terrae, 129-138.

LESSER, G. R. (2000). *Computation of three-dimensional suspended sediment transport within the Delft3D-FLOW module*, Report WL | Delft Hydraulics Z2396, Delft, 123p.

LESSER, G. R., ROELVINK, J. A., VAN KESTER, J. A. T. M., and STELLING, G. S. (2004). "Development and validation of a three-dimensional model" *Coastal Engineering*, 51, 883-915.

LI, C., and VALLE-LEVINSON, A. (1998). "Separating baroclinic flow from tidally induced flow in estuaries" *Journal of Geophysical Research*, 103(C5), 10405-10417.

LI, C., BLANTON, J., and CHEN, C. (2004). "Mapping of tide and tidal flow fields along a tidal channel with vessel-based observations" *Journal of Geophysical Research*, 109(C04002), 10.

LIGTENBERG, J. (1998). *De rol van het getij bij de aanzanding van het Marsdiep, voor en na de afsluiting van de Zuider Sea (in Dutch)*, Report RIKZ-OS-98.106x. Rijkswaterstaat RIKZ, The Hague.

LIN, W., SANFORD, L. P., and SUTTLES, S. E. (2002). "Wave measurements and modeling in Chesapeake Bay" *Continental Shelf Research*, 22, 2673-2686.

LOBO, F. J., HERNANDEZ-MOLINA, F. J., SOMOZA, L., RODERO, J., and MALDONANDO, B., A. (2000). "Patterns of bottom current flow deduced from dune asymmetries over the Gulf of Cadiz shelf (southwest Spain)." *Marine Geology*, 164, 91-117.

LORENTZ, H. A. (1926). *Verslag Staatscommissie Zuiderzee 1918-1926 (in Dutch)*, Report. Rijkswaterstaat, The Hague.

LOUTERS, T., and GERRITSEN, F. (1994). *The Riddle of the Sands. A Tidal System's Answer to a Rising Sea Level.*, Report RIKZ-94.040. Rijkswaterstaat RIKZ, The Hague.

LUMBORG, U., and PEJRUP, M. (2005). "Modeling of cohesive sediment transport in a tidal lagoon - an annual budget" *Marine Geology*, 218(1-4), 1-16.

MERCKELBACH, L. M., and RIDDERINKHOF. (2006). "Estimating suspended sediment concentration using backscatterance from an acoustic Doppler profiling current meter at a site with strong tidal currents. *Ocean Dynamics*, doi: 10.1007/s 10236-*005-0036-2.*

MULDER, J. P. M. (2000). *Zandverliezen in het Nederlandse kustsysteem. Advies voor dynamische handhaven in de 21e eeuw (in Dutch)*, Report RIKZ/2000.36. Rijkswaterstaat RIKZ, The Hague.

NWO-ALW. (1999). *Outer Delta Dynamics: process analysis of water motion, sediment transport and morphologic variability*, Project proposal, Utrecht University, Utrecht.

O'BRIEN, M. P. (1931). "Estuary tidal prisms related to entrance areas" *Civil Engineering*, 1, 738-739.

O'BRIEN, M. P. (1969). "Equilibrium flow areas of inlets and sandy coasts" *Journal of Waterways, Harbors, and Coastal Engineering*, 95, 43-55.

OERTEL, G. F. (1972). "Sediment transport on estuary entrance shoals and the formation of swash platforms" *Journal of Sedimentary Petrology*, 42, 858-868.

OERTEL, G. F. (1975). "Ebb-tidal deltas of Georgia Estuaries", *Estuarine research*, L. E. CRONIN, ed., Academic press, New York, 267-276.

OERTEL, G. F. (1988). "Processes of sediment exchange between tidal inlets, ebb deltas and barrier islands", *lecture notes on coastal and estuarine studies*, Vol. 29; Hydrodynamics and sediment dynamics of tidal inlets, L. W. D.G. AUBREY AND L. WEISHAR, eds., Springer-Verlag, New York.

OLD, C. P., VENNELL, R.,. (2001). "Acoustic Doppler Current Profiler measurements of the velocity field of an ebb tidal jet" *Journal of Geophysical Research*, 106(4), 7037-7049.

OOST, A. P., and DE BOER, P. L. (1994). "Sedimentology and development of barrier islands, ebb-tidal deltas, inlets and backbarrier areas of the Dutch Wadden Sea" *Senckenbergiana Maritima*, 24, 65-115.

OOST, A. P. (1995). *Dynamics and sedimentary development of the Dutch Wadden Sea with emphasis on the Frisian Inlet. A study of barrier islands, ebb-tidal deltas, inlets and drainage basins*, Geologica Ultraiectina, Mededelingen van de Faculteit Aardwetenschappen no. 126, Utrecht University, 454 p.

PARKER, B. B. (1991). "The relative importance of the various nonlinear mechanisms in a wide range of tidal interactions (Review)", *Tidal Hydrodynamics*, B. B. PARKER, ed., John Wiley & Sons, New York, 237-269.

PONS, L. J., and VAN OOSTEN, M. F. (1974). *De bodem van Noord-Holland*, Stiboka, Wageningen.

POSTMA, H. (1954). "Hydrography of the Dutch Wadden Sea" *Arch. Neerl. Zool.*, 10, 405-511.

POSTMA, H. (1961). "Transport and accumulation of suspended matter in the Dutch Wadden Sea" *Netherlands Journal of Sea Research*, 1(1/2), 148-190.

POSTMA, H. (1967). "Sediment transport and sedimentation in the estuarine environment", *Estuaries*, G. H. LAUFF, ed., AAAS Publ., 158-179.

POSTMA, H. (1981). "Exchange of materials between the North Sea and the Wadden Sea" *Marine Geology*, 40, 199-213.

RAB, M. (2003). *Morfologische onderzoek zeegat van Texel. Meetverslag (in Dutch)*, Report RWS-DNH-ANI-report 03.07. RWS directie Noord-Holland, Informatiedienst water, IJmuiden.

RAB, M. (2004a). *Stroommeting Nieuwe Schulpengat*, Report ANI-05.05. RWS directie Noord-Holland, Informatiedienst water, IJmuiden.

RAB, M. (2004b). *Stroommeting Molengat, September 2003*, Report ANI-04.02). RWS directie Noord-Holland, Informatiedienst Water, IJmuiden.

RANASINGHE, R., and PATTIARATCHI, C. (1999). "The seasonal closure of tidal inlets: Wilson Inlet, a case study" *Coastal Engineering*, 37, 37-56.

RANASINGHE, R., PATTIARATCHI, C., and MASSELINK, G. (1999). "A morphodynamic model to simulate the seasonal closure of tidal inlets" *Coastal Engineering*, 37, 1-36.

RIBBERINK, J. S., and DE VRIEND, H. J. (1995). *"Morphodynamics of a meso-tidal barrier-island coast.", Morfodynamiek van de Nederlandse kust op verschillende tijd- en ruimteschalen. Een samenvatting in 3 rapporten van de kennis verkregen in het project Kustgenese*, WL | Delft Hydraulics, Delft, pp. 34.

RIDDERINKHOF, H. (1988a). "Tidal and residual flows in the western Dutch Wadden Sea. I: Numerical model results." *Netherlands Journal of Sea Research*, 22(1), 1-21.

RIDDERINKHOF, H. (1988b). "Tidal and residual flows in the western Dutch Wadden Sea. II: An analytical model to study the constant flow between connected tidal basins." *Netherlands Journal of Sea Research*, 22, 185-198.

RIDDERINKHOF, H. (1997). "The effect of tidal asymmetries on the net transport of sediments in the Ems Dollard estuary" *Journal of Coastal Research*, 25(SI).

RIDDERINKHOF, H., VAN HAREN, H., EIJGENRAAM, F., and HILLEBRAND, T. (2002). "Ferry observations on temperature, salinity and currents in the Marsdiep tidal inlet between the North Sea and Wadden Sea." *Proceedings of the second international conference on EUROGOOS. Operational oceanography: implementation at the European and regional scales.* FLEMMING, N.C. *et al.*, eds., Elsevier Oceanography Series, 66, pp: 139-148.

RIETVELD, C. F. W. (1962). "The natural development of the Wadden Sea after the enclosure of the Zuider Sea." *Proc. of the 8th International Conference on Coastal Engineering*, Mexico City, 765-781.

RIJZEWIJK, L. C. (1986). *Overzichtskaarten zeegaten van de Waddenzee, 1976-1985 (in Dutch)*, Report 86.H208. Rijkswaterstaat RIKZ, The Hague.

RINGMA, S. H. (1953). *Scheepvaartdrempels rond het zeegat van Texel (in Dutch)*, Report 53.2. Rijkswaterstaat, Hoorn.

RIS, R. C., BOOIJ, N., HOLTHUIJSEN, L.H. (1999). "A third-generation wave model for coastal regions, Part II: verification" *Journal of Geophysical Research*, 104(4), 7649-7666.

ROELSE, P. (2002). *Water en zand in balans. Evaluatie zandsuppleties na 1990; een morfologische beschouwing (in Dutch)*, Report RIKZ/2002.003. Rijkswaterstaat RIKZ, The Hague.

ROELVINK, J. A., VAN DER KAAIJ, T., and RUESSINK, M. G. (2001a). *Calibration and verification of 2D/3D flow models*, Report Z3029.11. WL | Delft Hydraulics, Delft.

ROELVINK, J. A., VAN DER KAAIJ, T., and RUESSINK, M. G. (2001b). *Set-up, calibration and verification of large-scale hydrodynamic models.*, Report Z3029.10. WL | Delft Hydraulics, Delft.

ROELVINK, J. A., and WALSTRA, D. J. (2004). "Keeping it simple by using complex models", 6th International Conference on Hydroscience and Engineering, *Advances in Hydro-Science and -Engineering,* Brisbane, Australia.

ROGERS, W. E., HWANG, P. A.,WANG, D. W. (2003). "Investigation of wave growth and decay in the SWAN model: Three regional-scale applications" *Journal of Physical Oceanography*, 33, 366-389.

ROSKAM, A. P. (1988). *Golfklimaten voor de Nederlandse Kust (in Dutch)*, Report GWAO-88.046. Rijkwaterstaat RIKZ, The Hague.

SCHOORL, H. (1973). *Zeshonder Jaar Water en Land (in Dutch)*, Wolters-Noordhoff, Groningen.

SCHOORL, H. (1999). *Het westelijk waddengebied en het eiland van Texel vanaf circa 1550: deel 2. (in Dutch)*, Pirola.

SHA, L. P. (1989a). "Sand transport patterns in the ebb-tidal delta of Texel inlet, Wadden Sea, the Netherlands." *Marine geology*, 86, 137-154.

SHA, L. P. (1989b). "Cyclic morphologic changes on the ebb-tidal delta, Texel Inlet, The Netherlands." *Geologie en Mijnbouw*, 68, 35-48.

SHA, L. P. (1989c). "Variation in ebb-delta morphologies along the west and east frisian islands, the Netherlands and Germany" *Marine Geology*, 89, 11-28.

SHA, L. P. (1989d). "Holocene-Pleistocene interface and three-dimensional geometry of the ebb-tidal delta complex, Texel Inlet, The Netherlands." *Marine Geology*, 89, 201-228.

SHA, L. P. (1990). *Sedimentological studies of the ebb-tidal deltas along the West Frisian Islands, the Netherlands*, Geologia Ultaiectina, Mededelingen van de Faculteit Aardwetenschappen no. 64, University Utrecht, p 159.

SPEER, P. E., AUBREY, D., and FRIEDRICHS, C. (1991). "Nonlinear hydrodynamics of shallow tidal inlet / bay systems", *Tidal Hydrodynamics*, B. B. PARKER, ed., John Wiley, New York, 321-339.

STEIJN, R. C. (1997). *Morphodynamische berekeningen ZW-Texel. Fase 1: Modelopzet en calibratie (in Dutch)*, Report A078.15 / Z2175. Alkyon / WL|Delft Hydraulics, Emmeloord.

STEIJN, R. C., and JEUKEN, C. (2000). *Vier mogelijke beheersingrepen in het Zeegat van Texel - morfodynamische modelberekeningen (in Dutch)*, Report A514/Z2742. Alkyon / WL|Delft Hydraulics, Emmeloord.

STELLING, G. S. (1984). "On the construction of computational methods for shallow water flow problems." *Rijkswaterstaat communication series No.* 35, The Hague.

STIVE, M. J. F., and EYSINK, W. D. (1989). *Voorspelling ontwikkeling kustlijn 1990-2090. fase3. Deelrapport 3.1: Dynamisch model van het Nederlandse Kustsysteem (in Dutch)*, Report H825. Waterloopkundig laboratorium, Delft.

STIVE, M. J. F., ROELVINK, J. A., and DE VRIEND, H. J. (1990). "Large-scale coastal evolution concept" *22nd International Conference on Coastal Engineering*, Delft.

STIVE, M. J. F., M., C., WANG, Z. B., RUOL, P., and BUIJSMAN, M. C. (1998). "Morphodynamics of a tidal lagoon and adjacent coast." *8th International Biennial Conference on Physics of Estuaries and Coastal Seas*, The Hague, 397-407.

STIVE, M. J. F., and WANG, Z. B. (2003). "Morphodynamic modeling of tidal basins and coastal inlets", *Advances in Coastal Modeling*, C. LAKHAN, ed., 367-392.

SUTHERLAND, J., WALSTRA, D. J., CHESTER, T. J., VAN RIJN, L. C., and SOUTHGATE, H. N. (2004). "Evaluation of coastal area modeling systems at an estuary mouth" *Coastal Engineering*, 51, 119-142.

TER WEE, M. W. (1962). "The Saalian Glaciation in the Netherlands" *Mededelingen Geologische Stichting*, 15, 57-76.

THIJSSE, J. T. (1972). *Een halve eeuw Zuider Zeewerken 1920-1970 (in Dutch)*, Tjeenk Willink, Groningen.

UNCLES, R. J. (2002). "Estuarine physical processes research: Some recent studies and progress" *Estuarine, Coastal and Shelf Sciences*, 55, 829-856.

VALLE-LEVINSON, A., and LWIZA, K. M. M. (1995). "The effect of channels and shoals on exchange between the Chesapeake Bay and the adjacent ocean." *Journal of Geophysical Research*, 100(C9), 18.551-18.563.

VAN DE KREEKE, J., and ZIMMERMAN, J. T. F. (1990). "Circulation in Well and Partially Mixed Estuaries." *The Sea*, B. LEMEHAUTE and D. M. HANES, eds., Springer Verlag.

VAN DE KREEKE, J., and ROBACZEWSKA, K. (1993). "Tide-induced residual transport of Coarse Sediment. Application to the Ems Estuary" *Netherlands Journal of Sea Research*, 31, 209-220.

VAN DER MOLEN, J., and DE SWART, H. E. (2001). "Holocene tidal conditions and tide-induced sand transport in the southern North-Sea" *Journal of Geophysical Research*, 106, 9339-9362.

VAN DER SPEK, A. J. F. (1994). *Large-scale evolution of Holocene tidal basins in the Netherlands*, Faculteit Aardwetenschappen, Utrecht Universiteit, Utrecht, 191p.

VAN DER SPEK, A. J. F. (1995). "Reconstruction of tidal inlet and channel dimensions in the Frisian Middelzee, a former tidal basin in the Dutch Wadden Sea" *Tidal Signatures in Modern and Ancient Sediments. Special Publications International Association of Sedimentologists*, 24, B. W. FLEMMING and A. BARTHOLOMÄ, eds., 239-258.

VAN DER SPEK, A. J. F., and VAN HETEREN, S. (2004). *Analyse van steekboringen verzameld in het Molengat en het Nieuwe Schulpengat*, Report. TNO-NITG, Utrecht.

VAN DER VEGT, M. (2006). *Modeling the dynamics of barrier coasts and ebb-tidal deltas*, Faculteit Betawetenschappen, Universiteit Utrecht, Utrecht.

VAN GOOR, M. A., ZITMAN, T. J., WANG, Z. B., and STIVE, M. J. F. (2003). "Impact of sea-level rise on the morphological equilibrium state of tidal inlets." *Marine Geology*.

VAN HETEREN, S., OOST, A. P., DE BOER, P.L., VAN DER SPEK, A. J. F., and ELIAS, E. P. L. (2004). "Island-terminus evolution as a function of changing ebb-tidal delta configuration: Texel, The Netherlands". Tidalities, 6th International Conference on Tidal Sedimentology, Copenhagen, Denmark.

VAN LEEUWEN, S. (2002). *Tidal inlet systems: bottom pattern formation and outer delta development*, Instituut voor Marien en Atmosferisch onderzoek Utrecht (IMAU), Faculteit Natuur- en Sterrenkunde, Utrecht University, Utrecht, p134.

VAN MAREN, D. S. (2004). *Morphodynamics of a cyclic prograding delta: The Red River, Vietnam*, Royal Dutch Geographical Society, Faculty of Geosciences, Utrecht University, 165 p.

VAN MARION, B. B. (1999). *Zandbalansen van het Zeegat van Texel met het invers sediment transport model (1931 tot 1997) (in Dutch)*, Report RIKZ/OS - 99.116X. Rijkswaterstaat RIKZ, The Hague.

VAN RIJN, L. C. (1986). "Sediment transport, Part II Suspended Load Transport", *Journal of Hydraulic Engineering, ASCE*, 110(11), 1613-1641.

VAN RIJN, L. C. (1993). "Transport of fine sands by currents and waves," *Journal of Waterway, Port, Coastal and Ocean Engineering*, 119(2), 123-143.

VAN RIJN, L. C. (1995). *Sand budget and coastline changes of the central coast of Holland between Den Helder and Hoek van Holland period 1964-2040*, Report H2129. WL | Delft Hydraulics, Delft.

VAN RIJN, L. C. (1997). "Sediment transport and budget of the central coastal zone of Holland" *Coastal Engineering*, 32, 61-90.

VAN RIJN, L. C. (2000). *General view on sand transport by currents and waves*, Report Z2899.20-Z2099.30- Z2824.30. WL | Delft Hydraulics, Delft.

VAN RIJN, L. C. (2002). *Approximation formulae for sand transport by currents and waves and implementation in DELFT-MOR*, Report Z3054.20. WL | Delft Hydraulics, Delft.

VAN STAALDUINEN, C. J. (1977). *Geology of the Netherlands Wadden Sea*, Report), Haarlem.

VAN STRAATEN, L. M. J. U., and KUENEN, P. H. (1957). "Accumulation of fine-grained sediments in the Dutch Wadden Sea" *Geologie en Mijnbouw*, 19, 329-354.

VAN KONINGSVELD, M., STIVE, M.J.F., MULDER, J.P.M. (2004). "Balancing research efforts and management needs. A challenge to coastal engineering " *Proc. of the 29th International Conference on Coastal Engineering*, Lisbon, Portugal, 2985-2997.

VAN VEEN, J. (1936). *Onderzoekingen in den Hoofden in verband met de gesteldheid des Nederlandse kust.*, Leiden University, Den Haag.

VAN VEEN, J. (1945). "Bestaat er een geologische bodemdaling te Amsterdam sedert 1700?" *Tijdschrift Koninklijk Nederlands Aardrijkskundig Genootschap*, 62, 2-36.

VAN VEEN, J. (1950). "Eb en vloedschaar systemen in de Nederlandse getijwateren (in Dutch)" Tijdschrift Koninklijk Nederlands Aardrijkskundig Genootschap, 303-325.

VAN VEEN, J. (1954). "Tide-gauges, subsidence-gauges and flood-stones in the Netherlands. Symposium: Quaternary Changes in Level, especially in the Netherlands" *Geologie en Mijnbouw*, 16(6), 214-219.

VAN VEEN, J., VAN DER SPEK, A. J. F., STIVE, M. J. F., and ZITMAN, T. J. (2005). "Ebb and Flood channel systems in the Netherlands tidal waters" *Journal of Coastal Research*, 21(6), 1107-1120.

VENNELL, R. (1994). "Acoustic Doppler current profiler measurements of tidal phase and amplitude in Cook Strait, New Zealand" *Continental Shelf Research*, 14, 353-364.

WALBURG, L. (2001). *De zandbalans van het Zeegat van Texel bepaald met verschillende buitendelta-definities (in Dutch)*, Report RIKZ/OS 2001. Rijkswaterstaat RIKZ, The Hague.

WALSTRA, D. J., ROELVINK, J. A., and GROENEWEG, J. (2000). "Calculation of wave-driven currents in a 3D mean flow model" *Proc. of 27th Conference on Coastal Engineering*, 1050-1063.

WALSTRA, D. J., and VAN RIJN, L. C. (2003). *Modeling of sand transport in Delft3D*, Report Z3624). WL | Delft Hydraulics, Delft.

WALTON, T. L., and ADAMS, W. D. (1976). "Capacity of inlet outer bars to store Sand" *Proc. 15th International Conference on Coastal Engineering*, Honolulu, 303-325.

WANG, Z. B., LOUTERS, T., and DE VRIEND, H. J. (1995). "Morphodynamic modeling for a tidal inlet in the Wadden Sea." *Marine Geology*, 126, 289-300.

WESTENBERG, J. (1974). "Kennemer Dijkgeschiedenis" *Verhandelingen Kon. Ned. Akad. Wetensch, Afd. Natuurk.*, 1e reeks(27 (2)), 1-159.

WIJNBERG, K. M. (1995). *Morphologic behavior of a barred coast over a period of decades.*, Faculteit Ruimtelijke Wetenschappen, University Utrecht, Utrecht, 245 pp.

WIJNBERG, K. M. (2002). "Environmental controls on decadal morphologic behavior of the Holland coast" *Marine Geology*, 189, 227-247.

WL | Delft Hydraulics. (2005). *Delft3D-FLOW; Simulation of multi-dimensional hydrodynamic flows and transport phenomena, including sediments*, User Manual Delft3D version 3.12, WL | Delft Hydraulics, Delft.

Zagwijn, W. H. (1986). *Nederland in het Holoceen*, Report. Geological Survey of the Netherlands, Haarlem.

Zimmerman, J. T. F. (1976). "Mixing and Flushing of Tidal embayments in the western Dutch Wadden Sea. Part 1: Distribution of salinity and calculation of mixing time scales" *Netherlands Journal of Sea Research*, 10(2), 149-191.

Zimmerman, J. T. F. (1981). "Dynamics, diffusion and geomorphological significance of tidal residual eddies." *Nature*, 290, 549-555.

ACKNOWLEDGEMENTS

"Peacefully drifting just waiting for sets. A little breeze, a few friends its as good as it gets". Angulo wrote this phrase describing the ultimate feeling of surfing. After struggling to get out of the surf, you will find an oasis of peace, out on the ocean. Just sit there, wait with your friends for that one perfect wave. The one wave that gives you the ride of your life.

This is how writing the acknowledgements after finishing your thesis feels. Sitting here, outside in the lovely California sun, the long road of alternating periods of despair and optimism, failure and success fade away. The ultimate reward is there: the Thesis. You feel lucky having accomplished this, with all the support, love and friendship of those you met on the road. This section is dedicated to them.

Doing research on a specific topic over a four year period is a luxury, that is not always recognized. Therefore sincere appreciation to the Delft University of Technology, the Dutch National Institute for Coastal and Marine Management (Rijkswaterstaat-RIKZ), WL | Delft Hydraulics, the Dr. Ir. Cornelis Lely Foundation and the Delft Cluster Project: Coasts 03.01.03. for the provided support and funding

It might come as a surprise for some people but this Delft University thesis does not deal with numerical models exclusively; the major part is based on field data analysis. This would not have been possible without the support of Rijkswaterstaat RIKZ. Thanks, Jelmer, John and Daan for sharing the relative unexplored treasures (data) of Rijkswaterstaat. Ad, the Chapter we wrote on 400 years of bathymetric change (Chapter 2) is still my favourite; thanks for your personal interest, support and cooperation. Although, a lot of field-data analysis is presented I am still more and more impressed by the endless opportunities that lie ahead in process-based modelling. Dano, your support and help in making models available and running is highly appreciated. Unfortunately, I could only incorporate a fraction of your suggestions. I still regret that I was not able to incorporate the long-term simulations in the Thesis, but at least that gives us some reasons for further joint research in the future.

A special word of appreciation to Marcel and Jelmer. Marcel, you are more then a promoter, all your former PhD's will agree on this. Many thanks for your personal interest, support and friendship. Jelmer, without you this thesis in its present form would not have existed. I enjoyed our conversations, discussions and cooperation at RIKZ. Many thanks for sharing your ideas and office (and all the reports and data in it).

The major part of the project was carried out at Delft University of Technology. Many thanks to all my former colleague's. Mark and Saskia you were the best room mates one can imagine. Not sharing offices anymore makes you realize this more and more. I think all of us went through joyful but also difficult times; thanks for all the support and friendship. Chantal thanks for all the conversations we had, your logistical support and help with printing of the thesis. Mark without you computers would have been a problem. Thanks for your support and providing the ultimate 'computational monsters' for doing the D3D simulations.

Field data and support was made available by Rijkstwaterstaat RIKZ. I really enjoyed working those Friday's at the Kortenaer Kade in Den Haag. Thank you Daan for making this exchange possible, and letting me browse around in the central library (and the personal library of Jelmer). Thanks to all my former colleagues at RIKZ for their interest, reviews, discussions, comments and contributions. WL | Delft Hydraulics is gratefully acknowledged making available the Delft3D model and support for scientific research. Looking forward to working with all of you for many years to come.

Last but certainly not least, the completion of this thesis would not have been possible with all the support and understanding of my parents, family and friends. Larissa thanks for all the happiness you brought into my life. Sorry for the long working hours; time flies when you are having fun (or when working on a thesis). I hope we can enjoy being together for many, many years to come.

Marcel, Jelmer, Dano, Ad, John, Co, Hans, Dirk-Jan and Tjerk thank you all for your contributions and sharing your knowledge with me. I hope you are just as proud on the end result: this thesis.

Edwin

Foster City California, June 2006.

About the author

Edwin Elias was born in Hontenisse, the Netherlands, on June 25th 1973. He graduated from secondary school, Jansenius College in Hulst. In Vlissingen he started his engineering studies at Hogeschool Zeeland and graduated at the Civil Engineering department in 1996. As part of this study work experience was gained at practical work in Witbank (South Africa) addressing the civil maintenance of the Duvha power station, and at HAM-VOW doing land surveys for the construction of the 'Kanaal door Zuid Beveland'.

Academic education was started at the Delft University of Technology in 1996. He did his final MSc-project at WL|Delft Hydraulics, entitled 'The Egmond Model. Calibration, validation and evaluation of Delft3D-MOR with field measurements' and graduated in 1999 at the Section of Hydraulic Engineering.

From 1999 till 2001 Edwin conducted research at Delft University on the erosion problems of the Abruzzo coastline (Italy). In May 2001 PhD-research was started at Delft University on the behaviour and evolution of Texel inlet, which resulted in the present thesis.

As of the 1st of October 2005, Edwin joined WL|Delft Hydraulics as a Researcher/Advisor on coastal morphodynamics. Presently, he is on a three-year deployment at the United States Geological Survey (Menlo Park/Santa Cruz, California, USA), where he participates in the Delft3D model studies of e.g. San Francisco bay, the Columbia river mouth and the Puget Sound.